

AIRCRAFT CONCEPTUAL DESIGN – AN ADAPTABLE PARAMETRIC SIZING
METHODOLOGY

by

GARY JOHN COLEMAN, JR.

Presented to the Faculty of the Graduate School of
The University of Texas at Arlington in Partial Fulfillment
of the Requirements
for the Degree of

DOCTOR OF PHILOSOPHY

THE UNIVERSITY OF TEXAS AT ARLINGTON

MAY 2010

Copyright © by Gary Coleman 2010

All Rights Reserved

ACKNOWLEDGMENTS

During the course of this research I have certainly stood on the *shoulders of giants* who came before and have been supported by many others. I would like to thank a few of them who have particularly helped me along the way.

First to my advisor Dr. Bernd Chudoba I would like to thank for the constant support and (often lengthy) suggestions and criticism. His high standards for quality and dedication to past knowledge are the foundation of this research and my career beyond.

To Prof. Paul Czysz (retired McDonnell Douglas) I would like to thank for opening his parametric sizing tool box and his wealth of experience and knowledge. The *design to mission* and his *clear thinking* approach to conceptual design provided the technical basis for this research.

I would also like to thank Andy Hahn, Mark More, and Dr. Dennis Bushnell of NASA LaRC for sharing their technical and philosophical feedback on this research through several AVD/NASA projects.

A special thank you to Dick Atkins (retired Vought Aerospace) and all the members of the Vought Retiree Club for their diligent work in collecting and maintaining the Vought Archive. The vast knowledge and insight gain through both exploring the achieve, and discussions with retired engineers has been an invaluable and exciting component of this research

A special thank you to AVD Lab past and current members, in particular Dr. Xiao Huang, Amit Oza, Lex Gonzalez, Andy Walker, Amen Omoragbon, Brandon Watters, and Reza Mansouri for their support and friendship.

Finally, I would also like to thank my family and friends for their love and support through my undergraduate and graduate career, In particular thank you to my wife Jessica, parents Gary and Janet Coleman and my brothers Danny, Dennis and Nick.

May 15, 2010

ABSTRACT

AIRCRAFT CONCEPTUAL DESIGN – AN ADAPTABLE PARAMETRIC SIZING METHODOLOGY

Gary John Coleman Jr., Ph.D.

The University of Texas at Arlington, 2010

Supervising Professor: Bernd Chudoba, Ph.D.

Aerospace is a maturing industry with successful and refined baselines which work well for traditional baseline missions, markets and technologies. However, when new markets (space tourism) or new constraints (environmental) or new technologies (composite, natural laminar flow) emerge, the conventional solution is not necessarily best for the new situation. Which begs the question ***“how does a design team quickly screen and compare novel solutions to conventional solutions for new aerospace challenges?”*** The answer is rapid and flexible conceptual design ***Parametric Sizing***. In the product design life-cycle, parametric sizing is the first step in screening the total vehicle in terms of mission, configuration and technology to quickly assess first order design and mission sensitivities. During this phase, various missions and technologies are assessed. During this phase, the designer is identifying design solutions of concepts and configurations to meet combinations of mission and technology. This research undertaking contributes the state-of-the-art in aircraft parametric sizing through **(1) development of a dedicated conceptual design process and disciplinary methods library, (2) development of a novel and robust parametric sizing process** based on ‘best-practice’ approaches found in the process and disciplinary methods library, and **(3) application of the**

parametric sizing process to a variety of design missions (transonic, supersonic and hypersonic transports), different configurations (tail-aft, blended wing body, strut-braced wing, hypersonic blended bodies, etc.), and different technologies (composite, natural laminar flow, thrust vectored control, etc.), in order to demonstrate the robustness of the methodology and unearth first-order design sensitivities to current and future aerospace design problems.

This research undertaking demonstrates the importance of this early design step in selecting the correct combination of mission, technologies and configuration to meet current aerospace challenges. Overarching goal is to avoid the reoccurring situation of optimizing an already ill-fated solution.

TABLE OF CONTENTS

ACKNOWLEDGMENTS.....	iii
ABSTRACT	v
LIST OF ILLUSTRATIONS.....	ix
LIST OF TABLES	xiii
NOMENCLATURE	xv
 Chapter	 Page
1. INTRODUCTION.....	1
2. LITERATURE REVIEW AND RESEARCH OBJECTIVES	8
2.1 Parametric Sizing	13
2.2 Configuration Layout	33
2.3 Configuration Evaluation	36
2.3 Research Objectives	42
2.4 Research Approach	44
2.5 Research Contribution Summary	47
3. CONCEPTUAL DESIGN PROCESS AND DELIVERABLES LIBRARY	48
3.1 Conceptual Design Processes Library	51
3.2 Disciplinary Methods Library Description	61
3.3 Contribution Summary	69
4. PARAMETRIC SIZING PROCESS AVD ^{SIZING} DESCRIPTION	71
4.1 Weight and Volume budget description	73

4.2 Trajectory and Constraint analysis.....	75
4.3 Geometry Module.....	81
4.4 Convergence Logic	93
4.4 Iteration of the slenderness parameter τ	95
4.5 Contribution Summary	97
5. TRANSONIC TRANSPORT CASE STUDIES	99
5.1 Summary of Results for TAC Transonic Transport Studies.....	100
5.2 Summary of Proposed Blended Wing Body Transonic Transport	114
5.3 Summary of Proposed Strut-Braced NLF Transonic Transport.....	119
5.4 Summary of Transonic Transport Studies	130
6. HIGH-SPEED COMMERCIAL TRANSPORT STUDIES	133
6.1 Summary of SSBJ Study Results Based on the LearJet 24 Airframe	134
6.2 Summary of Sanger EHTV and LAPCAT II Hypersonic Cruise Vehicle Studies..	147
6.3 Summary of Results and Contribution Summary.....	166
7. CONCLUSIONS AND SUMMARY OF CONTRIBUTIONS.....	168
Appendix	
A. AIRCRAFT CONCEPTUAL DESIGN PROCESS LIBRARY.....	175
B. EXCERPTS FROM PARAMETRIC SIZING METHODS LIBRARY	246
C. EXAMPLE AVDSIZNG INPUT FILE: B777-300ER MODEL.....	389
REFERENCES.....	420
BIOGRAPHICAL INFORMATION	427

LIST OF ILLUSTRATIONS

Figure	Page
1-1: Conventional aerospace vehicles.	1
1-2: Conceptual design compares alternative solutions in terms of cost, risk and benefit.....	2
1-3: Space tourism and hypersonic point-to-point solution concepts.	3
1-4: Aerospace Vehicle Design Process.....	5
1-5: Current state-of-the-art rest with preliminary and detail design phases of the Product Life-Cycle.	6
2-1: Conceptual design compares alternative solutions in terms of mission and the designs objective function.	8
2-2: Fundamental steps to aerospace vehicle conceptual Design.	12
2-3: Examples of weight estimation methods used in 'by-hand' and computer based sizing processes	17
2-4: Examples of trajectory analysis methods used in 'by-hand' and computer based sizing processes	18
2-5: Classical performance constraint diagram.....	20
2-6: Converged performance constraint carpet plot. The 2 nd segment climb and constrains have been omitted.....	21
2-7: Aspect ratio trade (AR) shown through 3 converged performance constraint carpet plots	22
2-8: General aircraft sizing process with fundamental steps high-lighted. This is the fundamental logic used in systems such as FLOPS, ANSYNT, and ASAP.....	23
2-9: Simplified sizing process, Roskam: Preliminary Sizing.	24
2-10: Comparison of the integration subsonic/supersonic and hypersonic aircraft	26
2-11: Hypersonic convergence sizing logic.	27
2-12: Explanation of Küchemann slenderness parameter.	28

2-13: Hypersonic Convergence sizing diagram illustrating the converged solution contour. The sizing problem is reduced to a single curve for hypersonic aircraft through including converging weight and volume.	29
2-14: Example Response Surface Equations demonstrating design sensitivities	31
2-15: Typical Procedure for Configuration Layout	33
2-16: Examples of Aircraft Specific Configuration Layout Software	35
2-17: Comparison of the 'By-hand' configuration evaluation methods from Roskam with the 'Computer-based' system PrADO	38
2-18: PrADO Execution, DMS and Disciplinary analysis modules	39
2-19: PrADO Visualization Capabilities.....	40
2-20: Examples of various applications of PrADO	41
2-21: Examples of AVD Lab Conceptual Design Studies	43
2-22: Summary of PhD. Research Approach.....	45
3-1: AVD 'Standard to Design'	48
3-2: Coupling of process, deliverables and methods library.	50
3-3: Loftin Aircraft Design Process.....	54
3-4: Comparison of Hypersonic Convergence and Classical Sizing Process.....	59
3-5: Fundamental AVD ^{sizing} Logic.	60
3-6: Comparison of Howe's semi-empirical wing weight method to the empirical General Dynamics methods(trade-study via AVD ^{sizing}).....	66
3-7: Development of trend data for strut and trust braced wings based on past experience with low-speed strut aircraft and Initial VPI FEM structural design study.....	68
4-1: Fundamental AVD ^{sizing} Logic.	72
4-2: Weight and balance convergence.....	73
4-3: Trajectory and constraint analysis.	76
4-4: For the given iteration the W/S is known and thus the maximum T/W required is computed from the performance constraints.	77
4-5: Illustration of drag polar location exponent $m^{(82)}$	78

4-6: Geometry Module.....	81
4-7: Modified Tail Volume Quotient.....	83
4-8: SBW/TBW Geometry Definition.....	84
4-9: Definition of the planform of a generic blending wing body.....	85
4-10: Definition of outer wing.....	87
4-11: Definition of the volume of an irregular prism.....	87
4-12: Assumed thickness distribution.....	90
4-13: Example delta wing planforms with various base areas.....	91
4-14: Example Propulsion Integrated Hypersonic Cruisers/Accelerators.....	91
4-15: Convergence of S_{pin} , and Weight.....	93
4-16: TOGW and S_{pin} , converges solution for a single value of τ	94
4-17: For each point a fully converged data set is compiled.....	95
4-18: Varying τ yields the simplified solutions space in terms of TOGW and S_{pin} . The grey area is the area for which the landing wing load constraint is no longer satisfied.....	96
4-19: Through trading AR three solutions curves are produced. The AR 9 wing provides a balance between fuel weight savings and maintenance costs.....	97
5-1: Modifications of the B777-300ER towards a TVC transport. The thrust vector control results in a significant reduction of both empty weight and aerodynamic efficiency.....	111
5-2: The Blended wing body has a compound cranked all-wing planform geometry allowing for increased cabin thickness relative to the remainder of the wing.....	114
5-3: Example TBW concepts for transonic flight incorporating natural laminar flow.....	119
5-4: Transitional Reynolds number for a NLF wing as determined from the F-14 wing glove experiment.....	122
5-5: Varying wing sweep and solving for wing area, aspect ratio and wing thickness demonstrates that NLF SBW benefits from higher sweep angles due to the high cruise Mach number.....	123
5-6: Percent change for the SBW relative to a cantilevered wing via the VPI, Analytic and Empirical Models.....	128

6-1: Size comparison of the LearJet 24 and Sukhoi Su-21 SSBJ	134
6-2: Drag components that constitute total supersonic drag and Mach 2, $C_L=0.1$	137
6-3: Possible engine installations for the SpiritLear SSBJ.....	138
6-4: Geometry results for the 4 primary trade-studies	141
6-5: Geometry results for the 4 primary trade-studies	142
6-6: Sanger II is a proposed hypersonic cruiser based on the first stage of the Sanger TSTO launch system	147
6-7: LAPCAT program proposed Hypersonic Cruiser Designs.....	148
6-8: Overall propulsion efficiency and aerodynamic efficiency as Mach number increases	150
6-9: Kuchemann diagram demonstrating the optimum range normalized to global range as a function of Mach number and vehicle slenderness, (s/l).....	150
6-10: Recreation of Kuchemann’s solution-space topography, demonstrating examples of existing supersonic aircraft (note: in Figure 5-5 Mach number is on a logarithmic scale).	151
6-11: Reduction in overpressure on ground due to increase cruise altitude and Mach possible for a Mach 4.4 cruiser relative to Mach 2 or 3 aircraft.....	152
6-12: For 7,000 to 10,000 km design ranges little time savings is achieved for design speeds past Mach 4.5	153
6-13: Mach 4.4 demonstrates an operational optimum in terms of flights per day and km per day	154
6-14: Nominal trajectory for the hypersonic cruise aircraft.....	156
6-15: Selected Configurations for the Sanger EHTV and LAPCAT II missions along with explanation of Kuchemann’s τ correlation parameter.	157
6-16: Selected Structural Indices for the Sanger EHTV and LAPCAT II Missions.	158
6-17: HYCAT turbo-ramjet propulsion system model used for the AVD ^{sizing} Sanger II model.	159
6-18: ONERA ejector ramjet performance chart	160
6-19: Sanger II design space for two structural indices.	161
6-20: LAPCAT 8 M, 18,000 km blended-body compared to Sanger II 4.4 M, 10,500 km wing-body reference vehicle.	163

LIST OF TABLES

Table	Page
2-1: 'By-Hand' conceptual design texts and course material	10
2-2: Selected 'Computer-Integrated' conceptual design synthesis systems.....	11
2-3: Classical Performance Constraints for Subsonic Transport Aircraft.....	19
2-4: Further advancements to the classical sizing logic.....	30
3-1: Representative 'By-Hand' conceptual design processes.....	52
3-2: Representative 'Computer-Integrated' conceptual design processes	52
3-3: NS Flow Chart Definitions	53
3-4: Process overview card	56
3-5: Example missions and configurations which do not necessarily conform to the classical aircraft sizing logic	58
3-6: Example Methods Overview Card	63
4-1: Weight and Volume Budget Terms from Hypersonic Convergence	74
4-2: Trajectory options in MISSION	79
4-3: Wing Definition for Transonic Transports	82
4-4: Fuselage definition for transonic transports.....	83
4-5: Typical shape factors for geometric shapes	88
4-6: Planform definitions for the blended wing body	89
5-1: TAC Transport Validation Case Studies Mission Summary	101
5-2: Sizing Objective Direct Operating Cost Weight Factors	102
5-3: Sizing design variables and aircraft definition.....	103
5-4: Summary of TAC Transonic Transport Validation Studies	104
5-5: Summary of Composite B777-300ER Study	107

5-6: Summary of Composite B737-800 Study.....	109
5-7: TAC Transport Validation Case Studies Mission Summary	115
5-8: TAC Transport Validation Case Studies Mission Summary	116
5-9: TAC Transport Validation Case Studies Mission Summary	120
5-10: Sizing design variables and resulting aircraft definition.....	124
5-11: Comparison of VPI results to AVD ^{sizing}	125
5-12: Comparison of VPI Results to AVD ^{sizing}	127
6-1: Comparison of Selected SSBJ Projects.....	135
6-2: Design Missions for the SpritLear SSBJ	136
6-3: Summary of SSBJ Comparison Study	139
6-4: Summary of LearJet 24-Constrained SSBJ	140
6-5: Comparison sizing results for the of Selected SSBJ Projects	144
6-6: Sanger II Hypersonic Transport Validation Case Mission Summary	154
6-7: LAPCAT II Mach 8 Mission Summary.....	155
6-8: Sanger Hypersonic Transport Validation Summary.....	162

NOMENCLATURE

Symbol	DESCRIPTION
AR	Aspect ratio
b	Wing span
c	Chord length
\bar{c}	Mean aerodynamic chord
C_D	Drag coefficient
C_L	Lift coefficient
C_{Lmax}	Maximum lift coefficient
c_r	Root Chord
c_{sr}	Strut root chord
c_{st}	Strut tip chord
c_t	Tip Chord
c_{tr}	Truss member chord
c_{sys}	Fixed systems weight
D_{max}	Fuselage maximum diameter
e	Oswald's efficiency factor
E_{TW}	Engine thrust to weight ratio
ff	Fuel fraction, $W_{fuel}/TOGW$
f_{sys}	Ratio of systems weight to OEW
h/w	Fuselage cabin height to width ratio
h_{cab}	Cabin height

h_{fus}	Fuselage height
I_{str}	Structural index
k_{crw}	Crew volume coefficient
k_{sf}	Irregular prism shape factor
k_w	Ratio of wetted area to planform area
k_{ve}	Engine volume coefficient
k_{vs}	Systems volume coefficient
k_{vv}	Void volume coefficient
L'	induced drag factor, $1/(\pi A R e)$
l/d	Fuselage length to diameter ratio
L/D	Lift to drag ratio, aerodynamic efficiency
l_{fus}	Length of the fuselage
m	Drag polar location, C_L^m/C_D
M	Mach number
M_{cr}	Critical Mach number
N	Number of engines
N_{crew}	Number of crew members
OEW	Operating empty weight, $TOGW - W_{fuel} - W_{pay}$
OWE	Operating weight empty, $OEW + WW_{pay}$
q	Dynamic pressure
S	Planform or reference area
s/l	Wing semi-span divided by vehicle length
SFC	Specific fuel consumption
S_{LF}	Landing field length
S_{pln}	Planform area

S_{ref}	Reference area
S_{TOFL}	Take-off field length
S_{wet}	Wetted area
T	Thrust
t/c	Airfoil thickness to chord ratio
T/W	Thrust loading
T/W_{eng}	Engine thrust to weight ratio
t_{climb}	Time to climb
$TOGW$	Take-off Gross Weight
V	Velocity
V_{crew}	Crew volume
V_{eng}	Engine volume
V_{fuel}	Fuel volume
V_{HT}	Volume quotient, horizontal tail
V_{pay}	Payload volume
V_{sys}	Systems volume
V_{total}	Total vehicle volume
V_{wing}	Wing volume
V_{void}	Void volume
V_{VT}	Volume quotient, vertical tail
R	Range
W/S	Wing loading
W_{ai}	Air induction system weight
W_{api}	Air-conditioning, pressurization and electronics weight
W_{apu}	Auxiliary power unit weight

W_{aux}	Auxiliary gear weight
W_{arm}	Armaments weight
W_{bal}	Ballast weight
W_{bc}	Baggage handling equipment weight
W_{cprv}	Crew provisions weight
W_{crw}	Crew weight
W_{emp}	Empennage structural weight
W_{eng}	Engine weight
W_{els}	Electrical system weight
W_{etc}	Extra items weight
W_f	Fuselage structural weight
W_{fc}	Flight control system weight
W_{feq}	Fixed equipment weight
w_{fus}	Width of the fuselage
W_{fuel}	Fuel weight
W_{fur}	Furnishing's weight
W_{fs}	Fuel systems weight
W_{glw}	Guns launchers and weapons provisions
W_{hps}	Hydraulic and pneumatic system weight
W_{iae}	Instrumentation, avionics and electronics weight
W_{ops}	Operational items weight
W_{ox}	Oxygen system weight
W_p	Propeller weight
W_{pay}	Payload weight
W_{prop}	Propulsion systems weight

W_{pt}	Paint weight
W_{pwr}	Powerplant weight
WR	Weight ratio, $TOGW/OWE$
W_{str}	Structural weight
W_W	Wing structural weight
x/c	Ratio of cabin length to airfoil length

Acronyms	DESCRIPTION
AVD	Aerospace Vehicle Design
BWB	Blended Wing Body
CAD	Computer Aided Design
CCV	Control Configured Vehicle
CFD	Computation Fluid Dynamics
CGR	Climb gradient
DMS	Database Management System
DOC	Direct Operating Cost
DOC_{fly}	Flying direct operating cost
DOC_{maint}	Maintenance direct operating cost
DOC_{dep}	Depreciation direct operating cost
DOC_{LNTF}	Landing, navigation and taxi fees direct operating cost
EHTV	European Hypersonic Transport Vehicle
ESA	European Space Agency
FEM	Finite Element Method
FWC	Flying Wing Configuration
GUI	Graphical User Interface

KBS	Knowledge Based System
LAPCAT	Long-term Advanced Propulsion Concepts and Technologies
LaRC	Langley Research Center
LM	Lockheed-Martin
MDA	Multi-Disciplinary Analysis
MDO	Multi-Disciplinary Optimization
ML	Methods Library
MLW	Maximum landing weight
NASA	National Aeronautics and Space Administration
NIA	National Institute of Aeronautics
NLF	Natural Laminar Flow
NS	Nassi-Schneiderman flow diagram
OEI	One-engine Inoperable
OFWC	Oblique Flying Wing Configuration
PL	Process Library
SAI	Supersonic Aerospace International
SBW	Strut-Braced Wing
SM	Static margin
SSBJ	Supersonic Business Jet
TAC	Tail-aft Configuration
TBO	Time between overhauls
TBW	Truss-Braced Wing
TFC	Tail-first Configuration
TVC	Thrust Vector Control

VAC	Vought Aerospace Company
VPI	Virginia Polytechnic Institute

Subscript	DESCRIPTION
<i>b</i>	Blended wing section
<i>c</i>	Cruise, cabin
<i>c/4</i>	Quarter chord
<i>c/2</i>	Half chord
<i>cab</i>	Cabin
<i>flap</i>	Flap, high-lift device
<i>h</i>	Horizontal tail
<i>LE</i>	Leading edge
<i>TE</i>	Landing gear
max	Maximum
<i>r</i>	Root
<i>SL</i>	Sea-Level
<i>TE</i>	Trailing edge
<i>TO</i>	Take-off
<i>w</i>	Wing
<i>wi</i>	Wing inboard
<i>wo</i>	Wing outboard

Greek Symbols	DESCRIPTION
β	Supersonic Compressibility factor, $\sqrt{M^2 - 1}$
Δ	Increment

η	Strut-wing intersection point, percent span
λ	Tapper Ratio
Λ	Sweep angle
μ_a	OEW margin
ρ	Density
ρ_{pay}	Payload weight
ρ_{ppl}	Propellant weight
σ	Ratio of Density at current altitude to sea-level
τ	Kuchemann slenderness parameter, $V_{total}/S_{pln}^{1.5}$

CHAPTER 1
INTRODUCTION

Aerospace is a maturing industry with successful and refined baseline products (tail-aft commercial transports, expendable launchers, see Figure 1-1). Therefore, any improvement to these products requires extensive research and development (R&D) with an increase in the products risk. For example, the tail-aft configuration is typically selected for commercial transports not because it promises the best performance for a mission, but because it offers a better balance of risk and reward. Since companies have to generate profit in a highly competitive environment, a compelling performance improvement case would be required to offset the risk in selecting an unconventional solution.



Fig 1-1: Conventional aerospace vehicles.

While the above situation is the norm, several projects and programs have proposed radical departures in configuration with limited success (Figure 1-2). For most of these cases the performance improvements have been promising; however, the risk involved with these

aircraft resulted in decision makers to eventually opting for more proven concept. In a highly competitive, expensive and mature industry, why would one risk the future of a company on such risky endeavors? With established products and high risk of unconventional solutions it stands to reason that the industry would stay conservative.



Fig 1-2: Conceptual design compares alternative solutions in terms of cost, risk and benefit (pictures via NASA, Aviation Weekly, and Scaled Composites)

This conservative nature has led many decision makers to opt for derivative development, as seen by the B737, B747, B-52, F-16, F-18, F-15 product lines which have been in operation for the past 60 to 30 years. By selecting a proven vehicle and applying moderate modification the risk and cost of the products is reduced ⁽¹⁾, even though it may not perform as well as an aircraft which is specifically designed for the mission. The move to increased derivative development is logical, for product improvement if original design mission and markets have not dramatically changed.

However, in the case of unconventional design missions (such as space tourism ⁽²⁾) and radical changes regulation (CO₂ reduction) or economic environment (energy costs) the classical paradigm, which leads to the conventional solution, is no longer valid.

For example, if fuel costs permanently increase, either by environmental regulation or oil scarcity, design solutions which promise reduced fuel burn could challenge current paradigms. Even the classical transonic transport must re-evaluate the effects of higher risk technologies such as Natural Laminar Flow (NLF) ⁽³⁾, control configured vehicles (CCV) ⁽⁴⁾ or unique propulsion system integrations such as distributed propulsion ⁽⁵⁾, which now may be required to meet the economic environment. In this situation it may even be required to re-evaluate the design mission, reducing the cruise velocity in order to gain greater fuel efficiency. Such a situation changes the previous balance between risk, cost and reward.

The current case for commercial space flight, tourism and point to point hypersonic transportation represents a non-mature industry which does not yet have a clear and accepted solution, see Figure 1-3.

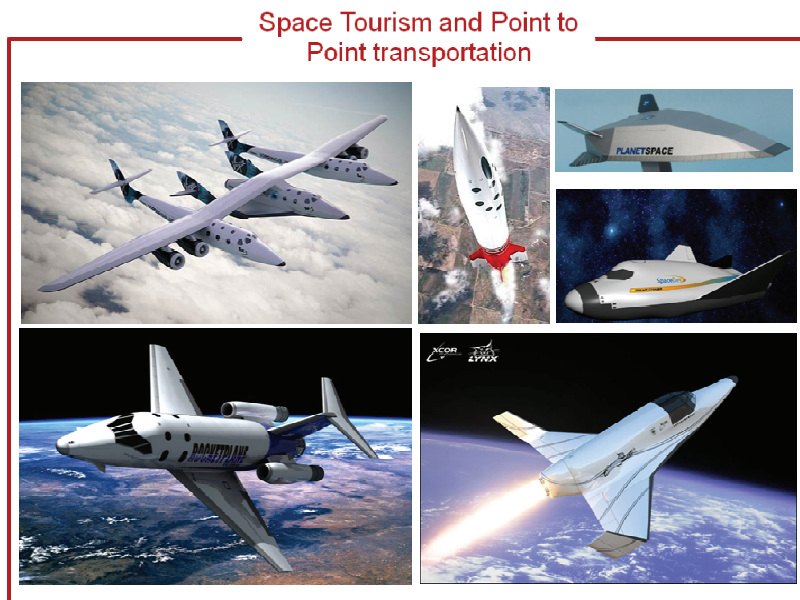


Fig 1-3: Space tourism and hypersonic point-to-point solution concepts (pictures, via space.com).

Significant change in design mission, or economic environment require the designer to re reexamining the classical paradigms and compare conventional and unconventional

solutions. Begging the question, “How to compare novel and classical configurations for new design objectives, constraints and missions?”

The design process

This situation of established baseline solutions and derivative development has created an interesting situation in aerospace vehicle design conceptual design. The need to develop better and better solutions for a well established markets and missions has design environments to trade rapid lower order design tools for more involved higher order design tools. This can be seen in the current torrent of work in conceptual design Multi-Disciplinary Optimization (MDO) ⁽⁵⁾ ⁽⁶⁾. The majority of these studies collect higher order CFD, FEM and simulation tools to optimize the vehicle for a given mission. In addition these studies assume the mission, configuration and technology level given and fixed. Little or no attempt is made to compare different solutions of variation in the problem, but rather the focus is on optimizing one solution.

When exploring this trend in the context of the design process it appears that what is being called conceptual design is really preliminary design with the conceptual design being performed through intuition. Figure 1-4 illustrates the fundamental aerospace design process.

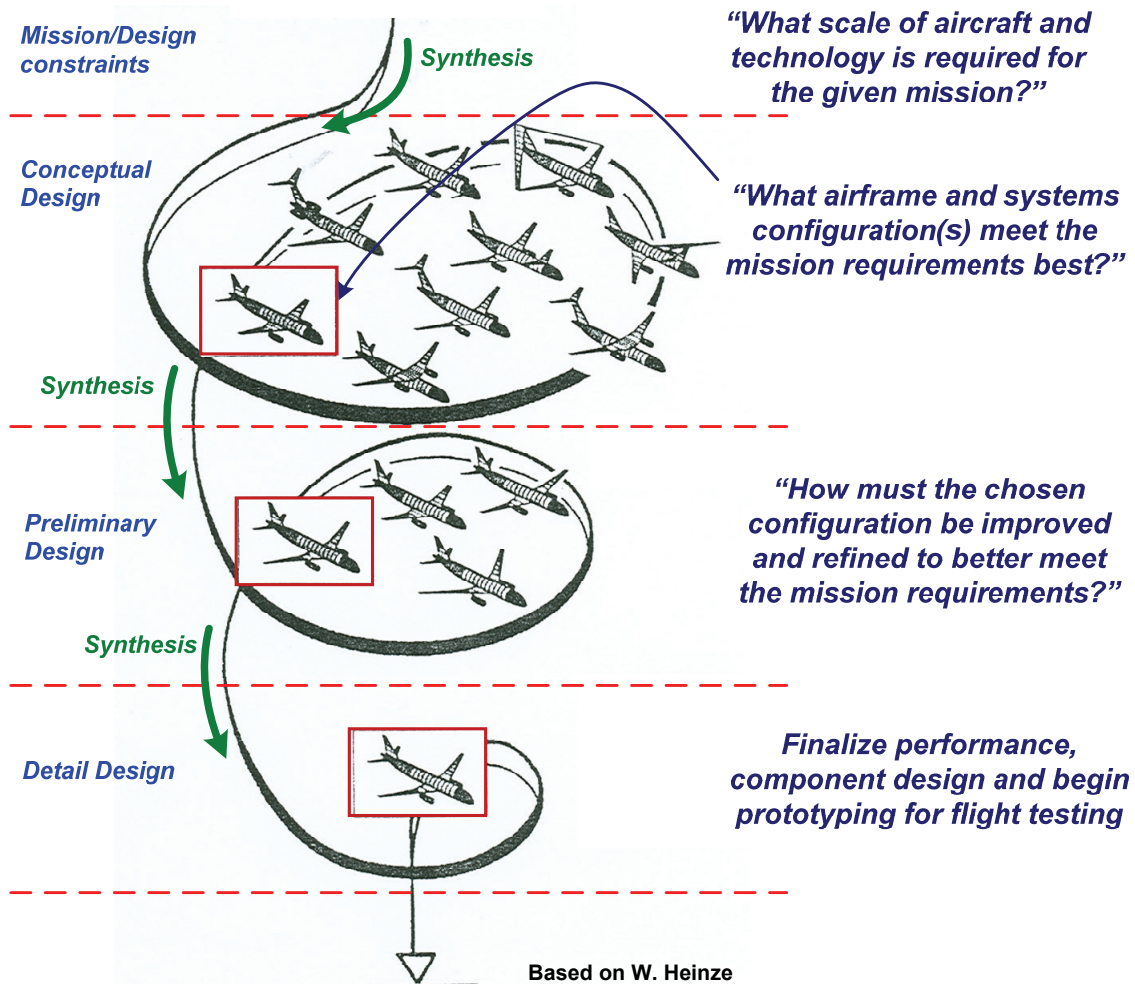


Fig 1-4: Aerospace Vehicle Design Process⁽⁷⁾

In this context, most MDO studies skip the solution space screening phase and begin by refining a specific solution concept. This type of approach may work for derivative development of vehicles for established markets but will most likely fail in an ill-conceived initial solution is selected, such as the LACPAT II Mach 8 cruiser (see Chapter 6).

This situation of developing higher order analysis tools for conceptual design and not focusing on clear and rapid comparison of various solutions has lead to the following level of understanding the aerospace design process as seen through the product life cycle (Figure 1-5

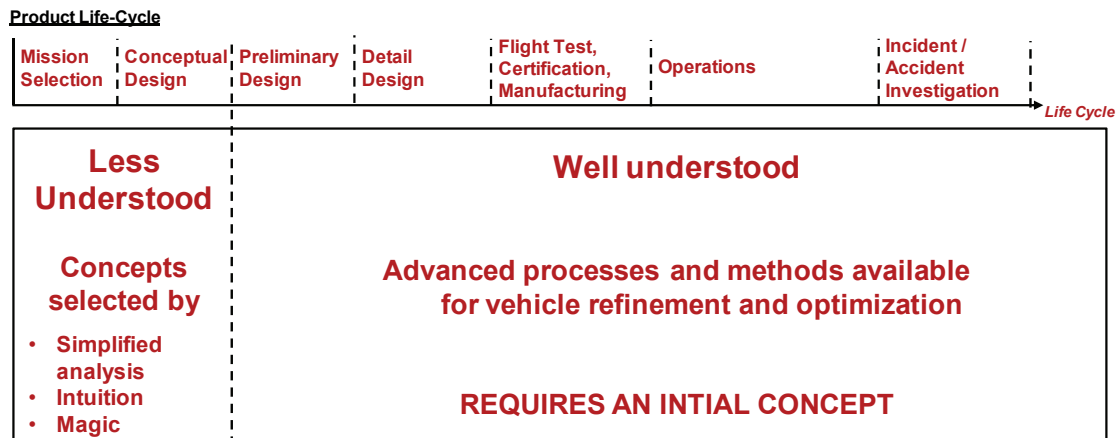


Fig 1-5: Current state-of-the-art rest with preliminary and detail design phases of the Product Life-Cycle.

The trend of increasing the refinement capability of the design process has led to a high level of understanding in preliminary design optimization and refinement⁽⁸⁾ with a neglect of how to screen and compare a large variety of solutions during conceptual design. This is not to say that high-fidelity modeling is not a useful tool. It simply increases the analysis time per top-level trade-study that the decision-maker needs to see. Thus, reducing the number and variety of options evaluated. This situation refines the previously posed question of how to compare novel and unconventional solutions to, ***“How to increase the capability and proficiency of the conceptual design phase where gross configuration, technologies and mission sensitivities are not pre determined?”***

Simply increasing the order (or fidelity) of conceptual design tools is not sufficient. The increase in input requirements and engineering time to execute higher order methods prohibits exploring a wide variety of solutions for novel designs in the time typically allotted for conceptual design. Clearly, the conceptual design phase is crucial to explore new design missions and technologies under existing and new objectives since the designer does not yet have the experience to predetermine the correct design solution space.

Therefore, the general objective of the current research undertaking is to revisit the classical approach to aerospace conceptual design and advance the state-of-the-art through increasing the flexibility and applicability of conceptual design processes and methods for novel design missions and configurations.

It is required that the conceptual designer be able to visualize and explain the solutions space topography in a meaningful way to the decision-maker. The fundamental challenge of provided time sensitive, meaningful solution recommendations and their associated risks is paramount to providing a single design solution.

CHAPTER 2

LITERATURE REVIEW AND RESEARCH OBJECTIVES

Aircraft conceptual design consists of (1) *running trade-studies* (2) *comparing the cost and benefits of each trade* and (3) *selecting the best overall aircraft for the mission* (Figure 2-1). The challenge for the conceptual designers is to conduct trade studies resulting in the correct solution space identification for typical conceptual design time slots available. Thus, ***the ultimate goal of the conceptual design is to select the combination of airframe and systems configuration which show the most promise for further refinement.***

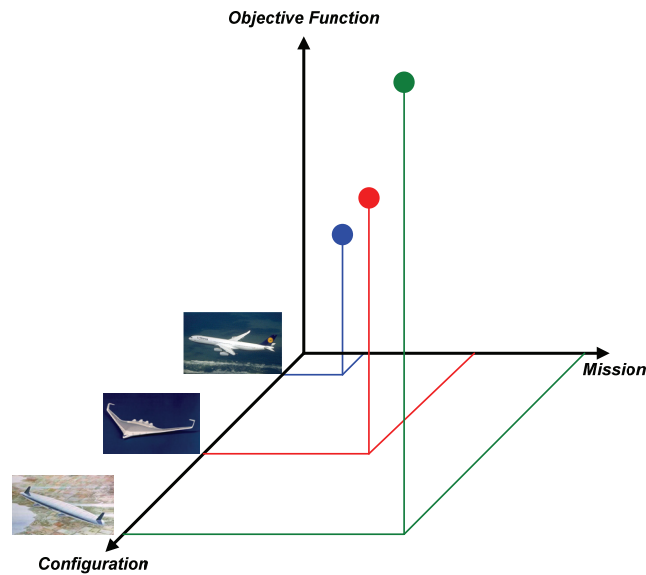


Fig 2-1: Conceptual design compares alternative solutions in terms of mission and the designs objective function.

When examining the conceptual design phase the first question to answer is “*how is the conceptual design trade-studies defined, organized and executed?*” Every aerospace

organization has its own method of executing a conceptual design, the details of which are typically kept proprietary. However, there is a wealth of examples in the public domain in the form of educational text books, short course notes, design code user's guides and papers which address this question. These references typical present the process established to execute conceptual design trade-studies with simple methods to compute the weight, aerodynamic, performance, etc. Table 2-1 lists the design texts and short courses reviewed and Table 2-2 lists the computer based processes reviewed. In addition to typical public domain sources this review also includes international and industrial reference providing a broad view of aircraft conceptual design.

The computer based-review is an expansion of the work done by Chudoba ⁽⁹⁾ and Huang ⁽¹⁰⁾. The computer based references are ones which possess adequate documentation of the process and/or methods utilized. The complete list of design synthesis systems explored by Chudoba and Xiao is included in the Process Library, Appendix A.

Table 2-1: 'By-Hand' conceptual design texts and course material

Reference	Year	Text/Course	Title
Warner (11)	1936	Text	Airplane Design - Performance
Wood (12)	1963	Text	Aerospace Vehicle Design Vol. 1, Aircraft Design
Brunk (13)	-	Notes	Handbook for Preliminary Design Engineers
Louthan (14)	1961	(VAC) Notes	Parametric Airplane Design and Sizing
Corning (15)	1979	Text	Supersonic and Subsonic, CTOL and VTOL, Airplane Design
Loftin (16)	1980	Text	Subsonic Aircraft: Evolution and the Matching of Size to Performance
Kossira (17)	1981	Course	Aircraft Design, Parts I-II
Torenbeek (18)	1982	Text	Synthesis of Subsonic Airplane Design
Stinton (19)	1983	Text	The Design of the Aeroplane
Nicolai (20)	1984	Text	Fundamentals of Aircraft Design
Renner (21)	1984	Course	Aircraft Design, Parts I-II
Hienemann (22)	1985	Text	Aircraft Design
Roskam (23)	1985	Text	Airplane Design, Parts I-VIII
Whitford (24)	1987	Text	Design for Air Combat
Shevell (25)	1989	Text	Fundamentals of Flight
Czysz (26)	1994	Course	Flight Vehicle Analysis and Design
Madelung (27)	1994	Course	Aeronautics, Parts I-II
Fielding (28)	1994	Text	Introduction to Aircraft Design
Huenecke (29)	1998	Text	Modern Combat Aircraft Design
Stinton (19)	1998	Text	The Anatomy of the Airplane
Kroo (30)	1998	Course	Introduction to Aircraft Design: Synthesis and Analysis
Scholz (31)	1999	Course	Aircraft Design
Thomas (32)	1999	Text	Fundamentals of Sailplane Design
Jenkinson (33)	1999	Text	Civil Aircraft Design
Heinze (34)	1999	Course	Aircraft Design, Parts I-II
Whitford (35)	2000	Text	Fundamentals of Fighter Design
Howe (36)	2000	Text	Aircraft Conceptual Design Synthesis
Schaufele (37)	2000	Text	The Elements of Aircraft Preliminary Design
Schaufele (38)	2003	Course	Aircraft Preliminary Design and Performance
Voit-Nitschmann (39)	2001	Course	Introduction to Aeronautics
Thorbeck (40)	2001	Course	Aircraft Design Parts I-II
Mason (41)	2002	Course	Airplane Design
Corke (42)	2003	Text	Airplane Design
Raymer (43)	2006	Text	Aircraft Design: A Conceptual Approach

Table 2-2: Selected 'Computer-Integrated' conceptual design synthesis systems

System	Full Name	Developer	Primary Application	Years
AAA (44)	Advanced Airplane Analysis	DARcorporation	Aircraft	1991-
ACES (45)	Aircraft Configuration Expert System	Aeritalia	Aircraft	1989-
ASAP (46)	Aircraft Synthesis and Analysis Program	Vought Aeronautics Company	Fighter Aircraft	1974
ACSYNT (47)	AirCRAFT SYNTHeSis	NASA	Aircraft	1987-1997
CASDAT (48)	Conceptual Aerospace Systems Design and Analysis Toolkit	Georgia Institute of Technology	Conceptual Aerospace Systems	late 1995
CPDS (49)	Computerized Preliminary Design System	The Boeing Company	Transonic Transport Aircraft	1972
DSP (50)	Decision Support Problem	University of Houston	Aircraft	1987
FLOPS (51)	Flight Optimization System	NASA Langley Research Center	?	1980s-
ICADS (52)	Interactive Computerized Aircraft Design System	Delft University of Technology	Aircraft	1996
MAVRIS (53)	an analysis-based environment	Georgia Institute of Technology		2000
MIDAS (54)	Multi-Disciplinary Integrated Design Analysis & Sizing	DaimlerChrysler Military	Aircraft	1996
NEURAL NETWORK FORMULATION (55)	Optimization method for Aircraft Design	Georgia Institute of Technology	Aircraft	1998
PACELAB (56)	knowledge based software solutions	PACE	Aircraft	2000
PASS (57)	Program for Aircraft Synthesis Studies	Stanford University	Aircraft	1988
PIANO (58)	Project Interactive Analysis and Optimization	Lissys Limited	Transonic Transport Aircraft	1980-
PrADO (7)	Preliminary Aircraft Design and Optimization	Technical University Braunschweig	Aircraft and Aerospace Vehicle	1986-
RDS (59)	(-)	Conceptual Research Corporation	Aircraft	1992
SYNAC (60)	SYNthesis of AirCRAFT	General Dynamics	Aircraft	1967
TASOP (61)	Transport Aircraft Synthesis and Optimization Program	BAe (Commercial Aircraft) LTD	Transonic Transport Aircraft	
TRANSYN (62)	TRANsport SYNthesis	NASA Ames Research Center	Transonic Transport Aircraft	1963- (25years)
TsAGI (63)	Dialog System for Preliminary Design	TsAGI	Transonic Transport Aircraft	1975
VDK/HC (64)	VDK/Hypersonic convergence	MacDonnell Douglas, Hypertec	SAV/Hypersonic Cruise	

When cross-referencing 'by-hand' and 'computer integrated' processes one sees clear patterns. Primarily, that the conceptual design phase may be broken down into 3 distinct steps (1) Parametric sizing, (2) Configuration Layout, and (3) Configuration Evaluation. (Figure 2-3)

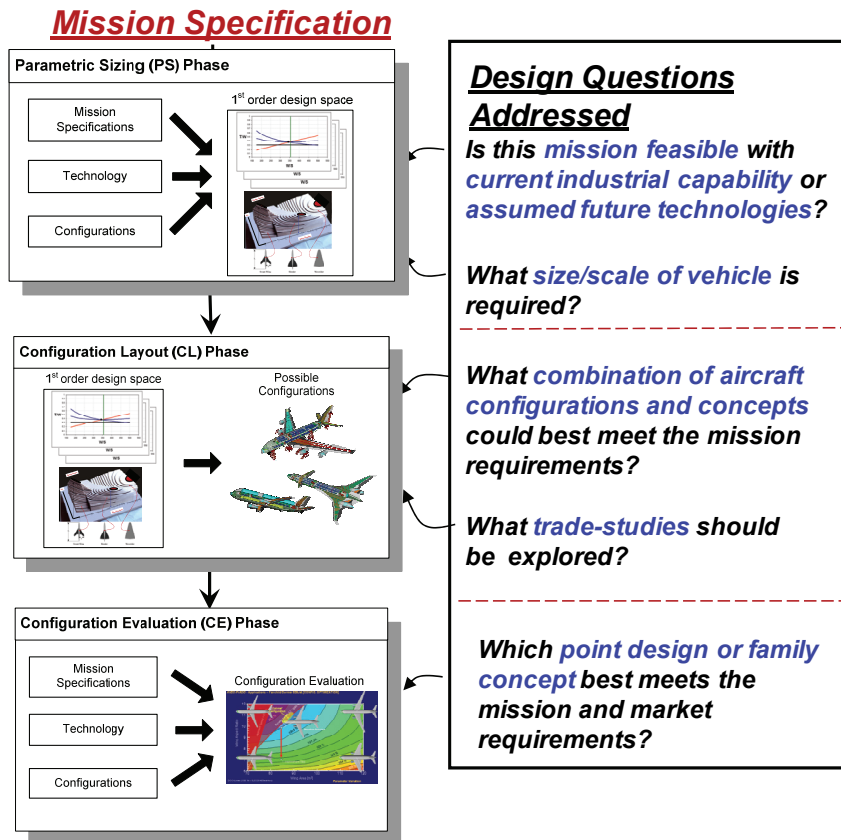


Fig 2-2: Fundamental steps to aerospace vehicle conceptual Design.

1. **Parametric Sizing** – The 1st order visualization of the solution space based on empirical data and reduced order models. Answers the questions; *is the mission feasible with current industrial capability? What, if any, new industrial capability is required? What is the scale of the aircraft required to complete the mission (S, AR, TOGW, etc)?* Typically considered the 1st step in conceptual design.

2. **Configuration Layout** – Integration and initial layout of the major aircraft components (i.e., wing, fuselage, propulsion system, empennage, etc.) in according to the parametric sizing results. The primary function is to fill in design details required for configuration evaluation, which are not explicitly required for parametric sizing. These features are then evaluated and traded during configuration evaluation.

3. **Conceptual Design Evaluation** – multi-disciplinary evaluation of integrated aircraft concepts. Answers the question: *which concept best meets the mission requirements?*

Before beginning the discussion and break-down of the phase of conceptual design some definitions are required. First, sizing processes explored can be categorized into two categories:

1. **'By-Hand' design processes** – Processes which the integration task is performed in a manual fashion. Consisting of design text books and short courses which reflect the classical method of disintegrated conceptual design.
2. **'Computer-Integrated' design Processes** – Processes which the integration task is performed in an automated fashion. Consisting of computer integrated design processes (i.e. disciplinary analysis is completed and pasted internally through the process).

This literature review will explore conceptual design for each of these steps to identify the current state of the art and potential for advancement during the current research. From this review to detail research objectives are derived.

2.1 Parametric Sizing

Parametric Sizing is the first step of the design process after the mission has been defined. This step serves to establish the 1st order solution space for the mission and gives the designer an idea related to the gross geometry, weight and cost of performing the mission. In

this step the designer begins with the (1) fixed mission, (2) gross configurations concepts and (3) disciplinary technology assumptions. Sizing allows for 1st order trading of these concepts and technologies.

Parametric sizing is the vital first step of any new aircraft project to gain both a 1st order understanding of the multidisciplinary effects of a new technologies and/or unconventional configurations. This step serves to justify the technology/configuration through demonstrating its multi-disciplinary potential, but also helps understanding the risk and cost involved in the project. With a well calibrated and flexible parametric sizing tool-box, designers can quickly screen configurations and technologies which warrant further conceptual design work.

In this review both the 'By-Hand' and 'Computer Based' design processes are compared and contrasted. Demonstrating the current state-of-the-art and allowing for identification of opportunities for advancement.

During this review it has been found that both 'By-hand' and 'Computer-Based' process share the same 6 fundamental elements which make-up the sizing process.

1. **Operating Empty Weight (OEW) estimation** – Based on the given or currently iterated geometry, payload weight and *TOGW*. This represents the vehicle structural, systems, operational items and propulsion system weight.
2. **Trajectory analysis (fuel weight estimation)** – Based on the required range and endurance requirements, the fuel weight is estimated. This step relies heavily on aerodynamic and propulsion disciplinary methods. In most 'by-hand' approaches these come from assumed values or highly simplified methods. In contrast computation tools tend to be semi-empirical in nature, requiring additional geometry input.
3. **Convergence logic** – In its simplest form, convergence is the method of solving the implicit function formed by the *OEW* estimation and Trajectory analysis. These two steps are fundamentally linked either by geometry (driving both aerodynamic and

structural weight) and *TOGW* (driving both fuel weight and structural loading). By holding the geometry constant one can solve this combined system iterative. Typically, geometry is held constant and an initial assumption of *TOGW* is made. *TOGW* is then iterated until the solution converges. Some 'By-hand' approaches reformulate this problem into an explicit function with simplified weight, aerodynamic and propulsion methods, thus eliminating the need for iteration.

4. **Constraint analysis** – From the mission and operational requirements such as take-off field length, maximum cruise speed, approach speed, OEI climb, etc., the required wing loading (W/S) and thrust loading (T/W) (or horsepower loading) are computed. Aerodynamic and propulsion disciplinary and performance estimation methods are required. These take the form of design constraints which provide boundaries for wing area and maximum sea-level thrust. In some cases wing fuel volume is included as a design constraint.
5. **Sizing logic** – A logic is imposed around the above 3 elements which iterates certain geometry variables (typically wing area) to meet some objective (typically, min *TOGW*). Generally speaking, sizing is an underdetermined system (more unknowns than equations). Therefore, we must assume certain unknowns constant and then solve the remaining. The solution for the specific sizing problem posed is called the '*sizing logic*'. For example, Roskam's sizing logic⁽²³⁾ the constraint analysis is utilized to select a wing loading which minimize the thrust loading required that meet the mission constraints.
6. **Trade studies** – By varying the assumed constants and solving the sizing logic for each new set of assumed constants, the designer gains a 1st order visualization of the design solution space. These trade-studies can take the form of geometric parameter variation, such as aspect ratio, or technology variation, such as composite vs. aluminum

materials). In some 'Computer-Based' processes optimizers are employed to perform trade-studies according to a prescribed objective function (Min *TOGW*, Min *DOC*, etc).

To examine the current state of the art in parametric sizing, first the fundamental elements of parametric sizing are explored followed by a discussion of the overall sizing processes.

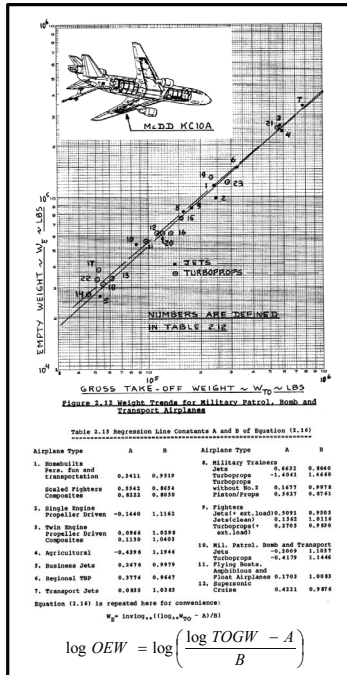
Operating Empty Weight Estimation

This step estimates the structural weight, fixed systems weight and propulsion systems weight for the given geometry. Often this requires an initial estimate of the *TOGW* in order to estimate the structural loads.

This step is typically computed with empirical and semi-empirical weight estimation methods during sizing. For example, in the 'by-hand' method proposed by Roskam⁽²³⁾ the total *OEW* is related to *TOGW* through a simple logarithm empirical correlation, while computer based process may use more detailed empirical relationships due to the increased computation capability, see Figure 2-4.

It is important to note that the more refined weight estimation requires more geometric detail than the simplified empirical correlation. This provides greater design resolution but comes at the cost of increased input requirements. It is important to balance the amount of design resolution required for the problem at hand with the engineering time required to prepare the model for execution.

Simplified Weight Estimation



Typically used for 'By-Hand' methods to reduce the number of calculations

Refined Weight Estimation

Detailed Weight Breakdown

$$\begin{aligned}
 OEW &= W_{str} + W_{feq} + W_{pwr} \\
 W_{str} &= W_w + W_{fus} + W_{emp} \\
 W_{feq} &= W_{fc} + W_{hps} + W_{els} + W_{iae} + W_{api} + W_{ox} \\
 &\quad + W_{apu} + W_{fur} + W_{bc} + W_{ops} + W_{arm} + W_{gbw} \\
 &\quad + W_{fit} + W_{aux} + W_{bal} + W_{pt} + W_{etc} \\
 W_{pwr} &= W_{eng} + W_{ai} + W_{prop} + W_{fs} + W_p
 \end{aligned}$$

Empirical and semi-empirical relationships for each item based on geometry and TOGW

Example: Wing group weight estimation, GD method, Nicolai

$$W_w = 0.00428 \frac{S_{pln}^{0.48} AR \cdot M_0^{0.43} (TOGW \cdot n_{ult})^{0.84} \lambda^{0.14}}{(100t/c)_{avg}^{0.76} \cos^{1.54} \Lambda_c / 2}$$

Typically used by computer based process to increase computational ability

Fig 2-3: Examples of weight estimation methods used in 'by-hand' and computer based sizing processes (23) (20)

Trajectory Analysis

Based on the aerodynamic (L/D) and propulsion (SFC) methods, the fuel fraction ($ff = W_{fuel}/TOGW$) or weight ratio ($WR = TOGW/(OEW+W_{pay})$) is computed to perform the design mission. For example, the Roskam (43) method uses Breguet range for cruise and climb with assumed weight fractions for taxi- take-off, descent and landing. In contrast computational systems, such as FLOPS (51), uses more elaborate methods. In FLOPS (51) an energy method is utilized to optimize the climb cruise and descent according to the specified objective (min fuel, min time, etc.) (Figure 2-2).

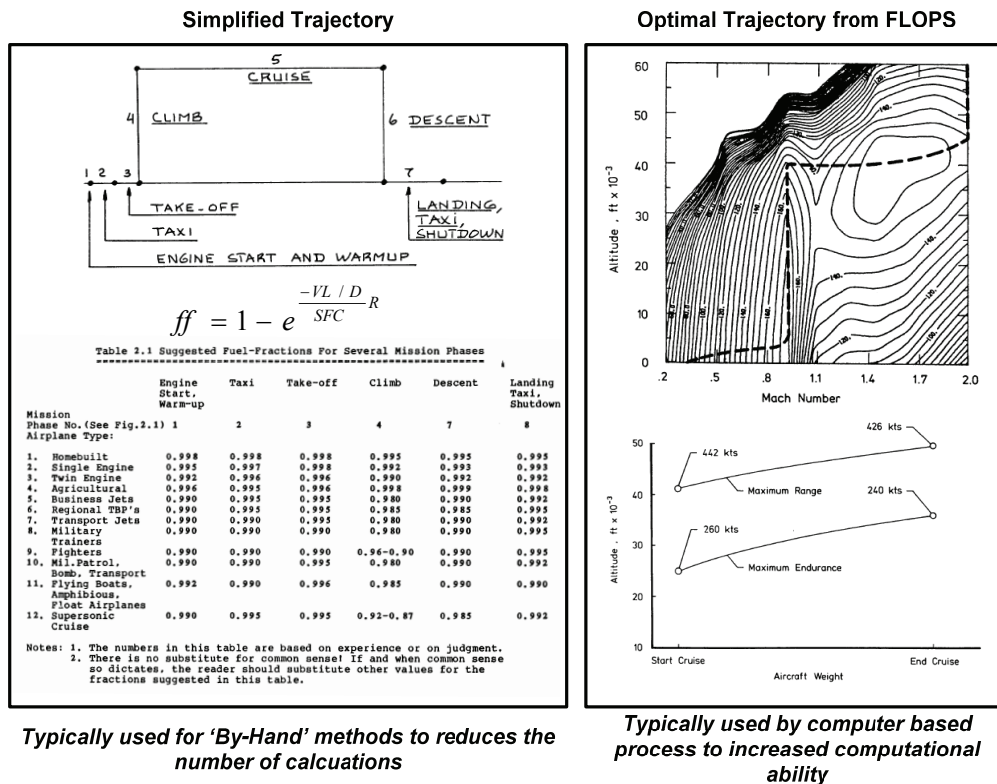


Fig 2-4: Examples of trajectory analysis methods used in 'by-hand' and computer based sizing processes ^{(23) (51)}

Convergence Logic

The convergence logic is the method of solving the implicit function formed by *OEW* and trajectory for a constant mission. Typically, convergence involves the *OEW* estimation and Trajectory analysis to converge the *TOGW* for a given geometry. For example, if we start with an initial *TOGW* and compute the *OEW* and fuel fraction Equation 2.1 can be used to compute the new fuel weight. If the convergence tolerance (Equation 2.2) is not met, any numerical method can be utilized to update the *TOGW* for the next iteration.

$$\text{New TOGW} \quad TOGW_{new} = W_{pay} + OEW + ff \cdot TOGW \quad 2.1$$

$$TOGW_{new} = \frac{W_{pay} + OEW}{1 + ff}$$

$$\text{Convergence} \quad |TOGW_{old} - TOGW_{new}| \leq tolerance \quad 2.2$$

Constraint Analysis

The next step is to take the converged design and compare it with the design constraints. Classically, the constraints take the form of thrust loading (T/W) and wing loading (W/S) derived from performance requirements. Some processes will include wing volume as additional design constraints.

The performance constraints can be written in closed form analytic expressions which demonstrate the relationship between T/W and W/S . Table 2-1 summarizes the classical performance constraints for a transport aircraft.

Table 2-3: Classical Performance Constraints for Subsonic Transport Aircraft

Constraint	Analytic Equation	Required Information
Approach Speed	$(W/S)_L = 1/2\rho V_S^2 C_{L_{\max(\text{landing})}}, V_A = \sqrt{\frac{S_{FL}}{0.3}}$	Landing field length or desired approach speed $C_{L_{\max}}$
Take-off	$(T/W)_{TO} = \frac{37.5(W/S)_{TO}}{\sigma C_{L_{\max}} S_{TOFL}}$	$C_{L_{\max}}$ Field length (S_{TOFL})
2 nd Segment Climb OEI and Aborted Landing Climb OEI	$(T/W)_{TO} = \frac{T}{T_{SL}} \frac{N}{N-1} \left[\frac{1}{L/D} + CGR \right]$	Drag polar Required climb gradient (CGR) Number of engines (N) Engine performance (T/Ts)
High-Speed Cruise	$(T/W)_{TO} = \frac{1}{(T_c/T_{SL})(L/D)_{\max}},$ $L/D_{trim} = \frac{C_L(L/D_{trim})}{C_{D0} + L'_w C_{L_w}^2 + L'_h C_{L_h}^2}, C_L = 2 \frac{(W/S)}{q}$	Trim solution for the given C_L , Drag polar Engine performance

From these expressions it is possible to build a constraint diagram which can be used to visualize the feasible solution and identify the design match point. The match point is the take-off wing loading which minimizes the take-off T/W required. This location typically provides a minimum $TOGW$ solution. Figure 2-6 provides a typical constraint diagram.

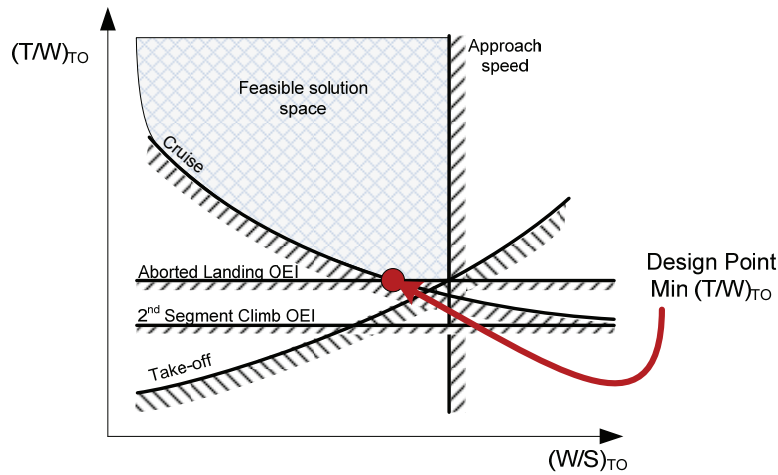


Fig 2-5: Classical performance constraint diagram

In the above example it can be seen that the approach speed, cruise and aborted landing constraints bound the feasible design space for this particular mission. This leads to the design point being located at the intersection of the aborting landing and approach speed constraints.

Physically this means that the propulsion system will have sufficient thrust for both OEI aborted landing and cruise. The wing will have sufficient planform area to allow for approach velocity with the available C_{Lmax} .

Figure 2-6 shows the constraint diagram typical of most 'by-hand' procedures. In these procedures the weight and aerodynamic methods are not sensitive to changes in T/W and W/S , because they are assumed based on typical values, and thus convergence can be performed independent of the constraint analysis. In essence the diagram assumes constant $TOGW$. Through combining the selected wing loading and thrust loading with the converged weight estimation, the required thrust and wing area for the mission can be computed.

In most computational systems the aerodynamic and weight methods are sensitive to T/W and W/S , because they are driven by geometry, therefore requiring the constraint analysis

to be included in the convergence logic. This removes the assumption of constant TOGW and allows for visualizing the effect of TOGW on design space (Figure 2-7).

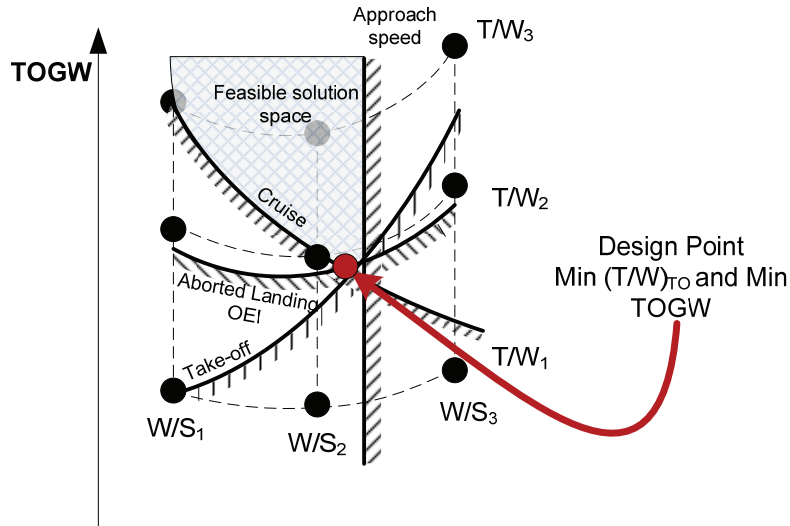


Fig 2-6: Converged performance constraint carpet plot. The 2nd segment climb and constraints have been omitted

The black points in Figure 2-7 are a 9 point carpet plot to demonstrate the curvature of the design space with respect to TOGW. By overlaying the converged constraint diagram it can be seen that the min TOGW corresponds to the minimum T/W for this design at the intersection of the cruise and aborted landing constraints.

Sizing Logic

The sizing logic is literally the method to which the design variables are solved for. In the previous example, wing loading (W/S) and thrust loading (T/W) have been utilized to size the aircraft to the *constant* mission (payload, range, field length, etc.), wing shape (AR , λ , $A_{c/4}$, etc) and type of propulsion system (turbojet, turbofan, etc.). Some methodologies will utilize wing area (S) and thrust (T) required directly in the sizing logic instead of T/W and W/S . This results in a different appearance of the design solution space relative to Figures 2-3 and 2-4.

Trade-Studies

With the sizing logic established, trade studies may be performed with the independent design variables (wing shape, type of propulsion system, etc) or the design mission to determine the most desirable configuration. Figure 8 demonstrates a simple wing aspect ratio trade example.

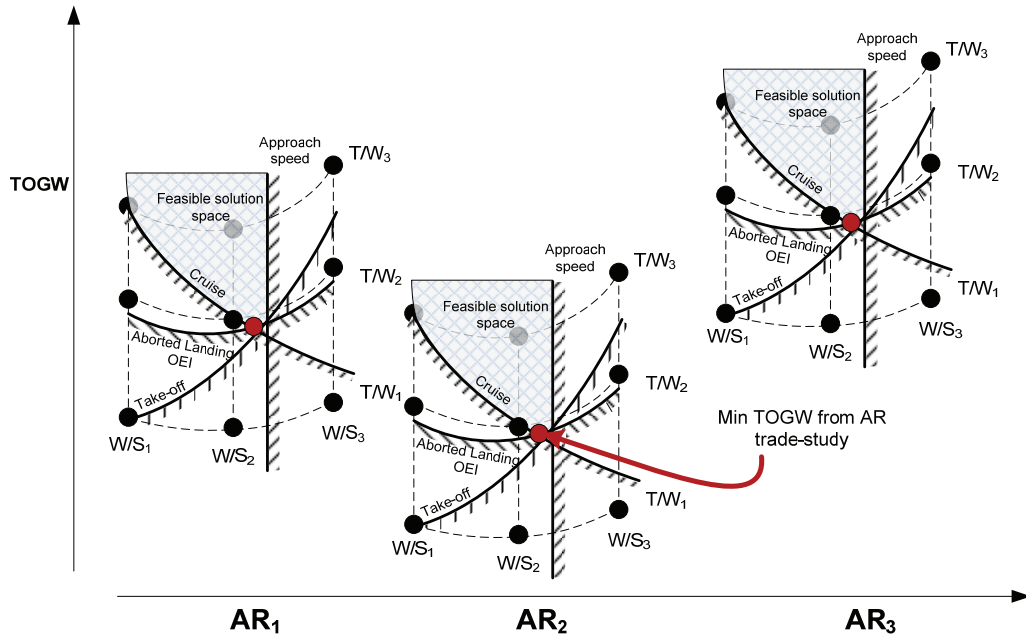


Fig 2-7: Aspect ratio trade (AR) shown through 3 converged performance constraint carpet plots

Discussion of Sizing Processes

With the 6 components of the parametric sizing process, (1) OEW, (2) Trajectory (3) convergence, (4) constraint analysis (5) sizing logic and (6) trade-studies described, we can now begin discussing how these elements are combined into the process.

Beginning with the general sizing methodology found implemented in the majority of modern, constant mission sizing, processes, one can see all 6 elements and how they combine to provide a parametric view of the solution space, see Figure 2-9. This 'general' process is representative of the processes proposed by classical reference such as Nicolai⁽²⁰⁾, Howe⁽³⁶⁾.

and Raymer⁽⁴³⁾ and it is representative for implementations in computer codes such as FLOPS⁽⁵¹⁾, ANSYNT⁽⁴⁷⁾, ASAP⁽⁴⁶⁾, etc.

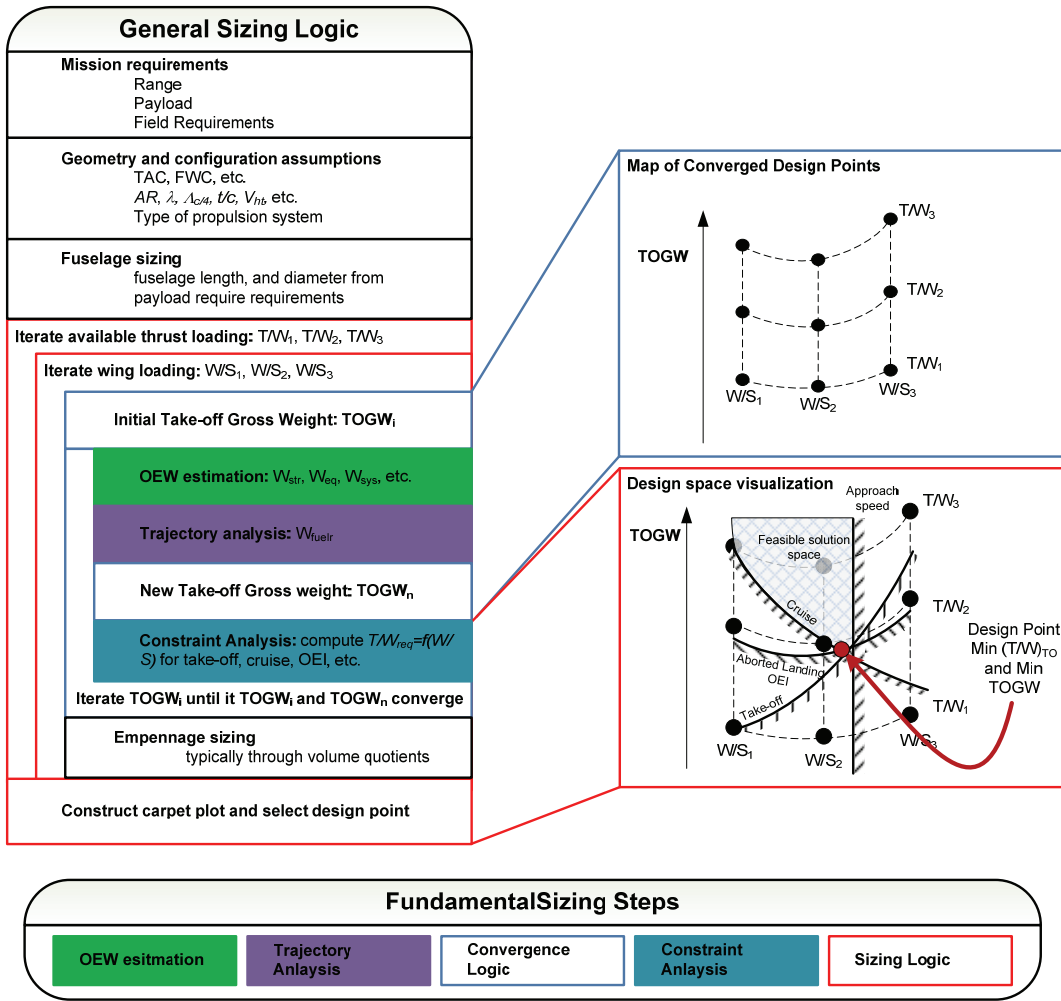


Fig 2-8: General aircraft sizing process with fundamental steps high-lighted. This is the fundamental logic used in systems such as FLOPS⁽⁵¹⁾, ANSYNT⁽⁴⁷⁾, and ASAP⁽⁴⁶⁾

In the above general process, the designer sets a range of wing loadings and thrust loadings and then converges each combination to the same design mission. Overlaying the constraints reveals the feasible design space and the designer can select the design point based on any figure of merit (such as minimum TOGW, fuel, DOC, etc). In Figure 2-9, the figure

of merit was TOGW and the designer selected the combination of W/S and T/W which yields a minimum TOGW within the feasible solution space. In practice this new point must be re-run through the convergence logic to generate the necessary design data.

Summary of the State-of-the-Art in Parametric Sizing

The majority of the 'by-hand' approaches tend to take short cuts when executing the convergence logic in an attempt to reduce the number of iterations required. A simple example of this can be found with Roskam⁽²³⁾, where the empty weight and fuel weight loop is solved by assuming very basic relationships between OEW and TOGW in combination with the Breguet range equation for fuel weight (assumed L/D and SFC from typical values). The constraint analysis is then performed and the proper (W/S)_{to} and T/W are selected with the assumed constant TOGW, see Figure 2-10.

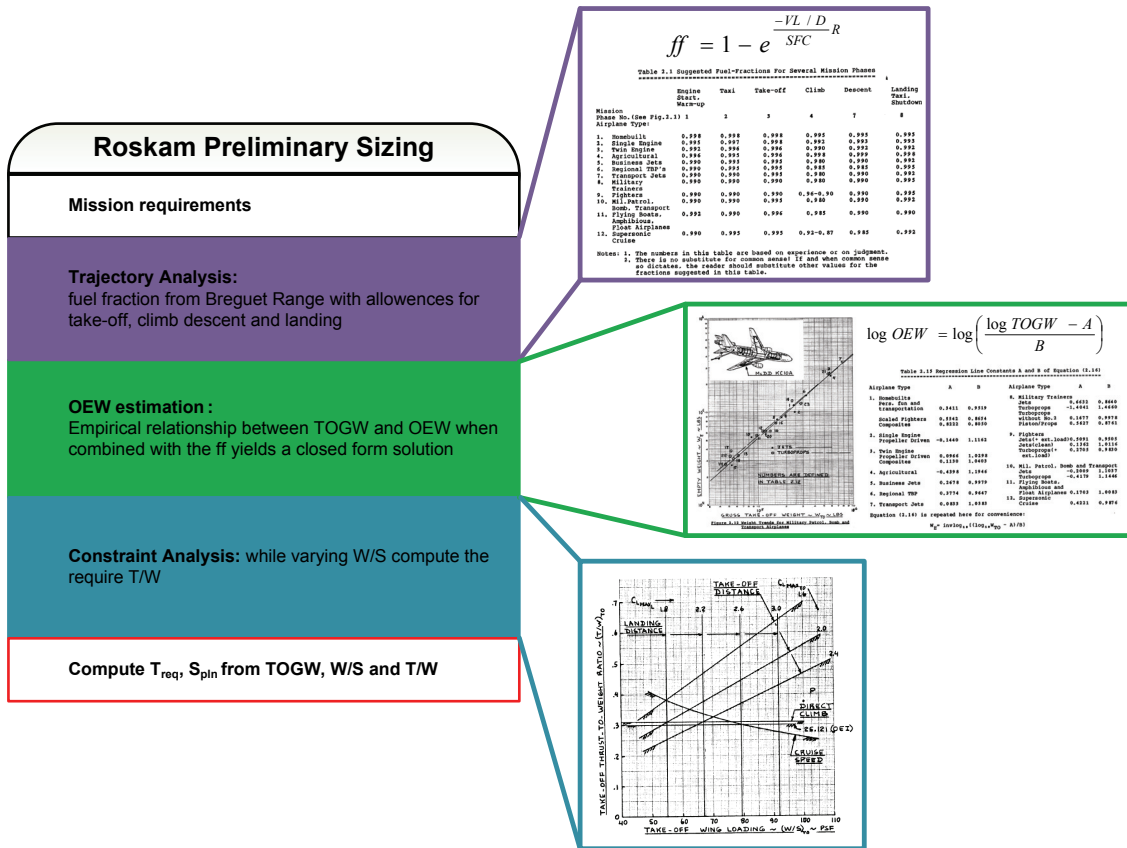


Fig 2-9: Simplified sizing process, Roskam: Preliminary Sizing (23).

Roskam's process results in a similar sizing diagram as shown in Figure 2-10 based on very general methods (such as assumed L/D , or an empirical relationship between OEW and $TOGW$). Thus, the process provides a very general result in terms of required vehicle geometry and performance. This process can be very useful for educational purposes where the nuances in the total process are emphasized. However the methods and process are too general for even simple trade-studies of the classical aircraft shape.

Most modern sizing 'computer-integrated' approaches utilize the general sizing method described in Figure 2-9 with minor nuances in the order in which the elements are arranged within the convergence logic. Such processes can be found in FLOPS⁽⁵¹⁾, ANSYNT⁽⁴⁷⁾, and ASAP⁽⁴⁶⁾.

The notable exception is found with a sizing logic for hypersonic launch vehicle and cruisers developed by VDK and Czysz⁽⁶⁴⁾ called Hypersonic Convergence. Due to the demanding aerothermodynamics environment of hypersonic flight vehicles, the design of this class of aircraft requires a unique aerodynamic, propulsion and structural integration logic, an integration level usually not found with subsonic and supersonic aircraft as illustrated in Figure 2-11.

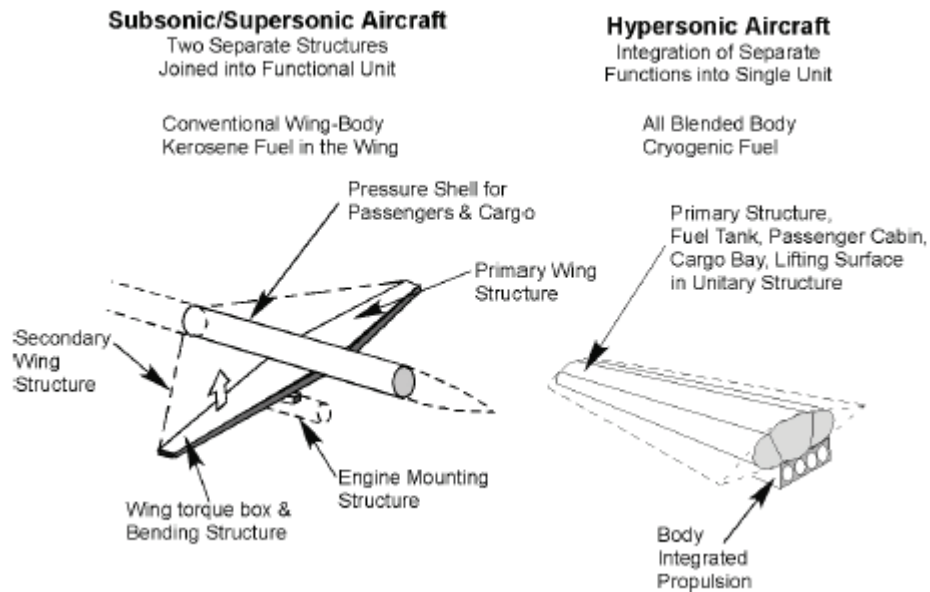


Fig 2-10: Comparison of the integration subsonic/supersonic and hypersonic aircraft ⁽⁶⁴⁾.

The design problem posed with hypersonic aircraft requires an advanced sizing logic since the hypersonic flight vehicle is a fully blended geometry, where the blended body must perform all functions (volume generation, lift generation, integrated propulsion, stability and control). As shown in Figure 2-9, typical subsonic/supersonic sizing methodologies size the wing and propulsion system simultaneously while the fuselage and empennage are sized independently ^{(51) (46)}. In contrast the hypersonic convergence logic considers the total aircraft integration within the convergence logic.

Integrating the volume supply (fuselage), aerodynamic surfaces (wing, empennage) and propulsion system simultaneously requires the explicit inclusion of volume in the convergence logic. In contrast, most subsonic design methodologies only check the wing fuel volume. This significantly advanced sizing logic is presented with Figure 2-12.

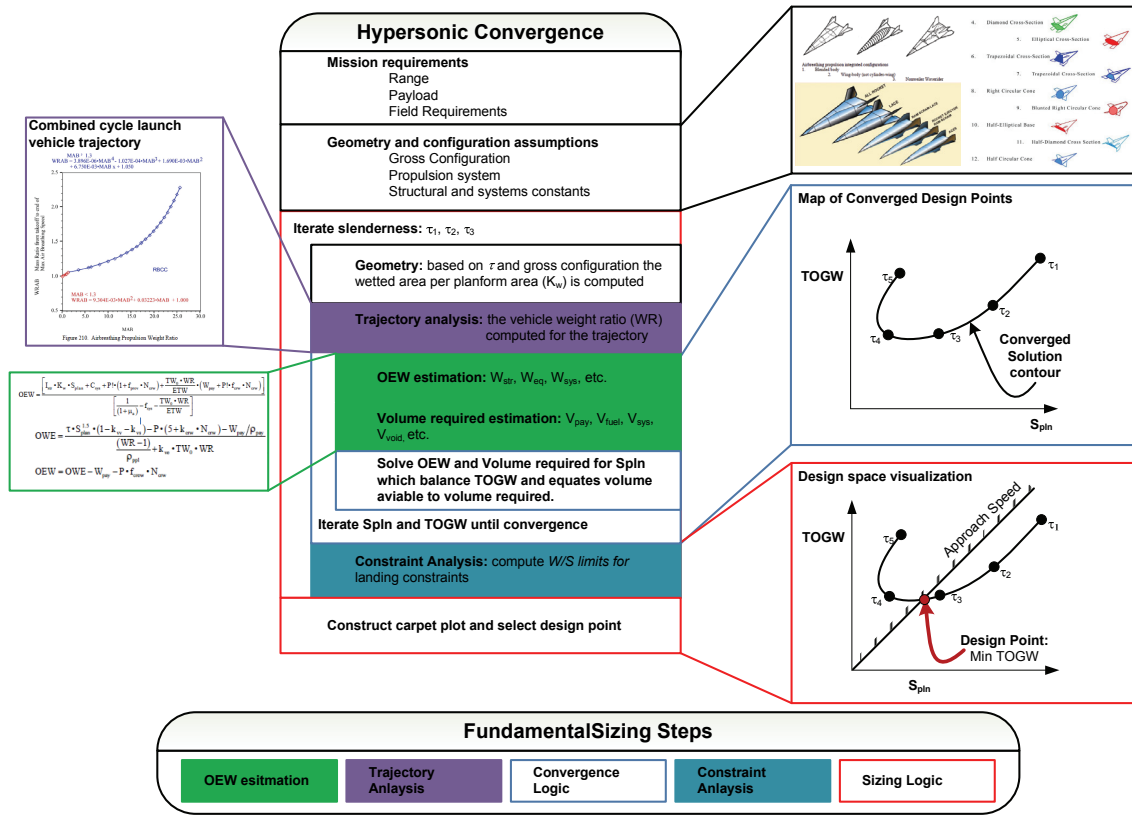


Fig 2-11: Hypersonic convergence sizing logic.

At the heart of Hypersonic Convergence is the system of two equations, which solves for weight and volume simultaneously, Equations 2.3 and 2.4.

$$\text{Weight Budget } OEW = \frac{I_{str} K_w S_{pln} + C_{sys} + W_{cprv} + \frac{T/W \cdot WR}{E_{TW}} (W_{pay} + W_{crw})}{1 + \mu_a - f_{sys} - \frac{T/W \cdot WR}{E_{TW}}} \quad 2.3$$

$$\text{Volume Budget } OWE = \frac{\tau \cdot S_{pln}^{1.5} (1 - k_{vv} - k_{vs}) - (v_{crw} - k_{crw}) N_{cew} - W_{pay} / \rho_{pay}}{\frac{WR - 1}{\rho_{ppl}} + k_{ve} \cdot T/W \cdot WR} \quad 2.4$$

Note: $OWE = OEW + W_{pay} + W_{crew}$

In these expressions, all of the variables have been solved for in the trajectory analysis or are constants except for OEW and S_{pln} allowing for a unique solution. Not that in this

formulation the wing load ($TOGW/S$) will be known when OEW and S_{pln} are solved for and therefore a new sizing variable must be utilized, τ .

The Küchemann slenderness parameter, τ , provides a link between the planform area and volume. When held constant in the convergence logic, the resulting OEW and S_{pln} provide the unique solution based on the required slenderness. With increasing τ , the vehicle will have more volume per unit planform area, thus will become stouter. Conversely, when τ is decreased, the vehicle will become more slender, see Figure 2-13.

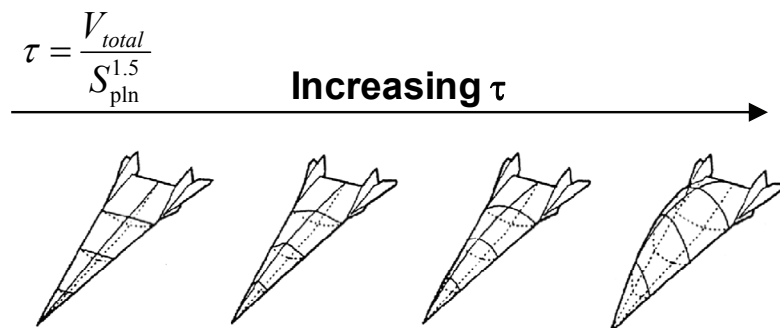


Fig 2-12: Explanation of Küchemann slenderness parameter.

In this integrated methodology, τ serves the same function as W/S does for the classical approach. However, instead of linking wing area to weight, τ connects wing area to volume. The total formulation allows for wing loading, weight and volume to be solved simultaneously.

The change in convergence logic and constant reduces the number of independent variables, resulting in a simplified solution space relative to the classical sizing process. Figure 2.14, which represent a typical converged solution curve for a hypersonic cruiser. In this figure a range of slenderness parameters, τ , have been specified and the resulting $TOGW$ and S_{pln} are solved for. Physically, this curve shows that as the slenderness of the aircraft is reduced (τ increases), the planform area shrinks while the height of the upper surface can increase to accommodate the required volume. As the slenderness decreases, the aircraft structural weight

will fortunately decrease while the aerodynamic efficiency will unfortunately decrease (due to increase wave drag). The result for τ larger than τ_4 the fuel weight increases such that it dominates the TOGW. Superimposing the wing loading required for landing, it can be seen that the slenderness ratio, that minimizes TOGW, will occur just above τ_3 .

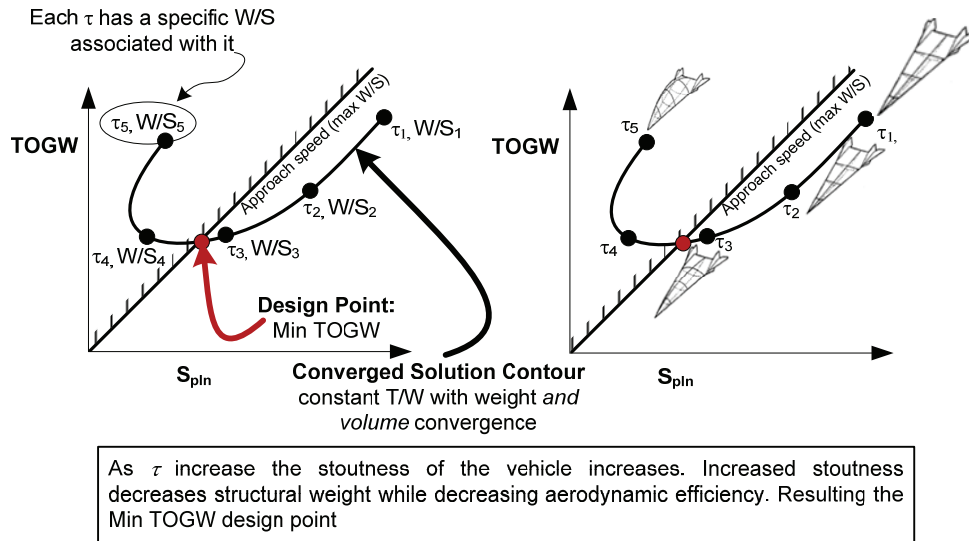


Fig 2-13: Hypersonic Convergence sizing diagram illustrating the converged solution contour. The sizing problem is reduced to a single curve for hypersonic aircraft through including converging weight and volume.

The hypersonic convergence logic provides an interesting simplification of the sizing process in that, (1) the total aircraft volume and weight are converged simultaneously and (2) the feasible design space for a given set of assumed constants is condensed into a single curve. Which leads to an interesting questions, ***Can the Hypersonic Convergence logic be modified for subsonic aircraft? Could elements of the general sizing logic be applied to allow for single logic applicable for subsonic through hypersonic aircraft? Would such a process provide the flexibility needed for consistent comparison of both conventional and unconventional configurations?***

In addition to the unique sizing logic provided by hypersonic convergence, several computer-based processes have made advancements relative to the classical sizing logic, see Table 2-2. These advancements have come from improvements in disciplinary methods and utilization the sizing process in unique ways.

Table 2-4: Further advancements to the classical sizing logic

System	Developer	Contribution
AAA	DARcorporation	Imbedded users guide
ACES	Aeritalia	Implementation of a Knowledge-based system
FLOPS	NASA Langley Research Center	Optimum performance trajectory code, noise and emissions methods
MAVRIS	Georgia Institute of Technology	Use of Metamodels and response surfaces for error propagation and risk assessment

AAA from DARcorporation utilizes the Roskam⁽²³⁾ methodology with an imbedded users guide for method utilization. While only a few methods are offered per classification of aircraft, the physical transparency of the methods is a feature not commonly found among synthesis systems.

The ACES system was a proposed system with a proposed Knowledge-based system (KBS) which would imbed certain design experience into the code. As the designer selected a type of aircraft or engine the code would output a description of the systems attributes. This early attempt at an integrating qualitative knowledge to quantitative knowledge is an intriguing advancement to the MDA frame-work.

FLOPS from NASA LaRC is a standard, open source sizing and performance evaluation code for transonic tail-aft and flying configurations. Of particular interest in this code the optimal performance trajectory code which has a wide variety of applicability as explained early in this chapter

The Mavirs system utilizes a standard MDA procedure for military aircraft with the use response surface models to visualize trade-study sensitivities (53). A response surface is a

visualization of the cause effect relationship between technology, design variables and top-level requirements to the design object and constrains, see Figure 2-15.

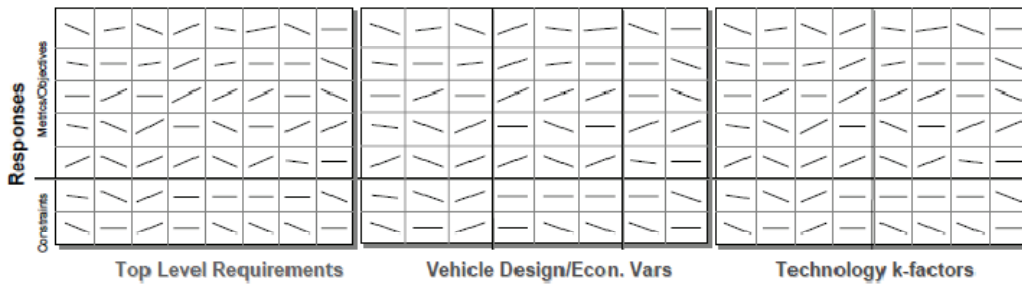


Fig 2-14: Example Response Surface Equations demonstrating design sensitivities ⁽⁵³⁾.

The response surface representation allows for visualization of the depended design variable gradients with respect to independent variables (Jacobian). This technique visualizes the sensitivity of design variables around a selected design point. When this technique is then multiplied by several design points the results is a metamodel that can be utilized as a query able design solution space of design points and gradients.

In theory this type of solutions space could yield a complete representation of the solution space, however, the large amount of data is difficult to visualize and interpret for the designer. Thus, the designer must rely on data mining techniques are required to explore the solution database.

In application, parametric sizing is performed at the beginning of the design cycle where little information is known about the solution space and such a bombardment of information can cause more confusion then it alleviates. From experience with sizing a large variety of aerospace vehicle (Chapters 5 and 6) it has been found that manually exploring the solution space during parametric sizing provides a more intimate understand of the solution space.

The use of Metamodels and Response surfaces are included here because they can be useful on the disciplinary level. For some unconventional vehicles not rapid analysis methods may exist for structural or aerodynamic prediction. These cases modern CFD and FEM analysis

can be quite useful, but computationally expensive and time consuming. Metamodels can be developed through parametric variation with off-line CFD and/or FEM methods to produce artificial experimental data^{(48) (65)}. This data set could be queried by the parametric sizing code in a quicker fashion than running the CFD or FEM code each iteration. This application is similar to the use of aerodynamic look-up tables in flight simulation.

In summary, the current state-of-the-art in parametric sizing resets with the MDA framework developed by VDK and Czysz in hypersonic convergence. While other advancements incorporate refinement to the general sizing process they tend to be configuration and flight regime specific. Hypersonic convergence provides a process in which the configuration can be varied without changing the sizing logic. This is a significant advancement considering the complexity of aerospace vehicle sizing which typically leads to simplifications which limit a process's capability.

Observations

During this review it became clear that a wide variety of design processes and disciplinary methods exist for aircraft parametric sizing. ***A well organized and condensed Process Library and Disciplinary Methods Library would provide the designer with a quick reference to the tools available, how and when to use them. Such a library would provide the elements for a rapid adaptation of a design process to a new design problem to be solved.***

2.2 Configuration Layout

The configuration layout phase begins with the configurations and technologies identified during the parametric sizing phase. The configuration phase is assembling a more detailed configuration around pre-selected start configurations and technologies. This phase is the creative design portion which requires the designer to use past experience and intuition in order to complement the parametric sizing phase and deliverables. For example, the parametric sizing phase may not require locating the landing gear, layout out the cabin or locate individual subsystems. The configuration layout phase adds this detail.

Several references, such as Raymer (59) and Roskam ⁽²³⁾, provide approaches to configuration layout in terms of process, simplified component analysis, design guidance and past aircraft geometry data. The fundamental steps typical for the configuration layout phase can be seen in Raymer ⁽⁴³⁾ Chapters 7-11 (Figure 2-16).

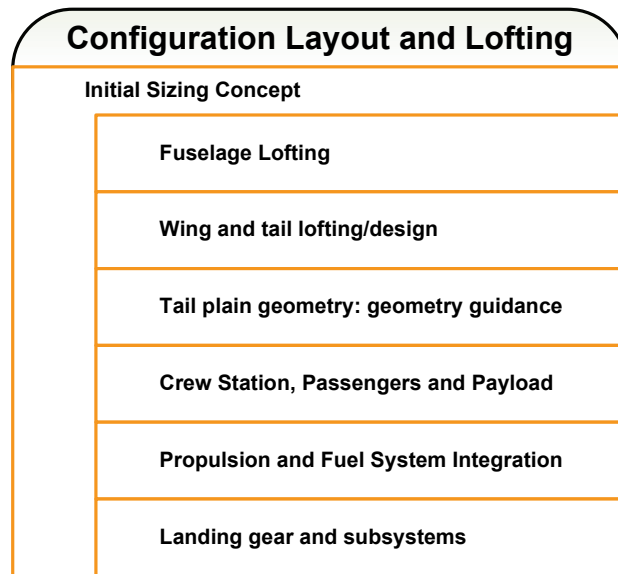


Fig 2-15: Typical Procedure for Configuration Layout ⁽⁴³⁾.

Note that *configuration layout* is not as dependent on the analysis procedure as parametric sizing. This is due to the fact that the configuration layout phase does utilize the

multidisciplinary design space as specified by the parametric sizing phase. The individual aircraft components are then defined within the given constraints. For example, in Roskam's⁽²³⁾ configuration layout phase (Preliminary Design I), the wing area is known from the earlier parametric sizing phase. However, the wing sweep, taper ratio, precise airfoil and flap dimensions are not yet known. Roskam provides empirical data of past aircraft to pre-select wing sweep, taper ratio and airfoils and uses reduce order models to design the flap system to provide the maximum lift coefficient assumed during parametric sizing. All of this analysis is done independently of the fuselage and empennage.

During the *configuration layout phase* it may be discovered that certain assumptions may not be valid; thus, the parametric sizing phase may need to be repeated with corrected assumptions. To continue the example from Roskam, if it is found that insufficient volume is available on the wing trailing edge to fit the required flap system. Consequently, the wing must be resized by iterating back to the parametric sizing phase to produce the lower maximum lift coefficient.

Once a reasonable configuration is layout has been establishes that promises functionality with view to the mission, the design proceeds to the *Configuration Evaluation Phase* where the proposed aircraft is thoroughly evaluated in the multi-disciplinary context.

State-of-the-Art in Configuration Layout

This design phase has been aided greatly from CAD systems to develop rapid 3-D models to aid the designer in visualizing the total aircraft integration with systems such as CATIA, Solid Works and ProE. Such systems have become standard across industry and across design phases.

However, some of these involved systems can be cumbersome and expensive for rapid aircraft conceptual design projects. Consequently, several aircraft conceptual design specific systems have also been developed and integrated into parametric sizing and configuration

evaluation tools. Systems such as NASA Langley's VSP (66), Raymer's RDS-DLM (Raymer Design System, Design Layout Module) (59) and PrADO's (Preliminary Analysis Design and Optimization CAD Kernel) (7), are examples, see Figure 2-17.

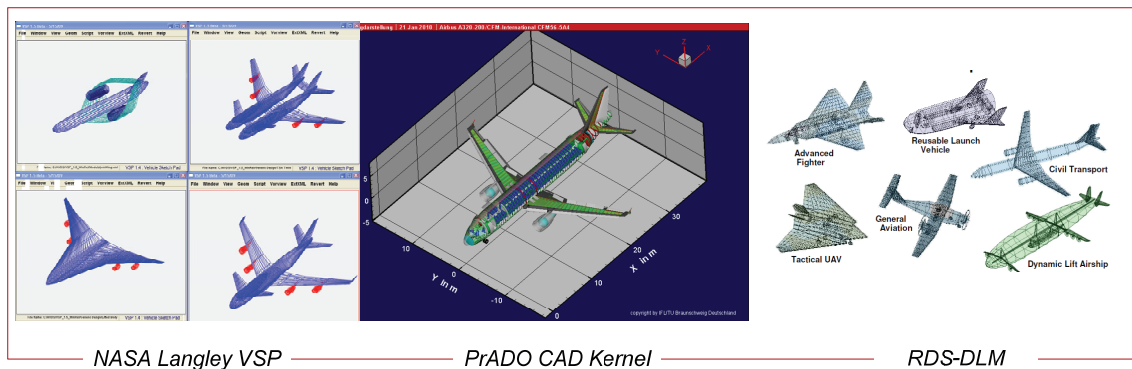


Fig 2-16: Examples of Aircraft Specific Configuration Layout Software (66) (7) (59) .

While this advancement in visualization has occurred, little has been done recently in the public domain to update or collect relevant aircraft design lessons learned from past projects. It could be assumed that historic lessons learned have been organized at proprietary commercial aircraft manufacturers, however, exposure with the commercial environments indicated that configuration layout knowledge is usually carried with individual engineers into retirement (67). The following references provide excellent guidance during the Configuration Layout Phase: Roskam (23), Raymer (43), Torenbeek (18) and Howe (36).

Observations

Improving the Configuration Layout Phase could come with organizing and presentation of design knowledge. As mentioned earlier, most of the public domain design knowledge and statistics are several decades old and are scattered across several references. A dedicated configuration layout Knowledge Based System could organize and make accessible the

qualitative and quantitative lessons learned from past design programs and projects. Such knowledge would be invaluable to the student and practicing engineer for applying past lessons learned to new design problems. This is admittedly easier said than done.

The Idea of a KBS is not a new one and development of such systems and their requirements are well established. See Davis ⁽⁶⁸⁾ for technical description of the systems requirements. As identified in Chudoba ⁽⁹⁾, the most difficult problem for such a system is the collection, organization and presentation of the design knowledge itself. Chudoba ⁽⁹⁾ begins the development of a dedicated conceptual design KBS with a systematic but 'manual KBS' for stability and control knowledge, aimed at presenting design lessons for both conventional and unconventional vehicles ⁽⁹⁾. Expanding this style of KBS toward other technical disciplines and design projects would be the next logical step in this research. ***A dedicated KBS for the Configuration Layout Phase should be the next step in this research.***

2.3 Configuration Evaluation

Having arrived at a sized and laid out configuration, it is required to generate conceptual design understanding by performing more detailed analysis of the identified aircraft proposals. Compared to the earlier two conceptual design phases, the Configuration Evaluation Phase is the better understood phase of the conceptual design steps due to its definite start point and analysis task. The fundamental objective of this final conceptual design phase is to satisfy the designer and the decision maker that the selected concept is worthy of preliminary design continuation with an acceptable level of risk. This is accomplished through,

1. **Check of critical design assumption used during *Parametric Sizing Phase*** – in order to get the project started it is necessary to make certain assumptions to develop an initial configuration. The assumptions which are crucial for the success of the vehicle must be addressed in a more rigorous fashion prior to preliminary design.

2. **Refine design decisions made during the *Configuration Layout Phase*** – This includes refinement of the wing, more through disciplinary analysis like performance and stability & control analysis, a though check of weight and balance, etc.

The elements representing the Configuration Evaluation Phase are similar to the Parametric Sizing Phase. Configuration evaluation contains weight estimation, trajectory analysis, constraint analysis, and convergences logic with an increase in the order (or fidelity) of the analysis. Additional analysis is also performed in disciplines like stability and control and structural analysis, disciplines which are thoroughly addressed during the Parametric Sizing Phase.

The Configuration Evaluation Phase executes the (MDA) framework first with parameter trade studies perturbing aircraft around the baseline concept, followed by mathematical optimizer studies, if required. In addition, due to the increase in disciplinary model fidelity, methods such as CFD and FEM do increase the processes sensitivity to 2nd order design variables.

State-of-the-Art in Configuration Evaluation

When comparing so called 'By-hand' and 'Computer-integrated' processes, the primary difference occurs in the iteration logic. Most 'By-Hand' approaches refer to its iteration logic by stating 'iterate as necessary'. This implies that the design team will make an interactive judgment call each iteration step as to what to change. In contrast, 'Computer-based' approaches are executing the iteration logic typically for pre-defined parameter sweep to visualize the design solution space. This systematic, and to some degree automated, assessment of the solution space does generate more physical insight to the design team to make the required decision for the design. The benefit of the computer integration can be seen in the process diagrams for Roskam ⁽²³⁾ and PrADO ⁽⁷⁾ (Preliminary Analysis, Design and Optimization), see Figure 2-18.

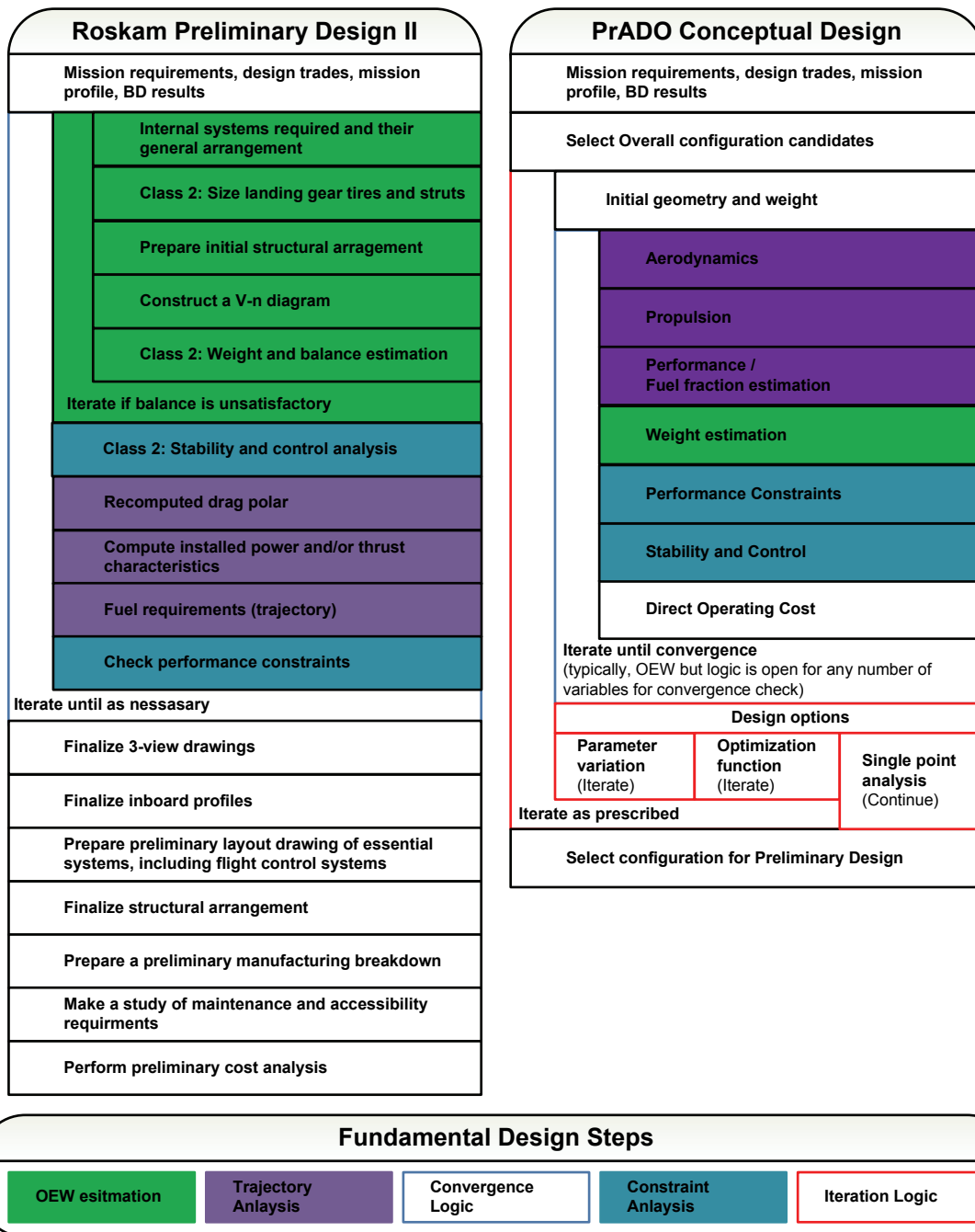


Fig 2-17: Comparison of the 'By-hand' configuration evaluation methods from Roskam⁽²³⁾ with the 'Computer-based' system PrADO

Chudoba⁽⁶⁹⁾ and Huang⁽¹⁰⁾ have been evaluating 'Computer-integrated' design synthesis systems, an activity which identified and selected PrADO as the state-of-the-art for

this phase of conceptual design. After revisiting this extensive review it was reconfirmed that PrADO is the most capable system reviewed for in depth configuration evaluation, while remaining flexible for modification.

PrADO contains a variety of attributes which make this tool a robust configuration evaluation tool.

1. **Modular design** – PrADO is built upon a custom database management system (DMS) which enables modules to access the latest model data. The DMS is developed such that variables must not necessarily be stored internally during iteration but rather are saved in a set of database text files that can queried at any time during the analysis. Therefore, to include a new disciplinary module only requires linking it to the DBS and the execution logic. This structure allows for methods to be added in the form of source code or executables, see Figure 2-12.

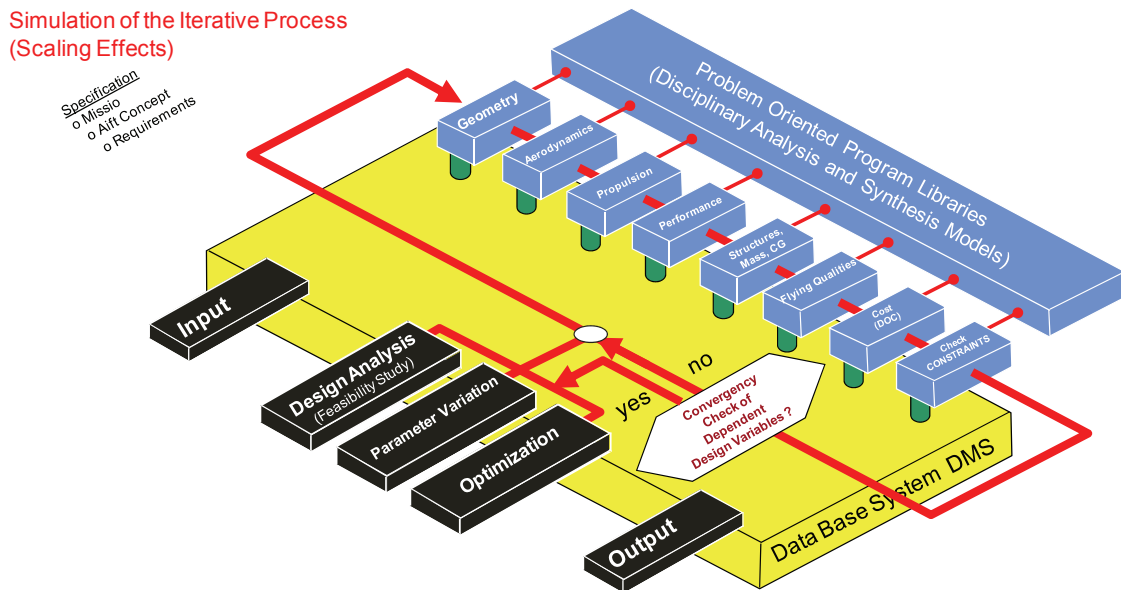


Fig 2-18: PrADO Execution, DMS and Disciplinary analysis modules ⁽⁷⁾

2. **Disciplinary Method Robustness** – PrADO incorporates a disciplinary analysis method library which is called by the disciplinary modules (Figure 2-12), giving another layer of robustness to the program. For example, since a single generic weight estimation method for all types of aircraft does not exist, it is, therefore, necessary to integrate the library of existing weight methods to enable evaluation of several different types of aircraft and technology concepts. These methods incorporate available analytical, empirical and numerical analysis tools.
3. **Data Visualization** – PrADO employs a custom CAD Kernel which visualizes both geometry and data through Tecplot® visualizations. The visualization capability is supplied with data stored in the DMS via a GUI interface, see Figure 2-21.

Technical Figures

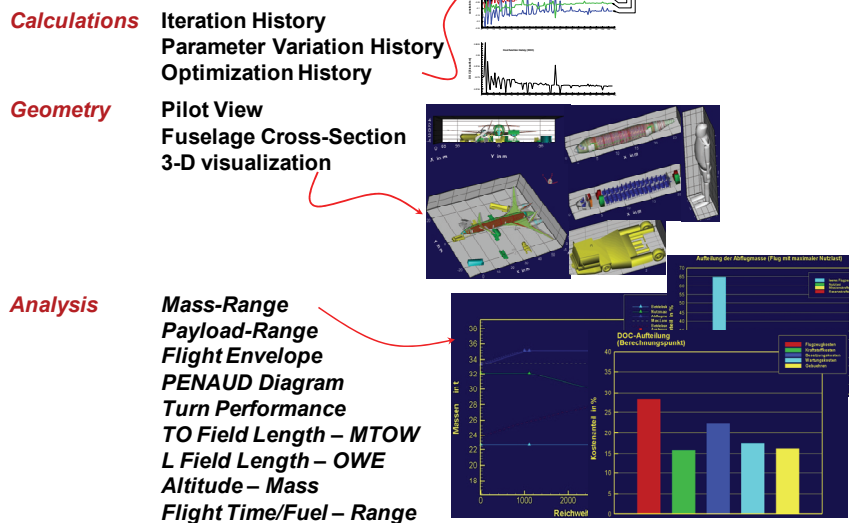


Fig 2-19: PrADO Visualization Capabilities ⁽⁷⁾

4. **Configuration Robustness** – PrADO has been developed to handle wide-variety of aircraft from flying wings to airships, see Figure 2-22. The application to a wide-

variety of configurations demonstrates the robustness of the overall program and its logic.

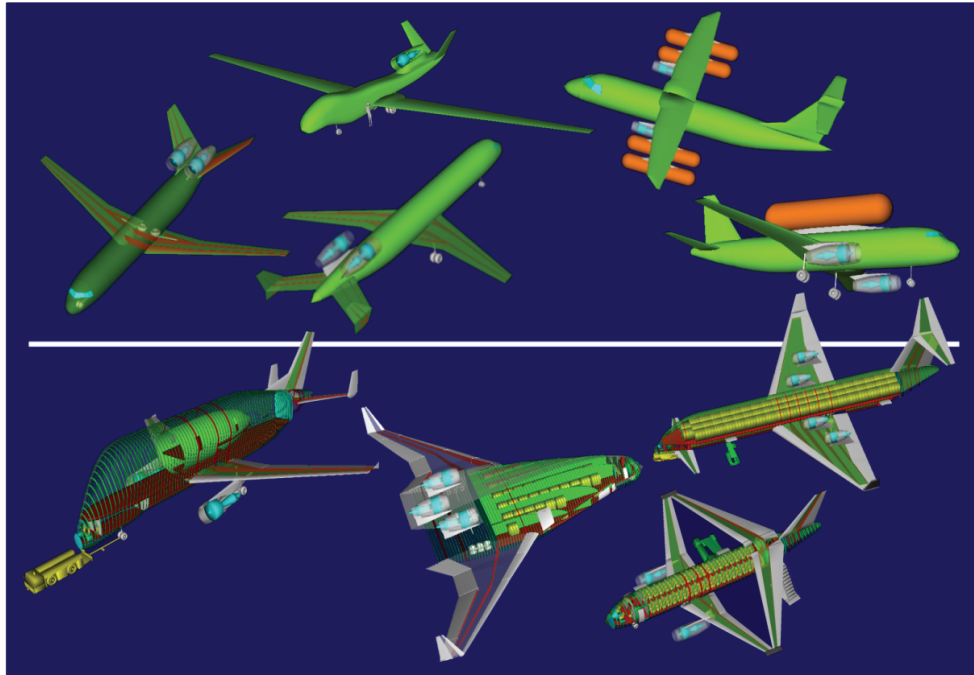


Fig 2-20: Examples of various applications of PrADO⁽⁷⁾

In recent years PrADO has been evolved to include an internal MDO capability to solve the Aero-Structural optimization problem as a sub-optimization problem with the convergence logic⁽⁷⁾. This capability allows PrADO to incorporate MDO into a true multi-disciplinary synthesis context. Even with PrADO's unique modular design and sophisticated disciplinary methods incorporated, there is room for improvement.

Observations

Currently the stability and control module in PrADO handles tail sizing in a very classical method which is only applicable for tail-aft configurations (TAC) or tail-first configurations (TFC). ***A unique opportunity exists to incorporate the generic stability and control analysis tool AeroMech⁽⁷⁰⁾ into PrADO to balance the higher-order aerodynamic,***

propulsion and performance analysis modules with an equivalently detailed stability and control module. This would allow for more accurate representation of unconventional configurations such as the blending wing body (BWB) or the oblique flight wing configuration (OFWC).

2.3 Research Objectives

From the above review, three separate PhD-worthy research directions emerge: (1) advanced parametric sizing processes library and methods library to quickly handle a wider variety of configurations (2) Develop a dedicated KBS for configuration layout, and (3) advance the aircraft synthesis system PrADO to incorporate a higher order stability and control analysis logic, *AeroMech*. The second option, the development of a dedicated KBS for configuration layout, is a large research topic and will require a significant amount of development. For the time being, it was decided to utilize the existing 'manual' KBS. This translates into two research options of significance to aerospace science: (a) parametric sizing and (b) configuration evaluation.

The original objective of this research was to advance the stability and control capability of the AVD Lab's design synthesis system *PrADO* which is a multi-disciplinary configuration evaluation tool. The fundamental goal was to enable complete multi-disciplinary design capability for control configured vehicles (CCV).

During the initial literature review of various approaches to conceptual design it was discovered that the first step in aircraft conceptual design, parametric sizing, has stagnated or has been ignored in the current literature. Current research in conceptual design has been focused on increasing the precision (fidelity) of the analysis of the configuration evaluation phase, while a worthy endeavor, a unique opportunity has been identified to advance the state-of-the-art in parametric sizing.

When a design project is first initiated, before any detailed analysis of a configuration can be performed, an initial start point must be defined. Parametric sizing is the step where the available solution space is identified and explored given a mission specification and general configuration concepts. For example, for a new long-haul transport, parametric sizing will determine possible solutions in the form of an initial geometry, weight, propulsion system, etc. to perform the mission. During this stage of conceptual design gross, configuration trades are performed to determine an appropriate start point for configuration layout and evaluation.

Recent AVD Lab experience with Rocketplane LTD’s Model XP space tourism vehicle ⁽⁷¹⁾, Sprit-wing Aviation’s Supersonic Business ⁽⁷²⁾ and NASA LaRC’s future efficient transport projects LaRC ⁽⁷³⁾, see Figure 2-23, demonstrate that these higher precision tools are not time effective for assessment of a wide variety vehicle concepts and technologies early in the conceptual design. ***The literature review and industry experience with AVD lab projects justify the adjustment of the PhD research objective to advance the state-of-the-art in parametric sizing with the following top-level objectives.***

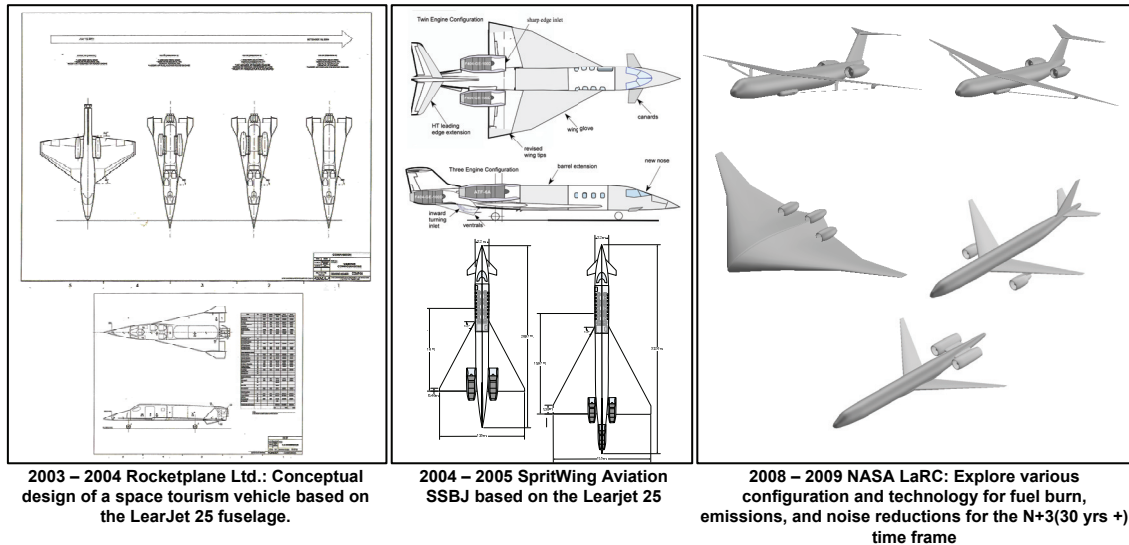


Fig 2-21: Examples of AVD Lab Conceptual Design Studies ⁽⁷¹⁾ ⁽⁷²⁾ ⁽⁷³⁾

In order to advance the state-of-the-art in aircraft parametric sizing, the following objectives have been defined.

Research Objectives.

1. ***Explore, catalog and compare the various approaches to aircraft conceptual design with emphasis on the Parametric Sizing Phase resulting in a design process library and disciplinary methods library.*** The design process library is a catalog of both 'by-hand' and computer-based conceptual design processes broken down by their fundamental process and cross-referenced for interpretation and application. The disciplinary methods library is a library of estimation methods for aerodynamics, propulsion, weight and balance, performance, cost, etc. Each method is broken down in a concise manner focusing on the applicability, assumptions and basic procedure of the method.
2. ***Assemble and develop a flexible and well-balanced aerospace vehicle sizing tool set.*** Experience and review has demonstrated a need for a sizing tool with a balance between input model requirements and design resolution.
3. ***Demonstrate the robustness and potential of such a tool set through case-studies.*** In order to prove such a system has been development, the tool has been applied to a wide verity of configurations within the PhD time frame, thus demonstrating the flexibility of the process and methods library approach.

2.4 Research Approach

To meet the objectives of this research investigation, a systematic literature review has been performed of aerospace vehicle design processes and disciplinary methods to build a solid foundation. Having assembled a representative cross-section of conceptual design

processes and disciplinary methods, the parametric sizing tool set has been assembled. The research follows the steps outlined in Figure 2-24.

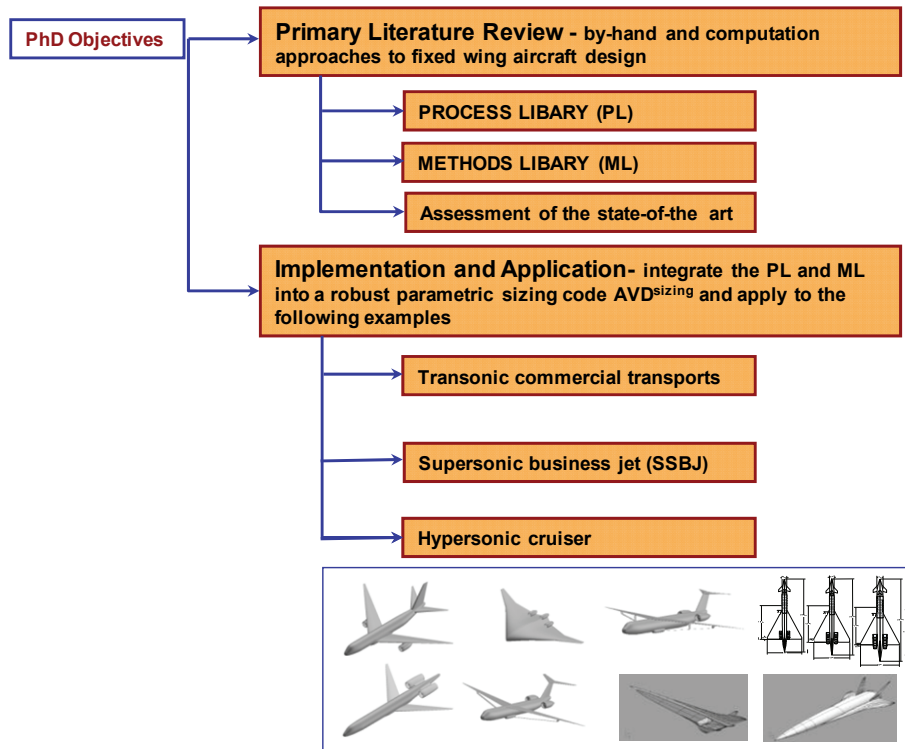


Fig 2-22: Summary of PhD. Research Approach.

The primary literature review consists of;

1. ***Comprehensive Literature Review of Hands-on conceptual design processes and methods*** – In addition to exploring the state of the art of conceptual design sizing, clear patterns can be found across the by hand methods of conceptual design available in the public domain.
2. ***Comprehensive Literature Review of computer based conceptual design process*** – Continuing the survey from Chudoba ⁽⁶⁹⁾ and Huang ⁽¹⁰⁾ on computer-integrated conceptual design processes, the available computer integrated methodologies have

been categorized and analyzed according to their specific conceptual design function (1) Parametric Sizing, (2) Configuration Layout, and (3) Configuration Evaluation.

3. ***Development of a conceptual design process library*** – When encountering new aerospace design challenges, the process by which the sizing, layout or evaluation is conducted may need to be altered. With a dedicated conceptual design process library at hand, the conceptual designer can quickly review, select or modify the baseline process to best address the specific design problem at hand. Aim is to identify the ‘best-practice’ baseline sizing process.
4. ***Development of a conceptual design parametric sizing methods library*** – Having first adjusted the baseline sizing process for the design problem at hand, the second step is to equip the process with the most appropriate disciplinary sizing methods representing aerodynamic estimation, weight estimation, etc.. Any disciplinary method underlies a certain set of assumptions which limits its range of applicability. Next to organizing the disciplinary methods into a user-friendly library or ‘designer toolbox’, it becomes essential to explicitly document the range of applicability for each method (development history, flight speed, aircraft configuration, etc.) From the literature review performed a collection of parametric sizing analysis methods is assembled in a documented parametric sizing methods library. From this organization scheme one is in the position to identify the availability and the lack of available sizing methods for specific design problems. Additional research in the AVD has been initiated to expand the methods library to address the Configuration Layout Phase and Configuration Evaluation Phase.

The development and application consists of:

1. ***Assemble an integrated and flexible parametric sizing program based on the process and methods library, AVD^{sizing}***– Through combining the process and

methods elements uncovered during the literature review, a flexible 1st order sizing code as been developed.

2. ***Validation and demonstration of AVD^{sizing} with existing commercial transports*** – representative aircraft case studies employing the conventional aircraft configuration have been selected to validate the methods and demonstrate the sizing process. In addition. The process is applied to various unconventional aircraft projects.
3. ***Application of AVD^{sizing} to novel configurations*** – In order to demonstrate the flexibility of the parametric sizing methodology, the system has been applied to a wide variety of configuration and technology combinations ranging from unconventional transonic transports to hypersonic cruisers.

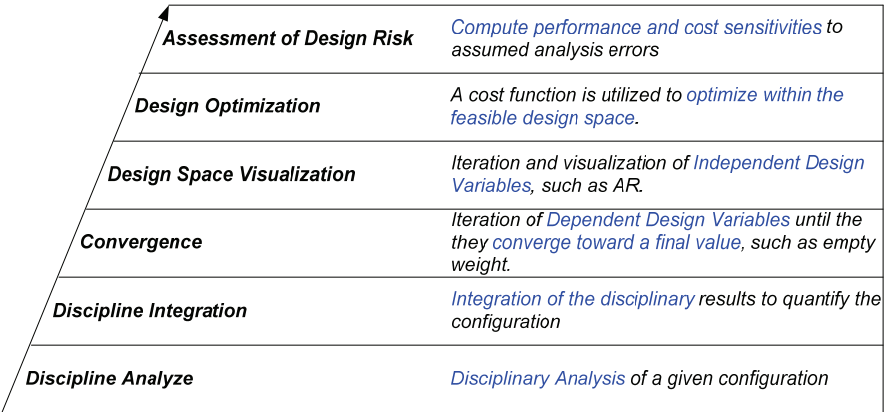
2.5 Research Contribution Summary

The original contribution of this research is the development of a dedicated (1) conceptual design process library, (2) parametric sizing methods library and (3) flexible and balanced parametric sizing code for subsonic to hypersonic aircraft.

CHAPTER 3

CONCEPTUAL DESIGN PROCESS AND DELIVERABLES LIBRARY

Once the mission has been selected and the first order trade-studies are defined (gross configuration candidates, propulsion systems, etc.), the designers must decide how to analyze, iterate and converge the aircraft to mission. These first fundamental steps in any conceptual design sizing process are visualized with the AVD ‘Standard to Design.’



Assessment of Design Risk	<i>Compute performance and cost sensitivities to assumed analysis errors</i>
Design Optimization	<i>A cost function is utilized to optimize within the feasible design space.</i>
Design Space Visualization	<i>Iteration and visualization of Independent Design Variables, such as AR.</i>
Convergence	<i>Iteration of Dependent Design Variables until they converge toward a final value, such as empty weight.</i>
Discipline Integration	<i>Integration of the disciplinary results to quantify the configuration</i>
Discipline Analyze	<i>Disciplinary Analysis of a given configuration</i>

Fig 3-1: AVD ‘Standard to Design’

First, to analyze the aircraft, the various disciplinary methods must be collected which are appropriate to the trade-study. The selection of disciplinary methods is not a trivial one; the accuracy of the design analysis and trends are dependent upon selecting the methods which are valid and sensitive to the design parameters to be quantified and varied.

Having selected the individual analysis methods, the integration of each method is organized with the design process. As discussed in Chapter 2, the classical parametric sizing process sizes the wing and propulsion system simultaneously but the payload bay and control surfaces are sized independently. While this works well for B707-type tail-aft aircraft, the

process requires significant modification for more integrated vehicles like the BWB, high-speed aircraft, CCV, etc.

During the literature review it has been found that a wealth of *configuration and mission specific* design processes and disciplinary methods exist for various applications. A concise library of these design ‘*puzzle pieces*’ would provide conceptual designers with an organized tool-box to (a) select existing design processes and methods and/or (b) discover the need to modify or develop new processes or methods for the new design problem.

A Process and Disciplinary Methods library provides conceptual designer with past design and disciplinary experience. In analogy to collected qualitative and quantitative design experience from various projects/programs (Jay miller's X-planes ⁽⁷⁴⁾, AIAA case studies of the F-16 fly-by-wire system ⁽⁷⁵⁾, Gulfstream III ⁽⁷⁶⁾, De Havilland STOL aircraft ⁽⁷⁷⁾, etc.), the process and methods library provides the analysis and integration “how-to” experience from past designers. Given the growing number of retiring, experience engineers in the industry and the relative inexperience of the engineers replacing them, such a library is critical for retention of design capability.

This design tool-box can be broken down into 3 fundamental elements.

1. **Design process library** – collection and comparison of both, (a) hands-on and (b) computational approaches to aircraft conceptual design. Yielding a clear understanding of how each design process has been approached and what improvements can be compiled into a best practice design process.
2. **Disciplinary methods library** – collection and organization of disciplinary methods to generate the required information (quantify parametric aircraft model) for the design process resulting in quantified deliverables. This library serves as a documentation platform which documents assumptions, applicability and disciplinary experience.

3. **Disciplinary deliverables library** – collection and analysis of the data which must be compiled at each step during the conceptual design processes. Yielding a clear understanding of what data and visualizations must be produced.

These three libraries are coupled. The conceptual design process is depended upon the anatomy of the methods employed and the deliverables will change to accommodate the new processes and methods, see Figure 3-1.

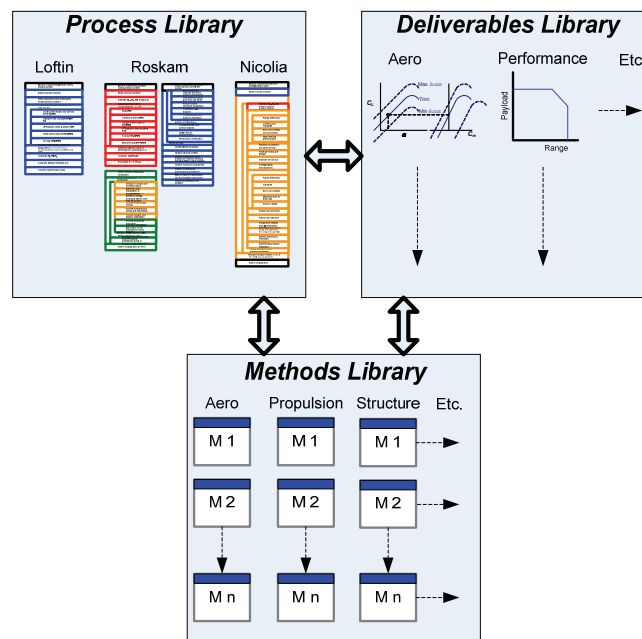


Fig 3-2: Coupling of process, deliverables and methods library.

Clearly, the development of ‘complete’ conceptual design process and disciplinary libraries is a never ending task. As such, the current research will focus on providing the foundation for the methods library by focusing on parametric sizing. The process library will provide an overview of public domain and industry developed (when available), ‘by-hand’ and ‘computer-based’ conceptual design processes. The development of the conceptual design deliverables library is beyond the scope of the present research investigation.

Development of these libraries is analogous to the development of a Knowledge Based System (KBS), which provides an organized and query able set of knowledge. The key development of such a system is first to collect the knowledge. Several search engines and KBS's exist for organizing and presenting the information and such this research is focused on collected the data. The process and methods libraries are presented in Appendices A and B in document form. Later research will convert these 'manual libraries' into searchable design KBS which would become the computation kernel of the AVD dedicated aerospace KBS.

3.1 Conceptual Design Processes Library

The design process library is intended to provide the conceptual designer with various options of exploring the solution space and to guide the designer through integration of the methods and deliverables. This chapter describes the Process Library in terms of (1) processes investigated, (2) process visualization, and (3) examples of the application of the process library to current design problems.

As introduced during the literature review, the process library is broken down into 'By-hand' and 'Computer-Integrated' design processes. From the total list of references explored in the literature review, a representative cross-section has been incorporated in the Process Library. Tables 3-1 and 3-2 provide the processes currently available in the process library.

Table 3-1: Representative 'By-Hand' conceptual design processes

Reference	Original Publication	Latest Publication	Text / Course	Title
Wood (12)	1934	1963	Text	Aerospace Vehicle Design Vol. I, Aircraft Design
Corning (15)	1953	1979	Text	Supersonic and Subsonic, CTOL and VTOL, Airplane Design
Nicolai (20)	1975	1984	Text	Fundamentals of Aircraft Design
Loftin (16)	1980	1980	Text	Subsonic Aircraft: Evolution and the Matching of Size to Performance
Torenbeek (18)	1982	1982	Text	Synthesis of Subsonic Airplane Design
Stinton (19)	1983	1983	Text	The Design of the Aeroplane
Roskam (23)	1985	2003	Text	Airplane Design, Parts I-VIII
Raymer (43)	1989	2006	Text	Aircraft Design: A Conceptual Approach
Jenkinson (33)	1999	1999	Text	Civil Aircraft Design
Howe (36)	2000	2000	Text	Aircraft Conceptual Design Synthesis
Schaufele (37)	2000	2000	Text	The Elements of Aircraft Preliminary Design

Table 3-2: Representative 'Computer-Integrated' conceptual design processes

System	Full Name	Developer	Primary Application	Years
AAA ³⁹	Advanced Airplane Analysis	DARcorporation	Aircraft	1991-
ACES ⁴²	Aircraft Configuration Expert System	Aeritalia	Aircraft	1989-
ASAP ⁵²	Aircraft Synthesis and Analysis Program	Vought Aeronautics Company	Fighter Aircraft	Paper 1974
FLOPS ⁷⁴	FLight OPTimization System	NASA Langley Research Center	?	1980s-
PrADO ⁹⁹	Preliminary Aircraft Design and Optimization	Technical University Braunschweig	Aircraft and Aerospace Vehicle	1986-
RDS ¹⁰¹	(-)	Conceptual Research Corporation	Aircraft	Paper 1992
VDK/HC ⁽⁶⁴⁾	VDK/Hypersonic convergence	MacDonnell Douglas, Hypertec	SAV/Hypersonic Cruise	

Visualization of Design Processes

In order to explore and compare the integration of these design processes each process is represented in a clear format. This is accomplished with color coded Nassi-Schneidermann (NS)⁽⁷⁸⁾ flow charts. NS flow flow-charts are used for structured programming, allowing to visualize complex algorithms in a simple, condensed form. The present context

employs NS charts to document the process flow of complex aircraft design processes. The basic components of NS flow charts are introduced with Table 3-3.

Table 3-3: NS Flow Chart Definitions ⁽⁷⁸⁾

Structure	Traditional Flow Diagram	N/S Structure	Comments									
Sequence		<table border="1"> <tr><td>Start</td></tr> <tr><td>Process X</td></tr> <tr><td>Process Y</td></tr> <tr><td>Process Z</td></tr> <tr><td>End</td></tr> </table>	Start	Process X	Process Y	Process Z	End	Represents a series of commands and procedures				
Start												
Process X												
Process Y												
Process Z												
End												
Selection		<table border="1"> <tr><td colspan="2">IF Condition is true</td></tr> <tr><td>Yes</td><td>No</td></tr> <tr><td>Process X</td><td>Process Y</td></tr> </table>	IF Condition is true		Yes	No	Process X	Process Y	If the condition is true then process x is executed, if false, process y is executed			
IF Condition is true												
Yes	No											
Process X	Process Y											
While Loop		<table border="1"> <tr><td>While Condition is true</td></tr> <tr><td>Process X</td></tr> </table>	While Condition is true	Process X	While the condition is true process x is repeated until the condition is no longer true							
While Condition is true												
Process X												
Until Loop		<table border="1"> <tr><td>Process X</td></tr> <tr><td>Until Condition is met</td></tr> </table>	Process X	Until Condition is met	Similar to a while loop. Typically used for a set iteration such as a do loop. Example, do for I=1 to I=10							
Process X												
Until Condition is met												
Switch		<table border="1"> <tr><td>Switch 'A'</td></tr> <tr><td>A = 1</td></tr> <tr><td>Process 1</td></tr> <tr><td>A = 2</td></tr> <tr><td>Process 2</td></tr> <tr><td>A = 3</td></tr> <tr><td>Process 3</td></tr> <tr><td>Default</td></tr> <tr><td>Process X</td></tr> </table>	Switch 'A'	A = 1	Process 1	A = 2	Process 2	A = 3	Process 3	Default	Process X	A second method of visualizing simple a selection in N/S diagrams
Switch 'A'												
A = 1												
Process 1												
A = 2												
Process 2												
A = 3												
Process 3												
Default												
Process X												

Color coding identifies individual process blocks according to **the following functionalities: Parametric Sizing (red), Configuration Layout (yellow), and Configuration Evaluation (green)**. The NS design process visualization enables to directly compare individual processes with each other. As a first example, the design process by Loftin (16) is presented with Figure 3-2.

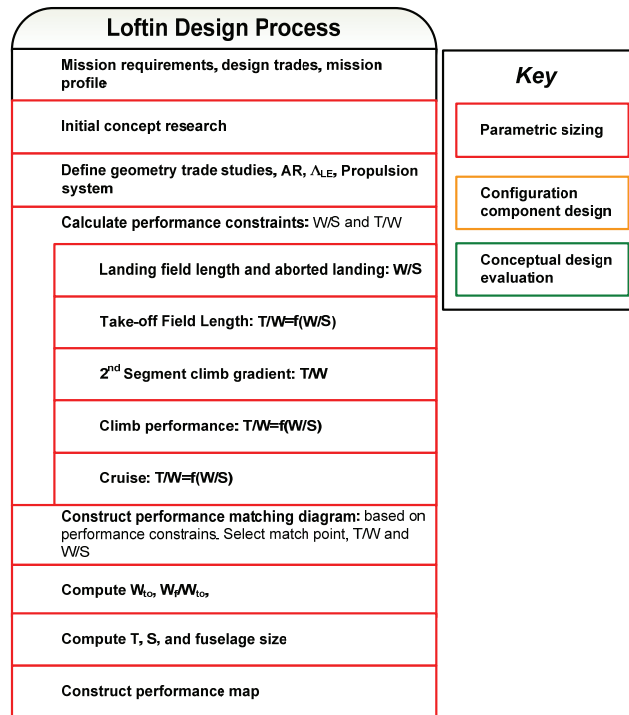


Fig 3-3: Loftin Aircraft Design Process.

The Loftin process demonstrates how individual analysis method selection can affect the process integration. In the classical design logic, see Chapter 2, empty weight estimation is performed first based on the initial TOGW and current geometry. In Loftin, the empty weight estimation method is based on the total aircraft T/W ratio, thus does not occur until after constraint analysis (performance matching). This type of process-customization is common for

'by-hand' processes where simplifications in analysis methods are uniquely implemented from reference to reference.

In addition to describing the physical integration of each process, the process library contains summary tables which highlight key attributes of the individual process, as demonstrated with the Loftin process documented in Table 3-4. This summary card provides a quick reference to the application and interpretation of the process. Similar processes are cross referenced and general comments are provided. More in depth description of the process is also included in narrative form.

Table 3-4: Process overview card

Processes Overview			
Design Phases	Author	Initial Publication Date	Latest Publication Date
Conceptual Design	Loftin	1980	1980
Reference: Loftin, L., "Subsonic Aircraft: Evolution and the Matching of Sizing to Performance," NASA RP1060, 1980			
Application of Process			
Applicability Primarily focused on parametric sizing of jet powered transports and piston powered general aviation aircraft			
Objective Determine an approximate size and weight of the aircraft to complete the mission from a 1 st level approximation of the design solution space			
Initial Start Point The processes begins with mission specification, possible configurations and fixed design variables such as AR.			
Description of Basic Execution From the mission specification, design statistics and basic performance relationships are used to determine relationships between T/W and W/S (performance matching). The aircraft is then sized around this match point.			
Interpretation			
CD Steps	Synthesis Ladder	Similar Procedures	
Parametric Sizing	Analysis Integrate Iteration of design Visualize design space	Roskam (preliminary sizing) Torenbeek (Cat 1 methods)	
General Comments One of the first published processes utilizing performance matching. Where Nicolai compares T/W and W/S after the complete convergence and interaction of the processes, Loftin derives basic relationships between T/W up front to visualize the solution space before initial sizing. Loftin essentially shortcuts the Nicolai approach by deriving an initial design space rather than an initial configuration.			

Application of the Process Library

After reviewing representative processes it became clear that most processes are configuration or technology specific. In other words, the process takes advantage of configuration assumptions in order to expedient process execution. This is seen in the classical tail-aft configuration design processes proposed by Loftin⁽¹⁶⁾, Roskam⁽²³⁾, Torenbeek⁽¹⁸⁾ which are integrated into design programs such as FLOPS and ACSYNT. Clearly, these mainstream processes are primarily addressing exclusively the traditional aircraft configuration, the tail-aft configuration. These processes have in common that the fuselage is designed first, based on the payload requirements. Then the wing and propulsion system are sized (majority of the analytical process). The process concludes with the sizing of the empennage based on the derived wing-body configuration. In summary, this process has evolved for the particulars of the transonic tail-aft configuration (TAC) where (1) the payload volume dominates the volume requirements compared to the volume demands posed by fuel and structures, (2) each primary hardware component (fuselage, wing, empennage, etc.) is designed for a primary function (disintegrated aircraft), and (3) some 100 years of design experience is available to the engineer.

However, apart from the transonic TAC, the majority of non-conventional aircraft configurations and missions do not conform to these assumptions, (1) supersonic/hypersonic aircraft; (2) flying wing configurations, (3) truss/strut braced aircraft, (4) hydrogen powered aircraft, see Table 3-5.

Table 3-5: Example missions and configurations which do not necessarily conform to the classical aircraft sizing logic

Configuration	Comments
Supersonic/Hypersonic Aircraft	Typically these configurations require a higher degree of aero-propulsion and structural integration compared to transonic aircraft
Flying Wing and Blended Wing-Body	The combination of the payload bay and lifting surface impose new constraints on both requiring a higher degree of integration.
Laminar flow Truss-Braced Wing	While still a tail-aft configuration, the thin laminar flow wings may require the fuselage to be enlarged based fuel requirements
Control Configured Vehicle	By designing the aircraft to be statically unstable trim drag is reduce. Resulting in reduced fuel burn, TOGW, wing size and tail size. A flight control system is required to provide artificial stability.
Hydrogen powered aircraft	The use of hydrogen (regardless of speed regime) increases the fuel volume relative to kerosene and requires storage in axisymmetric tanks which may not fit readily into the wing. Thus, additional volume may be required in the fuselage beyond the payload requirements.

In these examples the classical aircraft design sizing logic would require resizing the fuselage (and empennage in the case of CCV) each step outside of the wing-propulsion sizing. To meet the objective of sizing the total aircraft for a wide variety of missions, configurations and concepts it is required to open the general sizing logic. The best example of how to accomplish this can be found with hypersonic vehicle sizing, through the Hypersonic Convergence sizing Logic⁽⁶⁴⁾

Comparing Hypersonic convergence⁽⁶⁴⁾ to the classical sizing logic (subsonic aircraft compiled from Torenbeek⁽¹⁸⁾, Roskam (23), Raymer⁽⁴³⁾ and FLOPS (51)) 2 key points can be seen, see Figure 2-4:

1. Similar components – Each process contains the same functions of trajectory, empty weight and constraint analysis with hypersonic convergence having total volume explicitly involved in the convergence logic.
2. Hypersonic Convergence has the total aircraft geometry imbedded into the sizing logic, allowing the sizing logic to redefine the entire aircraft geometry. During each

iteration the total vehicle is modified to meet the performance and volume constraints.

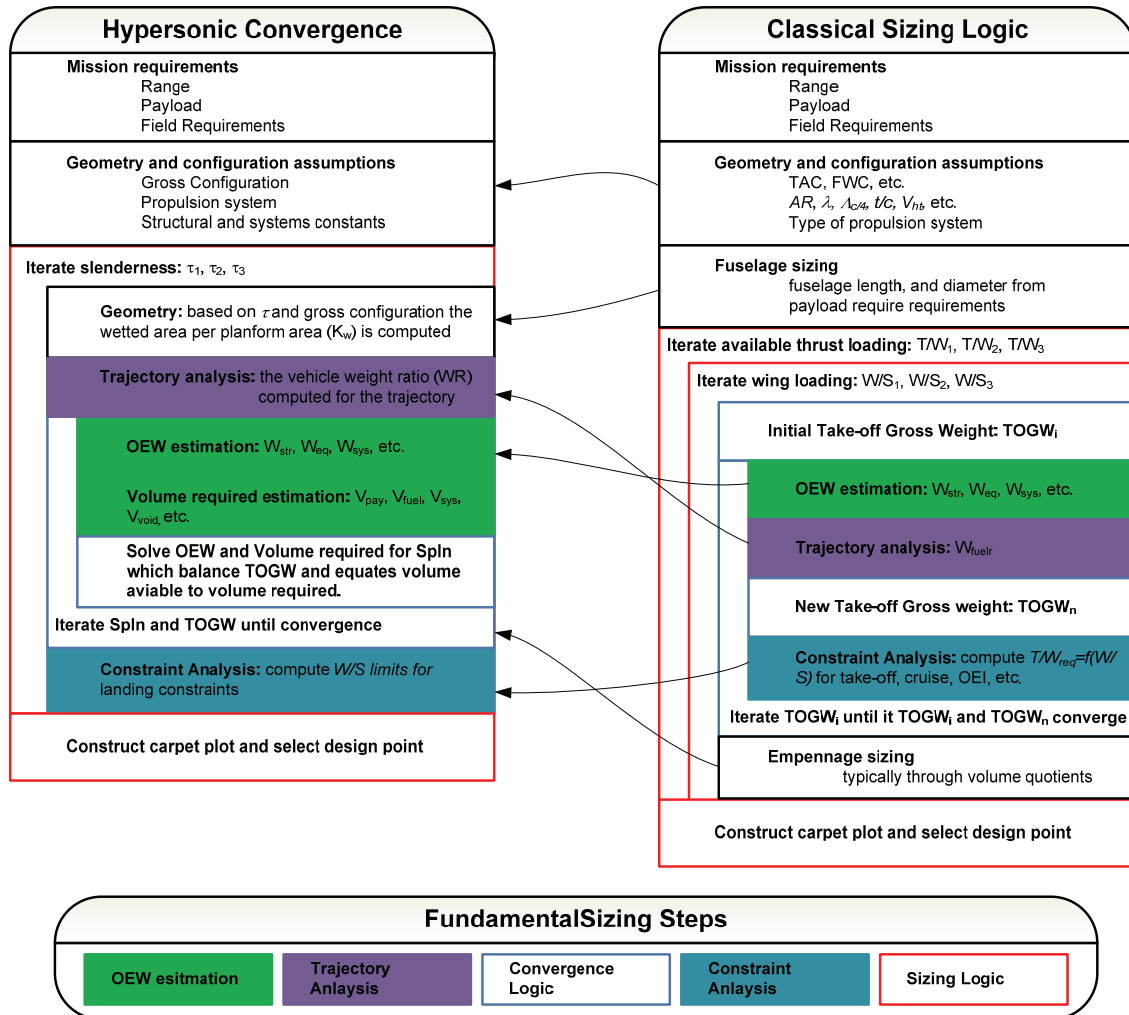


Fig 3-4: Comparison of Hypersonic Convergence and Classical Sizing Process.

These observations lead to the development of AVD^{sizing} (Chapter 5) where the hypersonic convergence sizing logic is adapted to handle any fixed wing aircraft/launch vehicle. In AVD^{sizing} the geometry and trajectory modules are included in the convergence logic allowing for modification of the entire aircraft within the inner most design loop, see Figure 3-5. The variation of vehicle geometry is controlled through the geometry module and a set of design

rules or constants utilized at the designers discretion. Through collected all of the geometry assumptions into an exchangeable module, configuration changes are easily incorporated while leaving the fundamental logic intact. In contrast, the general sizing logic implies that the fuselage is of fixed size within the wing-propulsion systems sizing. This requires adaptation of the process for some novel missions and configurations, where AVD^{sizing} does not.

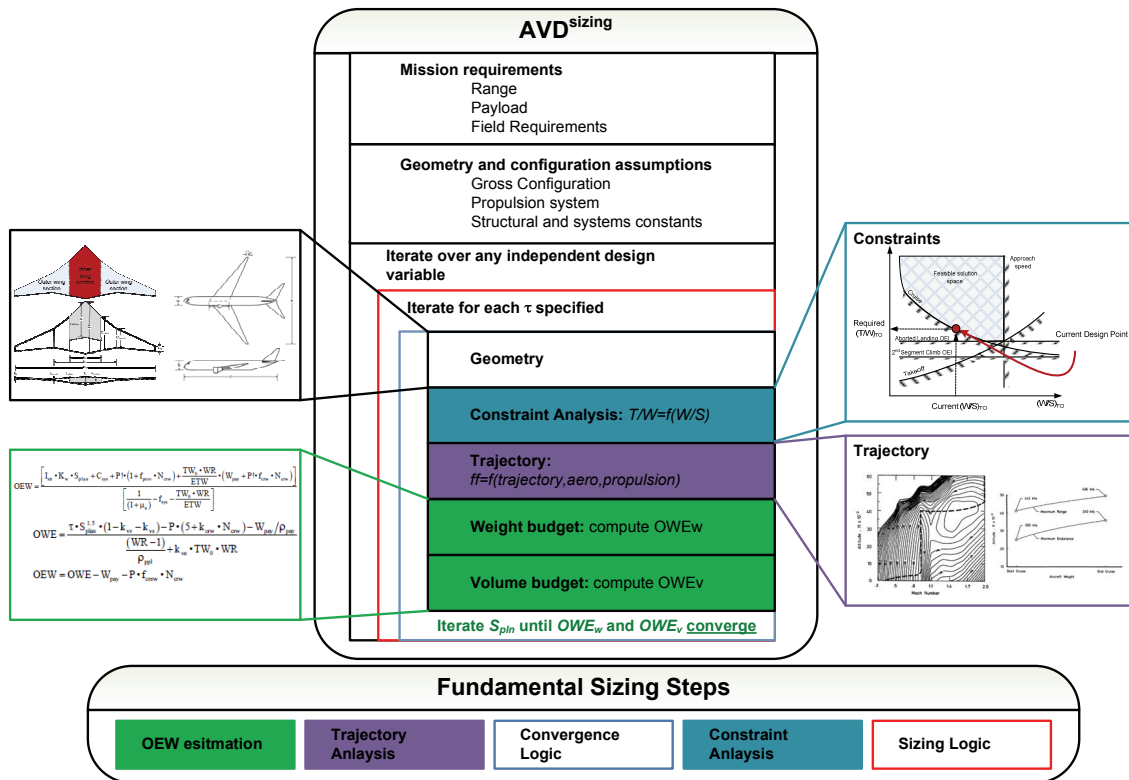


Fig 3-5: Fundamental AVD^{sizing} Logic.

As the development of AVD^{sizing} demonstrates, through cross-referencing with available design processes a new design process has been developed which builds from the strengths of past approaches to parametric sizing. Since the disciplinary methods will require adjustment with varying configurations and technologies, it is a requirement to develop a parametric sizing disciplinary methods library, see Chapter 3.2.

3.2 Disciplinary Methods Library Description

The disciplinary methods library consists of the disciplinary analysis methods which form the building blocks of the any aircraft design process. The objective of the methods library is to provide a standard documentation platform for:

1. **Database of existing methods** – Allowing the designer to select the most appropriate existing method for the given problem.
2. **Documentation of method experience** – Providing a central location for designers to document background, applicability, accuracy, and experience with the methods.
3. **Platform for documenting new methods** – If a method cannot be found in methods library this document serves as a starting platform of either researching or developing an appropriate method.

The collection and organization of disciplinary methods is a task which is critical for the advancement of aerospace science. This style of organization and presentation presents methods in a unique way which focuses application, rather than derivation and development which is typically found. Through focusing the methods library on the fundamental assumption, applicability and Input-Analysis-Output, the designer can gain quickly select the method which is most appropriate. The current research objective is to provide a template for such a library and collect methods which pertain specifically to parametric sizing, See Appendix B. Appendix B provides an excerpt from the master AVD disciplinary methods ⁽⁷⁹⁾ organized by which model they are applied to in Chapters 5 and 6. The total AVD disciplinary methods library is currently being prepared for publication.

Expanding upon this research several Masters topics have been initiated to collect methods for specific disciplines in the Aerospace Vehicle Design (AVD) Lab at the University of Texas at Arlington

Organization of the Disciplinary Methods Library

The parametric sizing disciplinary methods library is organized by disciplines. For each discipline, the methods are structured by function. For example, the aerodynamic chapter is broken down by parasite drag, induced drag, wave-drag, miscellaneous drag, lift curve and maximum lift.

For each method an overview card is produced which summarized each method based on:

1. Assumptions – detailing all simplifying assumptions used in the method.
2. Applicability – application validity (configuration/technology packages).
3. Basic Procedure – detailing the input requirements, basic analysis procedure and output.
4. Experience – documentation of design application and lessons learned in terms of accuracy, computation time and general comments.

Table 3-6 gives an example summary card for the drag polar method provided by Roskam, Part I (23). In this example the complete method description fits into the analysis description block. Other methods require additional documentation beyond the overview card; such is then provided in an additional description chapter following the method overview card.

Table 3-6: Example Methods Overview Card

Method Overview				
Discipline	Design Phase	Method Title	Categorization	Author
Aerodynamics	Parametric Sizing	Initial Drag polar estimation	Semi-Empirical	Roskam
<p>Reference: Roskam, J., "Airplane Design Part I: Preliminary Sizing of Airplanes," DARcorporation, Lawrence, Kansas, 2003</p>				
<p>Brief Description</p> <p>The drag polar is constructed using empirical relationships for parasite drag (based on gross weight), flap and landing gear effects. A classical definition of induced drag is used.</p>				
<p>Assumptions</p> <p>Increments of flap and landing gear taken from typical values</p> <p>Parasite drag coefficient is a function of take-off gross weight</p>		<p>Applicability</p> <p>Homebuilt aircraft propeller aircraft, single engine propeller aircraft, twin engine propeller aircraft, agricultural aircraft, business jets, regional turboprop aircraft, transport jets, military trainers, fighters, military patrol, bomb and transport, flying boats, supersonic cruise aircraft</p>		
Execution of Method				
<p>Input</p> <p>Mission profile, type of aircraft, take-off gross weight, AR, e, S estimate</p>				
<p>Analysis description</p> <p>Estimate $S_{wet}=f(W_{TO})$ empirical based on type of aircraft Fig 3.22</p> <p>Estimate $f=f(S_{wet})$ empirical based on type of aircraft Fig 3.21</p> <p>Assume average value of S</p> <p>Select Flap and landing gear effects for each mission segment Table 3.6</p> $C_D = f / S + \Delta C_{Dflap} + \Delta C_{DLG} + \frac{C_L^2}{\pi AR \cdot e}$ <p>Assume C_{Lmax} values from Table 3.1</p>				
<p>Output:</p> <p>Drag Polar</p>				
Experience				
<p>Accuracy</p> <p>Unknown</p>		<p>Time to Calculate</p> <p>Unknown</p>	<p>General Comments</p>	

Application of the Disciplinary Methods Library

Documentation and application of existing disciplinary methods

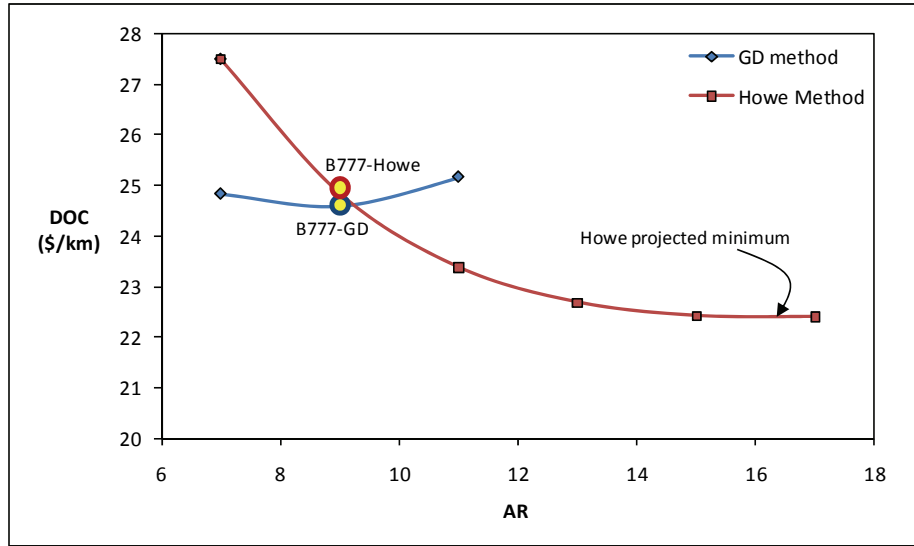
Currently, the parametric sizing methods library contains 79 individual methods covering Geometry (5 methods), Aerodynamics (17 methods), Propulsion (7 methods), Performance (15 methods), Stability and Control (2), Weight/structural estimation (28 methods) and Cost (5 methods). These methods have been integrated into AVD^{sizing} such that they can be activated and deactivated at the designer's discretion.

Documentation of design experiences

Through documenting design experience the Methods Library gives a platform to designers to share experiences. Weight and balance tends to be the place where most error in the total system originates and documenting their range of applicability is paramount. For example, a wide variety of weight methods exist for cantilever wings. These methods are based on various analytic expressions and past wing designs; however, some methods are unclear as to the range of applicability. From experience it has been found that the semi-empirical weight method from Howe is only applicable up to aspect ratio 9 wings. This method uses a closed form analytical expression for the weight of bending material required in the wing box and an empirical relationship for the shear and torsion structural weight. It has been discovered with experience that above an aspect ratio of 9 this method will under predict wing weight. In this case the designer must be aware of this experience to avoid improper usage of the method.

Figure 3-7 shows the results of the B777-300ER when using both Howe's Method ⁽³⁶⁾ and the General Dynamics (empirical) weight methods (20). In the case of Howe's method, the Aspect ratio 15 wing demonstrates a minimum in terms of direct operation cost (DOC). In contrast, the General Dynamics method predicts that an aspect ratio of 9 is more appropriate. While the Aspect ratio 9 wing agrees well with the actual B777 for both methods, see Figure3-7,

Howe's method does not correctly represent the weight penalty of the higher aspect ratio, thus leads to an incorrect trend. This issue has also been observed with the semi-empirical weight estimation used in FLOPS⁽⁸⁰⁾.



	B777-300ER	B777-GD	% error	B777-Howe	% error
Geometry					
τ		0.2		0.21	
AR	9.25	9.00	-2.69%	9.00	-2.69%
S_{pln} (m ²)	454.00	471.60	3.88%	457.46	0.76%
b (m ²)	64.80	65.15	0.54%	64.17	-0.98%
l_{fus} (m)	73.08	74.05	1.32%	74.22	1.56%
d_{fus} (m)	6.20	6.28	1.32%	6.30	1.56%
Weight					
TOGW (kg)	351535	352484	0.27%	352386.47	0.24%
W_{fuel} (kg)	145538	144607	-0.64%	148382.83	1.95%
MLW (kg)	251290	251956	0.26%	251885.85	0.24%
$(W_{PAY})_{design}$ (kg)	38168	38168	0.00%	38168	0.00%
OEW (kg)	167829	169709	1.12%	165835.64	-1.19%
Aero-Propulsion					
ff	0.41	0.41	-0.91%	0.421	1.71%
Thrust (kN/engine)	514.00	510.81	-0.62%	516.68	0.52%
Alt_{cruise} (m)		10731		10643	
L/D_{cruise}		18.19		18.01	
SFC_{cruise} (/hr)	0.56	0.55	-2.62%	0.56	0.00%
Cost					
DOC (\$/pax-km)		0.076		0.077	
Unit price (\$ M)	202	200	-1.09%	198.34	-1.81%

Fig 3-6: Comparison of Howe's semi-empirical wing weight method to the empirical General Dynamics methods(trade-study via AVD^{sizing})

This experience is documenting the significance of the methods library. Technical decision-making critically depends on results generated with methods which either accurately or falsely predict a technical outcome, mostly without the knowledge of the operating engineer. The weight method example vividly illustrates the problem at hand. The methods library becomes an essential tool to reduce the risk in technical decision-making.

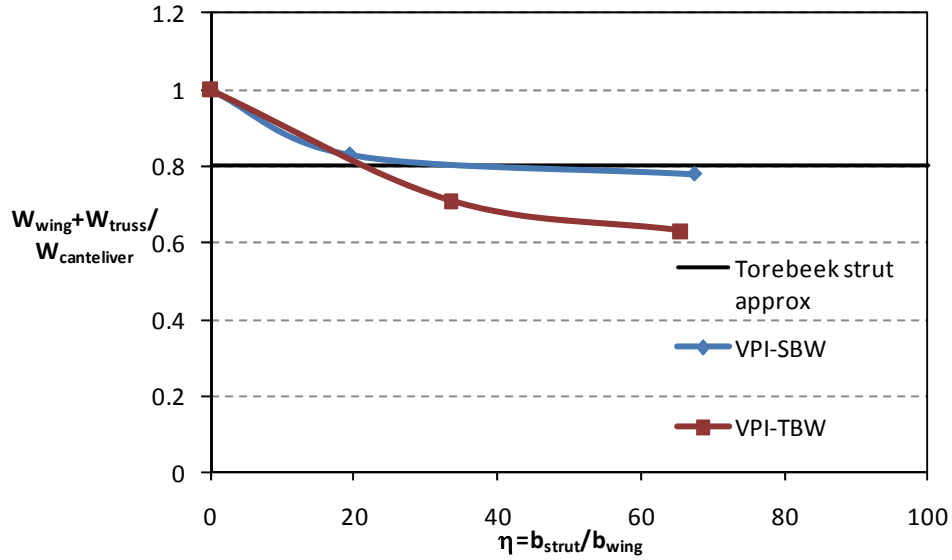
Development and Research of New Methods

In the case of many unconventional design and mission methods do not exist for the design problem and must be developed. In this case the designer must typically start with adapt an existing method and later initiate a technology investigation to develop a more appropriate method. For example, NASA LaRC (Langley Research Center in Hampton Virginia) is currently funding research into a laminar flow truss-braced wing for wide-body transports through Virginia Polytechnic Institute VPI⁽⁸¹⁾. In order to provide laminar flow the chord length must be reduced (increase aspect ratio) and thin airfoils are required, however, the resulting wing will suffer a sever weight penalty. External bracing is proposed to reduce this weight penalty, resulting in a truss-braced wing.

An important element in analysis of such a configuration is to estimate the total wing group weight. Methods exist for smaller, slower strut-braced wings such as Torenbeek's 80% correction factor which states that a strut braced wing will weigh 20% less than a cantilevered wing⁽¹⁸⁾. Since this correction was derived for much slower aircraft, VPI ran a series of FEM experiments with various strut locations for comparison with a classical cantilever wing.

During a review of this work the author superimposed these results on top of the 80% correction factor and found that VPI results asymptotically approach the 80% correction factor for strut braced wings and approach 60% for truss braced wings (Figure 3-8) In Figure 3-8 the

strut wing intersection (η) is varied and the resulting ratio of the wing-truss weight to the baseline cantilever wing is shown.



Design	# Members	0	1	1	3	3
	Telescopic	-	Yes	No	Yes	No
Configuration	Wing location member 2 % halfspan	-	87.5%	19.5%	32.8%	17.08%
	Wing location member 3 % halfspan	-	-	-	65.5%	33.5%
Results	Wing bending material weight	9057 kg	3739 kg	5769 kg	3835 kg	3908 kg
	Truss weight	0 kg	3279 kg	1755 kg	2515 kg	1879 kg
	Total weight	9057 kg	7077 kg	7524 kg	6350 kg	5787 kg
	Weight reduction wrt. cantilever wing	-	21.86 %	18.93 %	29.89 %	36.10 %

Fig 3-7: Development of trend data for strut and trust braced wings based on past experience with low-speed strut aircraft and Initial VPI FEM structural design study⁽⁸¹⁾. Remove bar graph ad graphic⁽⁸¹⁾

With this information at hand, a classical cantilever wing weight estimation method can be used during parametric sizing and total wing group weight can be corrected based on the strut wing intersection-location.

This example demonstrates how an existing method can be modified for a new design problem. The incorporation of FEM analysis to gain an understanding of the 1st order effects of external bracing can be incorporated into the methods library for future strut and truss braced wings.

This approach should not be confused with full aero-structural MDO (Multi-disciplinary Optimization), which occurs later in the design phase. The objective is not to determine the optimal wing strut combination but rather to identify the first order structural sensitivities and effects of the external bracing such that a multidisciplinary assessment of the total aircraft will be possible in a reasonable amount of time. If the 1st order assessment of external bracing identifies a significant performance improvement, then more rigorous MDO analysis is warranted in a later step.

3.3 Contribution Summary

The disciplinary methods library consists of the disciplinary analysis methods which form the building blocks of the any aircraft design process. The following presents the contribution summary.

Process and Disciplinary Methods Library Contribution Summary

1. A practical design library for organizing the designer's tool box.
2. A unique cross-section of design processes from 1936 to the present, consistently documented, analyzed, and interpreted.
3. A standard presentation of existing methods for parametric sizing, allowing the designer to select the most appropriate method for the given problem.
4. A standard documentation platform for documenting method experience. Thereby indicating a more specific range of applicability for the method.

5. A standard documentation platform for new methods. Adding in the identification of the need for new methods.
6. In general, a standard platform for retaining disciplinary and multi-disciplinary knowledge.

CHAPTER 4

PARAMETRIC SIZING PROCESS AVD^{SIZING} DESCRIPTION

In order to develop a flexible and well balanced parametric sizing process it is necessary to have the logic organized such that,

1. Geometry and configuration assumptions must be collected in a central location in the sizing logic
2. Wide variety of disciplinary methods must be integrated
3. Consistent Visualization of the design space across all vehicles and missions.

The sizing process presented is based on the constant mission sizing logic of Hypersonic Convergence by Paul Czysz⁽⁶⁴⁾. The process is based on an algebraic sizing process which solves for weight and planform area simultaneously through converging weight and volume for a given set of design variables. Most sizing processes, see Chapter 3, converge weight only (i.e. compute the fuel and empty weight for a given trajectory), then volume is checked as an inequality constraint. For hypersonic aircraft (cruisers or launchers), fuel volume is typically more constraining than payload (opposite to transonic aircraft). Thus, by using volume as equality constraint instead of an inequality constraint the sizing problem can be reduced to fewer fundamental design variables. Numerically, the reduction of one design variables (via 1 additional equation, volume) is not significant. However, for design space visualization this technique has proven useful for increasing the physical understanding of the design space for both unconventional and conventional aircraft.

In order to adequately describe the sizing process employed in AVD^{sizing}, the process description and derivation will begin at the heart of matter, convergence of the volume and weight budget. From the weight and volume budgets, the trajectory (fuel required estimation),

and constraint analysis ($T/W=f(W/S)$) are described. These elements provide the fuel fraction, and T/W required to perform the mission. The weight and volume budgets, trajectory analysis and constraint analysis all utilize modules representing the classical aerospace disciplines of aerodynamics, propulsion, structures, stability and control, and weight and balance, which are described in the disciplinary methods library, see Appendix B.

Feeding these methods is the geometry of the aircraft. The geometry module acts as the 'gearbox' of the system aircraft where the geometry is specified through algebraic equations and constant values which adapt the configuration for each new planform area, see Figure 4.1.

Formulated in this manner, the fundamental process is applicable to any fixed wing aircraft or launcher with changes in the disciplinary methods and geometry module when appropriate.

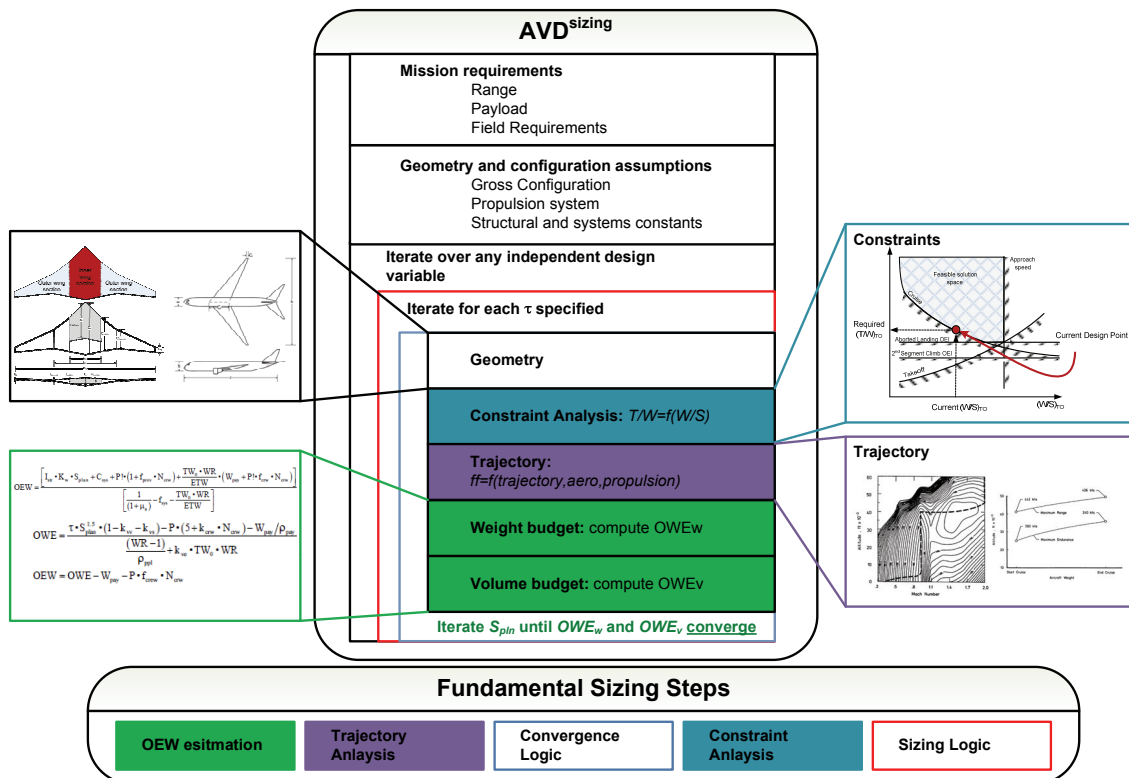


Fig 4-1: Fundamental AVD^{sizing} Logic.

4.1 Weight and Volume Budget

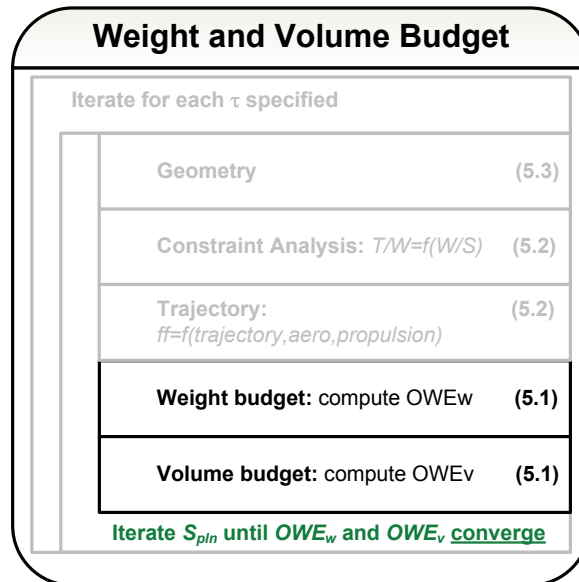


Fig 4-2: Weight and balance convergence

At the heart of the process is the convergence of the weight and volume budgets, see Figure 4-2. Fundamentally, convergence can be thought of an algebraic system of two equations and two unknowns. In this case Equations 4.1 and 4.2 are the total weight and volume of the aircraft, with the two unknown OEW and S_{pln} . Through the substitutions in Table 4.1 it is clear

Weight Budget $OEW = W_{str} + W_{eng} + W_{sys} + W_{operationa\ l\ items}$ 4.1

Volume Budget $V_{tot} = V_{fuel} + V_{sys} + V_{eng} + V_{void} + V_{pay} + V_{crew}$ 4.2

Table 4-1: Weight and Volume Budget Terms from Hypersonic Convergence ⁽⁶⁴⁾

Variable	Description	Hypersonic Convergence Relationship
Weight Budget		
W_{str}	Structural weight	$W_{str} = I_{str} S_{wet}$
W_{sys}	Systems weight	$W_{sys} = C_{sys} + f_{sys} W_{OEW}$
W_{eng}	Engine weight	$W_{eng} = \frac{T/W \cdot WR}{E_{TW}} OWE$
C_{sys}	Constant systems weight	-
f_{sys}	Variable systems weight	-
E_{TW}	Engine thrust to weight ratio	-
I_{str}	Structural index	See methods library
Volume Budget		
V_{fuel}	Fuel volume	$V_{fuel} = \frac{OWE \cdot (WR - 1)}{\rho_{fuel}}$
V_{fix}	Fixed system volume	$V_{fix} = V_{un} + V_{optems}$
V_{sys}	Total system volume	$V_{sys} = V_{fix} + k_{vs} V_{tot}$
V_{eng}	Engine volume	$V_{eng} = k_{ve} \cdot T/W \cdot WR \cdot OWE$
V_{void}	Void volume	$V_{void} = k_{vv} V_{tot}$
V_{pay}	Payload volume	$V_{pay} = W_{pay} / \rho_{pay}$
V_{crw}	Crew volume	$V_{crw} = k_{crw} N_{crw}$
V_{tot}	Total volume	$V_{tot} = \tau \cdot S_{pln}^{1.5}$
V_{un}	Unused volume	-
V_{optems}	Operational items volume	-
ρ_{fuel}	Fuel density	-
ρ_{pay}	Payload density	-
k_{ve}	Engine volume coefficient	-
k_{vv}	Void volume coefficient	-
k_{vs}	Variable systems volume	-

Since τ is utilized as a design variable (constant at the time of convergence), it is possible to find a numerical solution to this system for OEW and S_{pln} simultaneously, see Equations 4.3 and 4.4.

$$\text{Weight Budget} \quad OEW = \frac{W_{str} + W_{sys} + W_{operational\ items} + \frac{T/W \cdot WR}{E_{TW}} (W_{pay} + W_{crew})}{\frac{1}{1 + \mu_a} - f_{sys} - \frac{T/W \cdot WR}{E_{TW}}} \quad 4.3$$

$$\text{Volume Budget} \quad OWE = \frac{\tau \cdot S_{p\ln}^{1.5} (1 - k_{vw} - k_{vs}) + V_{pay} + V_{crew}}{\frac{WR - 1}{\rho_{ppl}} - k_{ve} \cdot T/W \cdot WR} \quad 4.4$$

Note: $OWE = OEW + W_{pay} + W_{crew}$

Inside the iterative solution, various methods can be utilized for the estimation of structural weight and systems weight, which are typically a function of *TOGW* and geometry. In order to proceed with the solution, an estimate of *T/W* and *WR* are required which come from the constraint and trajectory analysis. The remaining variables are held constant during convergence. See Methods Library, Appendix B for description of methods. It is important to note that this logic requires an initial estimate of *TOGW* and *S_{p_{ln}}*.

4.2 Trajectory and Constraint analysis

In order to converge to *OEW* and *S_{p_{ln}}* for a given tau value, the total *T/W* required and *WR* (or fuel fraction *ff*) are required. The required *T/W* is a function of the performance constraints and the *WR* is a function of the flight path trajectory. This chapter will discuss the implementation of these modules (Figure 4-3).

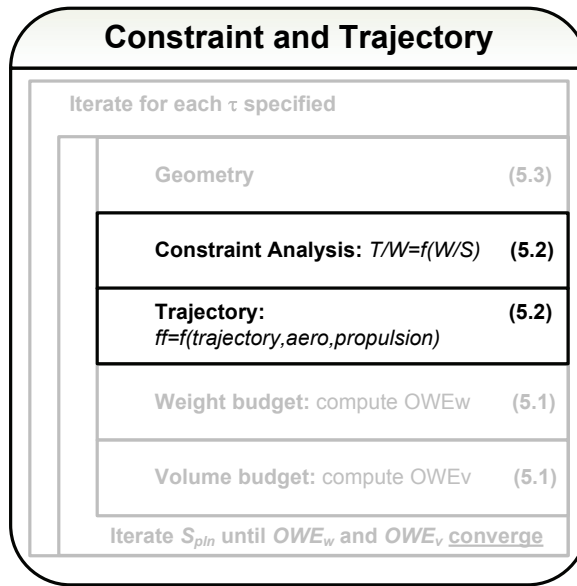


Fig 4-3: Trajectory and constraint analysis.

Constraint Analysis

The constraint analysis is analogous to the performance matching method described by Loftin ⁽¹⁶⁾. Where Loftin varies W/S and computes the T/W required for each mission phase, AVD^{sizing}'s sizing logic is constantly updating $TOGW$ and S_{pln} with W/S becoming an output. During each iteration $(W/S)_{TO}$ is known, thus the constraint analysis computes the T/W required for each mission segment and maximum T/W required is taken forward into the weight and volume convergence logic, see Figure 4-4.

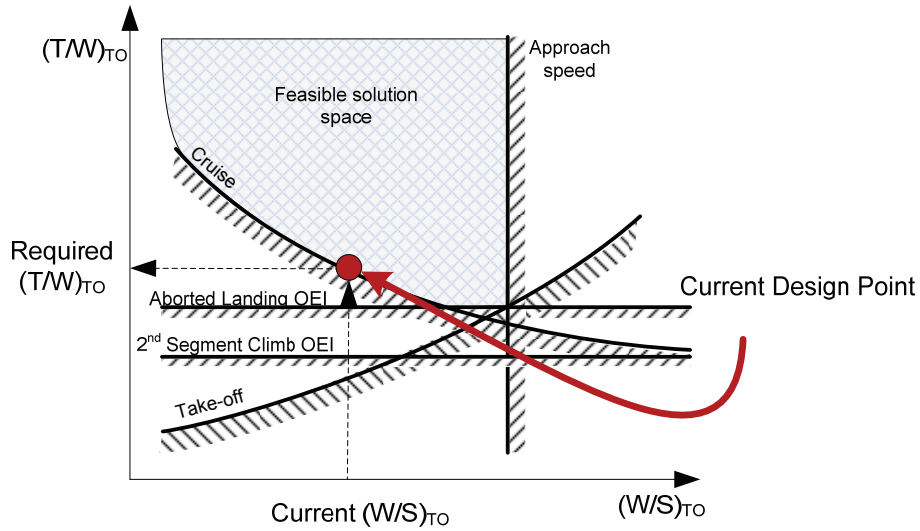


Fig 4-4: For the given iteration the W/S is known and thus the maximum T/W required is computed from the performance constraints.

Trajectory Analysis

The objective of the trajectory analysis is to compute the fuel fraction required to perform the specified mission. There are many methods available to perform this analysis ranging from Breguet range to a minimum fuel burn trajectory method as used in FLOPS⁽⁵¹⁾. AVD^{sizing} offers two trajectory options for transonic transports and one method for hypersonic cruisers.

Breguet based trajectory

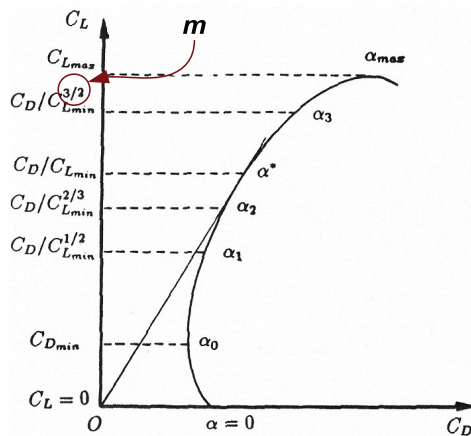
This method is based on the classical mission breakdown with the fuel fraction for taxi, take-off, descent and landing being assumed from typical values. Climb and cruise fuel fractions are computed from the Breguet range and endurance equation.

The climb fuel fraction is estimated with the L/D and SFC from the optimum cruise velocity for the required time to climb, see Equations 4.5 – 4.6.

Climb velocity $V_{\text{climb}} = \sqrt{\frac{2(W/S)}{\rho C_{L/D \max}}} \quad 5.5$

Fuel fraction $f_{\text{climb}} = 1 - e^{\frac{-T_{\text{climb}} SFC}{L/D}} \quad 5.6$

For the cruise mission segment, there are two options available: (1) Constant altitude cruise, and (2) constant cruise-climb. In both cases the cruise range is broken into several small increments. The cruise altitude can be specified in both cases as a design constant or can be solved for based on the desired drag polar location, see Figure 4-5 as demonstrated by Vihn⁽⁸²⁾. As shown, the requirement to cruise at L/D max can lead to an excessive thrust requirement for the cruise segment. By designing the aircraft to fly at a lower cruise L/D, a smaller and lighter engine can be used.



$$C_L = \sqrt{\frac{m}{m-1}} \sqrt{\frac{C_{D0}}{L}}, \quad L/D = \frac{\sqrt{m(2-m)}}{2\sqrt{L C_{D0}}}$$

Fig 4-5: Illustration of drag polar location exponent m ⁽⁸²⁾.

Knowing the required C_L , and having calculated the cruise velocity and wing loading (W/S) with the sizing logic, it is then possible to numerically solve for the required cruise altitude. This method is derived from a similar cruise altitude method proposed by Loftin⁽¹⁶⁾.

The cruise-climb option re-computes the cruise required cruise altitude across each range segment with the updated wing loaded (weight reduced by the fuel burned in previous range segments). Reserve fuel is computed at a specified velocity and altitude with either an endurance or range requirement.

FLOPS Trajectory subroutine MISSION⁽⁵¹⁾

The trajectory method in Flops uses an integration technique across all segments of fight to provide precise values for fuel burned, elapsed time, distance covered and changes in altitude and speed⁽⁵¹⁾. The primary integration occurs over climb, cruise and descent with various options for each as summarized in Table 4-4.

Table 4-2: Trajectory options in MISSION⁽⁵¹⁾

	Climb	Cruise	Descent
<i>Description</i>			
	For climb optimization the climb is divided into a series of energy steps and then the optimum path can be found according to the options specified	Using a finite difference method the range is divided into several components. At each component the drag, thrust and fuel flow are computed. The required cruise trajectory is then determined using optimization according to the following options.	Descent is divided into a series of energy steps and then the path is determined along the following options
<i>Options</i>			
Minimum time to climb	<u>Altitude</u>	<u>Mach</u>	<u>Objective</u> Specified profile
Minimum fuel	Optimum	Optimum	Range Constant CL
Minimum time to distance (interceptor mission)	Optimum	Fixed	Range Maximum L/D
Minimum fuel to distance (most economical)	Fixed	Fixed	-
	Fixed	Optimum	Range
	Fixed	Optimum	Endurance
	Fixed	Variable	Constant CL
	Optimum	Fixed	Endurance
	Optimum	Optimum	Endurance
	Fixed	Maximum	Max Speed
	Optimum	maximum	Max Speed
	Variable	Fixed	Constant CL

Energy integration for a typical hypersonic cruiser climb cruise and descent trajectory

This method is very similar to the FLOPS MISSION method described above with the climb set to a specified profile, cruise performed at a constant C_L and descent at maximum L/D . The method is currently only available for hypersonic cruisers. With the inclusion of the FLOPS MISSION subroutine this method is no longer required but is available for backward compatibility of the Hypersonic cruiser models.

With the required T/W and fuel fraction in hand, all of the information is available for weight and volume convergence. The remaining elements to be described are the geometry which drives the disciplinary methods and the numerical convergence methods.

4.3 Geometry Module

The geometry module updates the geometric properties during the convergence logic. As the planform area is updated by the weight and volume budget the, other geometric parameters may change with constant τ . These can be constant or change by a geometric relationship depending on the configuration, see Figure 4-6. The best way to describe the geometry module is through an example.

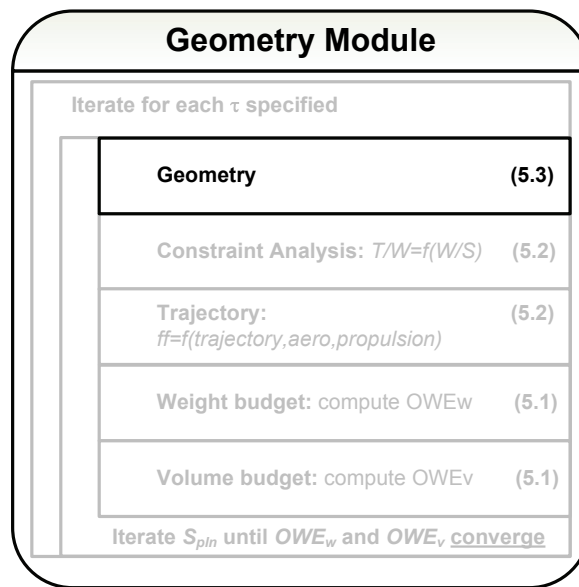


Fig 4-6: Geometry Module.

Tail-Aft Transonic Transport

Wing and Fuselage

Through the convergence logic the value of the slenderness parameter τ ($\tau = V/S_{pln}^{1.5}$) is constant and the latest estimate of planform area (S_{pln}) is known, thus the total volume required is known. This leaves the designer the option of deciding how to distribute this volume across the aircraft. For the traditional tail-aft aircraft the intent is to optimize the wing primarily for aerodynamic performance, while the fuselage represents the primary volume supply. Thus,

by specifying the wing shape and fuselage shape parameters, we size the aircraft's wing and fuselage simultaneously for τ . The wing size (S_{pln}) is known to the geometry module, thus the fuselage will be resized (l_{fus} , d_{fus}) according to τ .

The shape of the wing is specified as summarized in Table 4-5. The planform is defined by aspect ratio, taper ratio and sweep angle where the thickness ratio is computed from transonic critical Mach number expression from Howe (36), analogues to the Korn equation⁽⁸³⁾.

Table 4-3: Wing Definition for Transonic Transports

Variable	Description
<i>Given</i>	
AR	Aspect ratio (input)
λ	Tapper ratio (input)
Λ_{LE}	Leading edge sweep (input)
M_{cr}	Desired wing critical Mach number (input)
<i>Computed</i>	
b	Span $b = \sqrt{AR \cdot S_{pln}}$
c_r	Root chord $c_r = \frac{2}{1 + \lambda} \frac{S_{pln}}{b}$
c_t	Tip chord $c_t = \lambda \cdot C_r$
\bar{c}	Mean aerodynamic chord $\bar{c} = \frac{2}{3} c_r \frac{1 + \lambda + \lambda^2}{1 + \lambda}$
$(t/c)_{avg}$	Average wing thickness $(t/c)_{avg} = 0.95 - 0.1(C_L)_{cruise} - M_{cr} \cos^m \Lambda_{c/4}$
V_{wing}	Wing volume $V_{wing} = 0.54 \cdot \frac{S_{pln}^2}{b} b \cdot (t/c)_{avg} \frac{1 + \lambda + \lambda^2}{(1 + \lambda)^2}$

With the wing volume computed, the fuselage size can be found to yield the desired τ by specifying the desired shape of the fuselage (l/d , h/w) as demonstrated in Table 4-6.

Table 4-4: Fuselage definition for transonic transports

Variable	Description	
<i>Given</i>		
l/d	Fuselage slenderness ratio (input)	
h/w	Cabin eccentricity (high/width) (ADD CONSTANT CABIN)	
<i>Computed</i>		
d_{max}	Maximum diameter of fuselage	$d_{max} = \frac{\tau \cdot S_{pln}^{1.5} - V_{wing}}{\left(\frac{\pi}{4} l/d \left(1 - \frac{2}{l/d}\right)\right)^{1/3}}$
l_{fus}	Length of fuselage	$l_{fus} = d_{max} \cdot l/d$
w_{fus}	width of fuselage	$w_{fus} = d_{max} / \sqrt{h/w}$
h_{fus}	height of fuselage	$h_{fus} = w_{fus} \cdot h/w$

Note, if the nacelles are located on pylons under the wings, no volume is added to the volume budget nor is it required by the geometry.

Control Surfaces

The control surface sizing is linked to the wing area through the use of a modified volume quotient method from Hahn⁽⁸⁰⁾ and modified by Morris⁽⁸⁴⁾, see Figure 5-7. See methods library for further description.

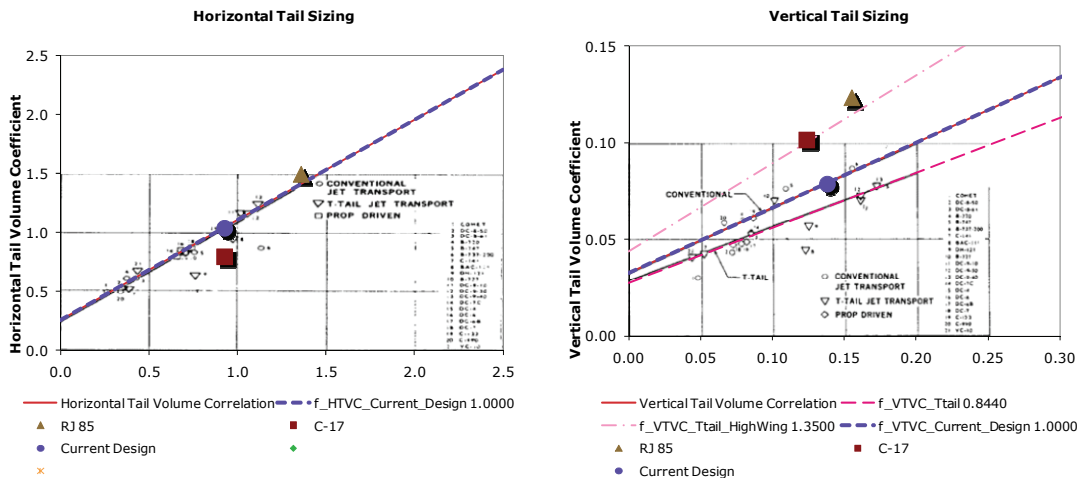


Fig 4-7: Modified Tail Volume Quotient⁽⁸⁰⁾.

Truss braced wing (TBW) and Strut braced wing (SBW) Tail-Aft Transonic Transport

The TBW/SBW's fuselage wing and empennage are treated in a similar fashion to the TAC with additional struts added under wing, see Figure 4-8.

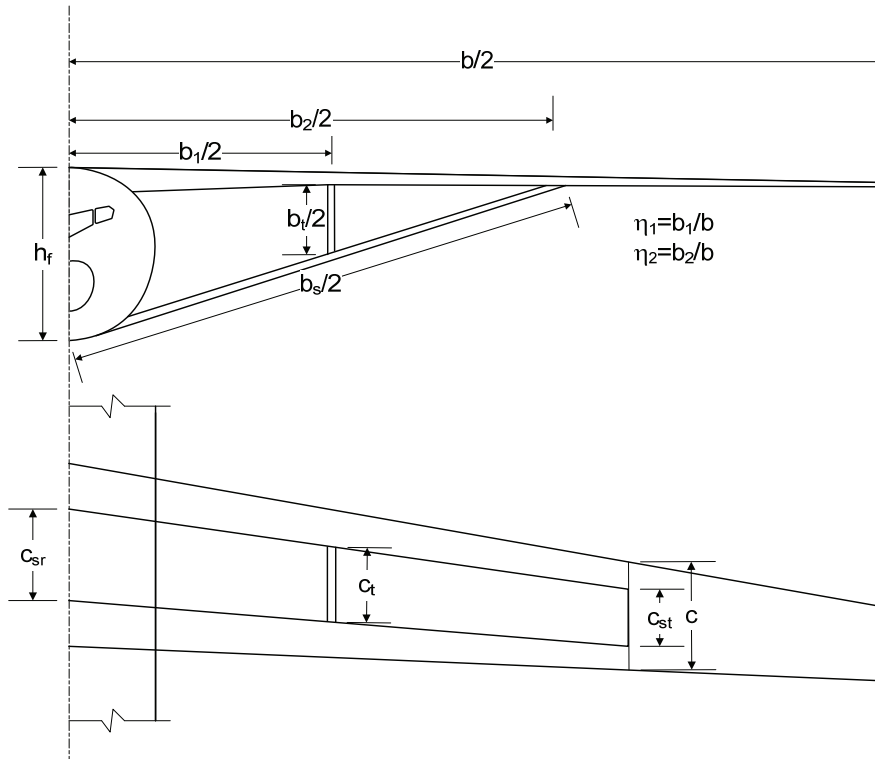


Fig 4-8: SBW/TBW Geometry Definition.

The spanwise location and percent of wing chord and t/c of the strut and truss members are specified as independent design variables. The volume and wetted area of these members are computed using the same relationships for the wing. Additional methods are required for interference and weight effects, see methods library Appendix B.

Flying Wing Transonic Transport

The flying wing configuration (FWC) or blended wing body (BWB) presents the challenge of combining the primary volume supply, lift supply and control into one lifting surface. The coupling of these surfaces requires the wing thickness to vary such to meet current τ and platform values. As with tail aft aircraft, the wing thickness is coupled to the wing sweep angle

through critical Mach number effects. This creates an aircraft which is very geometrically responsive to changes in planform area and τ . The build up the analytic equations for the Blended Wing Body (BWB), the planform is broken down into (1) inner wing planform, (2) outer wing planform, and (3) total volume, see Figure 5-8.

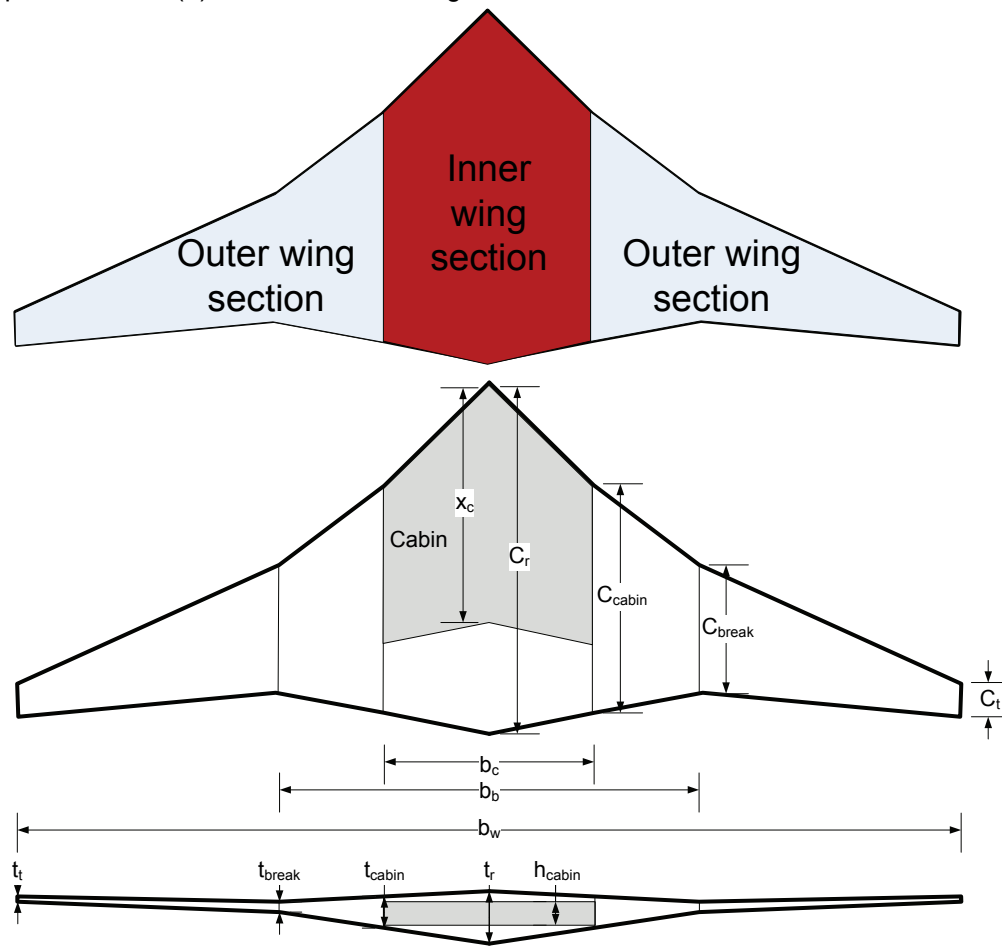


Fig 4-9: Definition of the planform of a generic blending wing body.

Definition of the inner wing planform

The inner wing planform consists of two parts, the cabin and aft section, see Figure 4-8. The cabin presents the first constraints for the BWB in terms of (1) cabin height (2).cabin floor area and (3) cabin aspect ratio. The cabin height requires that the outboard section of the cabin must be sufficiently thick to accommodate the passengers, overhead bins and structure. This

constraint does not explicitly apply to the root where the airfoil thickness could be higher compared to the minimum height required for the cabin.. In the AVD^{sizing} the required passenger volume is known; then by specifying cabin height the cabin floor area is known. The cabin aspect ratio controls the shape of the cabin floor for passenger cabin evacuation. If the cabin aspect ratio is too low, the number of emergency exits will be insufficient along the side of the aircraft. Leibeck⁽⁸⁵⁾ states, as a rule of thumb, that the cabin aspect ratio should be larger than 4.0 for proper cabin evacuation. This provides three geometric relationships, see Equations 4.7, 4.8 and 4.9.

$$\text{Cabin height} \quad t_c = h_{cab} \Rightarrow \left(\frac{t}{c}\right)_c = \frac{h_{cab}}{c_r \lambda_c} \cdot (h_{cab}/t_c)_{req} \quad 4.7$$

$$\text{Cabin floor} \quad S_{cab} = V_{pax} / h_{cab} \quad 4.8$$

$$\text{Cabin Aspect ratio} \quad AR_{cab} = \frac{b_c^2}{S_{cab}} \Rightarrow b_c = \sqrt{AR_{cab} S_{cab}} \quad 4.9$$

The final piece required to define the cabin section is the percent of the chord the cabin occupies (x/c). Having defined the chord-occupation of the cabin, the cabin area plus the aft body area (S_f) and wing area can be defined as shown in Figure 4-8.

In summary, the cabin and aft section of the BWB are controlled by the height cabin (h_{cab}), the cabin chord wise occupation (x/c), and cabin aspect ratio (AR_{cab}).

Definition of wing section planform

To define the wing planform, a new variable is introduced with η_b which is defined along with the outer wing taper ratios relative to the chord length at the edge of the cabin, see Figure 4-10. This is done to allow for typical taper ratios of transonic transport wings.

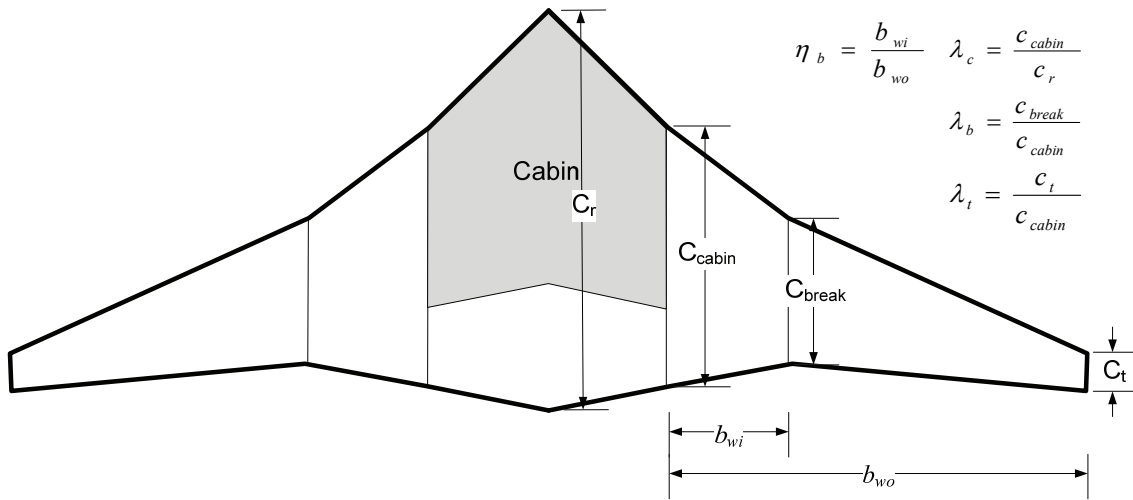


Fig 4-10: Definition of outer wing.

By specifying the outer wing AR and given the current estimate of planform area required, the total span breakdown can be computed.

Total Volume Definition

Starting from the volume of an irregular truncated prism with a defined thickness (t) and length (c), all that is required is a shape variable (k_{sf}) describing the area, see Figure 4.11.

Typical shape variables are listed in Table 4-7.

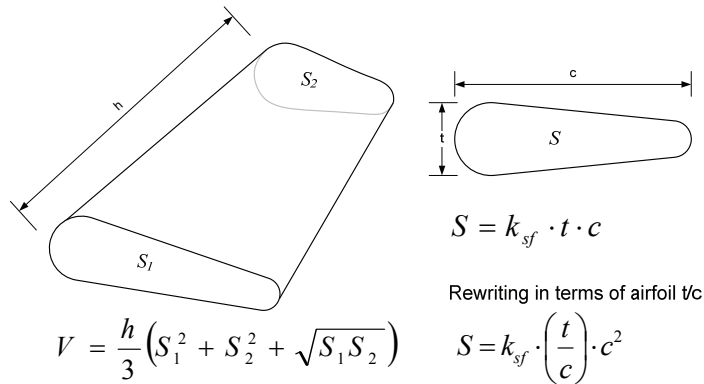

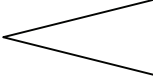
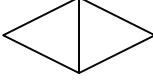



Fig 4-11: Definition of the volume of an irregular prism⁽⁸⁰⁾.

Table 4-5: Typical shape factors for geometric shapes

Shape		k_{sf}
Square		1
Triangle		1/2
Diamond		1/2
Torenbeek approximation of a fuel tank within a wing structure ⁽¹⁸⁾		0.54

Defining the planform according to Figure 4-8, each wing section can be treated as an irregular truncated prism and the sum of the section volumes yields Equation 4.9. The variables are described in Table 4-8.

$$V_{total} = k_{sf} c_r^2 b \left[\begin{aligned} & \eta_1 \left(\frac{t}{c} \right)_r (1 + \lambda_c^2 + \lambda_c) + \\ & + \lambda_c^2 \left((\eta_2 - \eta_1) \left(\left(\frac{t}{c} \right)_c + \left(\frac{t}{c} \right)_t \lambda_b^2 + \sqrt{\left(\frac{t}{c} \right)_c \left(\frac{t}{c} \right)_t} \right) \lambda_b \right) + \\ & + (1 - \eta_2) \left(\left(\frac{t}{c} \right)_c \lambda_b^2 + \left(\frac{t}{c} \right)_t \lambda_t^2 + \left(\frac{t}{c} \right)_t \lambda_b \lambda_t \right) \end{aligned} \right] \quad 4.7$$

Table 4-6: Planform definitions for the blended wing body

Variable	Description	
η_1	Ratio of span location of cabin to total span to	$\eta_1 = \frac{b_c}{b_w}$
η_2	Ratio of wing break to total span	$\eta_2 = \frac{b_b}{b_w}$
$\left(\frac{t}{c}\right)_r$	Airfoil thickness ratio at root	
$\left(\frac{t}{c}\right)_c$	Airfoil thickness ratio at edge of cabin	
$\left(\frac{t}{c}\right)_t$	Airfoil thickness ratio at wing break point and wing tip	
λ_c	Tapper ratio at the edge of cabin	$\lambda_c = \frac{c_{cabin}}{c_r}$
λ_b	Tapper ratio at the wing break	$\lambda_b = \frac{c_{break}}{c_r}$
λ_t	Tapper ratio at the wing tip	$\lambda_b = \frac{c_t}{c_r}$

With the inner and outer wing planforms defined, the only variables left to be solved for are the wing thicknesses. The thickness ratios utilized in the sizing logic to geometrically fit the volume required to the volume available for the current estimate of planform area and value of τ . However, currently we have one equation for the volume, see Equation 5.7, and two unknown t/c_r and t/c_t . Recall that from the cabin height requirement, see Equation 5.7, we obtain a required t/c at the edge of the cabin.

To enable a closed form solution, an additional equation is required. Assuming a thickness to chord distribution provides such an equation. Assuming a similar thickness distribution as used by Liebeck⁽⁸⁵⁾, the thickness to chord ratio decreases linearly from the root to the outer wing break point and is then constant to the wing tip as shown in Figure 4-12.

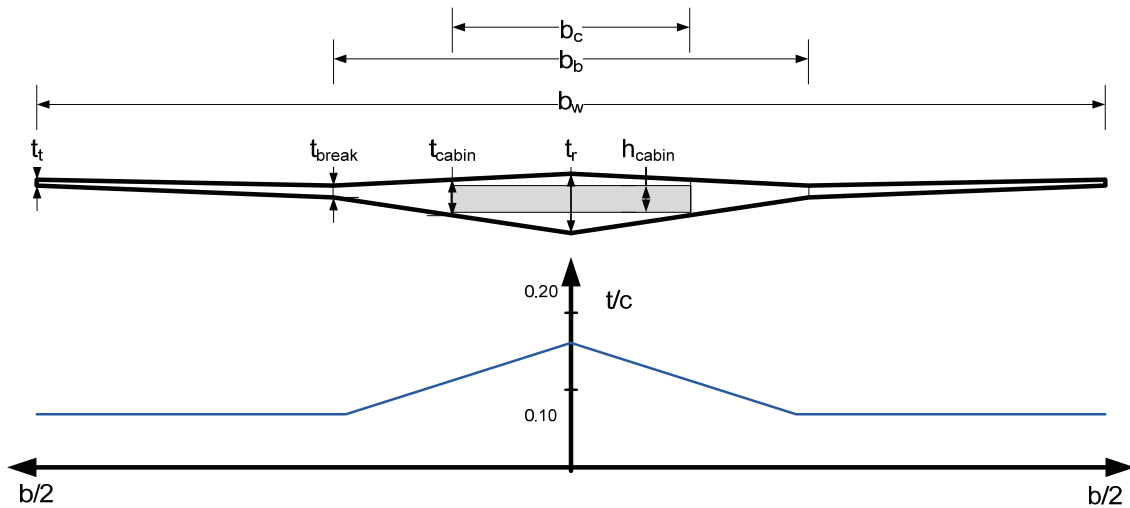


Fig 4-12: Assumed thickness distribution.

To completely describe the distribution, one of the following must be defined: (1) t/c_r , (2) t/c_t or (3) the slope of t/c from root to wing break. Of these three options, the most reasonable appears to be the outer wing thickness which can be selected based on past transonic wing designs. Therefore, in order to meet the required volume specified by τ and planform area, the root thickness to chord ratio and the slope of the thickness to chord ratio are solved for simultaneously via a numerical solution. See the methods library for a summary of all the geometric relationships.

Hypersonic Cruiser/Glider

Hypersonic cruisers in the AVD^{sizing} logic fall into one of two categories: (1) hypersonic gliders with flat bottom geometry, and (2) propulsion integrated hypersonic cruisers and accelerators.

Hypersonic Gliders

The lifting bodies are defined by a planform area and several combinations of base area shapes, see Figure 5-13.

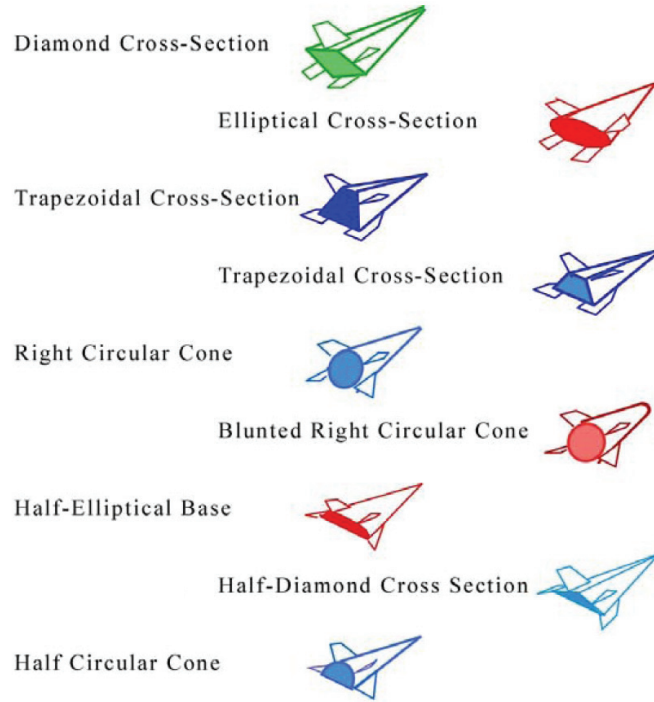


Fig 4-13: Example delta wing planforms with various base areas⁽⁶⁴⁾.

Through specifying the base shape, the required geometric relationships can be derived for wetted area and volume.

Integrated Hypersonic Cruisers/Accelerators

The wing body configurations are typically borrowed from past experience with hypersonic cruisers as shown in Figure 4-14.

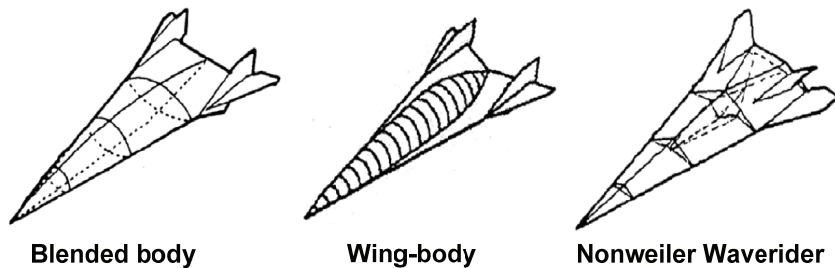


Fig 4-14: Example Propulsion Integrated Hypersonic Cruisers/Accelerators⁽⁶⁴⁾.

For each configuration, regressions are available for the wetted area and volume available based on previous design studies at McDonnell-Douglas (circa 1970). See the methods library for further details.

4.4 Convergence Logic

With the computation of the weight and volume budget, a numerical solution is required. Taking a variety of requirements and constraints into account (geometry, constraint analysis, and trajectory), the weight and volume budget equations represent a nonlinear system of equations. This requires an iterative solution, see Figure 4-15.

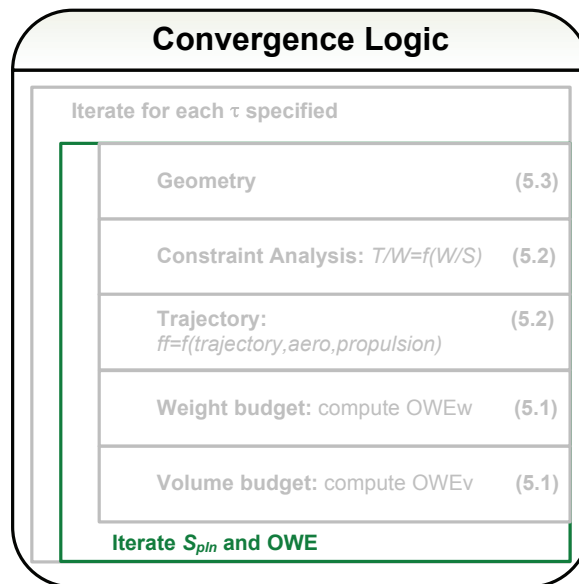


Fig 4-15: Convergence of S_{pln} , and Weight.

AVD^{sizing} is currently implementing three numerical solvers. In order to solve the two OEW equations derived from weight and volume budgets for planform area and OEW, a numerical solution is required. Currently there are three options available in AVD^{sizing}.

1. Fixed point iteration
2. Newton-Raphson solver
3. Bracketing Method

Once the solution has converged, this single design point can be plotted in the sizing diagram. For example, the primary sizing diagram for the B777 is presented in Figure 4-16.

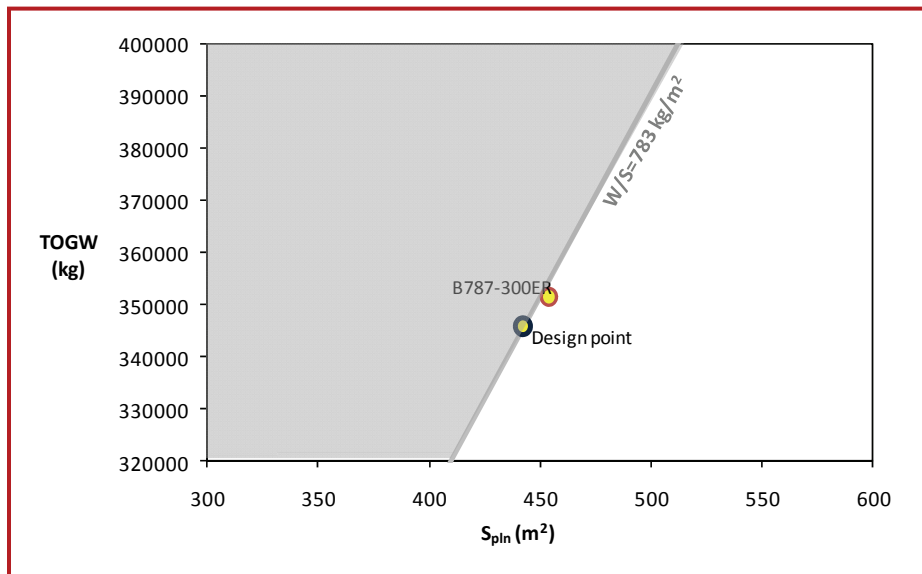


Fig 4-16: TOGW and S_{pln} , converges solution for a single value of τ .

For this design point, a complete converged aircraft data set has been saved in the database. This data-set contains all input data and all of the parameters computed for this aircraft point design, see Figure 4-17.

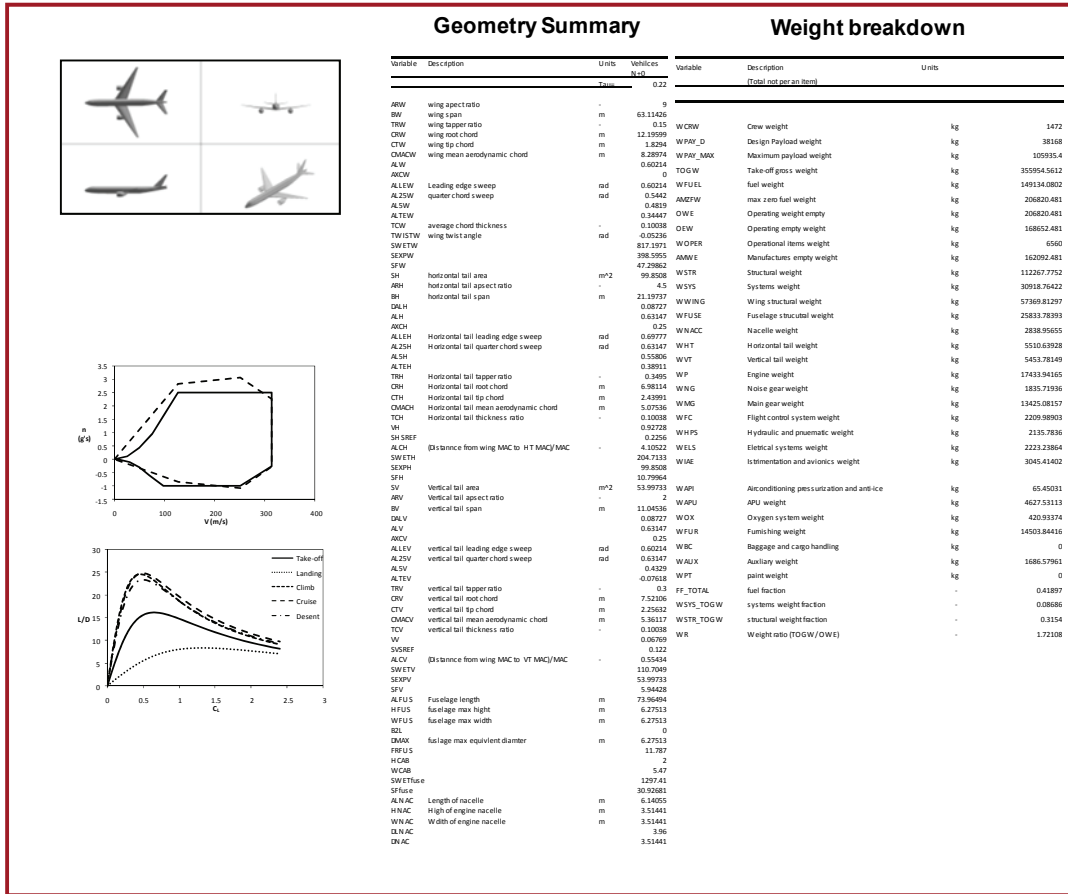


Fig 4-17: For each point a fully converged data set is compiled.

4.4 Iteration of the slenderness parameter τ

When repeating the convergence logic for several τ values yields a curve which represents all of the possible solutions for the given independent design variables, see Figure 4-18.

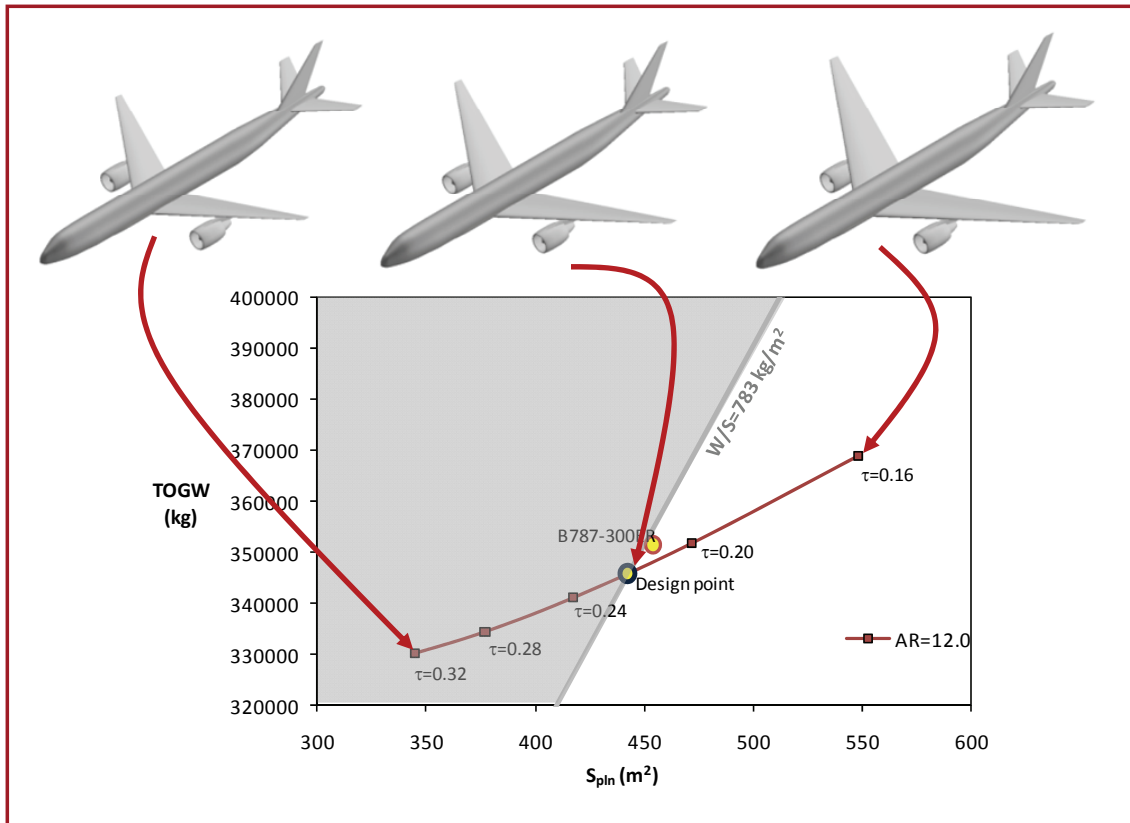


Fig 4-18: Varying τ yields the simplified solutions space in terms of TOGW and S_{plin} . The grey area is the area for which the landing wing load constraint is no longer satisfied.

The wing loading constraint (grey line) due to landing/stall does not need to be directly applied to the convergence logic since it is not a function of T/W . Landing distance is a function of approach speed, approach speed is a function of the stall velocity and thus is not a function of T/W . Thus, converged points can occur in the un-feasible side of the landing constraint. In this example for the B777, the solution which provides a minimum TOGW where the solution curve intersects the wings loading constraint.

Trade-studies can now be performed around this τ variation. For example, the B777's aspect ratio (AR) has been traded leading to three solution curves, see Figure 4-19. Comparing these curves based on TOGW, fuel weight and total DOC, it can be seen that depending on the objective function a different aircraft may be required.

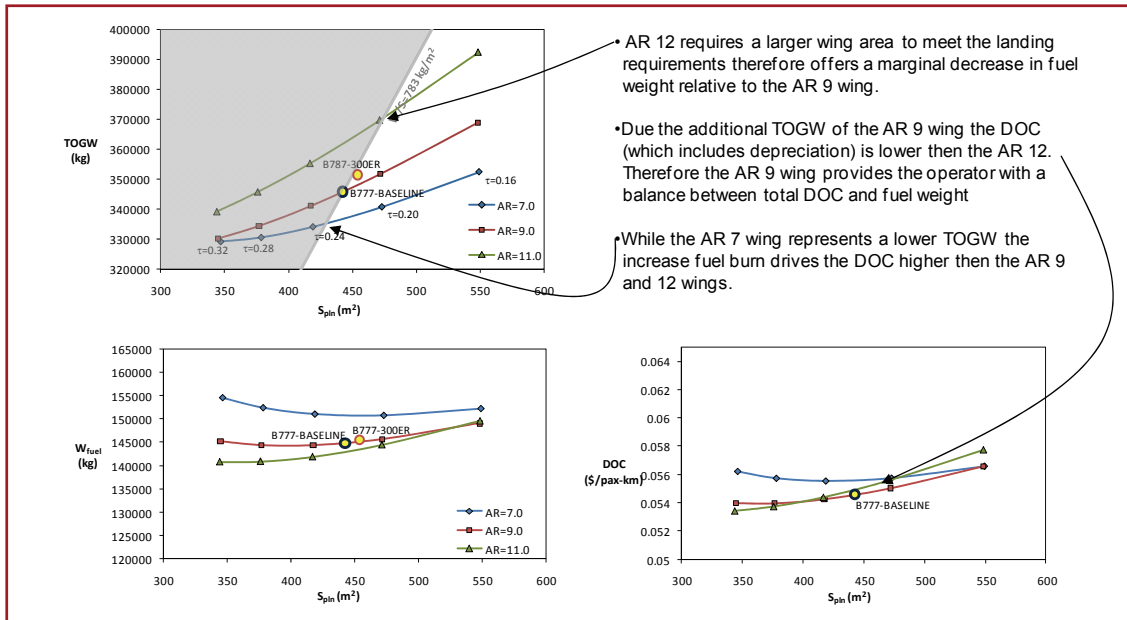


Fig 4-19: Through trading AR three solutions curves are produced. The AR 9 wing provides a balance between fuel weight savings and maintenance costs.

If minimum TOGW is the objective, then an AR 7 wing may be desirable. However, if a minimum fuel weight or DOC is the objective then the AR 9 wing is desired. This trade-study demonstrates that for a conventional TAC transport the aerodynamic benefit of high aspect ratio wings balances the higher structural weight of high aspect ratio wings around an AR of 9 for the B777 mission.

The input file for the B777-300ER AVD^{sizing} model is provided in Appendix C

4.5 Contribution Summary

1. A novel and modular design process. Allowing the same process to be applied to a wide variety of configuration and technologies with appropriate change in methods
2. Simplification of the design space visualization. By capturing the classical W/S and T/W trades into a single parameter (τ), what was once a collection of constrains can be reduced into a single curve.

3. Flexibility for process advancement. Based on the process and methods library, this process can be easily updated if new methods or process elements are found desirable.

CHAPTER 5

TRANSONIC TRANSPORT CASE STUDIES

Prior to applying any new methodology to a new product, it is important to first validate and calibrate the process with existing examples. To this end, AVD^{sizing} is applied to a wide variety of existing transonic, supersonic and hypersonic aircraft, both existing and proposed. This chapter will focus on transonic case studies examined during the PhD time frame. In order to demonstrate the unique flexibility of the methodology these studies include:

1. Tail-aft configuration (TAC) transonic transports
 - a. Business Jet - Cessna Citation X
 - b. Regional Jet – Embraer 170
 - c. Narrow Body Transport – Boeing 737-800
 - d. Wide Body Transport – Boeing 777-300ER
 - e. Wide Body Transport – Airbus A380
 - f. Composite Wide Body Transport
 - g. Composite Narrow Body Transport
 - h. Thrust Vector Controlled Wide Body Transport
2. Proposed Unconventional Transonic Transport Configurations
 - a. Boeing Blended Wing Body (BWB)
 - b. NASA LaRC/VPI Strut-Braced Wing

First then TAC studies are presented to demonstrate the accuracy and applicability of AVD^{sizing} to classical shapes and design mission. In addition these studies discuss the unique sensitive's various missions have on the classical shape.

Next, unconventional transonic transport studies are presented to demonstrate the flexibility of the methodology. When modeling project-level unconventional aircraft, there are no existing operational validation points. In order to benchmark AVD^{sizing}, the methodology is applied to the Boeing 800 pax blended wing body (BWB) study (85) and Virginia Polytechnic Institute's (VPI) strut braced wing (SBW) study (6) along their proposed design missions. The purpose of these studies is to independently assess the designs and be able to identify discrepancies in simulation results and their justification. In the case of the Boeing BWB, AVDsizing shows good agreement (Chapter 5.2), however, the VPI SBW shows serious discrepancies (Chapter 5.3).

5.1 Summary of Results for TAC Transonic Transport Studies

The TAC transonic transport case-studies are evaluated using the published formal design mission for each aircraft. AVD^{sizing} is utilized to derive the required (1) geometry, (2) weight, (3) thrust and wing location to satisfy (a) the mission, (b) minimum direct operating cost and (c) static stability with a static margin of, $0.05 < SM < 0.10$.

In addition two technology studies are briefly presented to demonstrate the capability of AVD^{sizing} to explore modifications to the classical TAC shape (1) composite B777-300ER and (2) Thrust vectored Control (TVC) B777-300ER.

Summary of Design Missions

Table 5-1 summarizes the design missions for the 5 TAC transonic transports. The transport pax payload ranges from the 6 pax design mission for the Cessna Citation X (86) to the 555 pax Airbus A380 (87). The selection of design case studies spanning this wide range of cruise range, payload and velocity is orchestrated to test the range of applicability of the methods library and process for TAC transports.

Table 5-1: TAC Transport Validation Case Studies Mission Summary^{(86) (88) (89) (90) (87)}

Mission	Citation X	E170	B737	B777	A380
Maximum payload	1,200 kg (2,645 lbs)	9,000 kg (20,062 lbs)	21,319 kg (47,000 lbs)	69,900 kg (154,000 lbs)	90,985 kg (200,587 lbs)
Design payload	6 pax 600 kg (1,320lbs)	70 pax 7,000 kg (15,400 lbs)	175 pax 17,060 kg (37,600 lbs)	325 pax 38,170 kg (84,150 lbs)	555 pax 51100 kg (119,000 lbs)
Range	5740 km (3,100 nm)	3892 km (2,100 nm)	5,560 km (3,000 nm)	14,075 km (8,000 nm)	14,186 km (7660 nm)
Velocity (design cruise)	0.85 M	0.78 M	0.78 M	0.85 M	0.85 M
Ceiling	15,500 m (51,000 ft)	12,200 m (40,000 ft)	12,200 m (40,000 ft)	12,200 m (40,000 ft)	12,200 m (40,000 ft)
Take-off Field Length (TOGW)	< 1556 m (5,100 ft)	< 1644 m (5,400 ft)	< 2286 m (7,500 ft)	< 3,048 m (10,000 ft)	2,750 m (9,020 ft)
Landing field length (MLW)	< 1036 m (3400 ft)	< 1274 m (4,180 ft)	< 1,645 m (5,400 ft)	< 1,770 m (5,780 ft)	1890 m (6,200 ft)
Reserve mission	45 min	370 km (200 nm)	370 km (200 nm)	926 km (500 nm)	926 km (500 nm)

Summary of Objective Functions

The objective function is simply the function the designer wishes to maximum or minimum to determine the 'best' vehicle for the given mission. Through utilizing the total Direct Operating Cost (DOC) (Equations 5.1 - 5.5) the designer can control the weighting of fuel burn, systems complexity and acquisition cost through economic parameters (fuel cost, development cost, maintenance cost and depreciation). The weighting factors for this study are summarized in Table 5-2

Total DOC	$DOC = DOC_{fly} + DOC_{maint} + DOC_{dep} + DOC_{LNTF}$	5.1
Flying DOC	$DOC_{fly} = f(\text{fuel burn, fuel cost, crew cost})$	5.2
Maintenance DOC	$DOC_{maint} = f(\text{TOGW, OEW, thrust, complexity})$	5.3
Depreciation DOC	$DOC_{dep} = f(\text{unit cost, time period, rate of depreciati on})$	5.4

Landing, Navigation
And taxi fees

$$DOC_{LNTF} = f(\text{empirical fraction of DOC})$$

5.5

Table 5-2: Sizing Objective Direct Operating Cost Weight Factors

Weighting Factor	Citation X	Embraer 170	B737	B777	A380
Fuel Cost	\$5.00/gal	\$5.00/gal	\$5.00/gal	\$5.00/gal	\$5.00/gal
Annual hull insurance rate	0.05	0.05	0.05	0.05	0.05
Crew Cost					
Captain	\$85,000/yr	\$30,000/yr	\$60,000/yr	\$85,000/yr	\$85,000/yr
1st Officer	\$50,000/yr	\$20,000/yr	\$50,000/yr	\$50,000/yr	\$50,000/yr
Attendants	\$32,000/yr	\$15,000/yr	\$25,000/yr	\$32,000/yr	\$32,000/yr
Propulsion Next Generation [TBO]	6,000	6,000	6,000	16,000*	16,000*
Depreciation factor	0.50	0.85	0.85	0.85	0.85
Depreciation time frame	10 yrs	15 yrs	15 yrs	20 yrs	20 yrs

*Increase in time-between overhauls (TBO) relative to narrow body aircraft due the increase time spent at cruise

Summary of Design Variables

In each study the total configuration arrangement is fixed (engine location, empennage location relative to fuselage, cabin cross-section, etc.) since the aircraft are reverse-engineered; AVD^{sizing} is utilized to solve for the following variables in Table 5.3.

Table 5-3: Sizing design variables and aircraft definition.

Iterate to minimize the objective function	Description
S_{ref}	reference wing area
τ	volumetric efficiency
AR	aspect ratio
$\Lambda_{c/4}$	quarter chord sweep angle
$(t/c)_{avg}$	average wing thickness
Remaining variables solve for each iteration	Derived From
Weight breakdown	from geometry, fuel burn and loads
Thrust required	thrust required from DCFC
Nacelle size	diameter and length from regressions based on thrust required
Fuselage length (constant cabin cross-section)	required volume with constant cabin cross-section
Tail-size	wing location with a modified tail-volume quotient method to approximate control power requirements
Wing location	relocated to provide required static margin during cruise; landing gear clearance checked manually after integration

Discussion of Existing Aircraft Results

Table 5.4 summarizes the selected design point for each case study. AVD^{sizing} demonstrates around +/-5% error across this range of aircraft when compared with published reference data.

Table 5-4: Summary of TAC Transonic Transport Validation Studies

	Cessna Citation X			Embraer 170			Boeing 737-800			Boeing 777-300ER			Airbus A380-800		
	Actual	Design Point	% error	Actual	Design Point	% error	Actual	Design Point	% error	Actual	Design Point	% error	Actual	Design Point	% error
Geometry															
τ	0.13	0.30		0.28	0.21		0.12								
AR	7.75	7.75	0.0%	9.30	9.50	2.2%	9.75	10.00	2.5%	9.25	9.00	-2.7%	7.52	7.50	-0.3%
S_{plan} (m ²)	49.02	49.53	1.0%	72.72	74.45	2.4%	120.8	117.2	-3.0%	454.0	457.5	0.8%	845.8	836.5	-1.1%
b (m)	19.49	19.59	0.5%	26	26.59	2.3%	34.32	34.24	-0.2%	64.8	64.17	-1.0%	79.75	79.21	-0.7%
l_{fus} (m)	17.78	18.04	1.5%	29.90	29.21	-2.3%	38.02	37.66	-0.9%	73.08	74.78	2.3%	72.57	73.58	1.4%
d_{fus} (m)	1.89	1.89	0.0%	3.17	3.18	0.2%	3.74	3.74	0.1%	6.20	6.20	0.0%	7.14	7.25	1.5%
Weight															
TOGW (kg)	16374	16722	2.1%	37200	37472	0.7%	79243	76822	-3.1%	351535	359391	2.2%	560000	554313	-1.0%
W_{fuel} (kg)	5729	6068	5.9%	9160	9378	2.4%	20894	20240	-3.1%	145538	148526	2.1%	243350	238322	-2.1%
$(W_{PAY})_d$ (kg)	600	600	0.0%	7000	7000	0.0%	16936	17066	0.8%	38168	38168	0.0%	54123	54123	0.0%
OEW (kg)	10036	10054	0.2%	21040	21094	0.3%	41413	39516	-4.6%	167829	172696	2.9%	270015	261867	-3.0%
Aero-Propulsion															
ff	0.35	0.36	3.7%	0.25	0.25		0.26	0.26	-0.1%	0.414	0.41	-0.2%	0.43	0.43	-1.1%
Thrust (kN/eng)	35	34	-2.0%	63	66	4.4%	117	117	-0.3%	514	548	6.6%	312	314	0.5%
$Alt_{cruise\ avg}$ (m)	12801	12801		-	11500		10668	11589	8.6%	-	10722		10660	10982	3.0%
L/D_{cruise}	-	11.83		-	12.94		-	16.44		-	17.46		-	17.02	
SFC_{cruise} (/hr)	0.68	0.68	1.3%	0.68	0.68	0.1%	-	0.64		0.56	0.56	-0.2%	0.52	0.53	1.9%
Cost															
DOC (\$/pax-km)	2.07	2.77		-	0.15		-	0.09		-	0.07		-	0.06	
Unit price (\$ M)	23	24.31	5.7%	34	37.46	10.2%	72	74.67	3.71%	202	205.39	1.7%	300	285	-5.1%

From these studies it is clear that different missions result in different aircraft shapes within the TAC family. The faster cruise speeds represented by the Citation X, B777 and A380 result in higher sweep angles due to wave drag considerations relative to the slightly slower B737 and Embraer 170. In addition, aspect ratio 9 wings tend to deliver the proper balance between structural efficiency and induced drag for most twin engine transports.

However, in the case of the 0.92 M Citation X, the increased wing sweep increases the aeroelastic torsion stress on higher aspect ratio wings. Consequently, a lower aspect ratio wing will result in a lighter wing. The best overall compromise between wing weight and induced drag results in a lower aspect ratio wing relative to the twin engine transport.

In the case of the Airbus A380, the lower aspect ratio wing selection is due to the larger concentration of payload weight at the wing root and the advantageous effect of increased Reynolds number. The larger concentration of payload at the root, due to the double deck cabin arrangement, requires a structurally advanced-efficiency wing relative to the single deck twin engine aircraft. The larger Reynolds number reduces the skin friction coefficient, thus adds aerodynamic improvement without relying on the induced drag reduction of a higher aspect ratio wing. Combining these effects creates a situation which will favor lower aspect ratio wings, relative to other twin engine transports. This effect is advantageous given the fact that an aspect ratio greater than 7 would result in violating the airport 80 meter box, which limits an aircraft span and length to below 80 meters.

From these trade-studies it is concluded that AVD^{sizing} is providing accurate (1) numerical results, see Table 5-4, and (2) correct, physically transparent design sensitivities for TAC aircraft, see abbreviated discussion above. The application of this configuration type to a wide variety of design missions it can be seen that the classical TAC involves a complex multidisciplinary iteration of design variables and is highly sensitive to mission selection.

Discussion of Technology Study Results

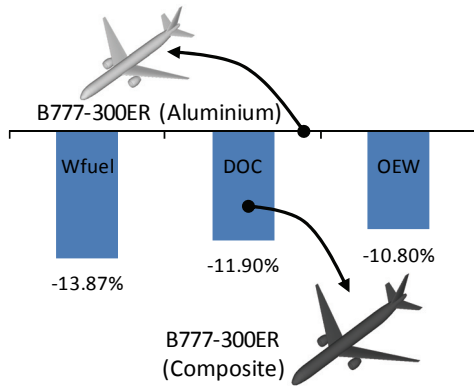
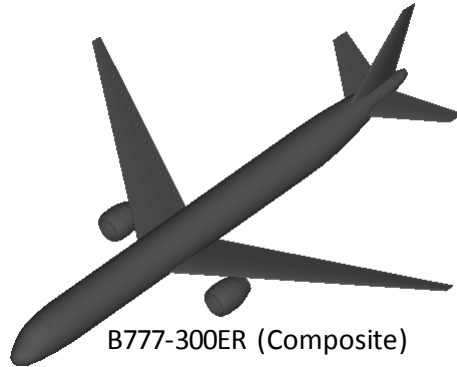
To demonstrate AVD^{sizing} capability to explore new technologies on the conventional TAC aircraft two configuration applied. (1) Composite B777-300ER and (2) Thrust vectored control (TVC) B777-300ER.

The composite primary structure (fuselage, wing, empennage) B777-300ER represents a possible next generation transport analogues to the B787 (however, the B787 has a different design payload range, and balance field-length). To model the composite structure a 15% reduction in the wing, fuselage, and empennage primary structure, as suggested by references (23), (7), (80)

The multi-disciplinary effects effect of the composite primary structure B777 show the approximate performance gains claimed by Boeing for the B787 relative to an aluminum structure (approx 20% fuel burn overall, included 8% increase due to improved SFC) ⁽⁹¹⁾ resulting in approximately 12% decrease in fuel burn attributed to composite structure, see Table 5-5

Table 5-5: Summary of Composite B777-300ER Study

	B777 (Aluminum)	B777 (Composite)	% change
Geometry			
τ	0.21	0.24	
AR	9.00	11.00	22.22%
S_{pln} (m ²)	457.49	413.73	-9.57%
b (m)	64.17	67.46	5.13%
l_{fus} (m)	74.78	74.87	0.13%
d_{fus} (m)	6.20	6.20	0.00%
Weight			
TOGW (kg)	359357	320112	-10.92%
W_{fuel} (kg)	148503	127904	-13.87%
MLW (kg)	256868	228816	-10.92%
$(W_{PAY})_{design}$ (kg)	38168	38168	0.00%
OEW (kg)	172686	154040	-10.80%
Aero-Propulsion			
ff	0.41	0.400	-3.31%
Thrust (kN/engine)	548	439	-19.93%
$Alt_{cruise\ avg}$ (m)	10722	11381	6.14%
L/D_{cruise}	17.46	18.24	4.44%
SFC_{cruise} (/hr)	0.56	0.56	-0.52%
Cost			
DOC (\$/pax-km)	0.073	0.064	-11.90%
Unit price (\$ M)	205	186	-9.55%



In the case of the composite wing the classical balance of wing aspect ratio is shifted for twin engine aircraft. The composite wing allows for an increase in aspect ratio (AR=11) relative to the aluminum (AR=9) wing due to the desensitizing the effect of wing weight in the

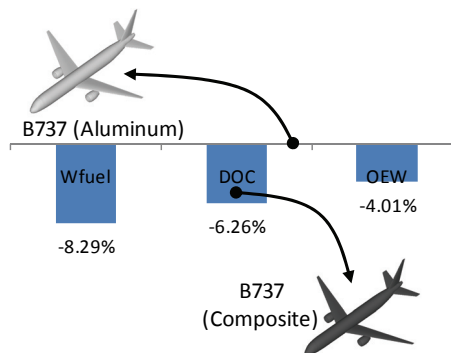
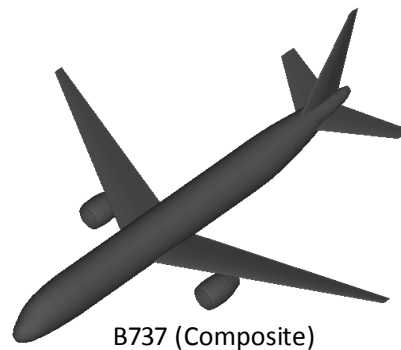
balance of structural wing weight verse aerodynamic efficiency. This effect is also seen in the B787 which as an AR=11 wing⁽⁹¹⁾

This new aircraft demonstrates and validates the B787/A350 current production lines and indicates that composite structure would most likely be implemented in all future long haul transports. However, this type of improvement is not seen with smaller transports

For example, applying composites to B737-800 model does not yield the same level of fuel burn reductions as found in the larger transports. If the same technology factors are applied to the B737 model, the resulting fuel burn is reduced to only an 8% improvement, see Table 5-6

Table 5-6: Summary of Composite B737-800 Study

	B737 (Aluminum)	B737 (Composite)	% change
Geometry			
τ	0.28	0.29	3.57%
AR	10.00	12.00	20.00%
S_{pln} (m ²)	117.21	113.88	-2.84%
b (m)	34.23535	36.97	7.98%
l_{fus} (m)	37.66	37.67	0.01%
d_{fus} (m)	3.74	3.74	0.00%
Weight			
TOGW (kg)	76822	73745	-4.01%
W_{fuel} (kg)	20240	18563	-8.29%
MLW (kg)	64147	61577	-4.01%
$(W_{PAY})_{design}$ (kg)	17066	17066	0.00%
OEW (kg)	39516	38116	-3.54%
Aero-Propulsion			
ff	0.263	0.252	-4.46%
Thrust (kN/engine)	117	116	-0.54%
$Alt_{cruise\ avg}$ (m)	11589	12152	4.86%
L/D_{cruise}	16.44	17.30	5.21%
SFC_{cruise} (/hr)	0.64	0.64	-0.04%
Cost			
DOC (\$/pax-km)	0.089	0.084	-6.26%
Unit price (\$ M)	74.67	73.56	-1.49%



The difference in benefit between the B777 and B737 is attributed to the reduce design range and payload of the B737. Thus, less time is spent during cruise, resulting in a reduced benefit in fuel required. The effect of scale the fundamental issue when addressing the next generation of narrow body transports. Future work is required to examine such technologies as

Pratt & Whitney's geared turbofan ⁽⁹²⁾ and improved natural laminar flow ⁽³⁾ could produce a viable replacement for the B737-800.

The thrust vectored transport is a concept that the AVD Lab was tasked to investigate as part of the Synergistic Efficiency Technologies for the truss-Braced Wing Workshop, hosted by the National Institute of Aeronautics (NIA) and NASA LaRC ⁽⁹³⁾.

Figure 5-1 demonstrates the change required to produce a TVC transport from the B777 and the multidisciplinary design effects of this technology. For this study the aim was take a first step into TVC by removing the empennage, relocating the propulsion system, and modify the engine while keeping the aircraft statically stable ⁽⁹³⁾

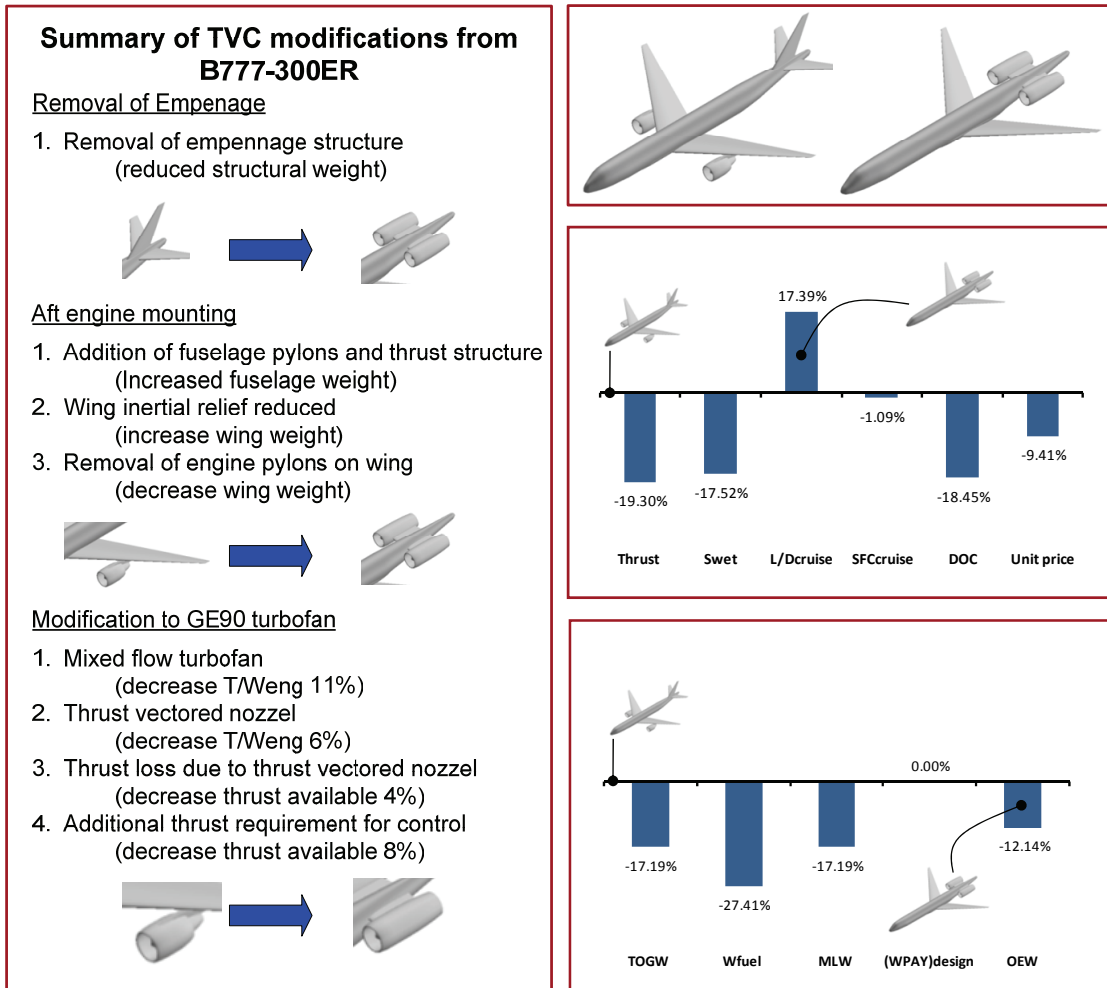


Fig 5-1: Modifications of the B777-300ER towards a TVC transport. The thrust vector control results in a significant reduction of both empty weight and aerodynamic efficiency

From an aerodynamic and weight stand point a TVC transport removes the trim drag and structural weight of the empennage. This in turn allows for smaller wing area and still meets the landing field length requirement. The reduction in wing area, removal of the empennage weight and trim drag off-set the adverse propulsion effects, results in a lighter and more fuel efficient vehicle.

However, it was demonstrated with *AeroMech* (a generic stability and control tool for conceptual design) ^(69; 70) in this study that this aircraft would require excessive thrust nozzle deflections for trim and would be uncontrollable during OEI conditions ⁽⁹³⁾. As such future work

will move towards a relaxed static stability 3 engine configuration. Decreasing the static margin through moving the wing forward would increase the lever arm between the TVC and c.g., thus reducing the control deflection required. The three-engine configuration would reduce the thrust and control loss during OEI, adding additional redundancy to both thrust and control functions.

Risk of Assumptions, Composite B777-300ER and TVC B777-300ER

For any novel configuration or configuration the conceptual design must make and disclose assumptions in order to start the design cycle. Sense little disciplinary has been performed this early, issues such as assumed structural concept, technology improvement and cost, etc. require reasonable assumptions in order to determine if the concept is worthy of further study. These assumptions represent the known unknowns of the design and therefore contribute the overall risk of the configuration and concept. Through openly disclosing the fundamental assumptions the later design phases have a start point for future disciplinary studies and risk mitigation.

Composite primary structure

For the composite model several structural assumptions have been built into the model in order to gain the 1st order multidisciplinary effects of the configuration,

1. 15% reduction in structural weight relative to an aluminum airframe
2. The structural sensitivities to t/c , $A_{c/4}$ and AR are the same for composites and aluminum construction. Sense a correction factor has been applied to an empirical, aluminum structural weight method the weighting of the design variables relative to each other has remained unchanged.
3. The difference between the B787 claimed fuel burn and the AVDsizing results are from a more fuel efficient engine on the B787 relative to the competition. AVDsizing used the same propulsion model for both the composite and aluminum models.

Thrust Vectored Control

For the TVC model several propulsion and structural assumptions have been built into the model in order to gain the 1st order multidisciplinary effects.

1. Weight penalty for aft fuselage mounted TVC engines is same as a the penalty for conventional aft fuselage mounted engines
2. Modification of the GE-90 is possible with the assumed increases in weight and thrust losses as shown in Figure 5-1.
3. A TVC transport is controllable in a twin engine, statically stable configuration. This assumption has already been shown to be false. Future studies will explore unstable and multiengine configurations.

5.2 Summary of Proposed Blended Wing Body Transonic Transport

The Boeing Blended Wing Body (BWB) is a flying-wing configuration (FW) which blends the cabin into an optimized transonic wing responsible as well to stabilize and control the aircraft. The BWB is significantly different from the classical flying wing which consists of a straight tapered wing as seen with the Northrop YB-49 (Figure 5-2). The blending of the cabin into the wing allows for thickening the cabin section independently of the outboard wing, thereby avoiding compromising the outer wing. The resulting aircraft planform resembles a cranked wing planform instead of the straight tapered wing seen with the YB-49.

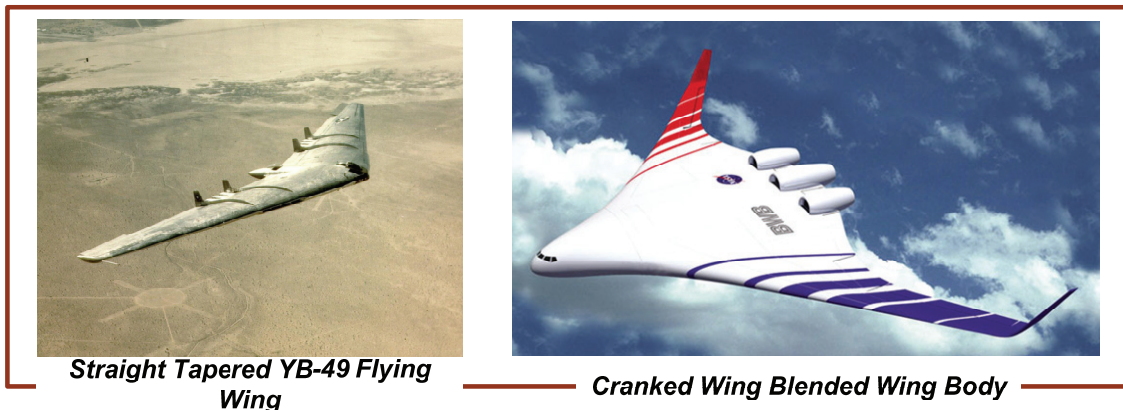


Fig 5-2: The Blended wing body has a compound cranked all-wing planform geometry allowing for increased cabin thickness relative to the remainder of the wing (picture via NASA.gov and aerospaceweb.org).

Summary of design missions

The Boeing study was performed with the intent of comparing the BWB to an aircraft similar to the Airbus A380; the 800 pax long range design mission was selected as the reference mission, see Table 5-7.

Table 5-7: TAC Transport Validation Case Studies Mission Summary (85)

M	Boeing BWB
Maximum Payload	1,200 kg (2,645 lbs)
Design payload	800 pax 600 kg (1,320 lbs)
Range	5740 km (3,100 nm)
Velocity (design cruise)	0.85
Ceiling	15,500 m (51,000 ft)
Take-off Field Length (TOGW)	< 1556 m (5,100 ft)
Landing field length (MLW)	< 1036 m (3400 ft)
Reserve mission	45 min

Summary of DOC objective functions

The BWB study does not explicitly state the objective function and therefore minimum DOC will be assumed. Minimum DOC results in a design-compromise between minimum TOGW and fuel weight.

Summary of design variables

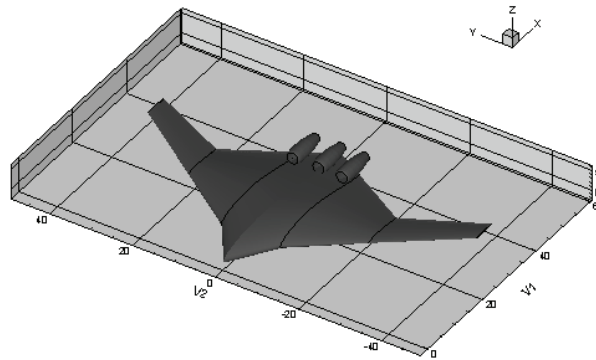
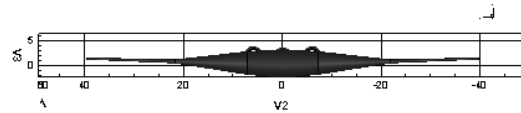
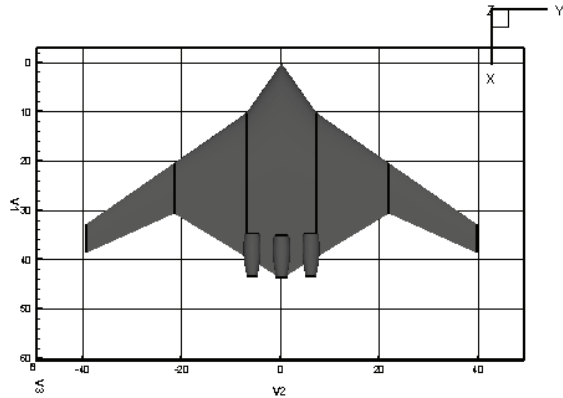
The BWB geometry is defined in Chapter 4. For this study the primary design variables explored were (1) cabin aspect ratio, (2) wing sweep and (3) cabin height.

Discussion of Results

The BWB model shows similar results to the published Boeing study for the same design mission⁽⁸⁵⁾ (Table 5-8)

Table 5-8: TAC Transport Validation Case Studies Mission Summary⁽⁸⁵⁾

Boeing BWB 800 PAX			
	Ref	Design Point	% error
<i>Geometry</i>			
T		0.10	
AR	4.72	5.00	5.9%
S _{plan} (m ²)	1424	1403	-1.5%
b (m ²)	82.00	83.75	2.1%
l _{fus} (m)	-	-	-
D _{fus} (m)	-	-	-
<i>Weight</i>			
TOGW (kg)	373140	363183	-2.7%
W _{fuel} (kg)	108243	103972	-3.9%
(W _{PAY}) _d (kg)	78016	78016	0.0%
OEW (kg)	186880	181196	-3.0%
<i>Aero-Propulsion</i>			
ff	0.29	0.29	-1.3%
Thrust (kN/eng)	276	268	-2.7%
Alt _{cruise avg} (m)	-	10073	-
L/D _{cruise}	23.00	23.08	0.3%
SFC _{cruise} (/hr)	0.47	0.48	3.2%
<i>Cost</i>			
DOC (\$/pax-km)	-	0.02	-
Unit price (M)	202.00	250.53	24.0%



The parametric trade studies identified that the cabin aspect ratio, cabin height and wing sweep angle are some of the most sensitive design variables in terms of aerodynamic performance and weight. Cabin aspect ratio controls the spanwise occupation of the cabin; typically a cabin aspect ratio 4 is considered the upper bound for cabin evacuation⁽⁸⁵⁾. A large cabin aspect ratio distributes the payload along the span which serves as load elevation (span-loading concept). The span-loading concept serves to reduce the wing structural weight.

However, the higher aspect ratio increases the airfoil thickness along the span due to the cabin height requirement. The increased thickness results in increased transonic wave drag and profile drag. If the cabin aspect ratio is too low the span-loading effect decreases, resulting in a heavier wing weight.

For the 800 pax BWB it is confirmed that a double deck cabin is required to maintain an adequate cabin aspect ratio and cabin height. A single deck arrangement would result in excessive cabin floor area and requiring an excessive overall wing area which would ultimately lead to an ill-condition design and violate the 80m box.

For the BWB, wing sweep tends to be higher relative to the TAC reference aircraft due to wave drag, volume and stability and control constraints. In case the wing sweep angle would be selected identical to the TAC reference aircraft, the airfoil thickness must be reduced to mitigate wave drag effects which results in an excessive wing planform area to maintain the total volume. In addition, such wing sweep angle would reduce the lever arm from the longitudinal control effectors on the wing trailing edge to the center of gravity, resulting in excessive control deflections thus increase trim drag penalties and excessive control deflections for maneuvering⁽⁶⁹⁾.

From the sensitivities generated it is possible that the BWB may only be applicable for large transports. Smaller transports (possibly less than 200 pax) will require an adverse ratio of cabin planform area to total wing planform area, resulting in an infeasible aircraft. Moving to a single deck configuration for thickness purposes would drive the wing area requirement away from the classical landing constraint for TAC. Thus, a larger wing area will be required for volume then for flight performance, resulting in an over engineered aircraft.

From this study it is concluded that AVD^{sizing} is in agreement with the Boeing study for this large BWB transport. The sensitivities discussed in this study show that AVD^{sizing} allows for modeling and design space exploration of flying wing configurations.

Risk of Assumptions

For any novel configuration or configuration the conceptual design must make and disclose assumptions in order to start the design cycle. Since little disciplinary has been performed this early, issues such as assumed structural concept, technology improvement and cost, etc. require reasonable assumptions in order to determine if the concept is worthy of further study. These assumptions represent the known unknowns of the design and therefore contribute the overall risk of the configuration and concept. Through openly disclosing the fundamental assumptions the later design phases have a start point for future disciplinary studies and risk mitigation.

For the BWB model several assumptions have been built into the model in order to gain the 1st order multidisciplinary effects of the configuration

1. Wing weight of the outer wing can be approximated as a straight tapered cantilever wing extending from the centerline to the wing tip (See Methods Library Appendix B.
2. A pressurized cabin can be designed with the weight as prescribed in Reference (94), see Methods Library Appendix B.
3. The aircraft is sufficiently controllable under all flight conditions. The current model has only account for trim in the stability and control analysis.

5.3 Summary of Proposed Strut-Braced NLF Transonic Transport

The concept of a strut braced wing (SBW) or truss braced (TBW) natural laminar flow wing (NLF) was originally proposed by Pfenniger in 1975⁽⁹⁵⁾ for transonic transports. This concept is currently under investigation by Virginia Polytechnic Institute (VPI) partnered with NASA LaRC⁽⁶⁾⁽⁸¹⁾ to develop a modern application of this concept (Figure 5-3).

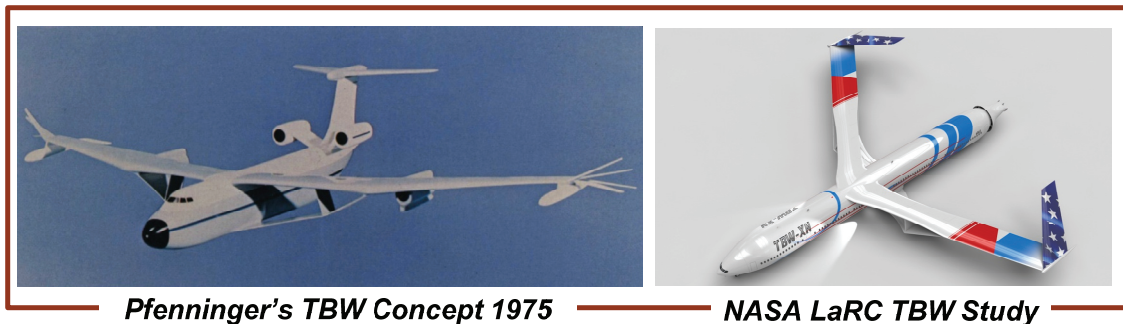


Fig 5-3: Example TBW concepts for transonic flight incorporating natural laminar flow⁽⁹⁶⁾

VPI's studies focus on showing the benefits of SBW/TBW natural laminar flow (NLF) through development of cantilever, strut and truss braced wing concepts. Each concept assumes a certain amount of laminar flow and is optimized for the given design mission⁽⁶⁾. The concepts are then compared with each other to understand the design sensitivities to deliver significant fuel burn reductions.

The presented AVD^{sizing} study focuses on the SBW for a clearly explanation of the design sensitivities. The same sensitive's can be found for the TBW, with the exception that the truss yields a larger improvement in fuel burn due to the improved structural efficiency which allows for larger aspect ratios and improved laminar flow⁽⁶⁾.

Summary of design missions

The VPI study focuses on the effects of SBW and TBW on long range, wide-body aircraft to provide a long cruise segment⁽⁶⁾. The long cruise segment allows for the reduced fuel

burn to have a greater impact on the total vehicle design and weight. Thus, the VPI study utilizes a modified B777 design mission (Table 5-9).

Table 5-9: TAC Transport Validation Case Studies Mission Summary ⁽⁶⁾

Mission	VPI SBW
Maximum payload	69,900 kg (154,000 lbs)
Design payload	325 pax 31,700 kg (69,900 lbs)
Range	13,900 km (7,5000 nm)
Velocity (design cruise)	0.85 M
Ceiling	12,200 m (40,000 ft)
Take-off Field Length (TOGW)	< 3350 m (10,100 ft)
Landing field length (MLW)	< 1767 (5,800 ft)
Reserve mission	926 km (500 nm)

Summary of Objective Functions

The VPI SBW study used three objective functions (1) minimum TOGW, (2) minimum fuel weight and (3) maximum L/D ⁽⁶⁾. For the sake of comparison, the minimum fuel weight solution is utilized in the current study.

The maximum L/D wing design produces a suboptimal wing structure which drives the aircraft TOGW and fuel weight beyond the minimum fuel- and TOGW-solutions ⁽⁶⁾. Therefore, maximum L/D is an erroneous objective function. The minimum TOGW is a reasonable objective function; however the minimum fuel weight better illustrates the possible fuel burn reductions of the SBW.

Summary of design variables

The same procedure is utilized for the SBW as with the TAC with a few notable exceptions. First, the span-wise intersection of the main strut is used as a design variable along with the strut chord length relative to the wing chord at the intersection point, see Chapter 4.

Discussion of Results

The primary difference between the SBW and a conventional cantilever wing is the use of an external support to promote natural laminar flow (NLF). The addition of this component requires a method of approximating the structural and weight implications, aerodynamic interference and extent of NLF obtainable under what conditions.

To model the structural implications of an external wing strut, the VPI FEM study (81) is utilized to develop a correlation between the strut-wing weight group relative to a cantilever wing weight. As described in Chapter 3, Figure 3-8, the VPI FEM study correlates well to the 80% correction factor proposed by Torenbeek ⁽¹⁸⁾. Thus, this correction factor is applied to the cantilever wing weight estimation method to approximate the strut structural benefit.

The aerodynamic interference is approximated with methods from Hoerner ⁽⁹⁷⁾ for subsonic wing intersections. It is assumed that an aerodynamic fairing can be developed to minimum wave drag at the strut wing intersection.

Laminar flow is approximated through an assumed transitional Reynolds number which is applied to the wing and strut. This transitional Reynolds number comes from experimental results obtained from the F-14 wing glove experiment ⁽³⁾ which demonstrates the transitional Reynolds number as a function of wing sweep (Figure 5-4).

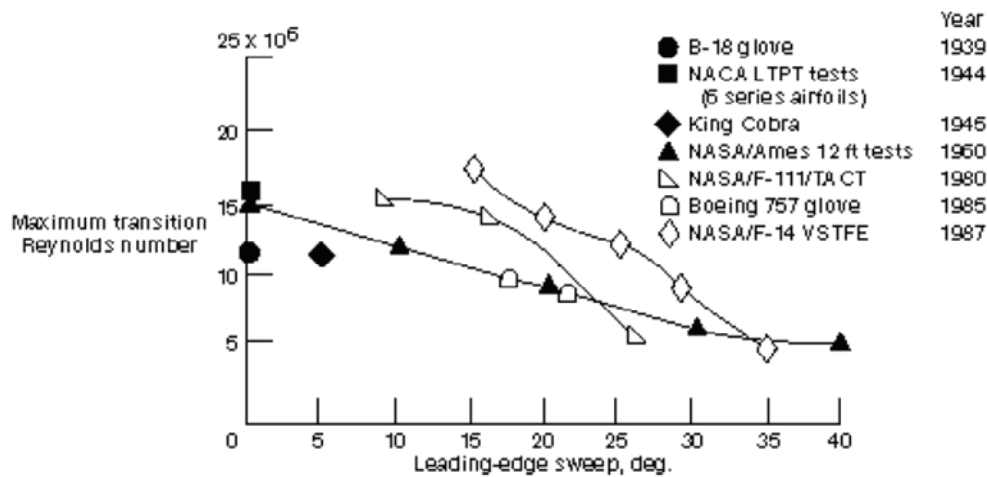


Fig 5-4: Transitional Reynolds number for a NLF wing as determined from the F-14 wing glove experiment ⁽³⁾

Before the SBW study can be executed, the validated B777-300ER model is modified in terms of (1) the mission for the VPI study (2) addition of strut geometry, (3) structural weight approximation applied to the empirical cantilever wing weight method, (4) removal of leading edge devices to promote laminar flow (reducing C_{Lmax}), and (5) the aerodynamic interference and natural laminar flow methods.

Through AVD^{sizing} the fundamental multi-disciplinary wing design problem for the strut braced transonic transport can be seen (Figure 5-5). An unswept wing is preferred for Natural laminar flow due to the increase transitional Reynolds number (Figure 5-4. The unswept wing requires a thinner airfoil to manage the transonic wave drag at this design speed. This thinner wing requires a stiffened and heavier wing structure. As demonstrated in Figure 5-4 these effects result in a 35 degree swept wing to balance these effects, even though an increased NLF wing would require a reduced sweep angle.

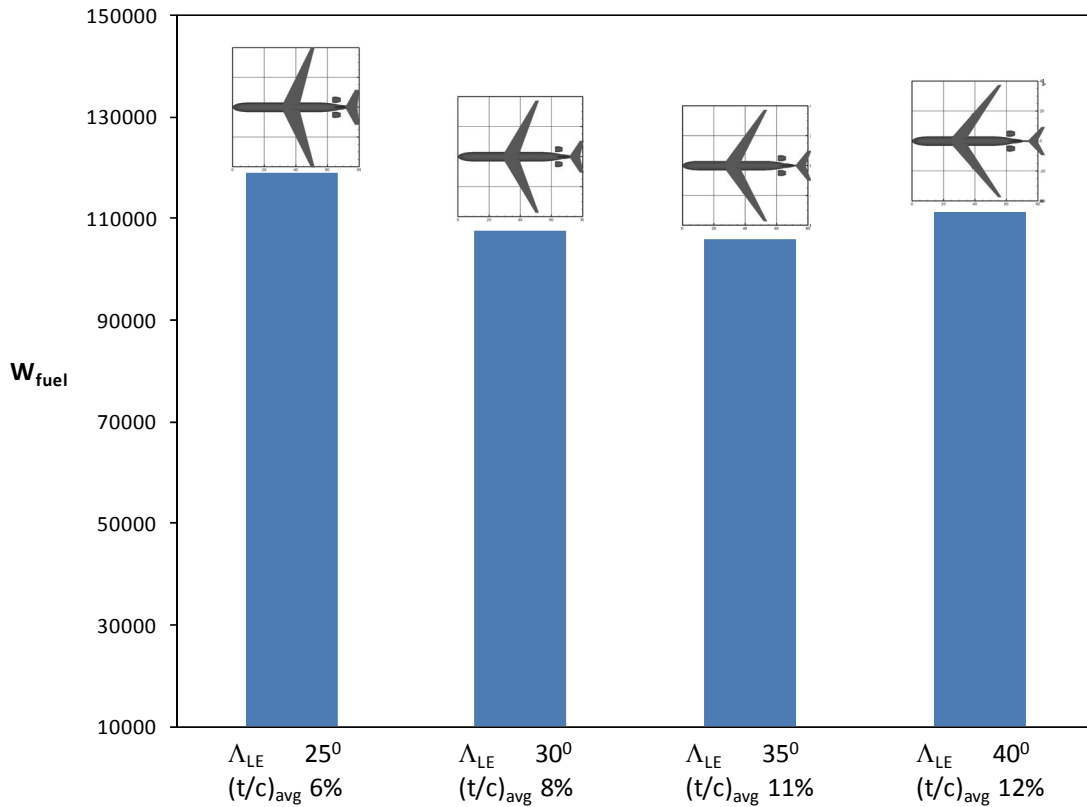


Fig 5-5: Varying wing sweep and solving for wing area, aspect ratio and wing thickness demonstrates that NLF SBW benefits from higher sweep angles due to the high cruise Mach number

It is clear that even with external bracing, the classical sweep and thickness (35 degrees leading edge sweep, 11% t/c_{avg}) results in a minimum fuel burn. From a multidisciplinary context, NLF, as produced by the F-14 wing glove experiment, plus the external structural support does not allow for an unswept wing due the weight and wave drag penalty for this mission.

Comparing the SBW to a baseline cantilever wing transport it is clear that the SBW demonstrates a small increase of L/D and reduction of OEW, which together reduce fuel burn, see Table 5-10. For both cases, the SBW and cantilever wing, the same transitional Reynolds relationship with sweep is assumed for NLF.

Table 5-10: Sizing design variables and resulting aircraft definition.

	Baseline Cantilever	SBW	% error
Geometry			
τ	0.18	0.21	
AR	9.00	12.00	33.33%
$S_{pln} (m^2)$	500.74	447	-10.80%
$b (m^2)$	67.13	73.21	9.06%
$l_{fus} (m)$	72.69	71.18	-2.08%
$D_{fus} (m)$	6.20	6.20	0.00%
Weight			
TOGW (kg)	332298.03	276794	-16.70%
$W_{fuel} (kg)$	126298.22	106045	-16.04%
MLW(kg)	237526.63	197853	-16.70%
$(W_{PAY})_{design} (kg)$	31694.00	31694.00	0.00%
OEW (kg)	174305.81	139056	-20.22%
Aero-prolusion			
ff	0.38	0.38	0.80%
Thrust			
(kN/engine)	527.08	328	-37.79%
$Alt_{cruise\ avg} (m)$	13583.28	12360	-9.01%
L/D_{cruise}	20.19	21.00	4.02%
$SFC_{cruise} (/hr)$	0.56	0.56	0.00%
Cost			
DOC (\$/pax-km)	0.06	0.06	-8.98%
Unit price (\$ M)	199.93	164.8	-17.55%

From this analysis it appears that the SBW allows for an increased aspect ratio due to external bracing. However, due to the similar wing sweep required for both the strut and cantilever wings, the reduced induce drag is offset by the interference drag and only amounts to a 4% increase in L/D. Combining this L/D improvement with the structural weight savings of the strut, the total fuel burn is reduced by 16%. By comparison total fuel savings of a full composite aircraft of this size is roughly 20%.

Comparing these results to the VPI results, it becomes clear that the VPI study ⁽⁶⁾ suggest larger aspect ratios compared to AVD^{sizing} results for both cantilever and SBW configurations. This yields significantly higher L/D's and reduced fuel burn results for the VPI study, see Table 5-11.

Table 5-11: Comparison of VPI results to AVD^{sizing}.

Strut Braced Wing (Min Fuel Weight)				Cantilever Wing (Min Fuel Weight)		
	SBW VPI	SBW AVD ^{sizing}	% error	Cantilever VPI	Cantilever AVD ^{sizing}	% error
<i>Geometry</i>						
τ		0.21			0.18	
AR	20	12.00	-40.00%	15.00	9.00	-40.00%
S_{pln} (m ²)	539	447	-17.10%	483	501	3.65%
b (m ²)	103	73.21	-28.92%	85.34	67.13	-21.34%
l_{fus} (m)	73.08	71.18	-2.60%	73.08	72.69	-0.53%
D_{fus} (m)	6.2	6.20	0.00%	6.20	6.20	0.00%
<i>Weight</i>						
TOGW (kg)	235868	276794	17.35%	258094	332298	28.75%
W_{fuel} (kg)	58513	106045	81.23%	74389	126298	69.78%
MLW (kg)	-	197853	-	-	237527	-
$(W_{PAY})_{design}$ (kg)	31525	31694	0.54%	31694	31694	0.00%
OEW (kg)	145830	139056	-4.65%	152011	174306	14.67%
<i>Aero-Propulsion</i>						
ff	0.309	0.383	23.99%	0.29	0.38	31.87%
Thrust (kN/engine)	-	328	-	-	527	-
Alt _{cruise avg} (m)	14000	12360	-11.72%	-	13583	-
L/D_{cruise}	39.00	21.00	-46.15%	31.00	20.19	-34.87%
SFC _{cruise} (/hr)	-	0.56	-	-	0.56	-
<i>Cost</i>						
DOC (\$/pax-km)	-	0.058	-	-	0.06	-
Unit price (\$ M)	-	165	-	-	200	-

After reviewing the VPI published work ⁽⁶⁾ on the strut and truss braced wing, the difference in results can be attributed, in part, to the wing weight estimation methods utilized. The VPI study utilized a dual plate FEM model for bending and an empirical relationship for the remaining wing structure. This method is analogous to the analytic wing weight method from Howe ⁽³⁶⁾ which utilizes an analytic solution for bending with empirical methods for the remainder of the structure. In Chapter 3 it has been shown that such methods tend to under predict the effect of aspect ratio for cantilever wings.

To test the above theory, the models were re-run using Howe's analytic wing weight method ⁽³⁶⁾, with the remainder of the model left unchanged. The result was a similar geometry to the VPI study with a differing weight breakdown, see Table 5-12.

Table 5-12: Comparison of VPI Results to AVD^{sizing}.

Strut Braced Wing (Min Fuel Weight)				Cantilever Wing (Min Fuel Weight)		
	SBW VPI	SBW AVD ^{sizing}	% error	Cantilever VPI	Cantilever AVD ^{sizing}	% error
<i>Geometry</i>						
τ		0.17			0.18	
AR	20	20.00	0.00%	16.00	15.00	-6.25%
S_{pln} (m²)	539	507	-5.84%	511	493	-3.48%
b (m ²)	103	100.73	-2.20%	90.80	86.01	-5.27%
l _{fus} (m)	73.08	71.33	-2.39%	73.08	74.12	1.42%
D _{fus} (m)	6.2	6.20	0.00%	6.20	6.20	0.00%
<i>Weight</i>						
TOGW (kg)	235868	264466	12.12%	259454	318097	22.60%
W_{fuel} (kg)	58513	82885	41.65%	70760	99750	40.97%
MLW (kg)	-	189041	-	-	227376	-
(W _{PAY}) _{design} (kg)	31525	31694	0.54%	31694	31694	0.00%
OEW (kg)	145830	149887	2.78%	157000	186653	18.89%
<i>Aero-Propulsion</i>						
ff	0.309	0.313	1.43%	0.27	0.31	14.98%
Thrust (kN/engine)	-	288	-	-	543	-
Alt _{cruise avg} (m)	14000	12948	-7.52%	-	13867	-
L/D_{cruise}	39.00	27.17	-30.32%	31.00	25.81	-16.76%
SFC _{cruise} (/hr)	-	0.56	-	-	-	-
<i>Cost</i>						
DOC (\$/pax-km)	-	0.050	-	-	0.06	-
Unit price (\$ M)	-	168	-	-	208	-

This comparison-table indicates that the VPI⁽⁶⁾ and Howe method⁽³⁶⁾ suffer the same error for high aspect ratio wings. In both models, the weight penalty for high aspect ratio wings is not sufficient to override the aerodynamic benefit. Thus, the minimum fuel burn solution is skewed toward a higher aspect ratio than is reasonable for such a swept wing. In both cases it

the resulting aircraft does account for the aeroelastic effects of high aspect ratio wings and thus both methods are improper for this configuration.

While the resulting geometry is similar, the fuel weight and L/D differ significantly. The fuel weight error is primarily caused by the VPI study L/D being 30% higher for the SBW and 16% for the cantilever. These errors are most likely due to the amount of laminar flow utilized in the VPI studies. In the VPI literature it is not explicitly stated how much laminar flow exists over the wing for this specific model. Some supporting material indicates up to 70% NLF⁽⁶⁾ while the AVD^{sizing} results, utilizing the F-14 wing glove model, are conservatively predicting only 35% laminar flow for the main wing and 80% on the strut due to the leading edge sweep angles.

All things considered, when comparing the cantilever wing to the SBW with the same wing weight method, the resulting reduction in fuel weight are similar(i.e. the VPI SBW relative to VPI cantilever, analytical model SBW relative analytical cantilever, and empirical SBW relative to empirical cantilever). (Figure 5-6).

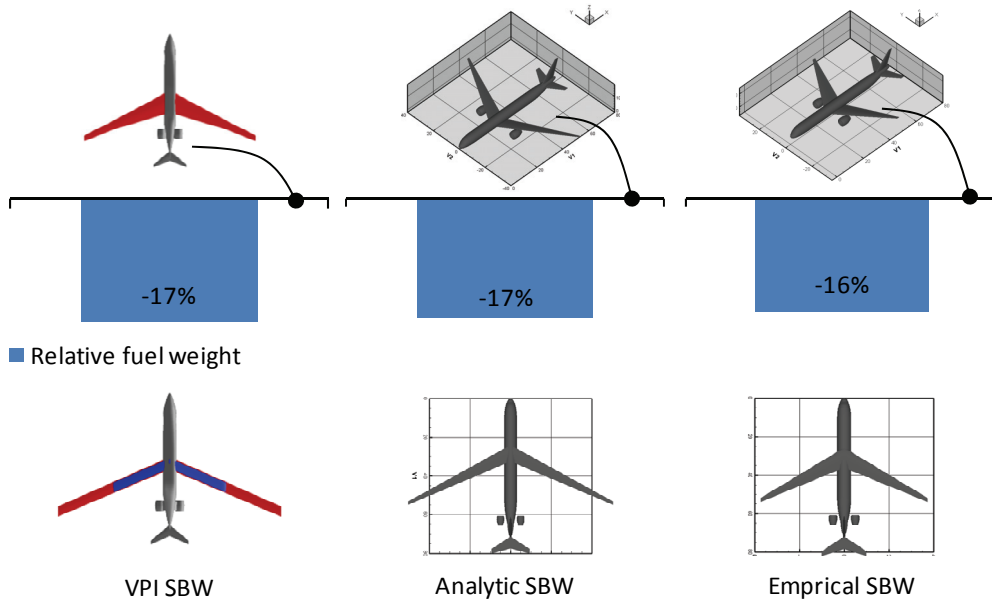


Fig 5-6: Percent change for the SBW relative to a cantilevered wing via the VPI, Analytic and Empirical Models (VPI results and figure from Reference (6)).

The fundamental lesson from this study is that selection of the correct wing weight method is critical for deriving an appropriate shape of vehicle. While the percent changes are in agreement for the various weight methods, the VPI model ⁽⁶⁾ and the analytic method from Howe ⁽³⁶⁾ suggest excessively high aspect ratio to achieve these results. The result is a perception that a SBW wing will have an aeroelastic problem due to this high aspect ratio. This problem is due to an inaccurate accounting of wing weight for both the baseline and the SBW, not from a need to have excessive aspect ratio. Such erroneous result during a conceptual phase can lead to unnecessary aeroelasticity studies of a high aspect ratio wing which is simply not required. It appears that a SBW will require only an aspect ratio 12 wing to provide a 16% reduction in fuel burn without suffering from severe aeroelastic problems.

In order to increase laminar flow contribution, the design cruise speed must be reduced. This will allow for reduced wing sweep without the need to reducing wing thickness due to wave drag effects, thereby resulting in a lighter and more aerodynamically efficient design. However, market and route research is required to determine if passengers will be willing to accept extended flight times in order to reduce ticket prices. Especially when considering that at Mach 0.85 the baseline mission translates already into a 17 to 18 hour flight time.

Risk of Assumptions

For any novel configuration or configuration the conceptual design must make and disclose assumptions in order to start the design cycle. Since little disciplinary has been performed this early, issues such as assumed structural concept, technology improvement and cost, etc. require reasonable assumptions in order to determine if the concept is worthy of further study. These assumptions represent the known unknowns of the design and therefore contribute the overall risk of the configuration and concept. Through openly disclosing the fundamental assumptions the later design phases have a start point for future disciplinary studies and risk mitigation.

For the SBW model several assumptions have been built into the model in order to gain the 1st order multidisciplinary effects of the configuration.

1. The SBW has the structural weight improvements as demonstrated in Figure 3-8.
2. The structural weight sensitivities to t/c , $\Delta c/4$ and AR are the same for a SBW and cantilever wing. Since a correction factor has been applied to an empirical, aluminum structural weight method the weighting of the design variables relative to each other has remained unchanged.
3. NLF can be achieved operational over the life of the vehicle, as determined by the F-14 wing glove experiment, see Figure 5-4
4. Wing-strut transonic interference is negligible and/or controllable with a properly designed intersection fairing

5.4 Summary of Transonic Transport Studies

Overall, AVD^{sizing} in combination with the Methods Library has proven to be a robust and accurate tool set for transonic aircraft parametric sizing. The approach demonstrates that a single process with variable methods can be applied to conventional and unconventional transonic aircraft of extreme mission. In summary, the follow conclusions can be drawn from the validation studies.

Methodology Conclusions

1. The total sizing methodology has proven flexibility and validity for a variety of transonic transport applications.
2. The methodology can be used to determine primary design drivers for a new engineering problem.
3. The selection of appropriate disciplinary analysis methods is critical. Incorrect methods tend to distort the conclusions, not only total accuracy but overall correctness of the solution space throughout the design process.

Lessons Learned – Aircraft Conceptual Design

1. TAC transports are highly sensitive to the mission due to the coupling of conflicting disciplines and requirements despite their disintegrated appearance (distinct wing, fuselage, empennage, etc.).
2. Composite structure provides a larger benefit for long-haul wide-body aircraft s (B777) than narrow body aircraft (B737/A320) due to the effects of scale, and time spent during cruise. Long haul aircraft are more sensitive to technology improvements because of the larger fuel requirement from the mission. As such developing a next generation narrow body aircraft (B737/A320) represents a more difficult technical challenge.
3. The thrust vectored transport shows significant performance improvement over the classical TAC, if the aircraft can be proven controllable in nominal and failure conditions (ex: OEI). The current design has proven to possess significant control problems. Further design iteration is required determine if these problems can be remedied.
4. The Blended Wing Body (BWB) demonstrates a strong sensitivity to cabin aspect ratio in terms of wave-drag and structural efficiency. It is imperative to correctly perform the cabin layout within the context of the total vehicle. The classical paradigm of disintegrated fuselage and wing design no longer hold.
5. The SBW shows modest improvements in fuel savings if (1) laminar flow can be maintained as determined by the F-14 wing glove experiment, if (2) transonic interference is manageable between the strut and the wing, and if (3) the strut can reduce the total wing group weight by 20%.

6. Slowing the SBW down would allow for reducing wing sweep without a reduction of wing thickness, thus allowing increased laminar flow without a wing weight penalty due to aeroelastic constraints.

CHAPTER 6

HIGH-SPEED COMMERCIAL TRANSPORT STUDIES

The high-speed regime spans from low supersonic aircraft (1.5 – 2.0 M) such as the supersonic business jet to hypersonic launch vehicles (5.0 M +). Over the past 5 years the AVD Lab has been tasked by industry and through internal projects to cover supersonic business jets (SSBJ) [SpiritLear Aviation]^{(72), (98), (99)} a reverse engineering of the Sanger EHTV (European Hypersonic Transport Vehicle) Mach 4.4 and ESA's (European Space Agency) LAPCAT (Long-Term Advanced Propulsion Concepts and Technologies) Mach 8 passenger transport in collaboration with the University of Rome⁽¹⁰⁰⁾. Across these studies, AVD^{sizing} has been utilized to determine the 1st order design sensitivities and solutions space screening.

These studies are summarized here to demonstrate the unique flexibility, range of applicability, but in particular relevance of the sizing process to actual projects in industry and research organizations. The following demonstrates how parametric sizing is utilized to assess new market opportunities, technical scenarios, overall resulting in the solution-space visualization for the decision-maker. These studies include the (1) Supersonic Business Jet (SSBJ) based on the Learjet 25 airframe, and the (2) comparison of technical and market implication of the LAPCAT Mach 8 commercial mission relative to the MBB Sanger EHTV Mach 4.4 commercial mission.

6.1 Summary of SSBJ Study Results Based on the LearJet 24 Airframe

The purpose of the SpiritLear SSBJ was to determine if it was technically possible and operationally practical to modify a LearJet 24 into a SSBJ (Figure 6-1). The technical design challenge is to retain as much of the LearJet vehicle while increasing the slenderness, modifying the wing and re-engining the aircraft. Details of this sizing study are published in Chudoba ⁽⁷²⁾.

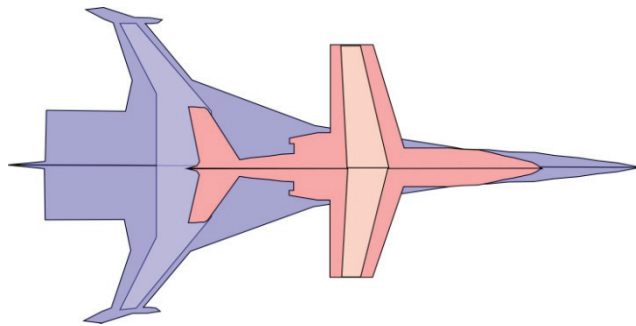


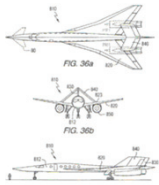
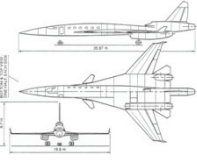
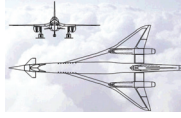
Fig 6-1: Size comparison of the LearJet 24 and Sukhoi Su-21 SSBJ ⁽⁷²⁾

Summary of Design Missions

References (98) and (98) present an applied market study for supersonic business jets performed by the AVD Lab under the SpiritLear contract. In these references it was determined that for a low cost, quick to the market business jet based on the LearJet airframe, it is necessary to have a high sonic boom design. In other words, no attempt is made to mitigate the sonic boom.

Several companies (Gulfstream, SAI, see Figure 6-2) are designing low-boom vehicles under the understanding that the prohibition of supersonic flight over land will be lifting if the sonic boom overpressure can be significantly reduced. It is believed that the SpiritLear SSBJ would be in the same holding pattern as Gulfstream and Lockheed-Martin/SAI, waiting for the regulation to change. Therefore a high-boom design is preferred for a quick to the market SSBJ

Table 6-1: Comparison of Selected SSBJ Projects

	LM/SAI QSST⁽¹⁰¹⁾	Sukhoi S-21⁽¹⁰²⁾	Dassault Trijet (103)
			
V_{cruise} , R	1.8M; 7,400 km	2.00M; 7,400 km 0.95M; 7,400 km	1.80M; 7,400 km 0.80M; 7,400 km
Pax design	8	4	8
max:	18	10	10
DOC	-	-	-
Price	\$80 mil/aircraft	\$40-50 mil/aircraft	\$70-80 mil/aircraft

Since the high-boom aircraft is not prohibited to fly supersonic over land, it must be designed to fly supersonic over water only, which means transatlantic and transpacific routes. These routes constitute design ranges of 7,400km (4,000 nm) as a minimum to make a two stop transpacific flight. In contrast, an early technical feasibility study performed by the AVD Lab determined the minimum change LearJet would only hold enough fuel to make a 5,560 km (3,000 nm) design range.

To explore both of these options more thoroughly, the practical mission of 7,400 km and the original LearJet 24 mission being constrained to 5,560 km mission are explored. Table 6-1 summarizes these two design missions.

Table 6-2: Design Missions for the SpritLear SSBJ

Mission Requirements	Practical Operational Mission	Learjet 24 Constrained Mission
Payload weight		
crew (2)	184 kg (410 lbs)	184 kg (410 lbs)
max passengers (8)	800 kg (1,764 lbs)	800 kg (1,764 lbs)
design passengers (4)	400 kg (881 lbs)	400 kg (881 lbs)
Range		
supersonic	7,400 km (4,000 nm)	5,560 km (3,000 nm)
transonic	7,400 km (4,000 nm)	7,400 km (4,000 nm)
Velocity		
supersonic cruise	1.4 – 1.8 M	1.4 – 1.8 M
transonic cruise	0.8 – 0.9 M	0.8 – 0.9 M
Altitude		
max operating	15,540 m (51,000 ft)	15,540 m (51,000 ft)
Take-Off Field Length [TOGW]	1,500 m – 2,440 m (6,000 -8,000 ft)	1,500 m – 2,440 m (6,000 -8,000 ft)
Landing Field Length [max landing weight]	1,520 m (6,000 ft)	2,438 m (6,000 ft)
Fuel Reserves	45 min, 1,524 km (5,000 ft)	45 min, 1,524 km (5,000 ft)

Summary of Objective Functions

The objective function for these vehicles is to minimize total DOC, as done with the transonic transports described in Chapter 5. This objective function allows for the weighting of both, fuel and TOGW, for the final SSBJ.

Summary of Design Variables

The analytical modeling of the delta wing body is generally similar to the TAC transport formulation, however it incorporates one significant modification. Instead of iterating the wing aspect ratio as a direct design variable, it is instead replaced with Küchemann's (s/l) slenderness parameter which is defined as the ratio of semi-span (s) the total length (l). This parameter fixes the ratio of span to length, thus as more volume is required for a given planform area, the wing aspect ratio changes accordingly.

When comparing the LearJet 24 to the Su-21, see Figure 6-1, it is clear that the LearJet 24 does not have the correct slenderness for a SSBJ design mission. Küchemann defines the minimum drag s/l as shown in Figure 6-2⁽¹⁰⁴⁾.

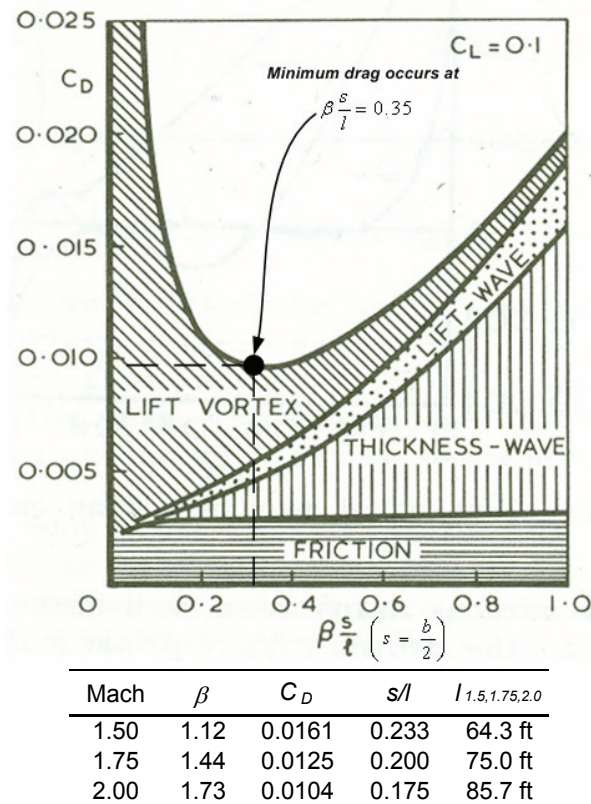


Fig 6-2: Drag components that constitute total supersonic drag and Mach 2, $C_L=0.1$ ⁽¹⁰⁴⁾

When utilizing this figure for guidance, then the design cruise Mach of 1.5 corresponds to a slenderness parameter of approximately 0.35. For example, to maintain this required slenderness parameter for supersonic flight, the LearJet 24 wing span fuselage length combination must be increased from 48 ft to 65 ft ⁽⁷²⁾.

The following demonstrates the sizing capability along two design trades: (1) 2 vs. 3 engine configuration, see Figure 6-3, and (2) stand-up cabin (2.3 m / 7.55 ft) vs. LearJet 24 sit-down cabin (1.6 m / 5.25 ft). These trades are performed to ascertain what modification would be required for the SpirtLear SSBJ while retaining the LearJet sit down cabin, and if such design would make sense from a performance and marketing point of view in the first place.

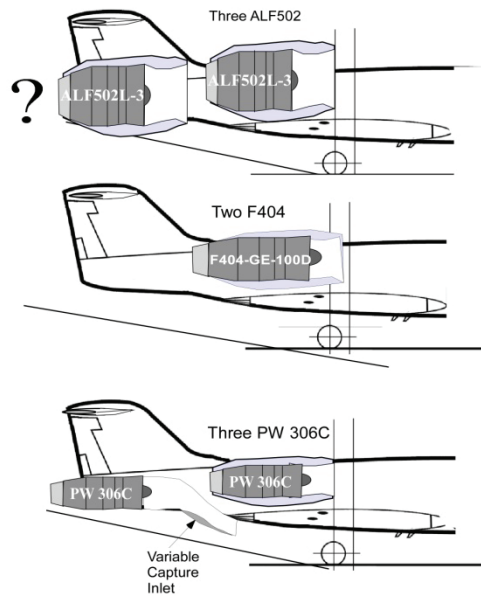


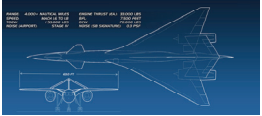
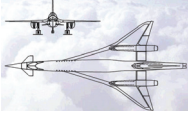
Fig 6-3: Possible engine installations for the SpirtLear SSBJ ⁽⁷²⁾

Discussion of Results

First, the results generated with AVD^{sizing} are compared with proposed SSBJ's in the literature. After review of several proposed business jet projects ⁽⁷²⁾, it was decided that the Dassault Trijet and LM/SAI QSST were the closest in shape to the proposed SpirtLear SSBJ, see Table 6-2.

The AVD^{sizing} modeling results for the Dassault Trijet and Lockheed-Martin/SAI QSST agree well with the published data from References (101) and (103), see Table 6-3. Note that the cost of the QSST per km (or nm) is significantly higher than the Trijet. This is due to the fact that the maximum payload of the QSST is 18 pax compared to the Trijet's 10 pax. This significant increase in payload for the QSST has a major impact on increased cabin volume required, enlarged wetted surface area, resulting in a much higher total TOGW and fuel weight, overall an increase in operating cost.

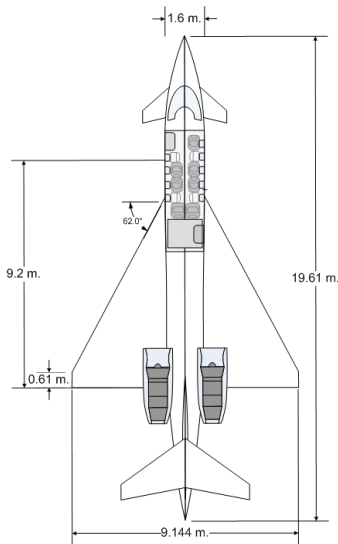
Table 6-3: Summary of SSBJ Comparison Study

Lockheed Martin/SAI QSST (101)				Dassault Trijet⁽¹⁰³⁾		
						
	Predicted	Actual	Error	Predicted	Actual	Error
Performance						
R _{SS} (km)	7,400	7,400	0.00%	7,400	7,400	0.00%
R _{TS} (km)	7,400	7,400	0.00%	7,400	7,400	0.00%
BFL (km)	2,286	2,286	0.00%	1,500	1,500	0.00%
Geometry						
S _{ref} (m ²)	183	197	-7.08%	133	130	2.36%
b (m)	19	19.204	-0.01%	17	17	0.00%
l (m)	40.4	40.4	0.00%	34	34	0.00%
Aerodynamics						
L/D _{SS}	6.3	-	-	6.1	-	-
L/D _{TS}	11.0	-	-	10.5	-	-
Propulsion						
TSFC _{SS} (/h)	0.819	-	-	0.828	-	-
T _{un} (kN)	317	294	7.96%	189	-	-
Weight						
OWE (kg)	31,020	31,751	-2.30%	19,114	18,241	4.79%
W _{fuel} (kg)	35,541	36,849	-3.55%	22,881	20,775	10.14%
W _{pay} (kg)	800	800	0.00%	800	800	0.00%
TOGW (kg)	67,545	69,400	-2.67%	42,979	40,000	7.45%
ff (kg)	0.53	0.53	-0.90%	0.53	0.52	2.50%
Cost						
(\$/unit)*	\$79	\$80	-1.52%	\$72	80	-10.45%
Supersonic**						
DOC \$/hr	13,393	-	-	9,238	-	-
DOC \$/km	8.89	-	-	6.10	-	-
DOC \$/nm	16.47	-	-	11.30	-	-
Transonic**						
DOC \$/hr	7,155	-	-	5,235	-	-
DOC \$/km	9.18	-	-	6.06	-	-
DOC \$/nm	17.01	-	-	11.22	-	-

Having demonstrated the overall validity of the sizing methodology with published data, the first trade-study of interest is the minimum-change SpirtLear SSBJ. The vehicle geometry is constrained by (1) the wing span of the existing wing LearJet wing, in order to retain the original structural wing box and structural hard-points, and (2) the original cabin section is to be retained (sit-down cabin). Thus, to maintain adequate vehicle slenderness (s/l), the fuselage is stretched (lengthened) accordingly. Table 6-4 summarizes the resulting aircraft.

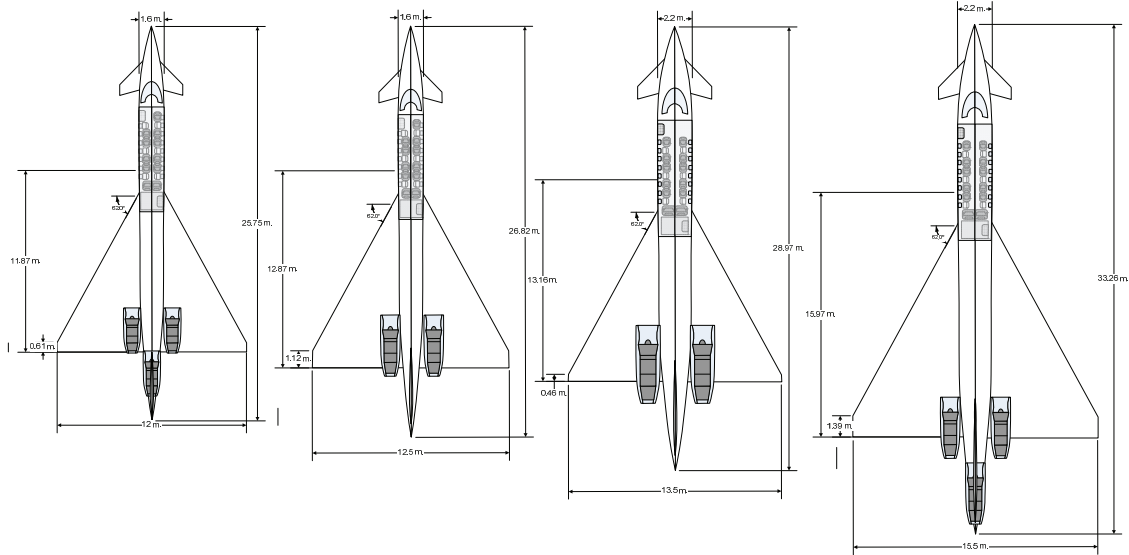
Table 6-4: Summary of LearJet 24-Constrained SSBJ

	SI	English
Performance		
h transonic (km-ft)	10.00	32,800
h supersonic (km-ft)	13.80	45,300
R supersonic (km-nm)	5,556	3,000
R transonic (km-nm)	7,400	3,996
BFL (m-ft)	2,440	8,000
Aerodynamics		
L/D transonic	8.22	-
L/D supersonic	5.93	-
C_{LA}	0.71	-
C_{LTO}	1.01	-
C_{Lmax} clean	1.20	-
Propulsion		
T_{sl} installed (kN-lbs)	92.2	20,721
T_{sl} uninstalled (kN-lbs)	101.4	22,793
Weight		
OWE (kg-lbs)	8,830	19,500
W_{fuel} (kg-lbs)	9,238	20,400
W_{pay} (kg-lbs)	400	882
$TOGW$ (kg-lbs)	18,700	41,000
ff	0.495	-
Cost		
Unit Cost \$/unit*	\$40,700,000	
DOC supersonic**		
\$/hr	\$4,319	
\$/km-\$/nm	\$3.26	\$6.04
DOC transonic**		
\$/hr	\$3,313	
\$/km-\$/nm	\$3.81	\$7.06



Comparing the SpiritLear SSBJ to the QSST and Trijet, it is clear that the SpiritLear will be significantly cheaper to purchase and operate. However, the design range constrains the aircraft to only short range over water flights. This will severely hinder the aircraft's marketability and utilization.

To determine the size and approximate cost of a practical high boom design, the primary design variables traded are the (1) number of engines, and (2) the cabin size applied to the practical design range of 7,400 km. Figure 6-5 is summarizing the resulting geometry and Figure 6-6 compares the cost, fuel weight and TOGW of the 4 designs considered.



	3 F404-100Dmod	2 JT8D-17AR	2 JT8D-216	3 JT8D-17AR
<i>Pax</i>	6	6	8	8
<i>R</i> (km-nm)	7,400 (4,000)	7,400 (4,000)	7,400 (4,000)	7,400 (4,000)
<i>BFL</i> (m-ft)	1,500 (8,000)	2,440 (8,000)	2,440 (8,000)	2,440 (8,000)
Cross-Section				
<i>w</i> (m-ft)	1.6 (5.25)	1.6 (5.25)	2.2 (7.22)	2.2 (7.22)
<i>h</i> (m-ft)	1.6 (5.25)	1.6 (5.25)	2.3 (7.55)	2.3 (7.55)
Aerodynamics				
<i>L/D</i> (1.5M)	6.76	6.69	6.44	7.00
<i>L/D</i> (0.9M)	9.40	9.47	9.50	9.84
<i>C_{Lmax} required</i>	1.78	1.26	1.50	1.45

Fig 6-4: Geometry results for the 4 primary trade-studies

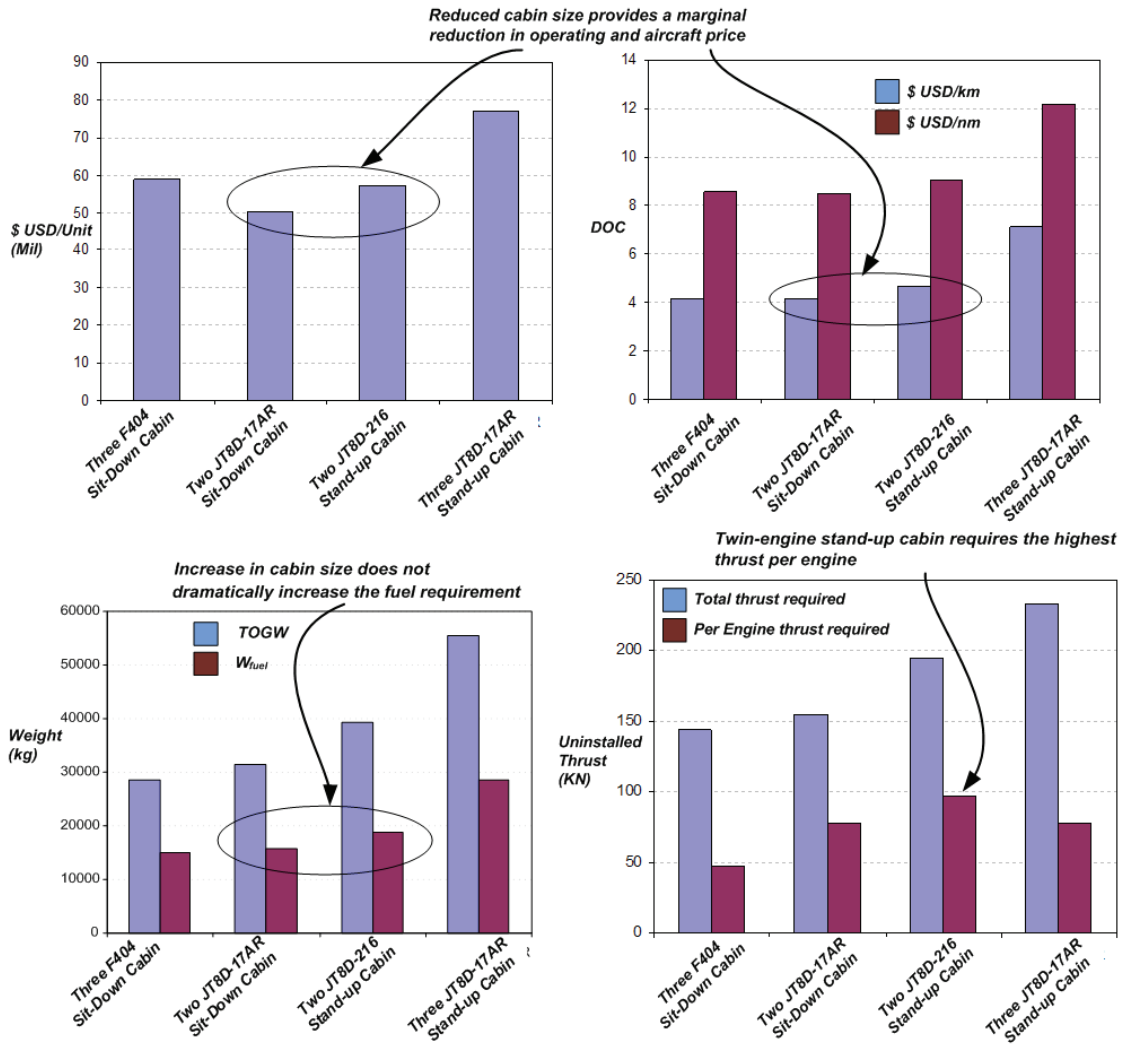


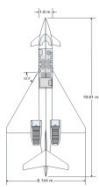
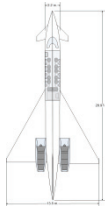
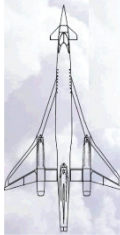

Fig 6-5: Geometry results for the 4 primary trade-studies

From these results two major conclusions can be drawn. First, the twin engine configuration is, relative to the tri-engine configuration, the lowest cost option in terms of maintenance and fuel burn. Second, transitioning to a stand-up cabin does not significantly increase the operating cost of the aircraft. This result suggests that, while a practical SSBJ can be produced with the same cabin of the LearJet 25, increasing the cabin to a stand-up cabin does not significantly affect the operating cost and fuel burn of the aircraft. Thus, the

marketability of a brand new aircraft, with a stand-up cabin would be improved without a serious performance impact.

All together, this study suggests that while a SSBJ can be developed from the LearJet 24, it will not have the same comfort as a modern business jets with a stand-up cabin while it would be severely limited on the over-water routes due to insufficient fuel volume. On the other hand, it does appear that an operationally sound 7,400 km range stand-up cabin SSBJ could be a quick to market and cost-effective alternative to the currently projected more complex SSBJ projects, see Table 6-5.

Table 6-5: Comparison sizing results for the of Selected SSBJ Projects

	3,000 nm <i>SpritLear</i>	4,000 nm <i>SpritLear</i>	Dassault <i>Trijet</i> ⁽⁵⁾	LM/SAI <i>QSST</i> ⁽³⁾
				
Weights				
<i>Pax</i>	4-6	8-12	8-12	8-18
<i>TOGW</i>	18,600 kg (41,100 lbs)	39,200 kg (86,500 lbs)	43,000 kg (94,700 lbs)	67,500 kg (149,000 lbs)
<i>ff</i>	0.495	0.478	0.532	0.526
Performance				
<i>R</i>	5,560 km (3,000 nm)	7,400 km (4,000 nm)	7,400 km (4,000 nm)	7,400 km (4,000 nm)
<i>M*</i>	1.5M/0.90M	1.5M/0.90M	1.8M/0.90M	1.8M/0.90M
<i>BFL</i>	2,440 m (8,000 ft)	2,440 m (8,000 ft)	1,500 m (4,900 ft)	2,440 m (8,000 ft)
Cost				
USD/unit**	\$40.1 mil	\$56.9 mil	\$71.6 mil	\$78.8 mil
USD/km***	\$3.26/\$3.81	\$4.67/\$5.11	\$6.10/\$6.06	\$8.89/\$9.18
Risk				
Propulsion	existing	existing	new	new
Aero/Structure	conventional delta wing	conventional delta wing	conventional delta wing	conventional delta wing
Sonic Boom	high-boom	high-boom	high-boom	low-boom
Supersonic	transatlantic	transatlantic/transpacific	transatlantic/transpacific	transatlantic/transpacific
Operation	moderate risk with existing technology and propulsion system; low operational performance	low risk with existing technology and propulsion system; adequate operational performance	moderate risk requiring new propulsion system; adequate operational performance	high risk due to new propulsion system and change in boom regulations; superior performance
Comments				

Summary of Conclusions

From this study it can be concluded that AVD^{sizing} can be applied to SSBJ sizing as evidenced through the abbreviated QSST, Trijet, and SpirtLear SSBJ design studies presented here. Its flexibility in terms of methods and process allow for rapid evaluation of unconventional ideas such as a modified LearJet 24 SSBJ for different operational scenarios.

While an intriguing idea to modify an existing business jet for supersonic flight, the resulting aircraft is impractical in terms of range. A high-boom, quick to the market SSBJ with 7,400 km range could be developed with existing technology. However, given the current economic downturn, development of such a luxury vehicle will not occur in the near term. If a manufacture was to go ahead with a *'quick and dirty'* SSBJ program, it would be better to start with a new 'high-boom' aircraft based on existing systems, thereby compromising some of the cruise velocity and balanced field length performance.

Risk of Assumptions

For any novel configuration or configuration the conceptual design must make and disclose assumptions in order to start the design cycle. Sense little disciplinary has been performed this early, issues such as assumed structural concept, technology improvement and cost, etc. require reasonable assumptions in order to determine if the concept is worthy of further study. These assumptions represent the known unknowns of the design and therefore contribute the overall risk of the configuration and concept. Through openly disclosing the fundamental assumptions the later design phases have a start point for future disciplinary studies and risk mitigation.

For the SSBJ studies the majority of the uncertainly in the analysis is derived from,

1. Wing structural weight. The wing weight methods utilized for this study is an empirical method from Howe ⁽³⁶⁾ for delta-wing supersonic intercept fighters. The wing structural concepts are similar between delta wing SSBJs and intercept fighters, however,

structural design loads of a fighter are typically higher than transports. Even considering the possible discrepancy in loads the methods are in agreement with the QSST and Trijet studies. The remaining aerodynamic and propulsion methods have been applied and validated for vehicles and scale and velocity.

2. The largest assumption in the SpiritLear SSBJ study is that business travelers would accept a SSBJ which can only fly supersonic over water due to the high sonic boom design. This noise constraint limits the applicability of the vehicle and could shrink the projected niche SSBJ market.

6.2 Summary of Sänger EHTV and LAPCAT II Hypersonic Cruise Vehicle Studies

AVD^{sizing} has been utilized for two hypersonic cruise vehicle studies, the (1) MBB Sänger EHTV, and the (2) ESA LAPCAT II transport. These case studies together illustrate the need for a sizing capability able to identify market potential and technical feasibility of proposed flight vehicle products

The MBB Sänger EHTV has been a modification of the 1st stage of the Sänger II two-stage to orbit (TSTO) launch vehicle, see Figure 6-7.⁽¹⁰⁵⁾ The study objective has been to utilize the first stage as a hypersonic passenger transport and develop a hypersonic cruiser which could be an operational success⁽¹⁰⁵⁾.



Fig 6-6: Sänger II is a proposed hypersonic cruiser based on the first stage of the Sänger TSTO launch system⁽¹⁰⁵⁾

The ESA LAPCAT II program's objective is to “*Examine propulsion concepts and technologies required for reduced long distance flight times*”⁽¹⁰⁶⁾. This project is centered on providing customers with an antipodal range aircraft (18,000 km) with flight times of 2 to 4 hours, resulting in cruise speeds of Mach 4 to 8. This design mission has led to several proposed configurations, see Figure 6-8.

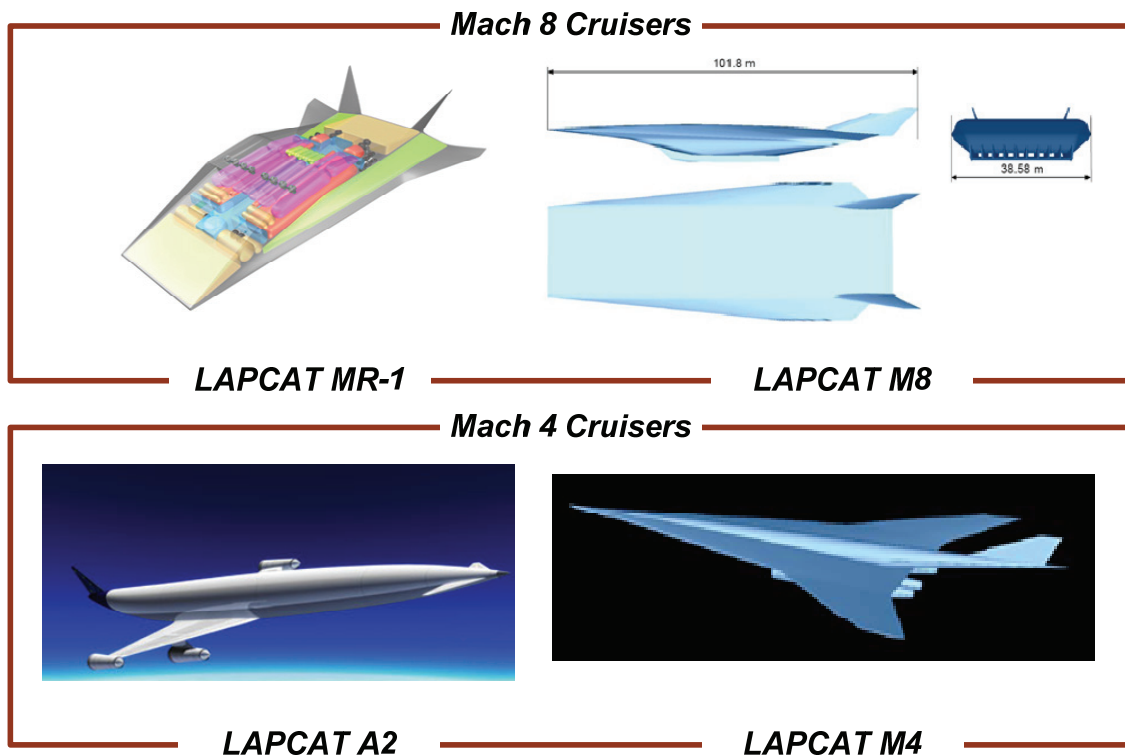


Fig 6-7: LAPCAT program proposed Hypersonic Cruiser Designs ⁽¹⁰⁶⁾

Recently, the AVD Lab has been engaged by the University of Rome to support a portion of the LAPCAT Mach 8 study ⁽¹⁰⁷⁾. For this study the University of Rome has been assigned to study a hypersonic M8 design employing the pre-cooled turbo-ramjet-scrumjet. In support of this activity, the AVD Lab at UTA MAE has utilized AVD^{sizing} for both, the pre-cooled turbo-ramjet and the ejector ram/scram jet powered aircraft. The ejector ram/scramjet has been explored as an alternative to the turbo-ramjet-scrumjet due to the large number of turbo-ramjets required for transonic acceleration.

The study results presented here directly compare the Sanger EHTV and LAPCAT II designs, using a consistent analysis framework in order to assess the correct mission for a hypersonic transportation system. As with the SSBJ study in Chapter 6.1, designing a commercial aircraft for an ill-conceived market will lead to overall failure of the program/project, see also Concorde, Tu-144, and others.

To facilitate this comparison, the Sanger EHTV has been sized to be the baseline or reference aircraft. The simulation results have been compared with published data available from MBB ⁽¹⁰⁵⁾. In a second step, the design mission has been changed, resulting in the study-vehicle LAPCAT II.

In the course of the LAPCAT II study it was determined that the ejector ram/scramjet is preferred to the pre-cooled turbo-ramjet scramjet. The ejector ram/scramjet yields a lighter total propulsion system compared to the turbo-ramjet propulsion system. The simulation clearly identifies that the acceleration phase through the transonic regime presents the most critical thrust requirement for this mission, resulting in a very high number (up to 20) pre-cooled-turbo-ramjets required for this scale of vehicle. This accumulation of turbo-machinery is simply impractical from a vehicle size, weight, and maintenance stand point. Thus, only the ejector ram/scramjet is presented in this chapter as a viable alternative for an operational Mach 8 mission.

Summary of Design Missions

Beginning with a first principles understanding of high-speed flight, it becomes clear that cruising between Mach 1 and 3 results in an energetic efficiency minimum (i.e. more fuel required traveling a specific range). Kuchemann ⁽¹⁰⁴⁾ illustrates that as the Mach number increases from 0 to Mach 10, the propulsion system overall efficiency increases while the aerodynamic efficiency reduces, see Figure 6-8.

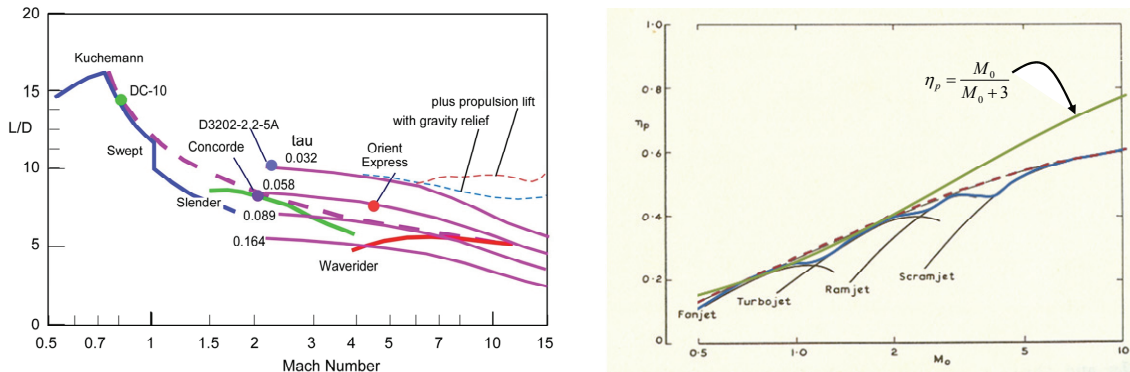


Fig 6-8: Overall propulsion efficiency and aerodynamic efficiency as Mach number increases (modified from Reference (104))

When superimposing the aerodynamic and propulsion effects, we do observe that the aerodynamic efficiency levels out as the propulsion efficiencies tend to increase past Mach 2. Applying these effects to three primary flight vehicle families (1) swept wing-body (e.g. B707), (2) slender wing-body (e.g. Concorde), and (3) an ideal Nonweiler waverider⁽¹⁰⁸⁾ configuration. Kuchemann identified for these flight vehicle families in Reference 50 three energetically optimal missions: (1) transonic 0.8 M, (2) supersonic, $3 < M < 5$ and (3) hypersonic 10 - 20 M+, see Figure 6-9⁽¹⁰⁴⁾. It is important to understand that the optimum at Mach 10 - 20 assumes an ideal waverider external combustion system.

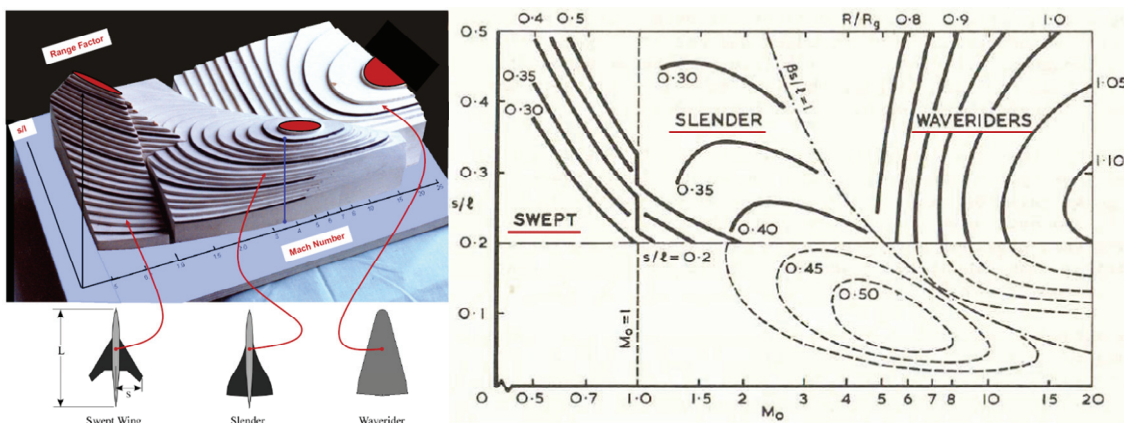


Fig 6-9: Kuchemann diagram demonstrating the optimum range normalized to global range as a function of Mach number and vehicle slenderness, (s/l) (modified from (104)).

When recreating this solution-space map from the theory presented in Küchemann⁽¹⁰⁴⁾, the following solution topography emerges, identifying that most supersonic aircraft reside near the energetic efficiency minimum (in this case for the same weight of fuel, reduced range capability) at the beginning of supersonic flight (Figure 5-6)

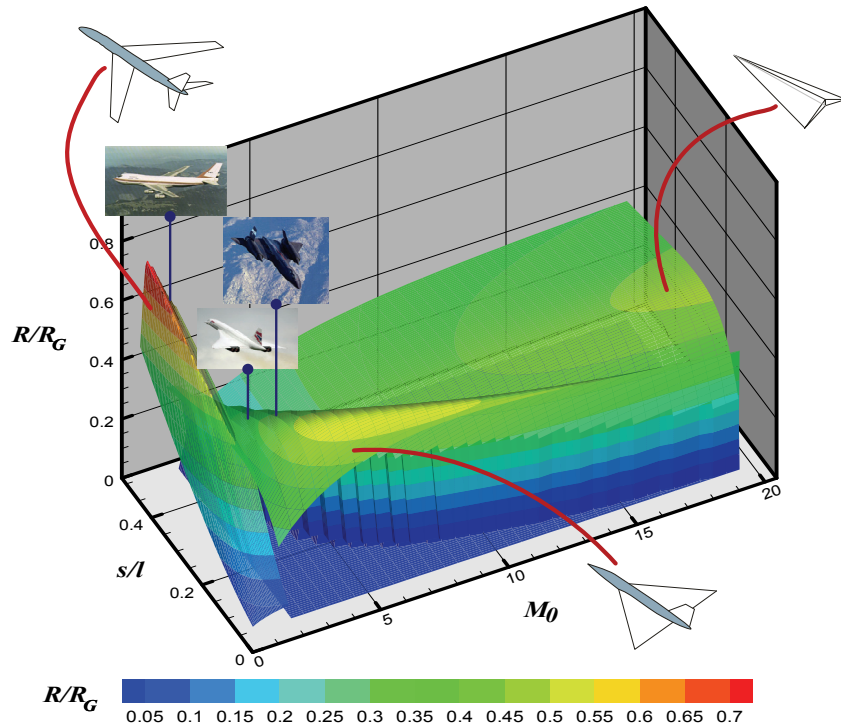


Fig 6-10: Recreation of Küchemann’s solution-space topography, demonstrating examples of existing supersonic aircraft (note: in Figure 5-5 Mach number is on a logarithmic scale).

As shown by this map between mach 4 and 6 rests a locally optimum cruise performance for slender aircraft in terms of aerodynamic and propulsion efficiency.

An additional consideration for a Mach 4 to 6 vehicle is the dissipation of the sonic boom. The MBB Sänger EHTV study, see Reference (105), determined that at the required cruise altitude for a Mach 4.4 vehicle (above the sensible ozone), the sonic boom will dissipate significantly before it reaches ground level, see Figure 6-11.

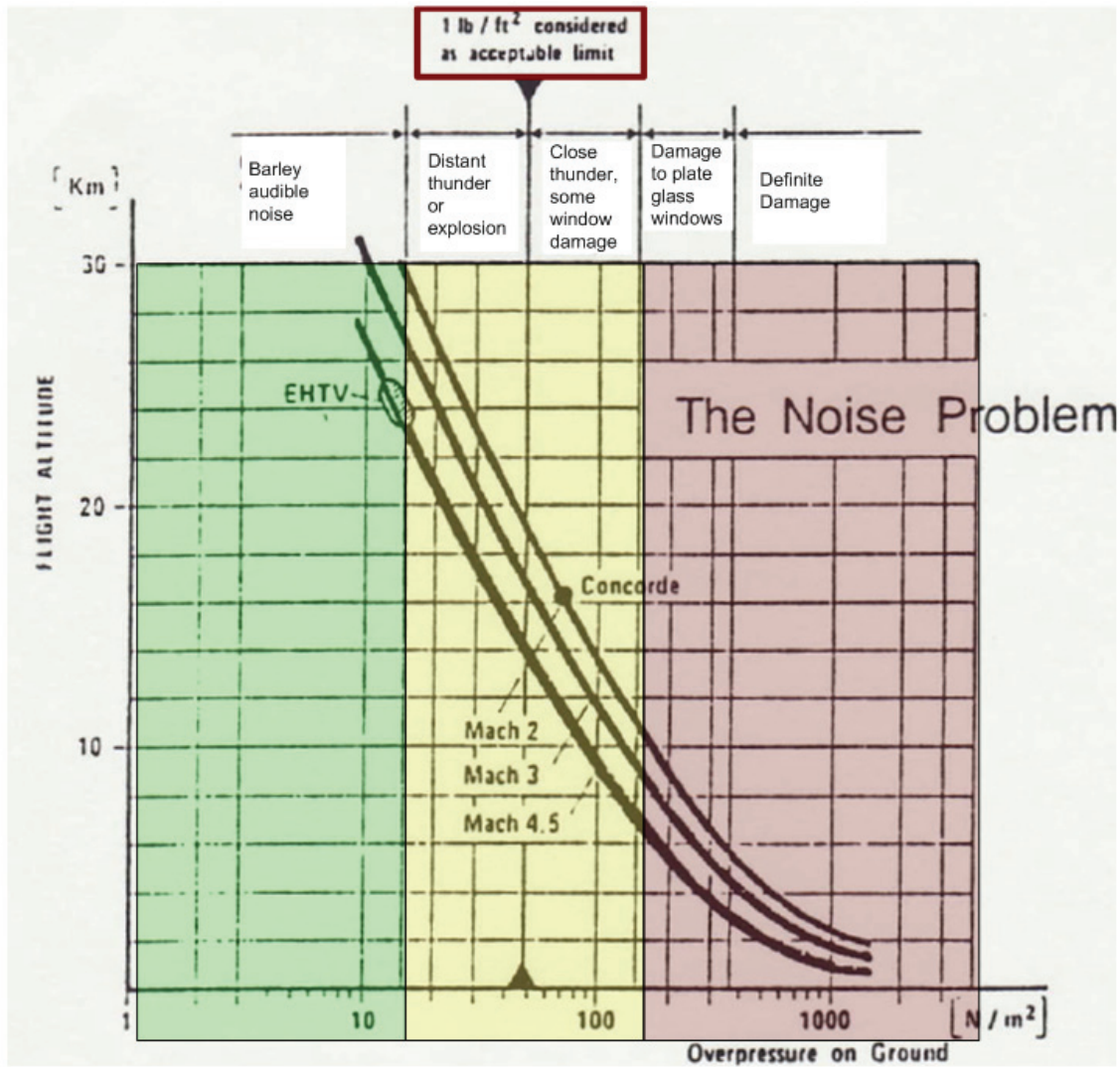


Fig 6-11: Reduction in overpressure on ground due to increase cruise altitude and Mach possible for a Mach 4.4 cruiser relative to Mach 2 or 3 aircraft (modified from Reference (105)).

The MBB Sanger EHTV study provides, interestingly, another piece to the high-speed puzzle from the stand point of operational constraints. Examining the block hours flown for the given design ranges, the flight duration begins to level-off just beyond Mach 4.5 for design ranges of 10,000 to 7,000 km, which are the most frequented international routes ⁽¹⁰⁵⁾, see Figure 6-11. This data suggests that a design range of 10,000 km at Mach 4.5 would allow for an operationally optimal vehicle.

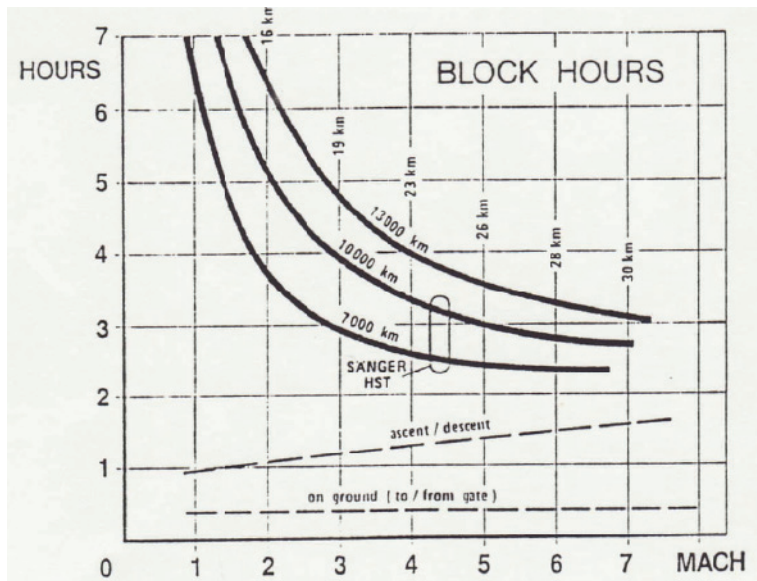


Fig 6-12: For 7,000 to 10,000 km design ranges little time savings is achieved for design speeds past Mach 4.5⁽¹⁰⁵⁾.

The MBB Sänger II study further demonstrates that the optimum Mach number for a high-speed transport ranges around Mach 4.4 from the stand point of flight hours per day and km per day, see Figure 6-12. This figure illustrates that including ground time in the analysis above Mach 5 results in a decrease in the number of trips per day⁽¹⁰⁵⁾. This is attributed to the maintenance associated to more sophisticated thermal protection system and cool down times.

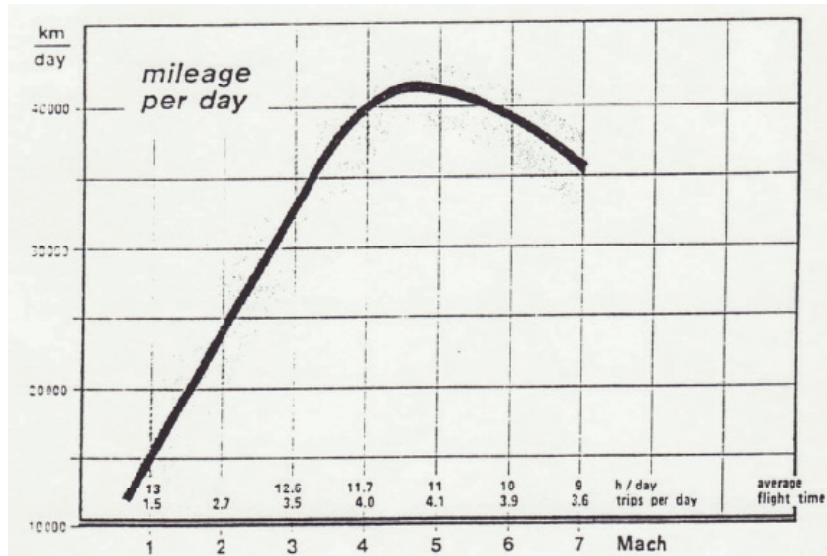


Fig 6-13: Mach 4.4 demonstrates an operational optimum in terms of flights per day and km per day

Combining the energetic optimum mission from Küchemann with the sonic boom mitigation and the operational constraints explored in the Sängler II study a Mach 4.4, the 10,000 km design range appears to be a very practical design mission for a hypersonic cruiser able to operate out of existing runways. Table 6.6 summarizes the Sängler II design mission.

Table 6-6: Sängler II Hypersonic Transport Validation Case Mission Summary

Mission	
Design payload	250 pax 250,000 kg (551,000 lbs)
Range	10,500 km (5670 nm)
Velocity(design cruise)	4.4 M
Initial Cruise Altitude	24,500 m (80,400 ft)
Take-off Field Length (TOGW)	< 3,340 m (11,000 ft)
Landing field length (MLW)	< 2180 m (7,150 ft)
Reserve mission	45 min

In this context, the LAPCAT II project, see Reference (106), does clearly not present a realistic business case for such a long range and high-speed mission. In light of the Sanger EHTV study it appears that the LAPCAT II mission is ill-conditioned from an operational and market point of view. Taking this mission-related understanding into mind, the LAPCAT II mission will be analyzed with AVD^{sizing} as described in Figure 6-7.

Table 6-7: LAPCAT II Mach 8 Mission Summary⁽¹⁰⁶⁾

Mission	
Design payload	300 pax 300,000 kg (662,000 lbs)
Range	18,000 km (9,700 nm)
Velocity(design cruise)	8.0 M
Initial Cruise Altitude	30,000 m (98,400 ft)
Take-off Field Length (TOGW)	< 3,340 m (11,000 ft)
Landing field length (MLW)	< 2180 m (7,150 ft)
Reserve mission	45 min

For LAPCAT II, a standard trajectory is assumed consisting of (1) climb to 10,000 ft, (2) constant altitude acceleration to 0.8 M, (3) constant Mach climb to 12,000, (4) constant altitude acceleration through the transonic region to maximum dynamic pressure, (5) constant dynamic pressure climb to cruise altitude, (6) cruise-climb to altitude, (7) maximum L/D descent, and (8) landing, see Figure 6-13.

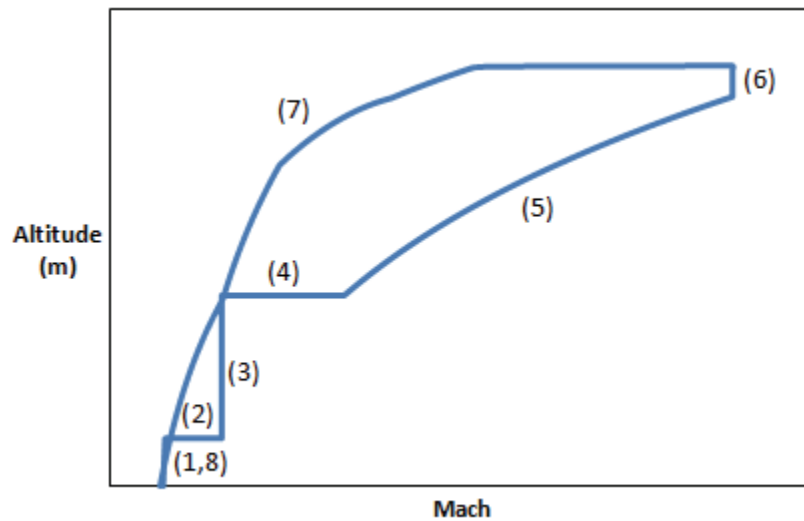


Fig 6-14: Nominal trajectory for the hypersonic cruise aircraft.

Summary of Objective Function

A rule of thumb in conceptual design is that a minimum TOGW solution will most likely lead to the minimum cost solution. It has been shown for transonic transports, see Chapter 5, that this is not always the case for transonic transports (Chapter 4.4). However, for hypersonic cruisers with fuel fractions larger than 50 to 60%, minimum take-off gross weight clearly corresponds to minimum fuel weight. Therefore, a minimum DOC-design would also correspond to a minimum TOGW-design solution. The only case where a minimum TOGW solution does not point towards minimum cost is when minimum TOGW does not correspond to minimum fuel. Therefore, a minimum TOGW objective function is utilized for this study.

Summary of Design Variables

For the Sänger EHTV, a wing body configuration is preferred due to improved low-speed and high-speed L/D relative to a blended body (64). On the other hand, The LAPCAT II mission prefers a blended-body configuration due to the large fuel volume required. A blended-body arrangement yields larger volumetric efficiency compared to the wing-body, thus the blended-body configuration results in a lighter vehicle for fuel dominated aircraft such as launch

vehicles (64) and in this case Mach 8 cruisers, see Figure 6-14. In both cases, the primary design variable for vehicle sizing is the Küchemann correlation parameter, τ , see (Figure 6-14.

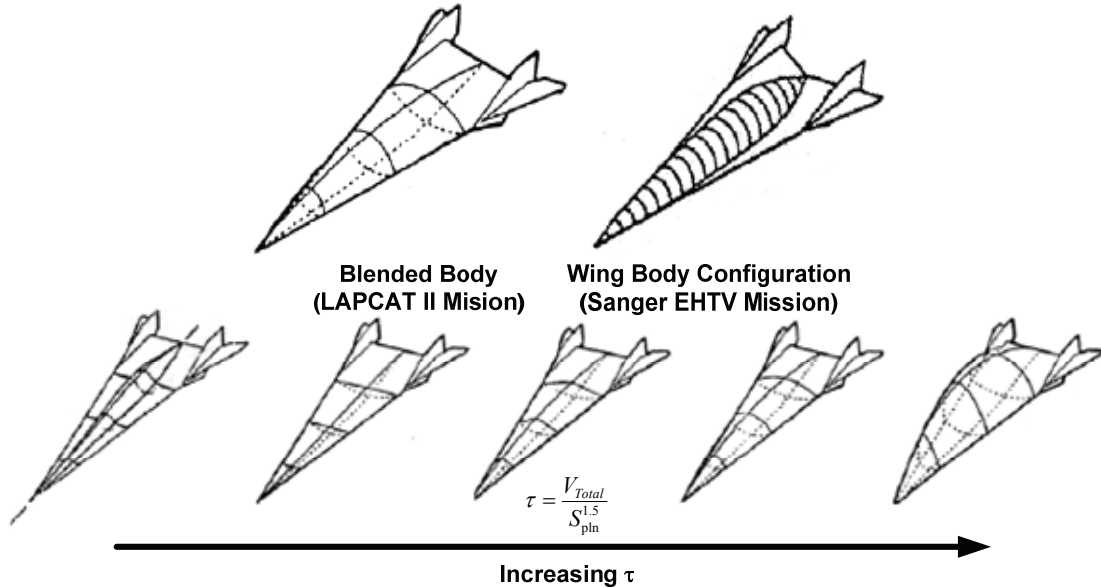


Fig 6-15: Selected Configurations for the Sänger EHTV and LAPCAT II missions along with explanation of Küchemann's τ correlation parameter.

In Hypersonic Convergence⁽⁶⁴⁾, the structural efficiency of the vehicle is controlled by the structural index as described in Figure 6-15. This trend was developed at McDonnell-Douglas circa 1970 for a combined thermal protection/primary structure sandwich⁽⁶⁴⁾. Thus by specifying the structural weight per surface area (or wetted area), a reasonably accurate estimate of the structural weight can be determined. For the Sänger II project, the curve describing in Figure 6-15 the cruiser aircraft with a passive thermal protection system is applied while the thermal environment of the LAPCAT II mission requires a thermally managed structure. Thus, a range of 18.0 to 21.0 kg/m² will be used for the Sänger EHTV mission and an 18.0 kg/m² will be used for the LAPCAT II mission (Figure 6-15).

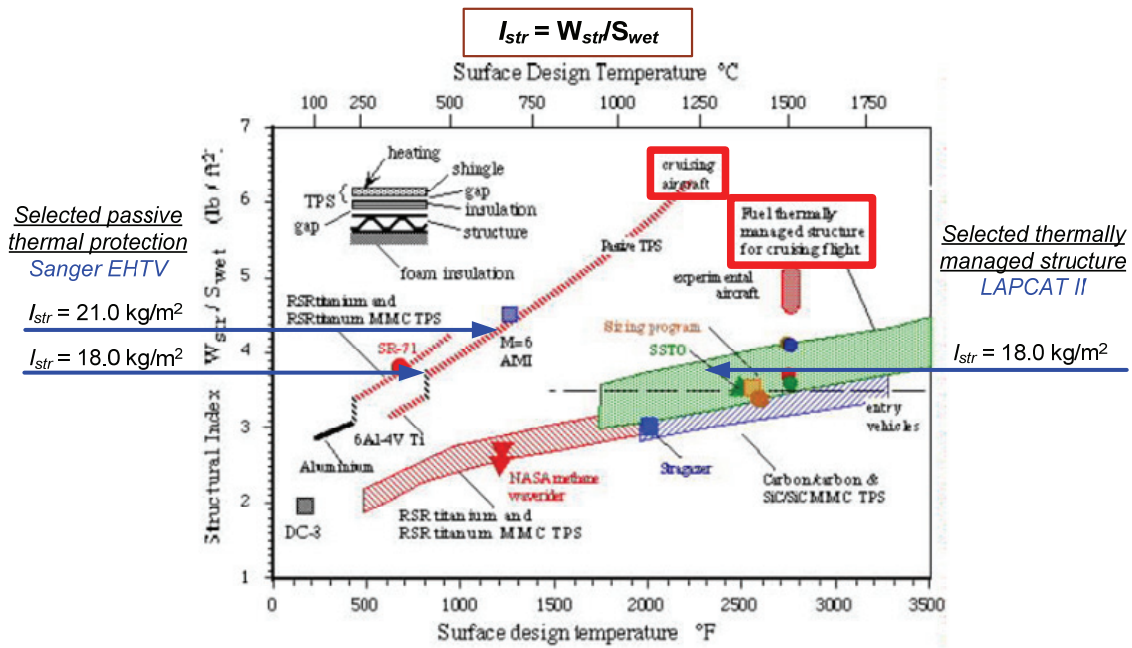


Fig 6-16: Selected Structural Indices for the Sanger EHTV and LAPCAT II Missions (modified from Reference (64)).

The propulsion system selected for the Sänger II was a dual turbo-ramjet cycle. To approximate such propulsion system, the cycle analysis data from the HYCAT⁽¹⁰⁹⁾ study is utilized as an initial propulsion model, see Figure 6-16. Note that the HYCAT turbo-ramjet propulsion system integration is similar to the Sänger II integration^{(105), (84)}.

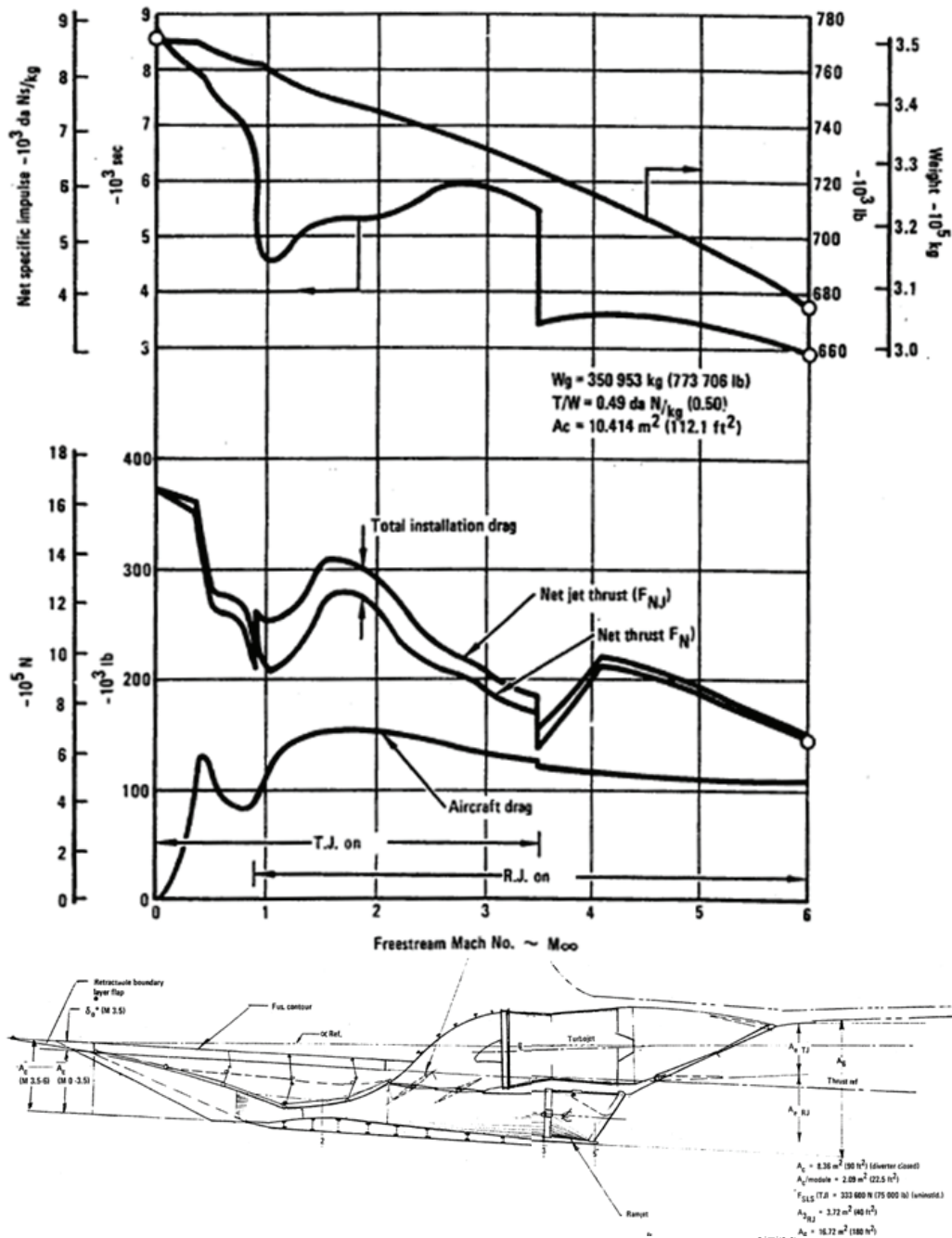


Fig 6-17: HYCAT turbo-ramjet propulsion system model used for the AVD^{sizing} Sänger II model (109)

For the LAPCAT II study, an ejector ram/scramjet is utilized similar to the system designed by ONERA in the mid 1980's⁽¹¹⁰⁾, see Figure 6-17. This data was used to approximate the engines performance through the prescribed trajectory.

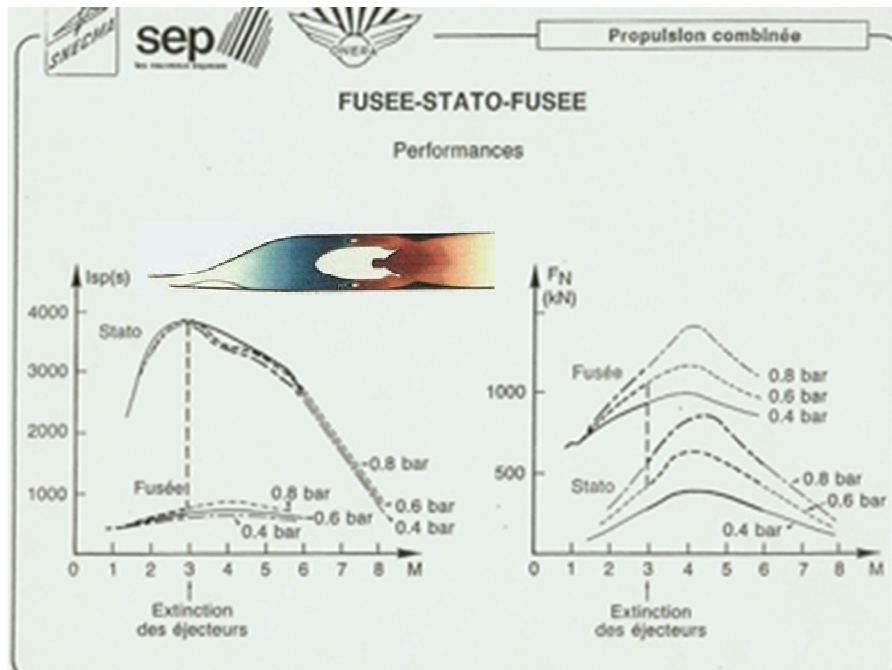


Fig 6-18: ONERA ejector ramjet performance chart⁽¹¹⁰⁾

Discussion of Results

Beginning with the Sänger EHTV, Figure 6-18 compares the solution curves for the two structural indices selected in Figure 6-15. As shown, the design match point occurs where the TOGW solution curve intersects the landing constraint. It is important to note that a minimum fuel weight solution occurs for a wing area which violates the landing wing loading constraint. Essentially, the mission constraint of operating out of existing runways is prohibiting a more fuel efficient vehicle. Thus, to be operationally successful, the Sänger design must have an oversized wing from a cruise performance standpoint. This is the same type of situation found with most transonic commercial transports. In this case if the runway length not an issue then a smaller wing could be used for cruise.

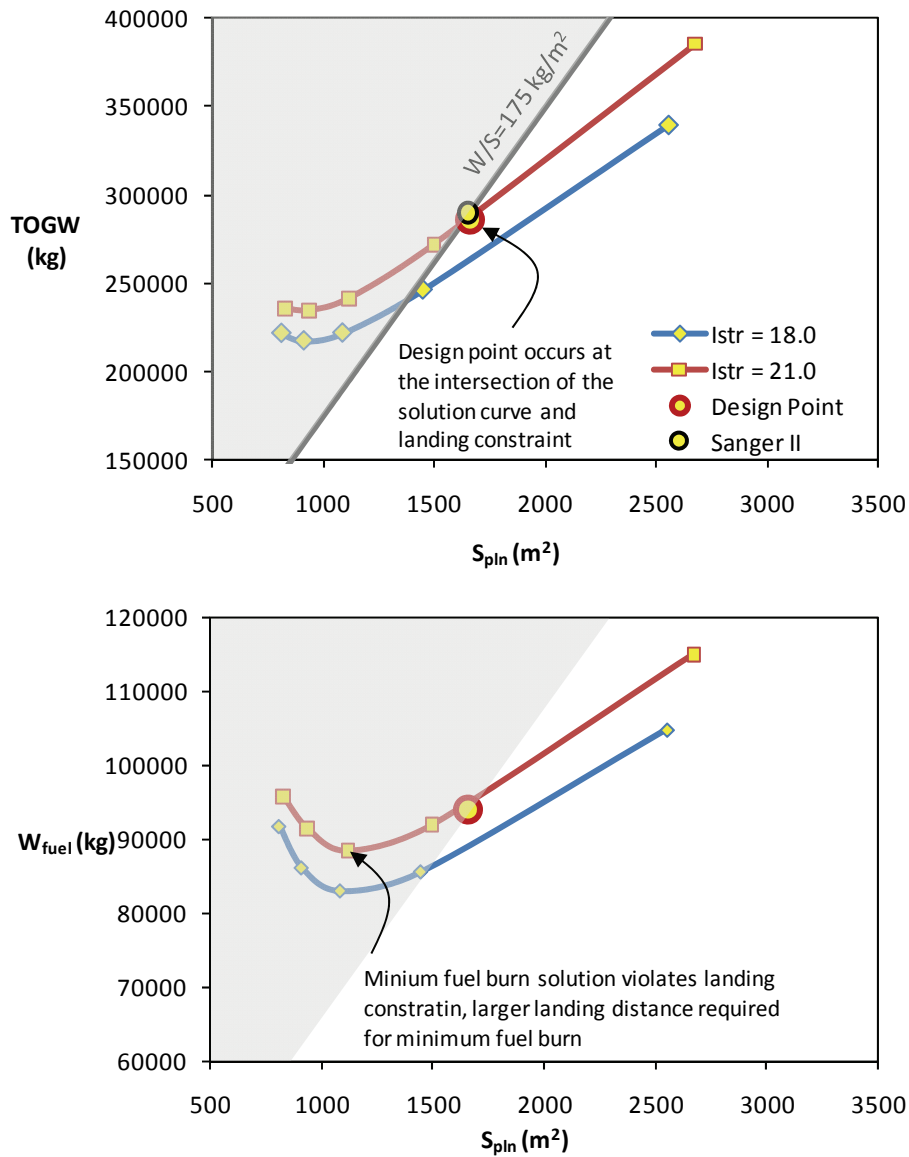


Fig 6-19: Säger II design space for two structural indices.

From Figure 6-18 it appears that the Säger II structural concept is conservative relative to the McDonnell Douglas structural index which indicates that $I_{str} = 21$ would be on the upper bound of the thermal protection and structural weight required. This is not surprising given MBB's philosophy of operational robustness⁽¹⁰⁵⁾.

Table 6-8 compares the AVD^{sizing} modeled baseline aircraft with original data for Sanger II from Reference (105). In this case, AVD^{sizing} is in agreement with the Sanger EHTV project.

Table 6-8: Sanger Hypersonic Transport Validation Summary (105)

	SANGER	BASELINE	Error	
				<i>Approximate Geometry (propulsion system not shown)</i>
Geometry				
τ	-	0.035		
S_{pln} (m ²)	1654.05	1656.27	0.13%	
b (m)	41.50	37.53	10.59%	
c (m)	0.00	0.00	-	
L (m)	84.50	88.27	4.27%	
h (m)	2.91	2.72	-6.80%	
Weight				
TOGW (kg)	290000	285663	-1.52%	
W _{fuel} (kg)	100000	94051	-6.33%	
W _{pay} (kg)	25000	25000	0.00%	
OEW (kg)	155000	166612	6.97%	
Aero-Propulsion				
ff	0.34	0.33	-4.74%	
Alt _{cruise avg} (m)	24500	24500	0.00%	
L/D _{cruise avg}	5.7	5.8	1.72%	
I _{SPcruise avg} (s)	3670	3740	1.87%	

When comparing the technical aspects of the dramatically different LAPCAT design mission, it is clear that the resulting vehicle will require an excessive amount of fuel relative to the slower market-derived Sanger II mission. Comparing the Sanger EHTV project solution to the LAPCAT II ejector ram/scramjet solution, see Figure 6-19, it is clear that the Sanger EHTV design represents a far lighter vehicle compared to LACPAT II.

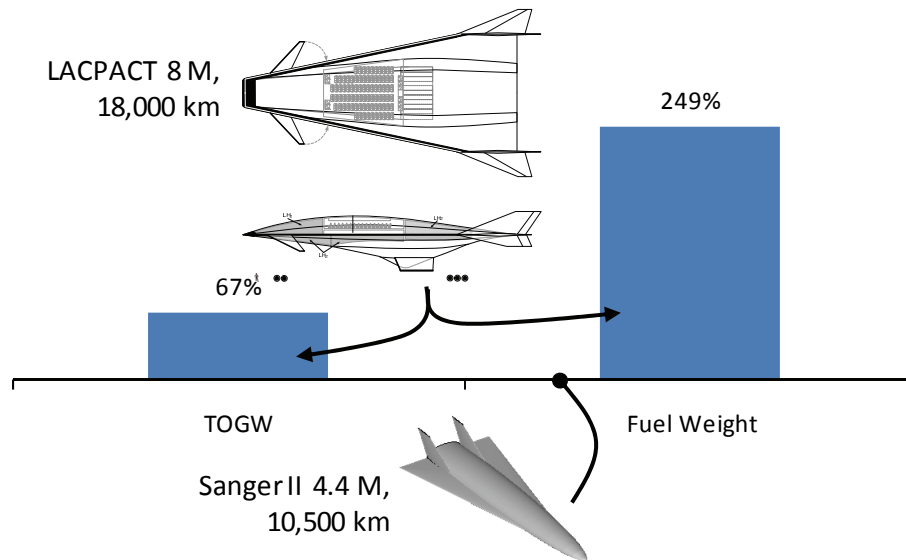


Fig 6-20: LACPACT 8 M, 18,000 km blended-body compared to Sanger II 4.4 M, 10,500 km wing-body reference vehicle.

The LACPACT mission results in a fuel weight increase by 250% due to the dramatic increase in design range and velocity, while the TOGW increase by only 67%. The TOGW does not increase by the same amount as the fuel weight since the blended-body configuration is volumetrically more efficient. The increased volumetric efficiency of the blended-body configuration is a critical design-choice for the Mach 8 mission, since L/D deteriorates slower compared to the increase in fuel volume available. ⁽⁶⁴⁾

Comparing these two near optimum solutions for minimum cost (via min TOGW), it is clear that an ill-conceived mission, such as the LACPACT II, results in an ill-conditioned aircraft. If a commercial manufacture is to seriously consider a hypersonic vehicle, it is clear that the Sanger EHTV mission results in a simpler technical solution while addressing a correctly identified business case.

Combining the LACPACT mission's questionable market placement and dramatically increased fuel requirements can mislead future technology planning and development. Since there is little justification nor need for a Mach 8 transport, and since a slower Mach 4.4 vehicle

will not dramatically increased travel time, the Mach 8 propulsion system design studies for a commercial transport appears to be a futile exercise.

Skepticisms aside, Mach 8 may be a tempted design speed for military hypersonic point-to-point (DARPA Falcon HT-2 Program ⁽¹¹¹⁾) Delivery of military supplies, troops, warheads or performing surveillance at such a velocities and range would be worthwhile, given the extreme time sensitivity of such military objectives.

Even though the Sanger EHTV looks technically and operationally feasible relative to LAPCAT II, it is still a challenging vehicle which will require extensive R&D, market development and infrastructure reform to make a viable product. In both the Sanger EHTV and LAPCAT II design cases, hydrogen is the selected fuel due to its superb energy efficiency. However, as of yet a hydrogen infrastructure does not exist at major international airports. Thus, the total air transportation systems should be examined in a later study in conjunction with the market and vehicle. Any hypersonic vehicle design study needs to be discussed in the broader context of the overall air transportation infrastructure.

Summary of Conclusions

It is concluded that the methods and the process underlying AVD^{sizing} provide an accurate representation for the Mach 4.4 Sanger II hypersonic cruiser. Applying this process to both, the Sanger EHTV and LAPCAT II designs, does demonstrate the meaningfulness of this capability to generate system-level information for the decision-maker involving gross-design disciplines and variables.

The total process also demonstrates the ability to complement market and mission planning by providing technical feedback to the overall feasibility of the mission. Comparing the design missions and resulting aircraft for the Sanger EHTV and LAPCAT II, it is clear the ill-conceived LAPCAT II mission results in an excessively large aircraft for a route which does not satisfy any customer demand. For the ill-defined mission, the resulting risk-level for the operator

would clearly represent a show-stopper; if the aircraft cannot be filled to capacity (300 pax) 3 to 4 times a day for an antipodal route, the losses in revenue would be staggering. Such risk is also prevalent for the Sanger EHTV. However, this smaller sized aircraft is inherently more flexible to operate on shorter and long international routes

Risk of Assumptions

For any novel configuration or configuration the conceptual design must make and disclose assumptions in order to start the design cycle. Sense little disciplinary has been performed this early, issues such as assumed structural concept, technology improvement and cost, etc. require reasonable assumptions in order to determine if the concept is worthy of further study. These assumptions represent the known unknowns of the design and therefore contribute the overall risk of the configuration and concept. Through openly disclosing the fundamental assumptions the later design phases have a start point for future disciplinary studies and risk mitigation.

For the Hypersonic cruiser study the uncertainty in the analysis is derived from,

1. Hydrogen infrastructure. In both cases liquid hydrogen is selected as the fuel source due to its high energy content. However, currently no hydrogen infrastructure exists to supply the amount of hydrogen required to major international airports.
2. Given the Concorde accident in July, 2000 ⁽¹¹²⁾ it is unlikely that regulatory bodies will allow turbojets podded in such proximity. In the cases where one engine failure could lead to a multiple engine failure (such as one engine failure damaging the adjacent engines or ingestion of debris/smoke by one engine could also be ingested by the other) the proximity of the turbojets makes the likelihood of total engine failure unacceptable. This constraint could prohibit the use of turbomachinery on hypersonic commercial transports. Propulsion system reliability is paramount for commercial application of highly integrated hypersonic configurations.

3. Market for Mach 4.4 is viable from an operational stand-point; however, no market currently exists for such a high-speed aircraft. The cost per passenger/cargo must be kept reasonable to justify the significant time savings.

6.3 Summary of Results and Contribution Summary

These two high-speed case studies demonstrate the usefulness of AVD^{sizing} and the methods library as an essential tool for high-speed mission- vehicle-design. Both design cases, the SSBJ and hypersonic cruiser studies, the methodology does generate correct trends and reasonable accurate results relative to representative published projects. Again, the focus of early design studies is not on accuracy but correctness, helping the designer to identify the gross design drivers and associated sensitivities for mission parameters.

These studies demonstrate how much physical insight the design team is able to gain utilizing a parametric sizing tool towards mission planning and market studies. In both cases discussed, the business case and technical detail has been assessed using parametric sizing in the quest to match technically feasible and economic vehicle to the correct market. The SpiritLear SSBJ demonstrated that it is technically feasible for a LearJet 24 to be modified into a SSBJ, however, the minimum modification design does not fit the market. When the SSBJ is designed for the market, little remains of the LearJet 24 to make the modification worthwhile.

This situation of matching the market to the vehicle is exemplified, again, through an evaluation of the Sanger EHTV and LAPCAT II programs. The Sanger EHTV is designed to a sound operational mission relative to the LAPCAT II. The result is a simpler technical challenge for the Sanger EHTV relative to the LAPCAT II. The increased technical difficulty and market risk of the LAPCAT II vehicle creates an impractical and irrelevant engineering problem from a commercial stand-point. The situation is in direct opposition to the given mission statement of the LAPCAT program, which is to “*Examine propulsion concepts and technologies **required** for*

reduced long distance flight times ⁽¹⁰⁶⁾". Reducing commercial flight times is irrelevant if the market cannot support the vehicle.

In summary, this research investigation as proven to generate a sought-after contribution to aerospace-science while delivering state-of-the-art understanding of high-speed vehicle synthesis and design. With the support of a rapid and physically transparent process and methods library, the designer is in a better situation to respond not only to a variety of technical challenges for a given mission, but, to evaluation those technical challenges from the perspective of the decision-maker.

CHAPTER 7

CONCLUSIONS AND SUMMARY OF CONTRIBUTIONS

The Aerospace industry may have passed through the 'golden years of aviation' in the 1930's and of space in the 1960's. However, aeronautics has only 'learned to walk' and space is still 'crawling'; there are immense challenges and development potential untapped for future industries! From low cost access to space to environmentally friendlier commercial transports, there is still the ever present question "*what is the best combination of market, configuration and technology?*"

The maturing aerospace industry provides current and future designers with baseline solutions, design processes, and methods developed to address product development issues. The presented research is based on, and expanded from, the best practices available for aircraft parametric sizing including, existing approaches, past design case studies, and design lessons-learned.

Conclusions derived from this research investigation are organized into a (1) research summary, (2) PhD. contribution summary to aerospace science, and finally (3) observations related to aircraft conceptual design.

RESEARCH SUMMARY

Process and Methods Library [Chapter 3]

1. CONTRIBUTION: The survey has produced a unique cross-section of design processes from 1936 to the present, consistently documented, analyzed, and interpreted through a dedicated *conceptual design process library*.
2. CONTRIBUTION: Consistent documentation of disciplinary methods provides the designer with a platform for (1) quick identification of appropriate methods for a given

design problem, (2) documented practical design experience with individual methods, (3) development of new design methods. During the course of this review it was determined that no public domain sources collect design methods libraries in such an organized or complete fashion for conceptual design.

3. CONTRIBUTION: The Methods library seeks not to recreate the derivation of methods but rather provide a reference for method applicability and documentation of method experience. A few select references have excellent discussions of the derivation and details of several methods, most notably Roskam ⁽²³⁾, Nicolai ⁽²⁰⁾ and Torenbeek ⁽¹⁸⁾. What makes the Methods library unique is the systematic summary and presentation of methods from a wide variety of public domain and industry sources, allowing for rapid selection of appropriate methods.

Robust and Flexible Parametric Sizing Process [Chapter 4]

1. CONTRIBUTION: A flexible and modular design process has been developed, allowing the same generic process to be applied to a wide variety of configuration and technologies with appropriate changes in methods and adjustment of the process to the problem.
2. CONTRIBUTION: Simplification of the design space visualization. By capturing the classical *W/S* and *T/W* trades into a single parameter (τ), it is now possible to reduce the solution space into a single curve from what was once a collection of constrains.
3. CONTRIBUTION: Flexible generic best-practice process. Based on the process and methods library, this process can be easily updated if new methods or process elements are found desirable.

Transonic Transport Design [Chapter 5]

1. CONTRIBUTION: The generic sizing methodology has proven flexibility and validity for a variety of transonic transport applications (business jets to wide-body transports).
2. CONTRIBUTION: The methodology can be used to identify primary design drivers for a new engineering problem as demonstrated through the composite B777, composite B737 and thrust vectored B777 studies.
3. CONTRIBUTION: Composite structure provides a larger benefit for long-haul wide-body aircraft (B777) compared to narrow-body aircraft (B737/A320) due to the effects of size and time spent in the cruise-phase. Long haul aircraft are more sensitive to technology compared to short-haul aircraft.
4. CONTRIBUTION: The thrust vectored transport shows significant performance improvement over the classical TAC, if the aircraft can be proven controllable in nominal and failure conditions like one-engine inoperative (OEI). The design presented is characterized by significant control challenges. Further design iterations are required to determine if these problems can be remedied.
5. CONTRIBUTION: The Blended-Wing Body (BWB FWC) demonstrates a strong sensitivity to cabin aspect ratio in terms of wave-drag and structural efficiency. It is imperative to correctly select the cabin layout within the context of the total vehicle. The classical paradigm of disintegrated fuselage and wing design no longer hold.
6. CONTRIBUTION: The SBW shows modest improvements in fuel savings if (1) laminar flow can be maintained, as demonstrated by the F-14 wing glove experiment, if (2) the transonic interference is manageable between the strut and the wing, and if (3) the strut can reduce the total wing group weight by 20%.

7. CONTRIBUTION: Reducing the flight speed of the strut-braced wing SBW allows reduces wing sweep without a reduction of wing thickness, thereby increasing laminar flow without a wing weight penalty due to aeroelastic constraints.
8. CONTRIBUTION: The selection of appropriate disciplinary analysis methods is critical. Incorrect methods tend to distort the conclusions, not only total accuracy but overall correctness of the solution space throughout the design process. Such has been vividly demonstrated with the strut-braced wing (SBW) study.

Supersonic and Hypersonic Transport Design [Chapter 6]

1. CONTRIBUTION: For both design cases, the SSBJ and hypersonic cruiser studies, the methodology generates physically correct trends and reasonable accurate results relative to representative published projects.
2. CONTRIBUTION: The SSBJ and hypersonic cruiser studies demonstrate how much physical insight the design team is able to gain utilizing a parametric sizing tool towards mission planning and market studies. In both cases discussed, the business case and technical detail has been assessed during parametric sizing in the quest to match technically feasible and economic viability.
3. CONTRIBUTION: The Sanger EHTV is designed to a sound operational mission relative to the LAPCAT II. The result is a reduced-complexity technical challenge for the Sanger EHVT relative to the LAPCAT II. The increased technical difficulty and market risk of the LAPCAT II vehicle creates an impractical and irrelevant engineering problem from a commercial point-of-view.

Ph.D. Contribution Summary

This research contributes to aerospace science by addressing the following fundamental research objectives.

4. **Objective:** Survey, investigate, catalog, document, and compare the various approaches to aircraft conceptual design with emphasis on the *Parametric Sizing Phase*.

Contribution: Organization of a dedicated design_process library and disciplinary methods library.

5. **Objective:** Specify and develop a flexible configuration-independent (generic) aerospace vehicle sizing methodology and software.

Contribution: Development of AVD^{sizing}, a flexible and well-balanced parametric sizing methodology and software incorporating 'best practices' identified through the comprehensive literature survey resulting in the unique process and method libraries.

6. **Objective:** Validate, calibrate and demonstrate the robustness and potential of the combined tool-set through relevant case-studies from subsonic to hypersonic speeds.

Contribution: The span of design case studies selected is meant to expose the generic, transparent, and robust character of this suggested practice key to the parametric sizing process. These case studies include: (1) existing transports ranging from business jets to wide-body transonic transports with both conventional aluminum and current composite construction for true validation purposes, (2) thrust vectored wide-body transport project, (3) blended wing body transport project, (4) strut-braced wing transport project, (5) supersonic business jet project, (6) Mach 4.4 commercial transport project, and (7) Mach 8 hypersonic commercial transport project.

Observation Related to Aircraft Conceptual Design

Early assumptions made during the sizing step of the conceptual design phase significantly impact the course of the project.

These decisions are based on assumptions which are required in order to start the design process. Design is an iterative process, an initial guess or assumption is often required

to initialize the iteration and finally determine a viable solution. These assumptions can take the form of *gross configuration assumptions* like “*The F-16 wing would make a good wing for a space tourism vehicle*”, or the form of *mission selection assumptions* like “*A Mach 8, 300 pax aircraft will find a market,*” or the form of *technology assumptions*, “*A composite wing will be 15% lighter relative to aluminum*”.

During this early phase of parametric sizing, designers tend to not disclose fundamental assumptions on which the project justification may hinge. This can be attributed to either insecurity related to the crudeness of analysis or the lack of backup material required to justify fundamental assumptions. At the beginning of a novel vehicle design projects the abstract nature of vehicle configurations or technologies requires some assumptions be made in order to initialize the design process.

With the prevailing risk adverse mindsets in industry and research environments, it is required for decision makers to understand the risk of novel projects in advance in order to take proactive steps to mitigate the inherent risks involved. Understanding the fundamental assumptions should be the first step in any risk assessment or risk mitigation. These assumptions represent the known-unknowns of the project. Later conceptual and preliminary designs phases phase are to re-evaluating the initial assumptions. The assumptions are iteratively improved and eventually replaced with a better understanding of the facts. This check of the fundamental assumptions can take the form of higher order disciplinary and multidisciplinary analysis, optimization, and experimentation.

Consequently, it must be an absolute requirement in any advanced project environment to rationally disclose in a transparent way the level of vagueness of all of the fundamental assumptions involved. In particular designers must specify what methods have been selected, in what process and what fundamental assumptions have been used. It is time to transition the conceptual design level decision-making from the ‘black-world mindset’ into a mindset of being

accountable related to fundamental early design decisions. The initiation of any true progressive flight vehicle program depends on an uncertainty-based, rigorous, transparent thus accountable forecasting process

With the required burden of full disclosure on the conceptual designer, it also required that Decision makers in the culture of risk aversion be open-minded of such assumptions. Pro-active treatment of these initial assumptions should be the goal, if the Decision maker decides that under these assumptions the vehicle shows potential. It is argued here that the first bit of risk information the decision maker should see are the known-unknowns or fundamental assumptions made. These assumptions take the form of (1) mission and market assumptions, (2) technology assumptions and (3) selected configurations. The key ingredient to initiating transparency and cooperation between designers and decision makers, early in the design process is the availability of the (1) methods library, (2) process library, and (3) a flexible flight vehicle parametric sizing process.

APPENDIX A
AIRCRAFT CONCEPTUAL DESIGN PROCESS LIBRARY

A.1 'BY-HAND' PROCESS LIBRARY

A.1.1 Wood - Aerospace Vehicle Design Vol. I, Aircraft Design

Processes Overview			
Design Phases BD, CD	Author Wood	Initial Publication Date 1934	Latest Publication Date 1963
Reference: Wood, K.D., "Aerospace Vehicle Design Volume I Aircraft Design," Johnson Publishing Company, Boulder, Colorado, 1963			
Application of Processes			
Applicability Primarily focused on commercial transports, fighters and supersonic aircraft			
Objective of Processes Estimate the size of an aircraft to meet the mission objective			
Initial Start Point The processes begins with mission specification and a gross assumption of the aircrafts configuration			
Description of basic execution Trends and statistics are used to first estimate the weight, wing area and propulsion system. the aircraft is then refined with better statistics and methods. Little or no design iteration			
Interpretation			
CD steps Mission feasibility Configuration sizing	Synthesis Ladder Analysis Integrate	Similar Procedures Coming Stinton	
General Comments: The earliest design process discussed here Based on gross design trends such as the gross weight is 4 times the payload weight Used to derive a single initial start configuration for preliminary design No discussion of various configurations BD and configuration sizing distinguished			

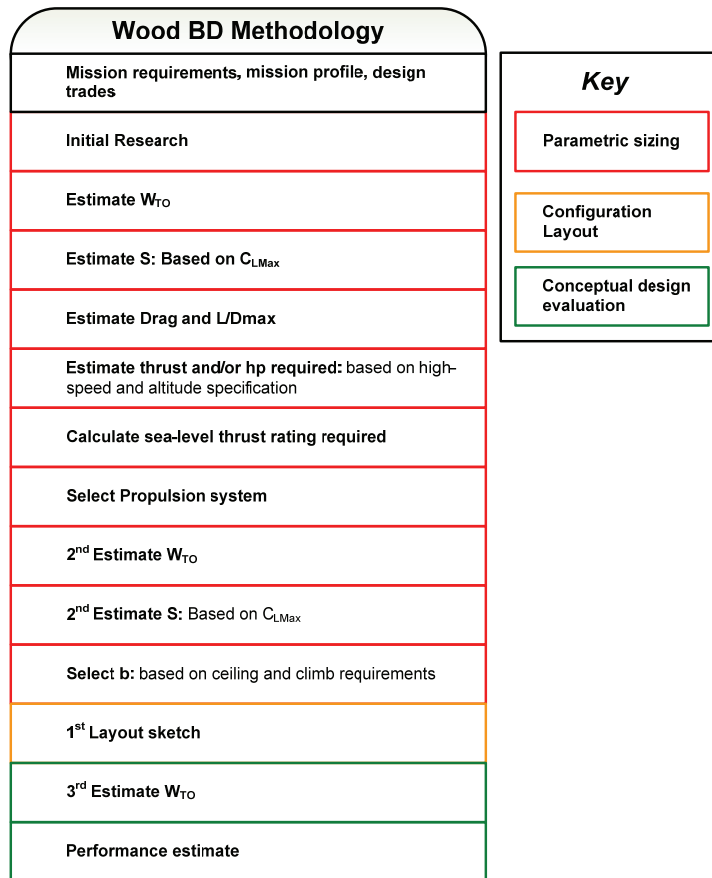


Fig A-1: Wood Aircraft Design Process

FURTHER DESCRIPTION

The earliest aircraft design methodology presented in this report, Wood demonstrates a direct sizing approach for configuration layout (Figure 2.1). This process defines the aircraft's weight, wing area, propulsion system size. This process is similar to the parametric sizing function where the basic parameters are estimated based on past aircraft experiments. From these approximations a configuration layout is defined followed by structural design, wing design, control surface sizing, landing gear design and fuselage design.

PARAMETRIC SIZING

This processes is called *layout design* in wood and is intended to get a ballpark approximation to take-off gross weight, wing area and prolusion system required. From an assumed TOGW ($TOGW=4W_{pay}$) wing area is computed from an estimated of the maximum lift coefficient (stall).

Propulsion system thrust is computed from a simple drag estimate, at the high speed level flight condition.

From these estimates the TOGW is refined and a new estimate for wing area is obtained. Next the span is computed through an aspect ratio trade study. From these basic parameters a configuration can be derived, thus completing the parametric design phase.

The approach to parametric sizing has been termed ***single-point sizing***. Single-point sizing is defined by utilizing a single flight condition to size each parameter. For example in Wood the wing area is estimated from stall and maximum thrust is estimated from high speed cruise. No attempt is made to explore the total performance of the vehicle during this phase of Woods methodology.

CONFIGURATION LAYOUT

The 1st conceptual sketch consists of a making design decisions for the vehicle based on experience and statistical data. No formal structure for this approach is provided.

The configuration layout is the most '*artistic*' component of conceptual design. The resulting vehicle concept is a product of the designer's creativity, physical understanding and personal preferences. No two designers' will come-up with the exact same solution, thus the *art* of conceptual design.

CONCEPTUAL DESIGN EVALUATION

The evaluation of the configuration begins with a 3rd weight and balance estimate. The configuration is modified to meet c.g. requirements of the landing gear and stability. Once the weight and balance is established a final performance estimate is performed. If the resulting design is feasible, then the process proceeds to preliminary design. This phase is the scientific component of conceptual design. The total aircraft is evaluated and iterated to converge on the most feasible form of the configuration posted.

OVERALL INTERPRETATION OF PROCESS

Wood presents relatively simple processes for conceptual design and provides a good foundation for the remaining design processes explored in this document. This process has been applied in wood for subsonic, transonic and supersonic aircraft. While the statistics and methods are limited to 1950's and 60's era aircraft, the overall approach remains relevant.

A.1.2 Corning – Supersonic and Subsonic Airplane Design - 1953 Basic Description

Processes Overview			
Design Phases BD, CD	Author Corning	Initial Publication Date 1953	Latest Publication Date 1979
Reference: Corning, G., “Supersonic and Subsonic Airplane Design,” Edwards Brothers, Inc., Ann Arbor, Mi, 1953			
Application of Processes			
Applicability Primarily focused on commercial transonic and supersonic transonic			
Objective of Processes Estimate the size of an aircraft to meet the mission objective along with optimization based on gross design drivers			
Initial Start Point The processes begins with mission specification, possible configurations and design variables for optimization			
Description of basic execution From the mission specification the wing sweep and thickness are first derived to appropriately place the critical mach number. From there the vehicle is sized and iterated			
Interpretation			
CD steps Mission feasibility Configuration sizing	Synthesis Ladder Analysis Integrate Integrate Optimization	Similar Procedures Wood Stinton	
General Comments: An improvement to the wood methodology with better empirical correlation Iterative base-lined design approach While this process appears to be a baseline design process at the time it was develop it would have been more appropriate as a conceptual design approach W/S and T/W are computed for a single flight condition Configuration layout and BD are somewhat distinguished			

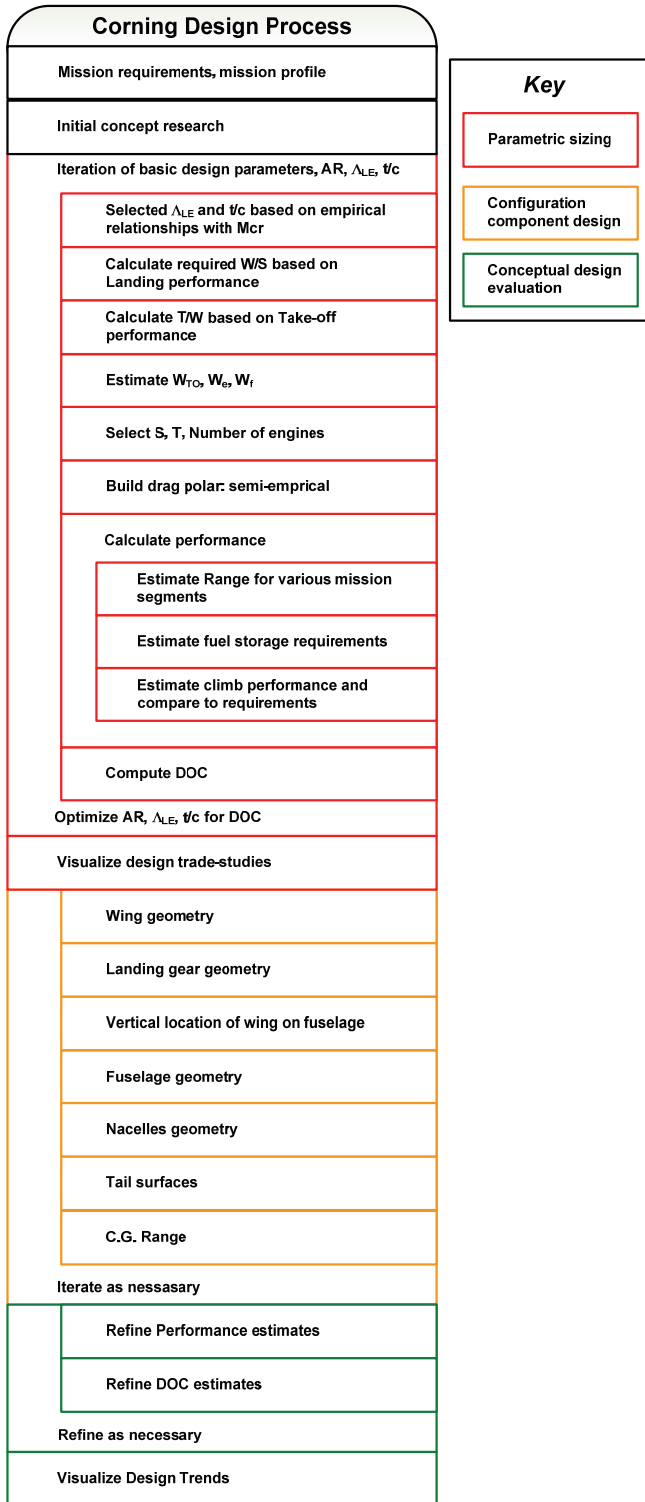


Fig A-2: Corning Aircraft Design Process

FURTHER DESCRIPTION

Corning is an improvement to the Woods processes through improving the structure and depth of all three conceptual design components,

PARAMETRIC SIZING

Corning first selects combinations of AR , A_{LE} and t/c which are required for the high-speed condition (typically transonic drag rise). Next the W/S and T/W are computed from landing performance and take-off performance respectively. This differs from Wood where the wing area and thrust are calculated first.

From this estimate of W/S , AR , \square_{LE} and t/c the weight is estimated using a statistical regression. With the weight estimate in hand the S and T required are easily computed. With these basic parameters the drag polar is estimated which enable a performance and DOC estimate.

Thus, with-out laying out a detailed configuration the input parameters of AR , \square_{LE} and t/c can be explored to determine an '*optimum*' performance and/or DOC.

From this analysis the basic weight and geometric requirements are established for the configuration layout phase.

Corning improves the depth of parametric sizing from Wood but still uses ***single-point sizing***. The W/S and T/W are estimated from single flight condition. Later design processes will show that W/S and T/W can be computed simultaneously considering all performance criterion.

CONFIGURATION LAYOUT

The structure of the configuration layout phase in Corning is improved from Wood. A step-by-step procedure is outlined with statistical trends to aid the designer in laying out the vehicle. In Corning the final weight and balance estimation is completed during this phase. More than one aircraft can be laid out for the conceptual design evaluation

CONCEPTUAL DESIGN EVALUATION

The evaluation of the configuration consists of refining the aerodynamics, performance and DOC estimates for the configuration provided. The process is repeated for the various configurations proposed. Through comparing the configurations an '*optimum*' configuration is selected based on performance and DOC estimates.

OVERALL INTERPRETATION OF PROCESS

Corning provides a clear and logical approach to aircraft conceptual design. The improvements of structure and depth to the Wood process give the design greater flexibility and insight during the design processes.

A.1.3 Nicolai – Fundamentals of Aircraft Design - 1975

Processes Overview			
Design Phases BD, CD	Author Nicolai	Initial Publication Date 1975	Latest Publication Date 1984
Reference: Nicolai, L., “Fundamentals of Aircraft Design,” METS, Inc., Ohio, 1975			
Application of Processes			
Applicability Primarily focused on transonic and supersonic fighters, could be applicable for transonic transports			
Objective of Processes Size, iterate and optimize the aircraft to best meet the mission			
Initial Start Point The processes begins with mission specification, possible configurations and design variables for optimization			
Description of basic execution From the mission specification the vehicle’s components are individually sized similar to Wood and Corning. This sizing the primary bulk of the work followed by a total vehicle performance and cost evaluation. For a specific set of design variables the process is iterated until the weight and performance data converge. The design variables are then iterated to determine the best configuration for preliminary design			
Interpretation			
CD steps Mission feasibility Configuration sizing Total a/c evaluation/iteration Comparison of possible a/c	Synthesis Ladder Analysis Integrate Convergence Iterate Visualize design space Optimization	Similar Procedures Jenkinson Corke Schaufele	
General Comments: advancement from the Corning approach which includes convergence of depended variables. Presents methods of visualizing the design space and selected the best configuration Sizing of components in involves checking several design cases BD, configuration sizing and CD evaluation steps are not distinguished			

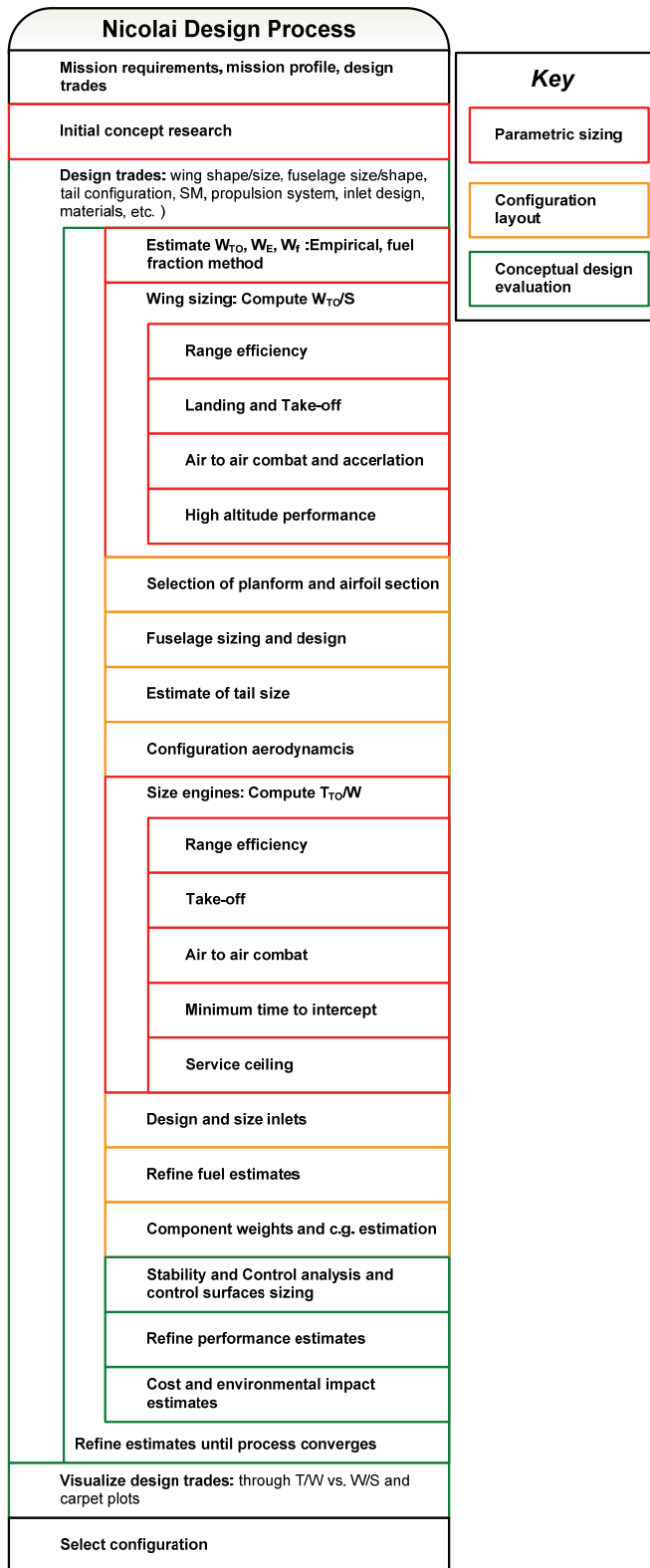


Fig A-3: Nicolai Aircraft Design Process

FURTHER DESCRIPTION

Nicolai presents a fundamentally different approach to Corning and Wood in that the functions of parametric sizing, configuration layout and conceptual design evaluation are combined. In addition Nicolai provides logic where *depended* design variables (such as weight) are iterated until they converge, thus, providing more accurate performance and cost estimates.

While Nicolai combines the three functions of conceptual design they will be analyzed separately for comparison purposes.

PARAMETRIC SIZING

Nicolai's process begins with identifying gross design trades, similar to Corning. From this point an estimate of weight is obtained and the W/S requirements are examined for several flight conditions. After the wing, fuselage empennage are sized the T/W requirements from several flight conditions are examined.

In both the W/S and T/W calculations the most demanding flight condition sizing the W/S and T/W, this is referred to as ***Multi-point sizing***. Multi-point sizing yields a better understanding of the requirements placed on the aircraft by the mission compared to the *single-point sizing* described in Wood and Corning.

CONFIGURATION LAYOUT

The configuration layout occurs in two places during this process, (1) after the W/S is selected and (2) after the T/W is selected. The configuration sizing is similar to Corning with more detailed statistics for military aircraft.

CONCEPTUAL DESIGN EVALUATION

The evaluation of each design trade is done in a similar fashion to Corning with performance and cost estimates. However, Nicolai includes stability and control estimates for an assessment of control power before the performance estimates. This allows for the inclusion of trim drag effects in range performance as well as giving a more complete picture of the design.

From this point the entire process is repeated until the weight estimates and performance results converge.

The process is then repeated in the outer loop for as many design trades as necessary. Example visualization of the trade studies is provided and the best compromise for the mission is selected.

OVERALL INTERPRETATION OF PROCESS

Nicolai represents several significant advancements in aircraft conceptual design (1) multi-point sizing, (2) Convergence of dependent design variables, (3) inclusion of stability and control in the design processes.

A.1.4 Loftin – Subsonic aircraft Evolution and the Matching of Size to Performance - 1980

Processes Overview			
Design Phases Conceptual Design	Author Loftin	Initial Publication Date 1980	Latest Publication Date 1980
Reference: Loftin, L., “Subsonic Aircraft: Evolution and the Matching of Sizing to Performance,” NASA RP1060, 1980			
Application of Processes			
Applicability Primarily focused on parametric sizing of jet powered transports and piston powered general aviation aircraft			
Objective of Processes Determine an approximate size and weight the aircraft to complete the mission from a 1 st level approximation of the design solution space			
Initial Start Point The processes begins with mission specification, possible configurations and design variables for optimization			
Description of basic execution From the mission specification statistics and basic performance relationships are used to determine relationships between T/W and W/S (Performance matching). The aircraft is then sized around this match point			
Interpretation			
CD steps Parametric Sizing	Synthesis Ladder Analysis Integrate Iteration of design Visualize design space	Similar Procedures Roskam (preliminary sizing) Torenbeek (Cat 1 methods)	
General Comments: One of the first published processes utilizing performance matching Where Nicolai compares T/W and W/S after the complete convergence and interaction of the processes, Loftin derives basic relationships between T/W up front to visualize the solution space before initial sizing. Loftin essential short cuts the Nicolai approach to derive an initial design space rather than an initial configuration.			

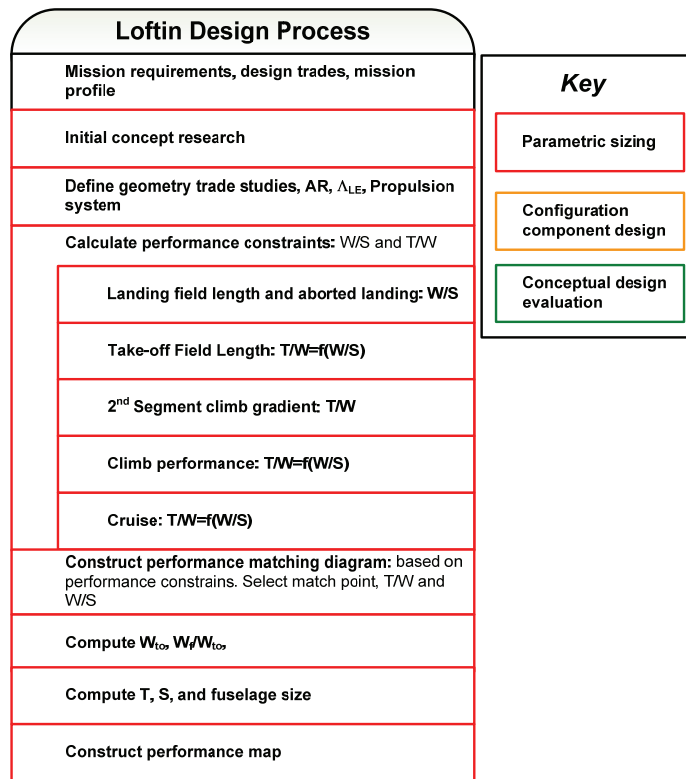


Fig A-4: Loftin Aircraft Design Process

FURTHER DESCRIPTION

Loftin's procedure represents a significant advancement in parametric sizing. The method does not address the functions of configuration layout and conceptual design evaluation.

PARAMETRIC SIZING

In the previous procedures the wing loading and thrust loading are selected for separate flight conditions. Lofting presents an approach called **Performance matching**, where the performance constraints are plotted in terms of T/W and W/S. In essence, a 1st order design space visualization is developed as shown in Figure 2.2. From this plot a 'optimum' T/W and W/S are selected which satisfied all of the performance requirements simultaneously.

OVERALL INTERPRETATION OF PROCESS

Performance matching allows for a 1st order design space visualization with minimal input. This approach gives designers an improved start point compared to Nicolai, Wood and Corning.

A.1.5 Torenbeek – Synthesis of Subsonic Airplane Design

Processes Overview			
Design Phases BD, CD	Author Torenbeek	Initial Publication Date 1982	Latest Publication Date 1982
Reference: Torenbeek, E., “Synthesis of Subsonic Airplane Design,” Delft University Press, 1982			
Application of Processes			
Applicability Primarily focused on commercial transonic transports			
Objective of Processes Determine an approximate size and weight the aircraft to complete the mission from a 1 st level approximation of the design solution space			
Initial Start Point The processes begins with mission specification, possible configurations			
Description of basic execution From the mission specification a Loftin style performance matching is performed to derive an initial visualization of the design space and to give a start point for the configuration development. From this point the aircraft components are individually sized and then the total aircraft is evaluated. The configuration development and evaluation processes are integrated to determine the best configuration			
Interpretation			
CD steps Mission feasibility Configuration sizing Total a/c evaluation/iteration	Synthesis Ladder Analysis Integrate Iteration Visualize design space Optimization	Similar Procedures Loftin (performance matching) Roskam	
General Comments: Loftin style performance matching Combines the Nicolai and Loftin approaches into a single conceptual design methodology Good explanation of methods for each step			

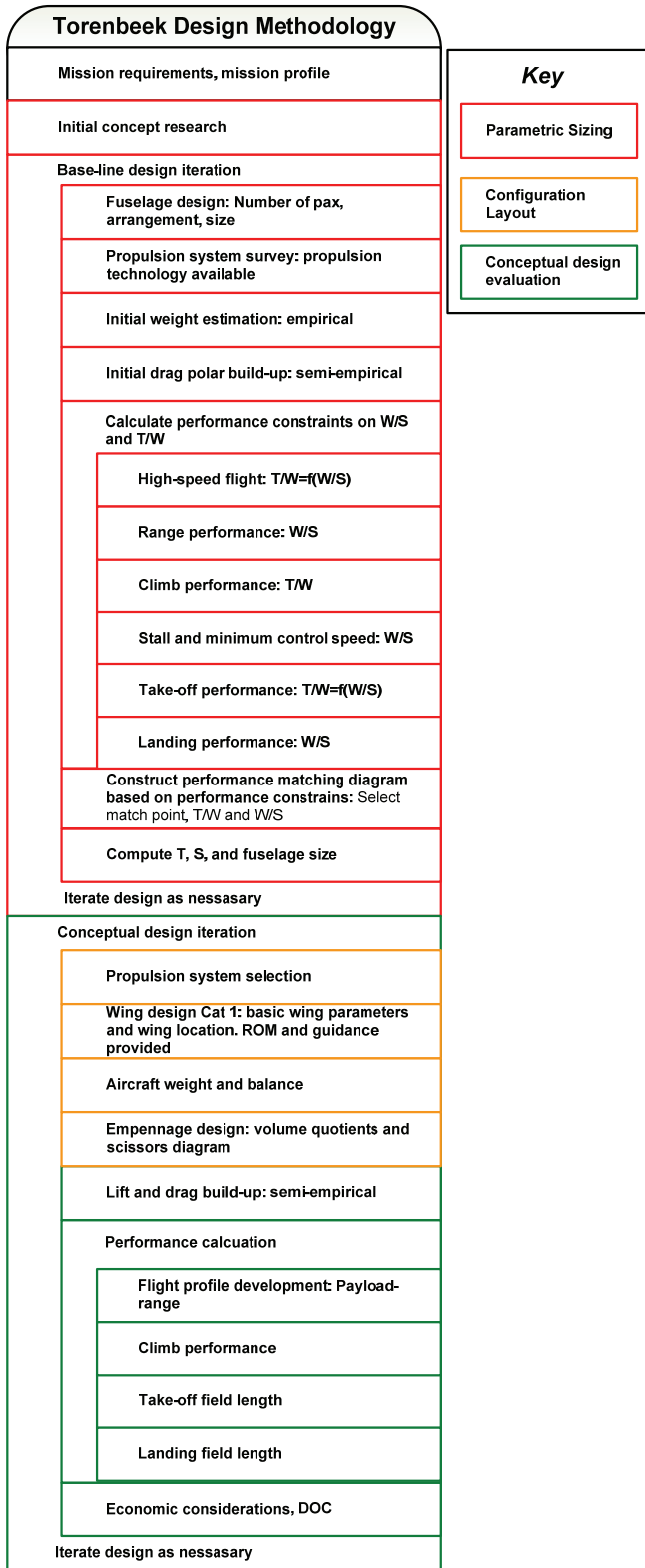


Fig A-5: Torenbeek Aircraft Design Process

FURTHER DESCRIPTION

Torenbeek combines the Loftin approach to Parametric sizing (Performance matching) with a configuration layout and conceptual design evaluation/iteration approach for subsonic commercial aircraft.

PARAMETRIC SIZING

Similar to Loftin, Torenbeek uses performance matching to describe the boundaries of the design space. Torenbeek adds the fuselage layout upfront to get a better approximation of the parasite drag and weight estimate before performance matching. In other words, Torenbeek determines the payout volume requirements prior to sizing the vehicle which helps constrain the final aircraft size to the mission payload.

CONFIGURATION LAYOUT

Torenbeek's configuration layout procedure consists of empirical data and reduced order models for propulsion system selection, wing design, and empennage sizing. This reference contains an excellent discussion of configuration layout with empirical data most applicable for transonic transports.

CONCEPTUAL DESIGN EVALUATION

With a configuration in hand, performance and cost estimates are obtained. A series of trade-studies are then run around this process.

OVERALL INTERPRETATION OF THE PROCESS

Torenbeek presents through processes for sizing and iterating transonic transports, while combining and advancing elements from previous design references.

A.1.6 Stinton – The Design of the Aeroplane

Processes Overview			
Design Phases BD, CD	Author Stinton	Initial Publication Date 1983	Initial Publication Date 1983
Reference: Stinton, D, "Design of the Aeroplane," BSP Professional Books, Oxford, 1983			
Application of Processes			
Applicability Primarily focused on general aviation aircraft			
Objective of Processes Determine the size and basic configuration of an aircraft to complete the mission			
Initial Start Point The processes begins with mission specification			
Description of basic execution From the mission specification a Wood style sizing and configuration layout is performed Followed by a conceptual design evaluation and iteration until the mission requirements are meet			
Interpretation			
CD steps Mission feasibility Configuration sizing Total a/c evaluation/iteration	Synthesis Ladder Analysis Integrate Iteration	Similar Procedures Wood Corning	
General Comments: Initial sizing very similar to the Wood processes with an extended performance and stability and control analysis / evaluation Contribution of this reference is primary in the physical description of the aircraft			

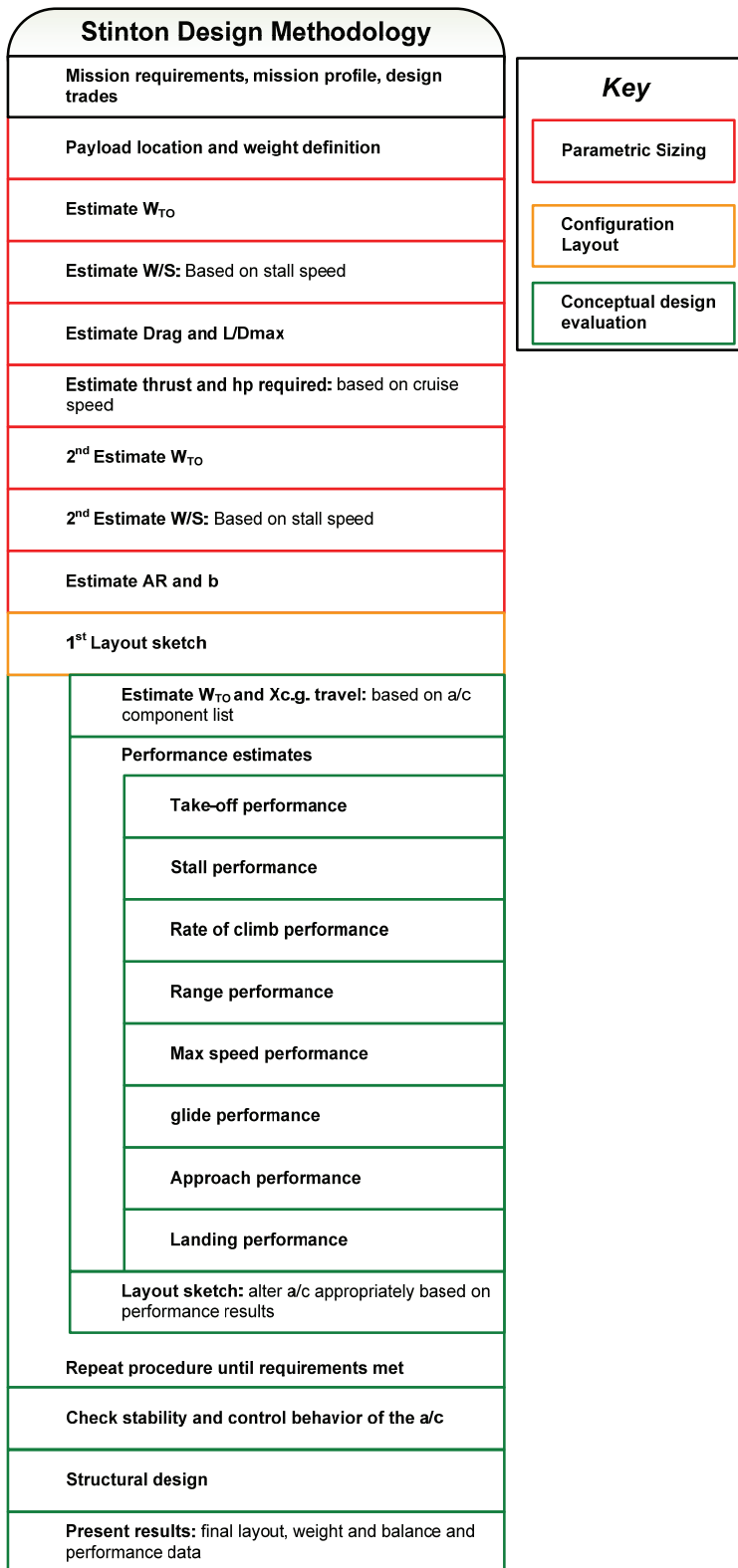


Fig A-6: Stinton Aircraft Design Process

FURTHER DESCRIPTION

Stinton presents a process very similar to Wood with the addition of stability and control and structural analysis after the performance evaluation.

PARAMETRIC SIZING

Identical to Wood

CONFIGURATION LAYOUT

Same as Wood with additional information for general aviation aircraft

CONCEPTUAL DESIGN EVALUATION

Same as Wood with stability and control and structural design added to the processes

OVERALL INTERPRETATION

While the process presented by Stinton is nothing new it does contain excellent descriptions of the physics of aircraft. This reference is recommend of obtaining the physically 'feel' of aircraft design.

A.1.7 Roskam – Airplane Design, Parts I-VIII

Processes Overview			
Design Phases BD, CD, PD	Author Roskam	Initial Publication Date 1985	Latest Publication Date 2003
Reference: Roskam, J., “Airplane Design Part I - VIII,” DARcorporation, Lawrence, Kansas, 2003			
Application of Processes			
Applicability Generic in application			
Objective of Processes Preliminary sizing, Configuration selection, preliminary design development			
Initial Start Point The processes begins with mission specification			
Description of basic execution There major components of this methodology <ol style="list-style-type: none"> 1. Preliminary sizing – BD design space visualization yielding a start point for configuration design 2. Preliminary design I – CD Development and comparison of several configurations 3. Preliminary design II – PD Refinement of selected configuration for DD 			
Interpretation			
CD steps Mission feasibility Configuration sizing Total a/c evaluation/iteration Comparison of possible a/c	Synthesis Ladder Analysis Integrate Converge Iteration Design space Visualization	Similar Procedures Wood Corning	

General Comments:

Most complete and in-depth design process described in this document

Combines a Loftin style BD with an in-depth configuration development and sizing CD and systematic PD refinement of the selected concept

Methods and processes developed to be applicable to a wide range of aircraft

In a computerized system, PD II could be run as CD

Convergence of depended design variable at a each phase, BD, CD, and PD

Design space visualization discussed but not explicitly shown

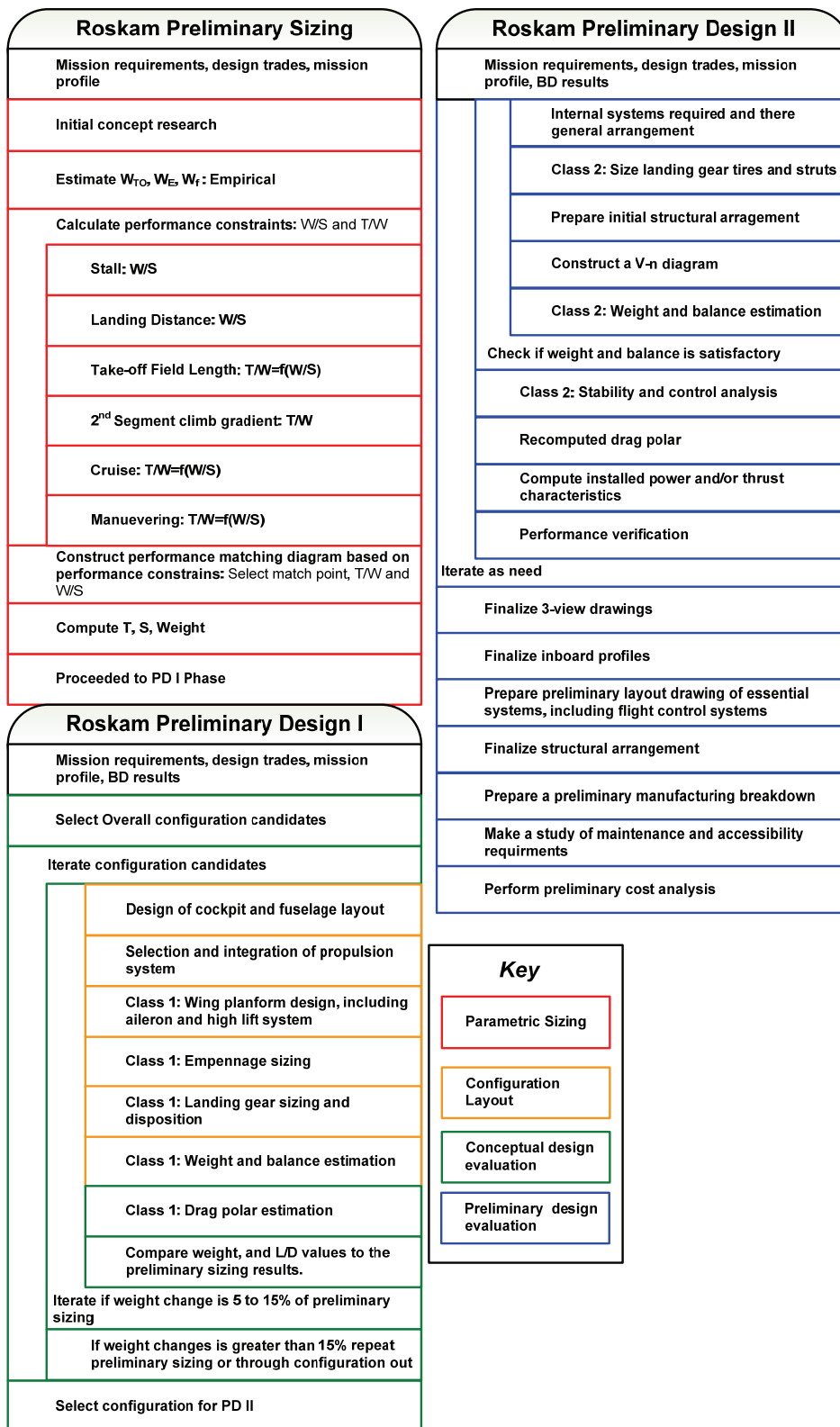


Fig A-7: Roskam Aircraft Design Process

BASIC DESCRIPTION

Roskam presents a comprehensive look at aircraft conceptual and preliminary design consisting of Parametric sizing (Preliminary Sizing), Configuration layout and Conceptual design evaluation (Preliminary Design I). In addition a Preliminary design evaluation procedure is also provided (Preliminary Design II). The distinction between conceptual design and preliminary design was made by looking at the objective of each process. Roskam's Preliminary design I is intended to determine the aircraft gross configuration and major subsystems (Conceptual design) and Preliminary design II is intended to refine the given aircraft and prepare it for detail design and manufacturing (Preliminary design).

PARAMETRIC SIZING

Similar to Loftin and Torenbeek, Roskam begins with a 1st order performance matching based on typical values and empirical relationships for a large variety of aircraft.

CONFIGURATION LAYOUT

With a wide variety of empirical data the major components of several aircraft are layout out around the results from the parametric sizing procedure. Each configuration is then iterated thought the conceptual design evaluation until the weight converges.

CONCEPTUAL DESIGN EVALUATION

The L/D and weights are compared to the parametric sizing results. If they differ slightly the configuration is adapted until the configuration layout results match the parametric sizing results. If they differ significantly the parametric sizing process must be repeated or the configuration is thrown out. From this work a configuration is selected based on performance estimates.

PRELIMINARY DESIGN EVALUATION

The selected configuration is refined through landing gear design, improved weight and balance, stability and control and performance and cost analysis. From this point it is decided if

the aircraft is ready for detail design, requires further refinement, or if a different concept is required.

OVERALL INTERPRETATION

The most comprehensive aircraft design text available today. Most methods have been Mechanized through the AAA software.

A.1.8 Raymer – Aircraft Design: A Conceptual Approach

Processes Overview			
Design Phases BD, CD	Author Raymer	Initial Publication Date 1989	Initial Publication Date 2006
Reference: Raymer, D., "Aircraft Design: A Conceptual Approach," 3 rd Edition, AIAA Educational Series, American Institute of Aeronautics and Astronautics, Virginia, 1999			
Application of Processes			
Applicability Generic			
Objective of Processes Size, trade and optimize various aircraft configuration to find the best configuration for the mission specification			
Initial Start Point The processes begins with mission specification and an initial sketch of the aircraft			
Description of basic execution From the mission specification and an initial sketch of the aircraft the vehicle is sized through a numerical Loftin style performance matching followed by a conceptual design evaluation and refinement of the total aircraft			
Interpretation			
CD steps Configuration sizing Total a/c evaluation/iteration	Synthesis Ladder Analysis Integrate Iteration Design space Visualization Optimization	Similar Procedures	
General Comments: Reader's digest version of Roskam Discussion of aircraft design Difficult to see the processes and is difficult to discern how each step is completed Configuration layout and baseline design are mixed Weak methods			

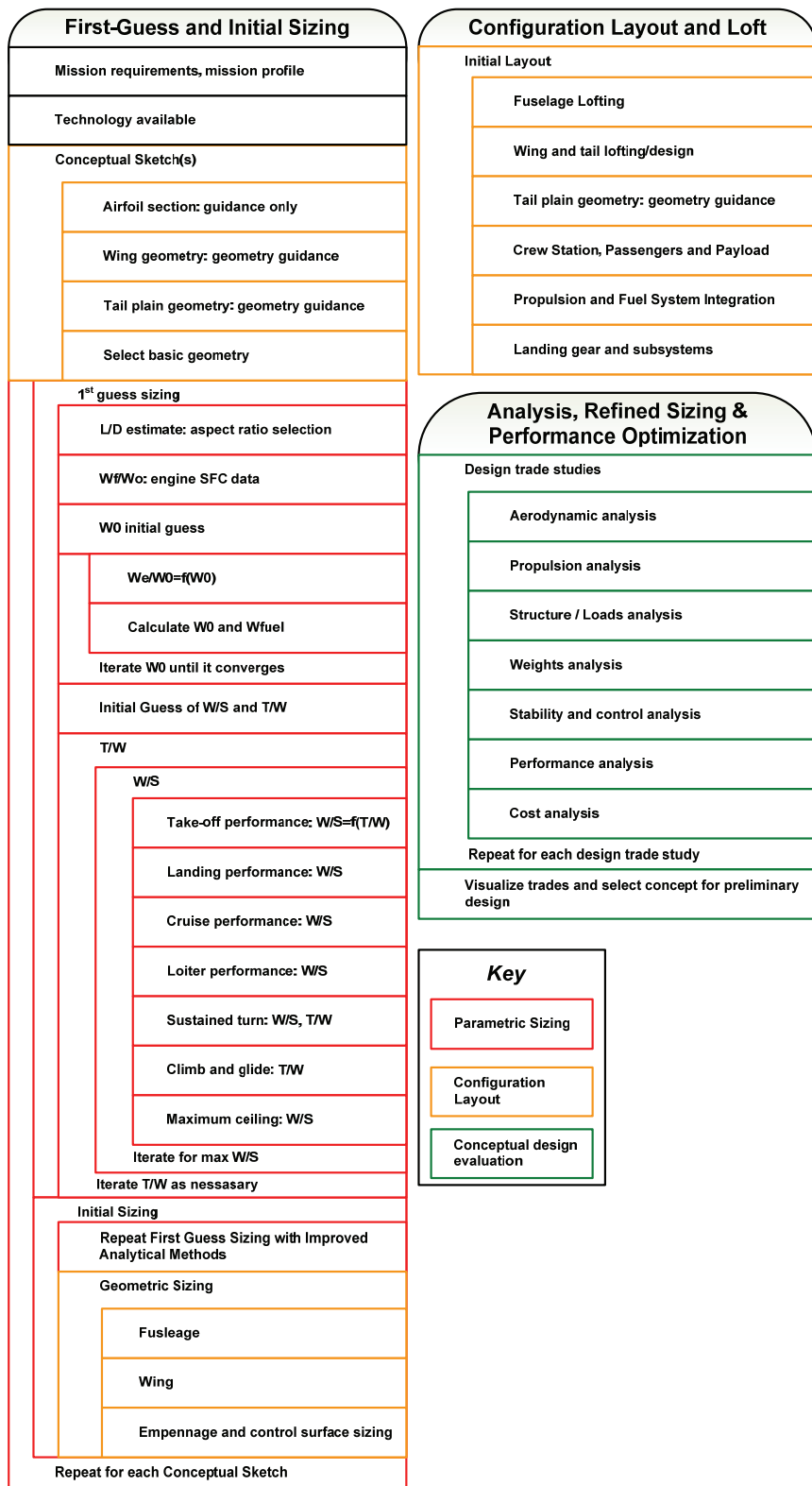


Fig A-8: Raymer Aircraft Design Process

BASIC DESCRIPTION

Raymer presents a processes similar to Roskam and Torenbeek but with a complicated parametric sizing processes and top-level descriptions of configuration layout and conceptual design evaluation. The process is presented in two places, Chapter 2 where a top level flow chart is presented and an intermission between Chapters 11 and 12 where a step by step procedure is presented. It is necessary to cross-reference these two and presentations of the processes study each component of the process to understand Raymer's approach to conceptual design

PARAMETRIC SIZING

Raymer begins with a technology survey as most references due and then brainstorms conceptual sketches to meet the mission. The idea of a conceptual sketch is explicitly mentioned in this reference as a means quickly visualizing design options but is not necessary.

First-guess sizing using empirical relationships to determine an appropriate initial estimate of aspect ratio, propulsion system, weight, T/W and W/S . This step is similar to the *Performance matching* found in Loftin, Roskam, and Torenbeek, but with reduced analytic complexity.

After the first guess sizing Initial sizing is performed in the exact same manner as First-guess sizing with comparable methods presented in Loftin, Roskam and Torenbeek. The Initial sizing methods presented are sufficient for parametric sizing and provide more physical information for parametric sizing. Thus, First guess sizing is an unnecessary step.

Raymer presents an iterative approach to computing the T/W and W/S which needlessly complicates performance matching. The graphical approach shown in Loftin, Roskam and Torenbeek is superior because it visualizing the design space, yielding better understanding the mission requirements effect on the design.

CONFIGURATION LAYOUT

The configuration layout and lofting approach proposed by Raymer provides insightful commentary into drafting and configuration layout. While little statistics or typical values are presented as in Roskam or Torenbeek the consideration presented by Raymer are worthy of note.

CONCEPTUAL DESIGN EVALUATION

The conceptual design evaluation and iteration process is sufficiently described and suggested visualizations for trade-studies are presented. The overall analysis approach is sufficient for conceptual design, but little or no analytic tools are provided.

OVERALL INTERPRETATION

Raymer's approach to conceptual design tends to complicate parametric sizing, under-represent the conceptual design evaluation while, providing insight into configuration layout. This reference would be recommended for students interested in drafting or configuration layout. However, there are better references for sizing and analysis.

A.1.9 Jenkinson – Civil Aircraft Design

Processes Overview			
Design Phases BD, CD	Author Jenkinson	Initial Publication Date 1999	Latest Publication Date 1999
Reference: Jenkinson, L., Simpkin, P., Rhodes, D., "Civil Jet Aircraft Design," AIAA Education Series, American Institute of Aeronautics and Astronautics, Inc., Virginia			
Application of Processes			
Applicability Primarily commercial transports			
Objective of Processes Size, trade and optimize various civil jet configuration to find the best configuration for the mission specification			
Initial Start Point The processes begins with mission specification			
Description of basic execution From the mission specification the initial design space is explored similar to Nicolai. From the selected design point several configurations are developed and evaluated. Each configuration is evaluated and optimized. The most promising configuration is selected			
Interpretation			
CD steps Mission feasibility Configuration sizing Total a/c evaluation/iteration Comparison of possible a/c	Synthesis Ladder Analysis Integrate Iteration Design space Visualization Optimization	Similar Procedures Nicolai Schaufele Corke	
General Comments: The initial sizing takes a step back to Nicolai in that the W/S and T/W are determined independently. Thus, instead of seeing the function relationship only design points are visualized not trends Simplistic conceptual design evaluation Nicolai for commercial transports			

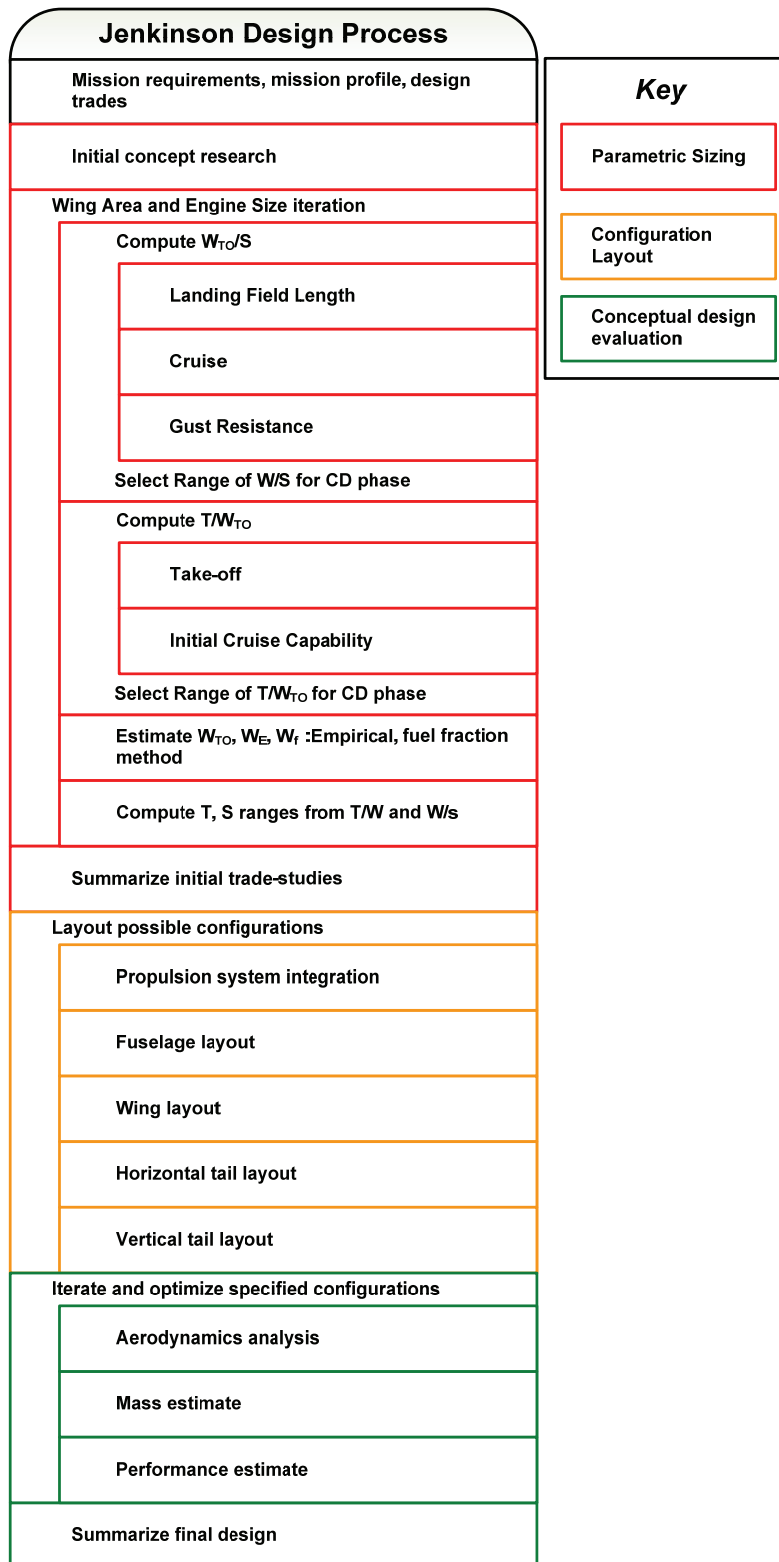


Fig A-9: Jenkinson Aircraft Design Process

BASIC DESCRIPTION

Jenkinson presents an aircraft design processes geared toward undergraduate students and thus the process has been simplified. The methods and statistics presented are primarily for transport aircraft.

PARAMETRIC SIZING

The parametric sizing in this reference goes back to multi-point sizing where the wing-loading and thrust loadings are computed separately for the most demanding flight conditions.

CONFIGURATION LAYOUT

The configuration layout is broken down into components and provides sufficient insight for undergraduate students

CONCEPTUAL DESIGN EVALUATION

The conceptual design evaluation is limited to performance and cost estimates. No attempt is made to analysis stability and control or structure.

OVERALL INTERPRETATION

This approach is to simplistic for practicing conceptual designers but provides a good introduction for undergraduate students. The process could be improved if performance matching where utilized instead of multi-point sizing for parametric sizing.

Simple examples are provided which reinforce the concepts presented in this reference.

A.1.10 Howe – Aircraft Conceptual Design Synthesis

Processes Overview			
Design Phases BD, CD	Author Howe	Initial Publication Date 2000	Latest Publication Date 2000
Reference: Howe, D., "Aircraft Conceptual Design Synthesis," Professional Engineering Publishing Ltd., UK, 2000			
Application of Processes			
Applicability Primarily commercial transports but could be applied for military aircraft as well			
Objective of Processes Size, trade and optimize various civil jet configuration to find the best configuration for the mission specification			
Initial Start Point The processes begins with mission specification			
Description of basic execution Three levels of conceptual design <ul style="list-style-type: none"> • Feasibility Design – BD, is the mission feasible and method of meeting the requirements • CD synthesis – several layers of iteration to size and select the best configuration 			
Interpretation			
CD steps Mission feasibility Configuration sizing Total a/c evaluation/iteration Comparison of possible a/c	Synthesis Ladder Analysis Integrate Convergence Iteration Design space Visualization	Similar Procedures Roskam	
General Comments: Distinction with adaptation, major modification and completely new design Configuration layout through an iterative Loftin style performance matching Obscure statistical methods CD evaluation similar to Nicolai and Jenkinson			

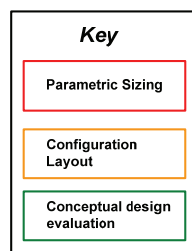
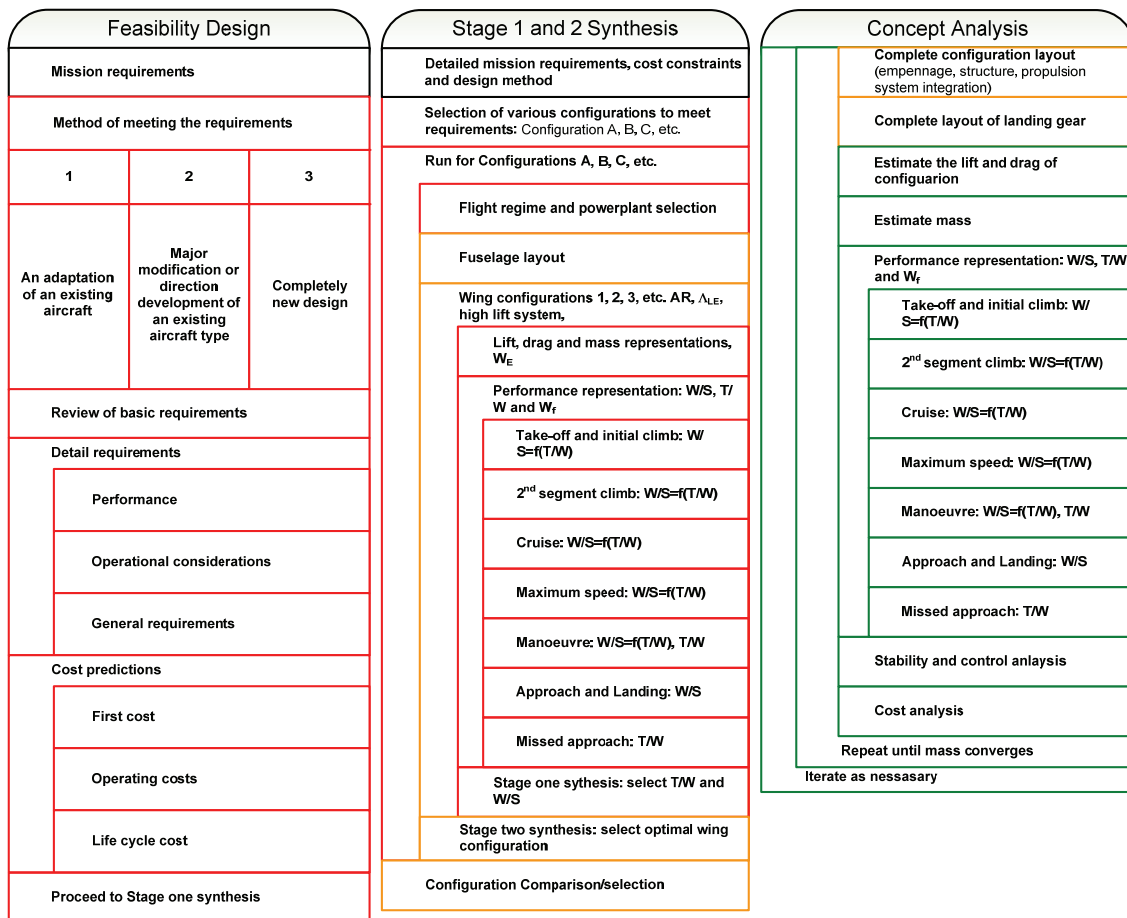


Fig A-10: Howe Aircraft Design Process

FURTHER DESCRIPTION

Howe’s conceptual design synthesis has several unique features. Most notably, a feasibility design phase has been added addressing qualitatively how best to meet the design requirements. In addition this reference demonstrates an integration of parametric sizing and configuration layout in a systematic design screening processes.

PARAMETRIC SIZING AND CONFIGURATION LAYOUT

Howe begins with a method of detailing the design requirements and the method of meeting the requirements in a process called Feasibility design. During this phase the mission requirements are transformed into design requirements and cost objectives. In addition the method of meeting the design requirements is selected between (1) adaptation of an existing aircraft, (2) Major modification or direct development from existing aircraft or (3) completely new design. This distinction up front allows the designer to streamline the conceptual design.

The actual parametric sizing and configuration layout is divided into 3 stages of synthesis.

- **Stage 1 synthesis** – selection of the optimal T/W and W/S for the given aircraft configuration and wing configuration (i.e. lowest T/W with highest W/S)
- **Stage 2 synthesis** – Comparison of the various wing configurations from stage 1 for weight and performance estimates
- **Configuration Comparison** – Comparison of the optimized configurations from stage 2 based on performance and weight estimates

This processes is a structured for configuration layout comparable to Nicolai where the configuration layout and parametric sizing are performed concurrently. In Howe's approach *performance matching* is used to size the specified wing.

CONCEPTUAL DESIGN EVALUATION

The conceptual design evaluation process presented here is similar to the approach for stage 1 synthesis with stability and control and cost analysis included. In addition improved empirical relationships are used for mass and aerodynamic estimation. No reference is made as to where the empirical relationships are derived.

Similar to Roskam and Torenbeek, the configuration analysis check that the mass estimates converge.

OVERALL INTERPRETATION

The process presented by Howe is a systematic and extensive approach to parametric sizing configuration layout and conceptual design evaluation. The methods presented in this text are all empirical by nature and do not reference their origin. Howe and Roskam represent the most complete aircraft conceptual design processes.

A.1.11 Schaufele – The Elements of Aircraft Preliminary Design

Processes Overview			
Design Phases BD, CD	Author Schaufele	Initial Publication Date 2000	Latest Publication Date 2000
Reference: Schaufele, R., "The Elements of Aircraft Preliminary Design," Aries Publications, California, 2000			
Application of Processes			
Applicability Primarily commercial transports			
Objective of Processes Size, trade and optimize various civil jet configuration to find the best configuration for the mission specification			
Initial Start Point The processes begins with mission specification			
Description of basic execution From the mission specification each component of the aircraft is designed individually and then trade-studies are run to determine the best configuration and combination of design variables			
Interpretation			
CD steps Configuration sizing Total a/c evaluation/iteration	Synthesis Ladder Analysis Integrate Iteration Design space Visualization	Similar Procedures Nicolai Jenkison Corke	
General Comments: No BD, being with initial component development W/S and T/W are utilized when sizing the wing and engine respectively Valuable design trends and lessons discussed Works well for major modification or family concept development			

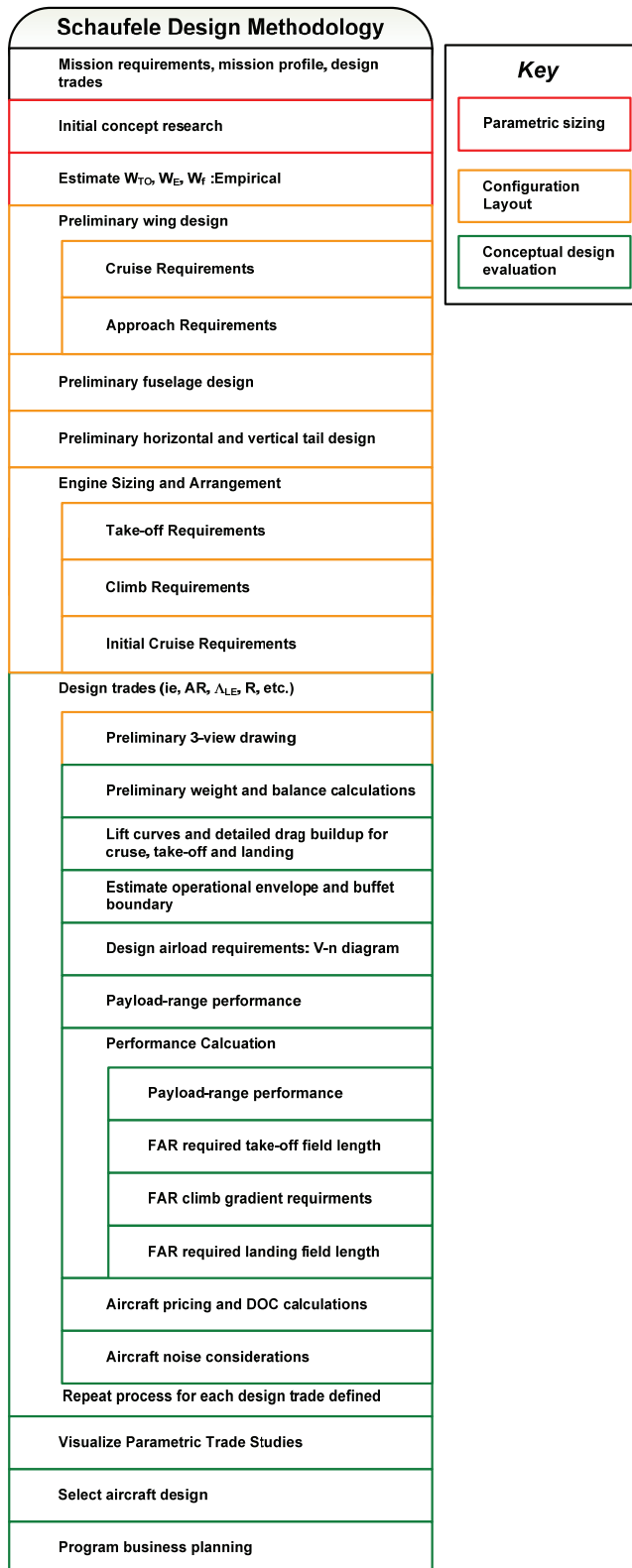


Fig A-11: Schaufele Aircraft Design Process

BASIC DESCRIPTION

Schaufele presents a focuses on the conceptual design evaluation and briefly touches on parametric sizing and configuration sizing. This process is primarily for commercial transport aircraft.

PARAMETRIC SIZING

The only components of this processes which are similar to the parametric sizing are the initial weight estimation. The wing and engine sizing is done through multi-point sizing.

CONFIGURATION LAYOUT

This reference presents clear guidance for the sizing of commercial transport major components. Examples and typical values are provided.

CONCEPTUAL DESIGN EVALUATION

The conceptual design evaluation consists of trade-studies based on performance, cost and noise estimates. Examples of trade-studies are provided along with various trade-study visualization techniques.

OVERALL INTERPRETATION

This reference provides a clear approach to configuration layout and conceptual design evaluation. Excellent physical descriptions and guidance are provided.

A.2 'COMPUTER-BASED' CONCEPTUAL DESIGN PROCESS LIBRARY

A.1.1 AAA – Advanced Aircraft Analysis

Processes Overview			
Design Phases BD, CD, PD	Author DAR corporation, Lawrence, Kansas	Initial Release Date 1991	Last known update 2009
Reference: Roskam, J., "Airplane Design Part I - VIII," DARcorporation, Lawrence, Kansas, 2003			
Application of Processes			
Applicability Generic in application			
Objective of Processes Preliminary sizing, Configuration selection, preliminary design development			
Description of basic execution With no imposed structure it is suggested to follow the process from Roskam's Airplane Design.			
Published Applications			
Description of basic execution With no imposed structure it is suggested to follow the process from Roskam's Airplane Design.			
Interpretation			
CD steps Parametric sizing Configuration layout Configuration evaluation	Synthesis Ladder Analysis Integrate Converge Iteration	Similar Codes	

General Comments:

Good collection of disciplinary methods

Difficult to iterate and converge a design but possible

Can be a good, if not difficult to use, tool for educational purposes. Each step must be done manually, thus, a good tool for teach the mechanics of aircraft design.

Not suggested for rapid conceptual design projects

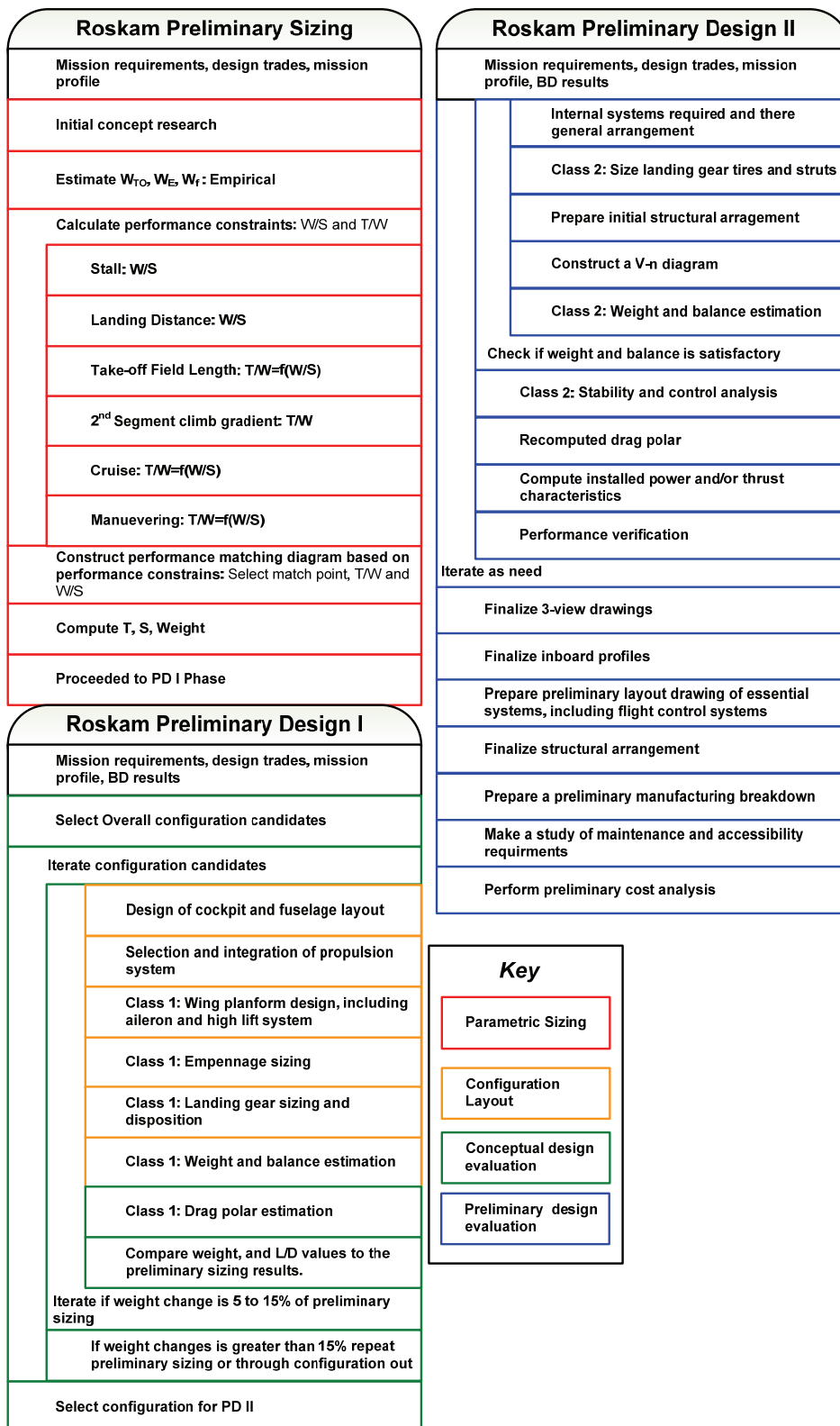


Fig A-12: AAA Aircraft Design Process

BASIC DESCRIPTION

See A.1.7 Roskam, Airplane Design, Parts I-VIII

A.1.2 ACES – Aircraft Configuration Expert System

Processes Overview			
Design Phases	Developer	Initial Release Date	Last known update
CD	Aeritalia-CSI (Centro Sitermi Informatici-Piemonte, Torino, Itally	1986	1989
Reference: Bargetto, R., et al, "Aircraft Configuration Analysis/Synthesis Expert System: A New Approach to Preliminary Sizing of Combat Aircraft," ICAS 88-1.11.2, 1988, pp. 1645-1649			
Application of Processes			
Applicability Generic in application			
Objective of Processes Generate a set of possible configurations beginning with the mission requirements and a set of design rules which constitute a knowledge-base. From these possible baseline the system helps the designer rank the configurations based on numerical weighing system			
Description of basic execution Define Mission requirements and design rules. From this point the system execute the			
Published Applications			
Interpretation			
CD steps	Synthesis Ladder	Similar Codes	
Parametric sizing	Analysis Integrate Converge Iteration Design space visualization		
General Comments: Very interested application of the classical sizing method through the iteration and weighting of certain design features			

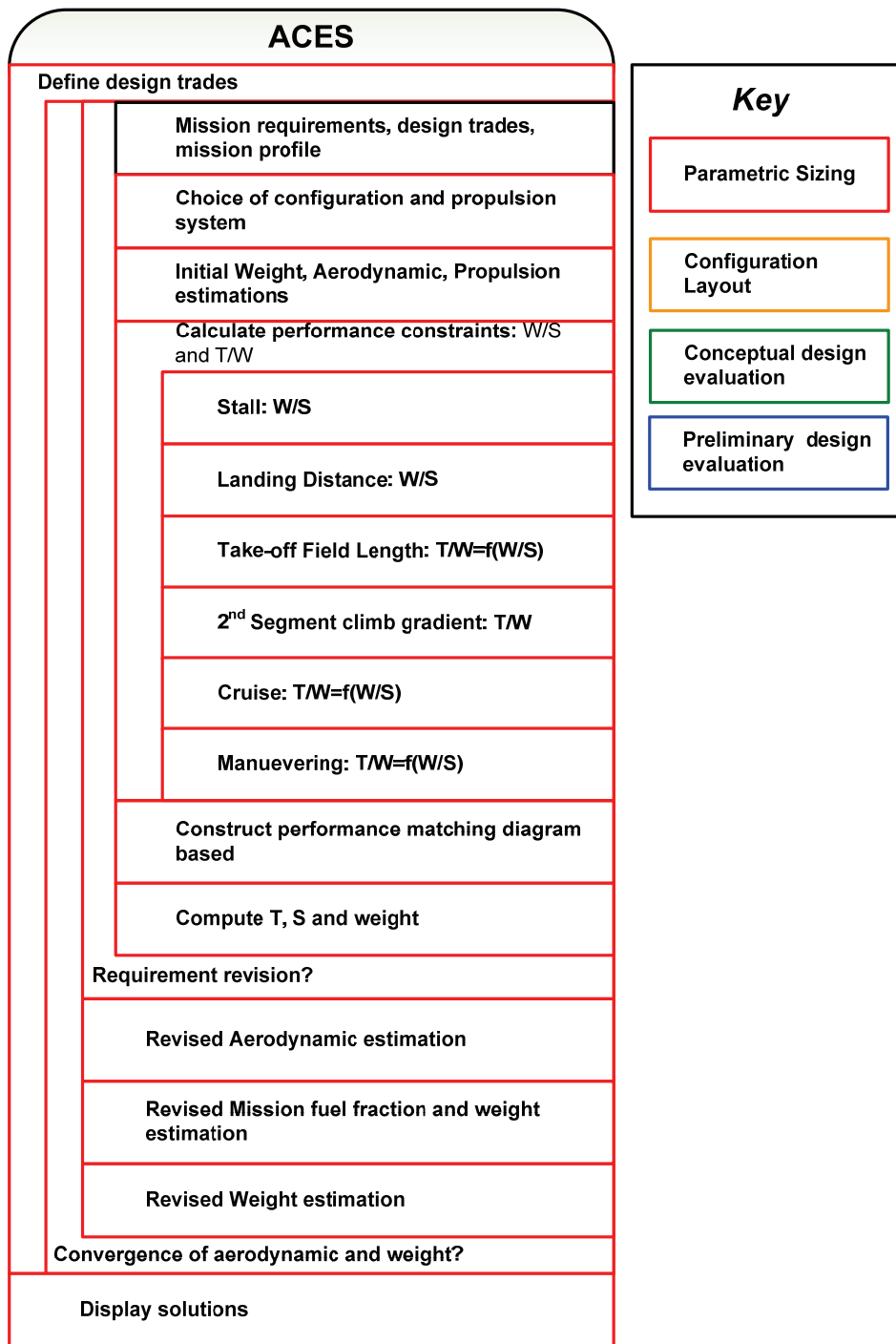


Fig A-13: ACES Aircraft Design Process

FURTHER DESCRIPTION

The Knowledge Base used in ACES is broken down into,

1. **Descriptive** – describing the category to which the aircraft belongs (Example: Transport – Civil- Regional)
2. **Operative** – collection of design rules which will apply different constraints on the aircraft (Examples: horizontal take-off, stealth, etc.)
3. **Technical** – collection of technical data for certain design features (Example: propulsion system data, inlet data, sub-systems, etc.). In addition reliability levels of teach system is also included and output to give the designer a heads up toward the total aircraft reliability.
4. **Calculation subprograms** – Disciplinary methods

These options can be varied as the designer sees fit to explore the solution space which makes ACES an interesting case-study for 1st order solution space screen.

A.1.3 ACSYNT – Aircraft Synthesis

Processes Overview			
Design Phases	Developer	Initial Release Date	Last known update
CD	NASA Ames Research Center, Systems Analysis Branch	1976????	Today
<p>Reference: ACSYNT Users Guide, NASA Ames Research Center, Systems Branch, http://fornax.arc.nasa.gov:9999/acsynt.html, Last Visited 12/21/1999</p> <p>Vanderplaats, G.,N., “Automated Optimization Techniques for Aircraft Synthesis,” AIAA. JoA , 1976 ??????</p> <p>Gelhausen, P., “ACSYNT – A Standards-Based System for Parametric Computer Aided Conceptual Design of Aircraft,” AIAA 92-1268, 1992 Aerospace Design Convergence, Irvine, CA., 1992</p>			
Application of Processes			
Applicability			
Transonic and supersonic transports, Supersonic CTOL, STOVL, fighters.			
Objective of Processes			
Rapid and accurate conceptual designs of many configurations.			
Description of basic execution			
Beginning with a mission specification, initial geometry and initial weight estimate the fuel and component weights are estimated and the initial weight estimate is updated until a converged weight estimate is obtained. Next the volume and performance constraints are overlaid. If the aircraft does not meet the mission constraints the wing are and engine size are sized automatically or manually. Around this logic parameter various or an optimization procedure is used to size the aircraft.			
Published Applications			
Advanced transonic commercial transports [AIAA 91-3082]			
High-Speed Civil Transport [AIAA 93-4006, ICAS 94-1.2.2]			
Supersonic STOVL Fighter Aircraft [AIAA 89-2112]			
Interpretation			

CD steps	Synthesis Ladder	Similar Codes
Parametric sizing Configuration Layout Configuration Evaluation	Analysis Integrate Converge Iteration Design space visualization	PrADO FLOPS
<p>General Comments:</p> <p>Long development history and application.</p> <p>Sizing logic focused on input geometry, with optimization required for aircraft sizing</p> <p>In 1997 was exclusively licensed to Phoenix Integration, inc. and possibly rolled into model center.</p> <p>Unknown status of current logic or utilization</p>		

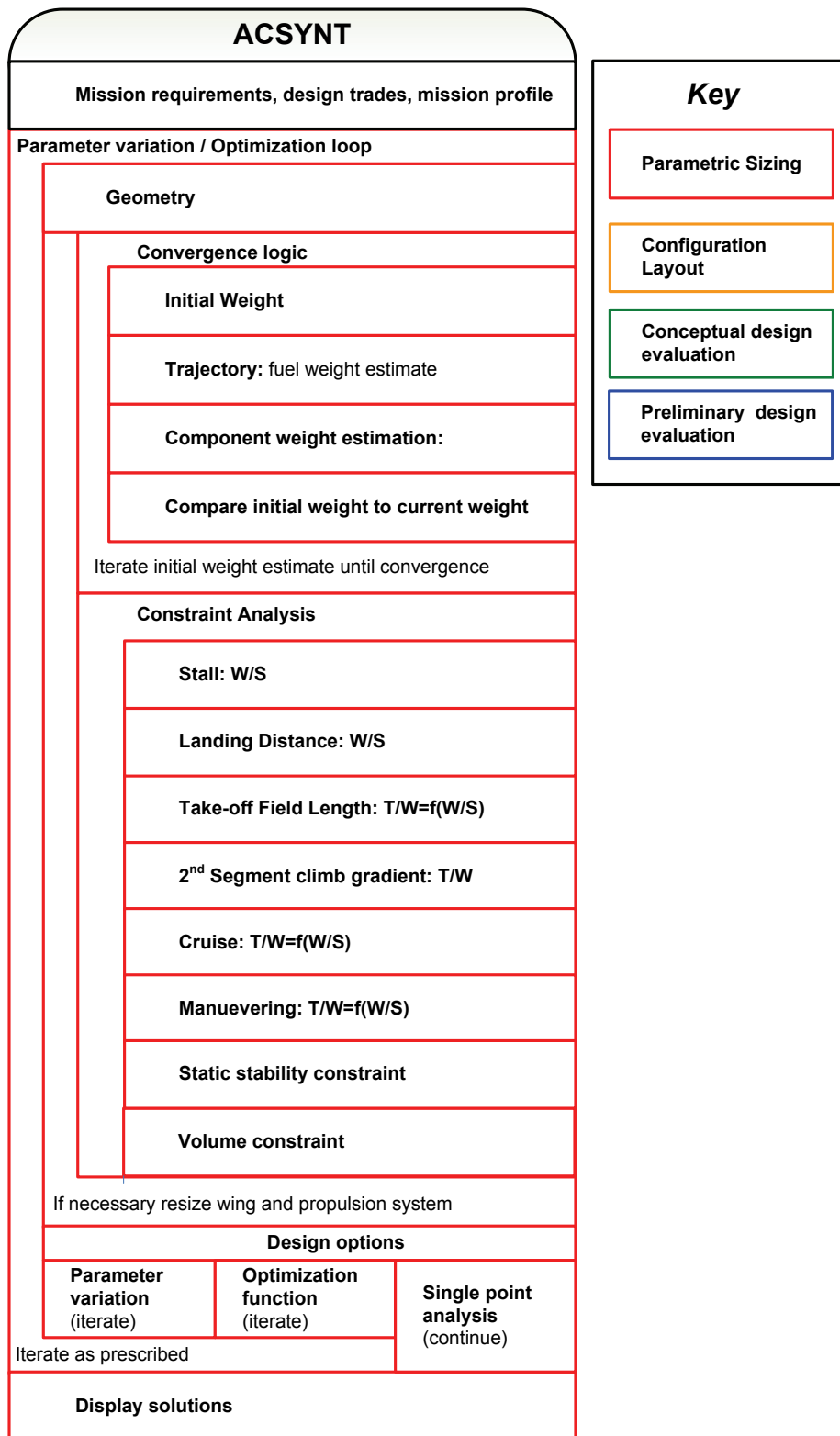


Fig A-13: ACSynt Aircraft Design Process

FURTHER DESCRIPTION

The above process describes the fundamental sizing and iteration logic of ACSYNT as described from the references. Additional functionality is available such as automated sensitivity studies and various CAD systems. In addition off line aerodynamic and structural tools can be integrated into the logic.

ACSYNT is based on a validated disciplinary Methods Library which consists of empirical and semi-empirical methods which can be seamlessly interchanged while using code. It is developed in a modal format allowing for timely adaptation and incorporation of disciplinary methods.

A.1.4 ASAP – Aircraft Synthesis Analysis Program

Processes Overview			
Design Phases	Developer	Initial Release Date	Last known update
CD	Vought Aeronautics Company, LTV Aerospace Corporation	1972	1985
<p>Reference: Ladner, F., Roch, A., “A Summary of the Design Synthesis Process,” SAWE Paper No. 907, 31st Annual Conference of the Society of Aeronautical Weight Engineers, Inc., Atlanta, Georgia, 1972</p> <p>“Aircraft Synthesis Analysis Program, ASAP,” Users manual and code documentation, Volumes II through IX, 2-52400/5R-17, LTV Aerospace and Defense, Vought Aero Products Division, Dallas, TX, 1985</p>			
Application of Processes			
Applicability			
Transonic and supersonic fighters with CTOL, STOVL, and VSTOL capabilities			
Objective of Processes			
To, size, optimize and visualize the total design space.			
Description of basic execution			
Beginning with a selection of two constants from W/S, T/W, S, and T the aircraft is fuel balanced. Fuel balancing is basically solving for the TOGW which gives just enough fuel to perform the mission. Next the constraints are computed [$T/W=f(W/S, L/D, T, \text{etc})$] and super imposed on the carpet plot produced based on varying the selected constants (W/S, T/W, S, T), This plot is then used to size the aircraft to some objective function (i.e. min TOGW). Around this loop optimization can be utilized.			
Published Applications			
Interpretation			
CD steps	Synthesis Ladder	Similar Codes	
Parametric sizing	Analysis Integrate Converge Iteration Design space visualization	FLOPS ACNST	

General Comments:

Detailed methods available for fighter design.

Conventional approach to automated aircraft sizing

Convergence is done to fuel balancing then constraint analysis.

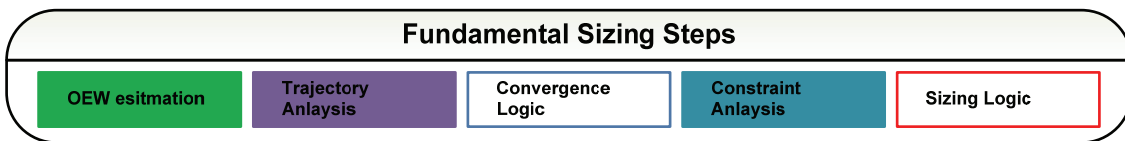
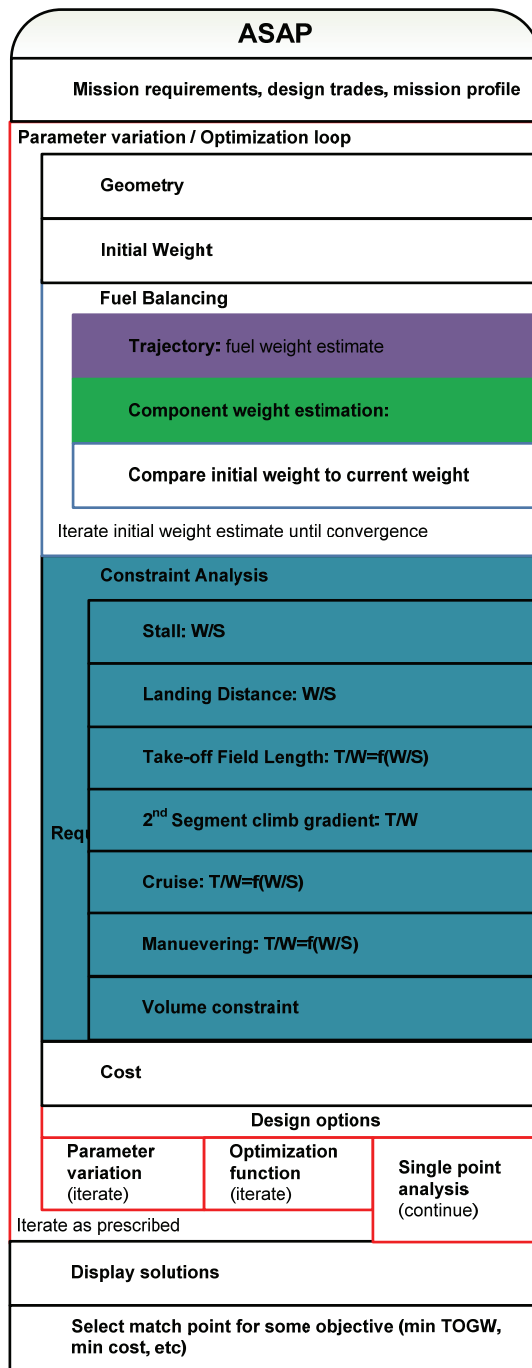


Fig A-13: ASAP Aircraft Design Process

FURTHER DESCRIPTION

This process was one of the earliest industry synthesis systems and follows a very straight forward sizing logic. The documentation makes an interest not that the process is not completely automated. The designer selects the design match point from the wing loading and thrust loading carpet plot. The documentation available discusses an automated optimization version but it is unclear if this version was ever developed.

A.1.5 FLOPS – Flight Optimization System

Processes Overview			
Design Phases CD	Developer NASA Langley Research Center	Initial Release Date 1982	Last known update 2005
Reference: McCullers			
Application of Processes			
Applicability Transonic and supersonic fighters with CTOL, STOVL, and VSTOL capabilities			
Objective of Processes To, size, optimize and visualize the total design space for the above types of aircraft. FLOPS is the standard performance evaluation and sizing tool at NASA LaRC			
Description of basic execution The process has both windows based text files interface and UNIX GUI version known as X-FLOPS. There are three options in flops (1) single point analysis, (2) parameter variation and (3) optimization. See the Users guides provided with FLOPS for more details			
Published Applications			
Interpretation			
CD steps Parametric sizing Configuration Evaluation	Synthesis Ladder Analysis Integrate Converge Iteration Design space visualization	Similar Codes ACNST ASAP	
General Comments: Detailed methods available for fighter design. Conventional approach to automated aircraft sizing Convergence is done to fuel balancing then constraint analysis.			

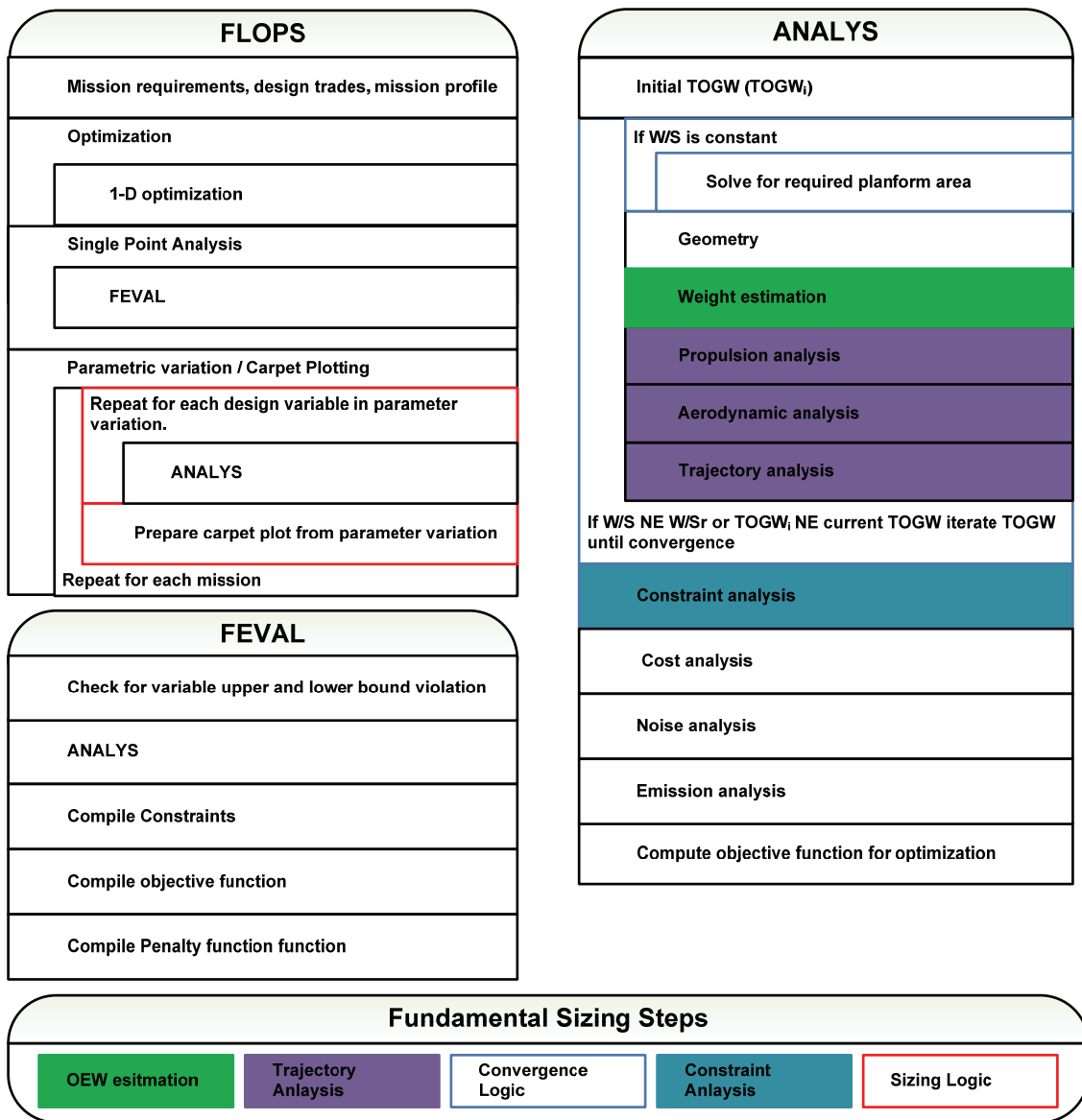


Fig A-13: FLOPS Aircraft Design Process

FURTHER DESCRIPTION

This system has been in development since the mid 1980s and has been applied to a large variety of aircraft. This system is the design synthesis system used throughout NASA. FLOPS follow a general sizing logic, incorporating cycle analysis, noise and emissions prediction methods.

A.1.6 PrADO – Preliminary Aircraft Design and Optimization

Processes Overview			
Design Phases	Developer	Initial Release Date	Last known update
CD	TU Braunschweig	1982	2005
<p>Reference: Heinze, W., <i>Ein Beitrag zur Quantitativen Analyse der Technischen und Wirtschaftlichen Auslegungsgrenzen Verschiedenster Flugzeugkonzepte fur den Transport grober Nutzlasten</i>. Braunschweig, Germany : PhD. Dissertation, Technical University Braunschweig, 1994.</p>			
Application of Processes			
<p>Applicability Transonic and supersonic transports, UAV, gliders, cryogenic aircraft, Blended wing body and multi-surface aircraft</p>			
<p>Objective of Processes This process is a basic evaluation process where the logic calls the appropriate disciplinary methods. What makes the process unique is the integration of each disciplinary module to a database management system which allows for rapid inclusion of new disciplinary methods and modification of the process when required.</p>			
<p>Description of basic execution This process can be executed in three modes (1) single design point, (2), Parameter variation and (3) optimization. Within each methods the convergence logic can utilize empirical, analytical and numerical methods including a structural/aerodynamic internal optimization</p>			
<p>Published Applications Various tail-aft commercial transports Blended wing Bodies Large Scale UAV Cryogenic transonic aircraft Hypersonic cruisers Airships</p>			
Interpretation			
CD steps	Synthesis Ladder	Similar Codes	
Configuration Evaluation	Analysis Integrate Converge Iteration Design space visualization	Piano	
<p>General Comments: .This system represents the state-of-the-art in configuration evaluation software amiable due its robustness, ease of modification level of fidelity in disciplinary methods.</p>			

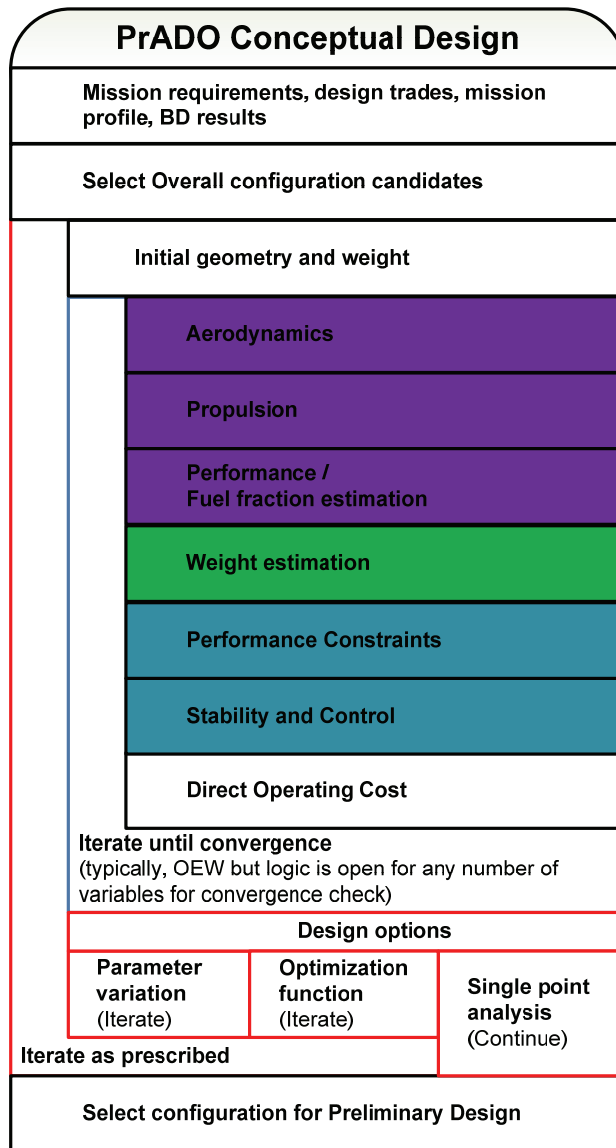


Fig A-14: PrADO aircraft design process

FURTHER DESCRIPTION

This system has been in constant development for the past 28 years. While the process is standard for configuration evaluation, the method of code integration through a database management system, range of fidelity in disciplinary methods and custom CAD kernel makes this software the state-of-the-art in conceptual design configuration evaluation and preliminary design.

A.1.7 Hypersonic Convergence

Processes Overview			
Design Phases	Developer	Initial Release Date	Last known update
CD	Czysz, McDonnell Douglass/Hypertec	1982	2005
Reference: Czysz, P.A., "Hypersonic Convergence," AFRL-VA-WP-TR-2004-3114, 2004			
Application of Processes			
Applicability			
Hypersonic launch vehicles and cruise aircraft			
Objective of Processes			
To provide a simple, volume based convergence logic to rapidly compare a wide-variety of approaches to space access and hypersonic cruise aircraft			
Description of basic execution			
From selection of mission, configuration and basic volume/weight constants the vehicle is sized for a specific range of Kuchemann slenderness parameters (τ). The t which minimizes the objective function is selected.			
Published Applications			
Curran, E., Murthy, S., "Scramjet Propulsion, Chapter 16: Czysz, P., Vandekerckhove, J., "Transatmospheric Launcher Sizing," , Progress in Astronautics and Aeronautics, American Institute of Aeronautics and Astronautics, Inc., Virginia, 2000			
Czysz, P.A., "Hypersonic Convergence," AFRL-VA-WP-TR-2004-3114, 2004			
Interpretation			
CD steps	Synthesis Ladder	Similar Codes	
Parametric Sizing	Analysis Integrate Converge Iteration Design space visualization	AVD ^{sizing}	
General Comments:			
This approach represents a more generic formulation of the parametric sizing process, through combining all generic assumptions into a single location, in steady of customizing the logic for a given configuration. In Addition this process benefits from simplifying the solution space for given aircraft into a single curve. Allowing for more complex trade studies to be visualized.			

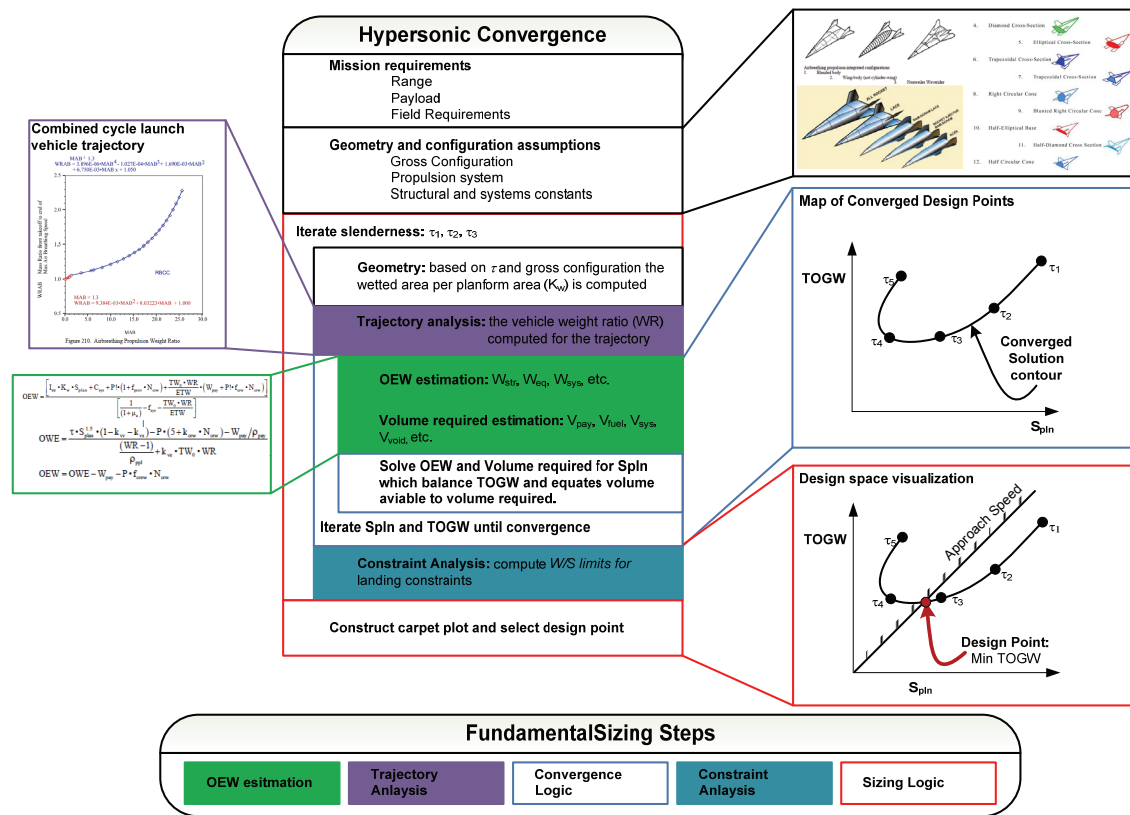


Fig A-15 HC aircraft design process

FURTHER DESCRIPTION

Due to the demanding aerothermodynamics environment of hypersonic flight vehicles, the design of this class of aircraft requires a unique aerodynamic, propulsion and structural integration logic, an integration level usually not found with subsonic and supersonic aircraft as illustrated in Figure 2-11.

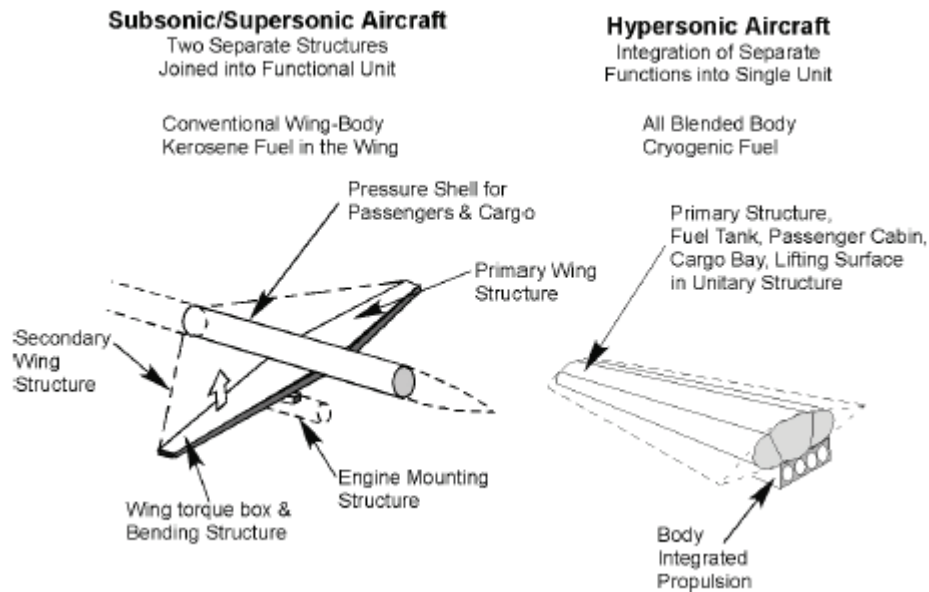


Fig A-16: Comparison of the integration subsonic/supersonic and hypersonic aircraft ⁽⁶⁴⁾.

The design problem posed with hypersonic aircraft requires an advanced sizing logic since the hypersonic flight vehicle is a fully blended geometry, where the blended body must perform all functions (volume generation, lift generation, integrated propulsion, stability and control). As shown in Figure 2-9, typical subsonic/supersonic sizing methodologies size the wing and propulsion system simultaneously while the fuselage and empennage are sized independently ^{(51) (46)}. In contrast the hypersonic convergence logic considers the total aircraft integration within the convergence logic.

Integrating the volume supply (fuselage), aerodynamic surfaces (wing, empennage) and propulsion system simultaneously requires the explicit inclusion of volume in the convergence logic. In contrast, most subsonic design methodologies only check the wing fuel volume. This significantly advanced sizing logic is presented with Figure 2-12.

At the heart of Hypersonic Convergence is the system of two equations, which solves for weight and volume simultaneously, Equations 2.3 and 2.4.

$$\text{Weight Budget } OEW = \frac{I_{str} K_w S_{pln} + C_{sys} + W_{cprv} + + \frac{T/W \cdot WR}{E_{TW}} (W_{pay} + W_{crw})}{\frac{1}{1 + \mu_a} - f_{sys} - \frac{T/W \cdot WR}{E_{TW}}} \quad 2.3$$

$$\text{Volume Budget } OWE = \frac{\tau \cdot S_{pln}^{1.5} (1 - k_{vv} - k_{vs}) - (v_{crw} - k_{crw}) N_{cew} - W_{pay} / \rho_{pay}}{\frac{WR - 1}{\rho_{ppl}} + k_{ve} \cdot T/W \cdot WR} \quad 2.4$$

Note: $OWE = OEW + W_{pay} + W_{crew}$

In these expressions, all of the variables have been solved for in the trajectory analysis or are constants except for *OEW* and *S_{pln}* allowing for a unique solution. Not that in this formulation the wing load (*TOGW/S*) will be known when *OEW* and *S_{pln}* are solved for and therefore a new sizing variable must be utilized, τ .

The Küchemann slenderness parameter, τ , provides a link between the planform area and volume. When held constant in the convergence logic, the resulting *OEW* and *S_{pln}* provide the unique solution based on the required slenderness. With increasing τ , the vehicle will have more volume per unit planform area, thus will become stouter. Conversely, when τ is decrease, the vehicle will become more slender, see Figure 2-13.

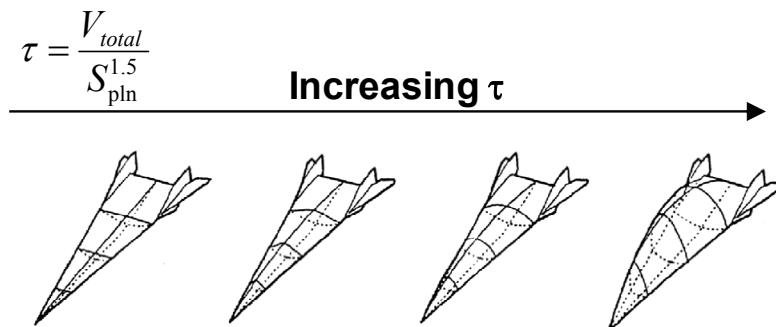
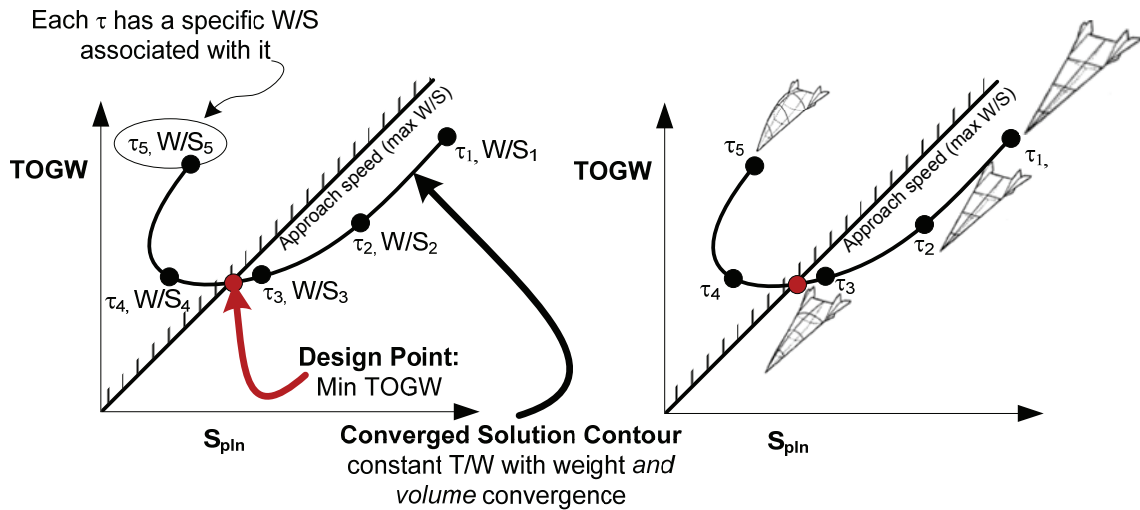


Fig 2-13: Explanation of Küchemann slenderness parameter.

In this integrated methodology, τ serves the same function as *W/S* does for the classical approach. However, instead of linking wing area to weight, τ connects wing area to

volume. The total formulation allows for wing loading, weight and volume to be solved simultaneously.

The change in convergence logic and constant reduces the number of independent variables, resulting in a simplified solution space relative to the classical sizing process. Figure 2.14, which represent a typical converged solution curve for a hypersonic cruiser. In this figure a range of slenderness parameters, τ , have been specified and the resulting $TOGW$ and S_{pln} are solved for. Physically, this curve shows that as the slenderness of the aircraft is reduced (τ increases), the planform area shrinks while the height of the upper surface can increase to accommodate the required volume. As the slenderness decreases, the aircraft structural weight will fortunately decrease while the aerodynamic efficiency will unfortunately decrease (due to increase wave drag). The result for τ larger than τ_4 the fuel weight increases such that it dominates the $TOGW$. Superimposing the wing loading required for landing, it can be seen that the slenderness ratio, that minimizes $TOGW$, will occur just above τ_3 .



As tau increase the stoutness of the vehicle increases. Increase stoutness decreases structural weight while decreasing aerodynamic efficiency. Resulting the Min $TOGW$ design point

Fig 2-14: Hypersonic Convergence sizing diagram illustrating the converged solution contour. The sizing problem is reduced to a single curve for hypersonic aircraft through including converging weight and volume.

AVD MASTER LIST OF DESIGN SYNTHESIS SYSTEMS

	Acronym	Full Name	Developer	Primary Application	Years
1	AAA	Advanced Airplane Analysis	DARcorporation	Aircraft	1991-
2	ACAD	Advanced Computer Aided Design	General Dynamics, Fort Worth	Aircraft	1993
3	ACAS	Advanced Counter Air Systems	US Army Aviation Systems Command	Air fighter	1987
4	ACDC	Aircraft Configuration Design Code	Boeing Defense and Space Group	Helicopter	1988-
5	ACDS	Parametric Preliminary Design System for Aircraft and Spacecraft Configuration	Northwestern Polytechnic University	Aircraft and Aerospace Vehicle	1991-
6	ACES	Aircraft Configuration Expert System	Aeritalia	Aircraft	1989-
7	ACSYNT	AirCRAFT SYNThesis	NASA	Aircraft	1987-
8	ADAM	(-)	McDonnell Douglas	Aircraft	
9	ADAS	Aircraft Design and Analysis System	Delft University of Technology	Aircraft	1988-
10	ADROIT	Aircraft Design by Regulation Of Independent Tasks	Cranfield University	Aircraft	
11	ADST	Adaptable Design Synthesis Tool	General Dynamics/Fort Worth Division	Aircraft	1990
12	AGARD				1994
13	AIDA	Artificial Intelligence Supported Design of Aircraft	Delft University of Technology	Aircraft	1999
14	AircraftDesign	(-)	University of Osaka Prefecture	Aircraft	1990
15	APFEL	(-)	IABG	Aircraft	1979
16	Aprog	Auslegungs Programm	Dornier Luftfahrt	Aircraft	
17	ASAP	Aircraft Synthesis and Analysis Program	Vought Aeronautics Company	Fighter Aircraft	1974
18	ASCENT	(-)	Lockheed Martin Skunk Works	AeroSpace Vehicle	1993
19	ASSET	Advanced Systems Synthesis and Evaluation Technique	Lockheed California Company	Aircraft	Before 1993
20	Altman	Design Methodology for Low Speed High Altitude UAV's	Cranfield University	Unmanned Aerial Vehicles	Paper 1998
21	AVID	Aerospace Vehicle Interactive Design	N.C. State University, NASA LaRC	Aircraft and AeroSpace Vehicle	1992
22	AVSYN	?	Ryan Teledyne	?	1974
23	BEAM	(-)	Boeing	?	NA
24	CAAD	Computer-Aided Aircraft Design	SkyTech	High-Altitude Composite Aircraft	NA
25	CAAD	Computer-Aided Aircraft Design	Lockheed-Georgia Company	Aircraft	1968

26	CACTUS	(-)	Israel Aircraft Industries	Aircraft	NA
27	CADE	Conceptual Aircraft Design Environment	McDonnell Douglas Corporation	Fighter Aircraft (F-15)	1974
28	CAP	Configuration Analysis Program	North American Rockwell (B-1 Division)	Aircraft	1974
29	CAPDA	Computer Aided Preliminary Design of Aircraft	Technical University Berlin	Transonic Transport Aircraft	1984-
30	CAPS	Computer Aided Project Studies	BAC Military Aircraft Division	Military Aircraft	1968
31	CASP	Combat Aircraft Synthesis Program	Northrop Corporation	Combat Aircraft	1980
32	CASDAT	Conceptual Aerospace Systems Design and Analysis Toolkit	Georgia Institute of Technology	Conceptual Aerospace Systems	late 1995
33	CASTOR	Commuter Aircraft Synthesis and Trajectory Optimization Routine	Loughborough University	Transonic Transport Aircraft	1986
34	CDS	Configuration Development System	Rockwell International	Aircraft and AeroSpace Vehicle	1976
35	CISE	(-)	Grumman Aerospace Corporation	AeroSpace Vehicle	1994
36	COMBAT	(-)	Cranfield University	Combat Aircraft	
37	CONSIZ	CONfiguration SIzing	NASA Langley Research Center	AeroSpace Vehicle	1993
38	CPDS	Computerized Preliminary Design System	The Boeing Company	Transonic Transport Aircraft	1972
39	Crispin	Aircraft sizing methodology	Loftin	Aircraft sizing methodology	1980
40	DesignSheet	(-)	Rockwell international	Aircraft and AeroSpace Vehicle	1992
41	DRAPO	Définition et Réalisation d'Avions Par Ordinateur	Avions Marcel Dassault/Bréguet Aviation	Aircraft	1968
42	DSP	Decision Support Problem	University of Houston	Aircraft	1987
43	EASIE	Environment for Application Software Integration and Execution	NASA Langley Research Center	Aircraft and AeroSpace Vehicle	1992
44	EADS				
45	ESCAPE	(-)	BAC (Commercial Aircraft Division)	Aircraft	1995
46	ESP	Engineer's Scratch Pad	Lockheed Advanced Development Co.	Aircraft	1992
47	Expert Executive	(-)	The Boeing Company	?	
48	FASTER	Flexible Aircraft Scaling To Requirements	Florian Schieck		
49	FASTPASS	Flexible Analysis for Synthesis, Trajectory, and Performance for Advanced	Lockheed Martin Astronautics	AeroSpace Vehicle	1996

		Space Systems			
50	FLOPS	FLight OPTimization System	NASA Langley Research Center	?	1980s-
51	FPDB & AS	Future Projects Data Banks & Application Systems	Airbus Industrie	Transonic Transport Aircraft	1995
52	FPDS	Future Projects Design System	Hawker Siddeley Aviation Ltd	Aircraft	1970
53	FRICION	Skin friction and form drag code			1990
54	FVE	Flugzeug VorEntwurf	Stemme GmbH & Co. KG	GA Aircraft	1996
55	GASP	General Aviation Synthesis Program	NASA Ames Research Center	GA Aircraft	1978
56	GPAD	Graphics Program For Aircraft Design	Lockheed-Georgia Company	Aircraft	1975
57	HACDM	Hypersonic Aircraft Conceptual Design Methodology	Turin Polytechnic	Hypersonic aircraft	1994
58					
59	HADO	Hypersonic Aircraft Design Optimization	Astrox	?	1987-
60	HASA	Hypersonic Aerospace Sizing Analysis	NASA Lewis Research Center	AeroSpace Vehicle	1985, 1990
61	HAVDAC	Hypersonic Astrox Vehicle Design and Analysis Code	Astrox		1987-
62	HCDV	Hypersonic Conceptual Vehicle Design	NASA Ames Research Center	Hypersonic Vehicles	
63	HESCOMP	HELicopter Sizing and Performance COMputer Program	Boeing Vertol Company	Helicopter	1973
64	HiSAIR/Pathfinder	High Speed Airframe Integration Research	Lockheed Engineering and Sciences Co.	Supersonic Commercial Transport Aircraft	1992
65	Holist	?	?	Hypersonic Vehicles with Airbreathing Propulsion	1992
66	ICAD	Interactive Computerized Aircraft Design	USAF-ASD	?	1974
67	ICADS	Interactive Computerized Aircraft Design System	Delft University of Technology	Aircraft	1996
68	IDAS	Integrated Design and Analysis System	Rockwell International Corporation	Fighter Aircraft	1986
69	IDEAS	Integrated DEsign Analysis System	Grumman Aerospace Corporation	Aircraft	1967
70	IKADE	Intelligent Knowledge Assisted Design Environment	Cranfield University	Aircraft	1992
71	IMAGE	Intelligent Multi-Disciplinary Aircraft Generation Environment	Georgia Tech	Supersonic Commercial Transport Aircraft	1998
72	IPAD	Integrated Programs for Aerospace-Vehicle Design	NASA Langley Research Center	AeroSpace Vehicle	1972-1980

73	IPPD	Integrated Product and Process Design	Georgia Tech	Aircraft, weapon system	1995
74	JET-UAV CONCEPTUAL DEISGN CODE		Northwestern Polytechnical University, China	Medium range JET-UAV	2000
75	LAGRANGE			Optimization	1993
76	LIDRAG	Span efficiency			1990
77	LOVELL				1970-1980
78	MAVRIS	an analysis-based environment	Georgia Institue of Technology		2000
79	MELLER		Daimler-Benz Aerospace Airbus	Civil aviation industry	1998
80	MacAirplane	(-)	Notre Dame University	Aircraft	1987
81	MIDAS	Multi-Disciplinary Integrated Design Analysis & Sizing	DaimlerChrysler Military	Aircraft	1996
82	MIDAS	Multi-Disciplinary Integration of Deutsche Airbus Specialists	DaimlerChrysler Aerospace Airbus	Supersonic Commercial Transport Aircraft	1996
83	MVA	Multi-Variate Analysis	RAE (BAC)	Aircraft	1991
84	MVO	MultiVariate Optimisation	RAE Farnborough	Aircraft	1973
85	NEURAL NETWORK FORMULATION	Optimization method for Aircrat Design	Georgia Institute of Technology	Aircraft	1998
86	ODIN	Optimal Design INtegration System	NASA Langley Research Center	AeroSpace Vehicle	1974
87	ONERA	Preliminary Design of Civil Transport Aircraft	Office National d'Etudes et de Recherches Aérospatiales	Subsonic Transport Aircraft	1989
88	OPDOT	Optimal Preliminary Design Of Transports	NASA Langley Research Center	Transonic Transport Aircraft	1970-1980
89	PACELAB	knowledge based software solutions	PACE	Aircraft	2000
90	Paper Airplane	(-)	MIT	Aircraft	
91	PASS	Program for Aircraft Synthesis Studies	Stanford University	Aircraft	1988
92	PATHFINDER		Lockheed Engineering Sciences Co. and	Supersonic Commercial Transport Aircraft	1992
93	PIANO	Project Interactive ANalysis and Optimization	Lissys Limited	Transonic Transport Aircraft	1980-
94	POP	Parametrisches Optimierungs-Programm	Daimler-Benz Aerospace Airbus	Transonic Transport Aircraft	2000
95	PrADO	Preliminary Aircraft Design and Optimization	Technical University Braunschweig	Aircraft and AeroSpace Vehicle	1986-

96	PreSST	Preliminary SuperSonic Transport Synthesis and Optimization	DRA UK	Supersonic Commercial Transport Aircraft	
97	PROFET	(-)	IABG	Missile	1979
98	RAE	Artificial Intelligence Supported Design of Aircraft	Royal Aircraft Establishment, Farnborough	Aircraft conceptual design	Early 1970's.
99	RAM		NASA	geometric modeling tool	1991
100	RCD	Rapid Conceptual Design	Lockheed Martin Skunk Works	AeroSpace Vehicle	
101	RDS	(-)	Conceptual Research Corporation	Aircraft	1992
102	RECIPE	(-)	?	?	1999
103	RSM	Response Surface Methodology			1998
104	Rubber Airplane	(-)	MIT	Aircraft	1960s-1970s
105	Schnieder				
106	Siegers	Numerical Synthesis Methodology for Combat Aircraft	Cranfield University	combat aircraft	Late 1970s
107	Spreadsheet Program	Spreadsheet Analysis Program	Loughborough University	Aircraft Design Studies	1995
108	SENSxx	(-)	DaimlerChrysler Aerospace Airbus	Transonic Transport Aircraft	
109	SIDE	System Integrated Design Environment	AstroX	?	1987-
110	SLAM	Simulated Language for Alternative Modeling	?	?	
111	Slate Architect	(-)	SDRC (Eds)	?	
112	SSP	System Synthesis Program	University of Maryland	Helicopter	
113	SSSP	Space Shuttle Synthesis Program	General Dynamics Corporation	AeroSpace Vehicle	
114	SYNAC	SYNthesis of AirCRAFT	General Dynamics	Aircraft	1967
115	TASOP	Transport Aircraft Synthesis and Optimization Program	BAe (Commercial Aircraft) LTD	Transonic Transport Aircraft	
116	TIES	Technology Identification, Evaluation, and Selection	Georgia Institute of Technology		1998
117	TRANSYN	TRANsport SYNthesis	NASA Ames Research Center	Transonic Transport Aircraft	1963-(25years)
118					
119	TRANSYS	TRANsportation SYStem	DLR (Aerospace Research)	AeroSpace Vehicle	1986-
120	TsAGI	Dialog System for Preliminary Design	TsAGI	Transonic Transport Aircraft	1975
121	VASCOMPII	V/STOL Aircraft Sizing and Performance Computer Program	Boeing Vertol CO.	V/STOL aircraft	1980

122	VDEP	Vehicle Design Evaluation Program	NASA Langley Research Center	Transonic Transport Aircraft	
123	VDI				
124	Vehicles	(-)	Aerospace Corporation	Space Systems	1988
125	VizCraft	(-)	Virginia Tech	Supersonic Commercial Transport Aircraft	1999
126	Voit-Nitschmann				
127	WIPAR	Waverider Interactive Parameter Adjustment Routine	DLR Braunschweig	AeroSpace Vehicle (Waverider)	
128	X-Pert	(-)	Delft University of Technology	Aircraft	Paper 1992

APPENDIX B

EXCERPTS FROM PARAMETRIC SIZING METHODS LIBRARY

This appendix details the disciplinary methods utilized for the studies described in this dissertation. They are taken from the master AVD disciplinary methods library (79). Each method will only be introduced once. If a method is used for two models the second model will refer to the first model. Each library is organized as follows,

GEOMETRY

AERODYNAMICS

- Fiction and form drag
- Drag due to flaps and landing gear
- Wave drag
- Induced Drag
- Lift Curve Slope
- Maximum Lift Coefficient
- Drag Polar Location Specification

PROPULSION

- Specific fuel consumption
- Thrust variation
- Propulsion system sizing

PERFORMANCE

- Landing Distance
- Take-off Distance
- Climb gradient requirement
- Design cruise
- Time to climb
- Descent performance
- Maximum velocity
- Ceiling
- Fuel weight estimation/Trajectory

STABILITY AND CONTROL

- Trim

WEIGHT AND BALANCE

- Structural Loads
- Empty Weight and Volume Formulation
- Structural weight
- Propulsion system weight
- Fixed equipment weight
- Operational items weight

COST

- Life Cycle Cost Formulation
- RDT&E estimation
- Manufacturing and acquisition
- Direct Operating Cost
- Block Mission

B.1 TAIL-AFT CONFIGURATION TRANSPORT METHODS

GEOMETRY

Method Overview				
Discipline	Design Phase	Method Title	Categorization	Author
Geometry	Parametric sizing	Transonic Tail-Aft Configuration	Analytical	Coleman
Reference: Dissertation				
Brief Description Derivation of the tail-aft configurations primary geometry, wetted area and volume used in AVD sizing. At the time when the geometry module is called assumed constants are combined with the given planform area and Küchemann's slenderness parameter to derive the geometry of the current aircraft				
Assumptions Strait tapered wings Fuselage Empennage		Applicability Most conventional tail-aft transonic transports		
Execution of Method				
Input $AR, \lambda, \Lambda_{LE}, M_{cr}, S_{pln}, \tau,$				
Analysis description Compute the wing dimensions, wetted area and volume Compute the fuselage dimensions and wetted area for the required volume. 2 methods are currently available in AVD ^{sizing} Fix fuselage l/d and h/w and solve for required cross-section Fix fuselage cross-section h and w and solve for fuselage length required See further description				
Output: $b, c_r, c_t, \bar{c}, (t/c)_{avg}, V_{wing}, d_{max}, l_{fus}, w_{fus}, h_{max}$				
Experience				
Accuracy Unknown	Time to Calculate Unknown		General Comments Has worked well for the B777, B787, A380 and Embraer 170	

Further Description

Wing

TABLE 5-5: Wing definition for Transonic Transports

Variable	Description
<i>Given</i>	
AR	Aspect ratio (input)
λ	Tapper ratio (input)
Λ_{LE}	Leading edge sweep (input)
M_{cr}	Desired wing critical Mach number (input)
<i>Computed</i>	
b	Span $b = \sqrt{AR \cdot S_{pln}}$
c_r	Root chord $c_r = \frac{2}{1 + \lambda} \frac{S_{pln}}{b}$
c_t	Tip chord $c_t = \lambda \cdot c_r$
\bar{c}	Mean aerodynamic chord $\bar{c} = \frac{2}{3} c_r \frac{1 + \lambda + \lambda^2}{1 + \lambda}$
$(t/c)_{avg}$	Average wing thickness $(t/c)_{avg} = 0.95 - 0.1(C_L)_{cruise} - M_{cr} \cos^m \Lambda_{c/4}$
V_{wing}	Wing volume $V_{wing} = 0.54 \cdot \frac{S_{pln}^2}{b} \cdot b \cdot (t/c)_{avg} \frac{1 + \lambda + \lambda^2}{(1 + \lambda)^2}$

Fuselage

TABLE 5-6: Fuselage definition for transonic transports with fixed l/d and h/w

Variable	Description
<i>Given</i>	
l/d	Fuselage slenderness ratio (input)
h/w	Cabin eccentricity (high/width)
<i>Computed</i>	
d_{max}	Maximum diameter of fuselage $d_{max} = \frac{\tau \cdot S_{pln}^{1.5} - V_{wing}}{\left(\frac{\pi}{4} l/d \left(1 - \frac{2}{l/d}\right)\right)^{1/3}}$
l_{fus}	Length of fuselage $l_{fus} = d_{max} \cdot l/d$
w_{fus}	width of fuselage $w_{fus} = d_{max} / \sqrt{h/w}$
h_{max}	height of fuselage $h_{fus} = w_{fus} \cdot h/w$

$$S_{wet\ fus} \quad \text{height of fuselage} \quad S_{wet\ fus} = \pi \cdot d_{max} l_{fus} \left(1 - \frac{2}{l./d_{fus}}\right)^{2/3} \left(1 + \frac{1}{(l./d_{fus})}\right)$$

TABLE 5-6: Fuselage definition for transonic transports with fixed cabin cross-section

Variable	Description	
<i>Given</i>		
h	Maximum fuselage height	
w	Maximum fuselage width	
<i>Computed</i>		
d_{max}	Maximum diameter of fuselage	$d_{max} = \sqrt{h \cdot w}$
l / d_{fus}	Fuselage fineness ratio	$l / d_{fus} = \frac{S_{pln}^{1.5} \tau - V_{wing}}{\pi / 4 d_{max}^3} + 2$
l_{fus}	length of fuselage	$l_{fus} = l / d_{fus} d_{max}$
$S_{wet\ fus}$	height of fuselage	$S_{wet\ fus} = \pi \cdot d_{max} l_{fus} \left(1 - \frac{2}{l./d_{fus}}\right)^{2/3} \left(1 + \frac{1}{(l./d_{fus})}\right)$

Empennage Definition

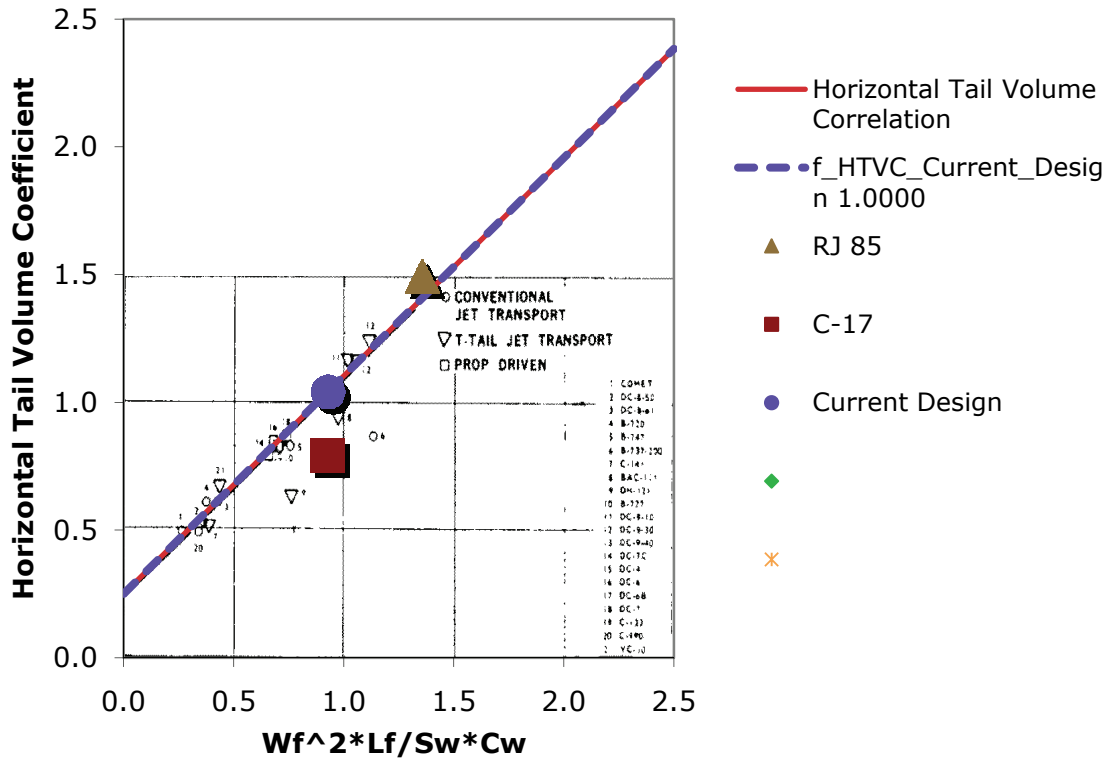
Method Overview				
Discipline	Design Phase	Method Title	Categorization	Author
Geometry	Parametric sizing	Modified Tail-Volume Quotient Method	Empirical	Hahn, Morris
<p>Reference: Morris, J, Ashford, D. M., "Fuselage Configuration Studies," SAE 670370 / Hahn, A., Modification in Spread-Sheet form, Personal Communitarian, July, 2009</p>				
<p>Brief Description Derivation empennage geometry based on a modified tail-volume coefficient methods</p>				
<p>Assumptions Wing-body combination Empennage</p>		<p>Applicability Most conventional tail-aft transonic transports</p>		
Execution of Method				
<p>Input $M_{HT}, B_{HT}, K_{VT}, M_{VT}$ and $B_{VT}, l/c$</p>				
<p>Analysis description Compute the new horizontal tail and vertical volume quotients from</p> $V_H = \frac{d_{\max}^2 l_{fus}}{S_{\text{pln}} \bar{c}} M_{HT} + B_{HT} \text{ and } V_V = K_{VT} \left(\frac{d_{\max}^2 l_{fus}}{S_{\text{pln}} b} M_{VT} + B_{VT} \right)$ <p>See further constants, $M_{HT}, B_{HT}, K_{VT}, M_{VT}$ and B_{VT} for definition From the definition of the volume quotient the horizontal and vertical tail areas are computed</p> $S_h = \frac{V_H}{l/c}, S_v = \frac{V_V}{l/b}$ <p>The remainder of the horizontal and vertical tail geometry is defined is a similar fashion to the wing</p>				
<p>Output: V_H, V_V, S_h, S_v</p>				
Experience				
<p>Accuracy Unknown</p>		<p>Time to Calculate Unknown</p>	<p>General Comments Appears to be a linear regression of the class critical Mach number charts (see USAF DATCOM)</p>	

Further Description

TABLE 5-6: Fuselage definition for transonic transports with fixed cabin cross-section

Variable	Description
<i>Horizontal Tail</i>	
M_{HT}	0.8532
B_{HT}	0.2500
<i>Vertical Tail</i>	
M_{HT}	0.3375
B_{HT}	0.0325
KHT	1.000 (HT attached to fuselage)
	0.844 (T-tail, mid to low wing)
	1.350 (T-tail, high wing)

Horizontal Tail Sizing



Vertical Tail Sizing

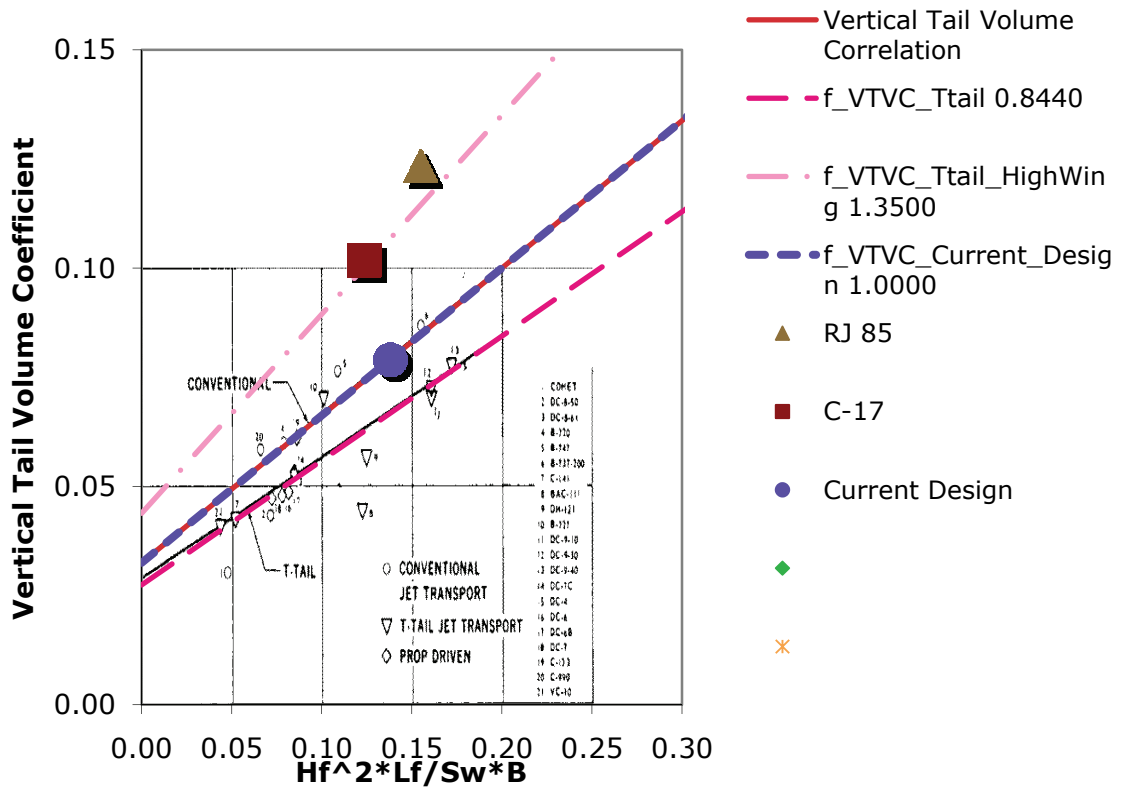


Fig 5-7: Modified Tail Volume Quotient⁽²⁵⁾.

AERODYNAMICS

Fiction and form drag

Method Overview				
Discipline	Design Phase	Method Title	Categorization	Author
Aerodynamics	Sizing	Subsonic skin friction estimation	Semi-Empirical	Smith
Reference: Smith, C.W., "Aerospace Handbook," 2 nd edition, General Dynamics Convair Aerospace Division, Fort Worth, TX, 1976				
Brief Description Construction of the skin friction drag coefficient using an equivalent flat plate method				
Assumptions Typical values		Applicability Subsonic aircraft		
Execution of Method				
Input Re, simple vehicle geometry and empirical constants				
Analysis description Estimate skin flat plat friction coefficient for example $C_f = 0.455/(\log R_e)^{1/5}$ $R_e < 5 \times 10^9$ for a turbulent boundary layer Estimate the equivalent component skin friction coefficient Compile total friction drag coefficient				
Output: Drag Polar, $(L/D)_{\max}$, $(C_L)_{\max}$ L/D, $C_{L\max}$, C_{LA} , C_{LT} , C_{L2}				
Experience				
Accuracy See Appendix on Page 170 Tables 3.II to 3.VI		Time to Calculate Unknown	General Comments This method gives the designer the freedom to estimate C_{D0} with minimum wing assumptions	

Further Description

The method involves computing the skin friction coefficient for each aircraft component and summing them together to compute the total aircraft parasite drag coefficient (Equation 2.2).

$$C_{Df} = \frac{\sum (C_f \cdot S_{wet})_{comp}}{S_{ref}} \quad (2.2)$$

Where, the individual skin friction coefficients for each component are estimated by Equations 2.3 to 2.5.

$$C_{f_{wing}} = C_{f_{FP}} \left[1 + L(t/c) + 100(t/c)^4 \right] R_{L.S.} \quad (2.2)$$

$$C_{f_{fuselage}} = C_{f_{FP}} \left[1 + \frac{1.3}{(FR)^{1.5}} + \frac{44}{(FR)^3} \right] R_{fus.} \quad (2.3)$$

$$C_{f_{nacelle}} = C_{f_{FP}} Q \left[1 + \frac{0.35}{(FR)} \right] \quad (2.4)$$

$$C_{f_{HT\&VT}} = C_{f_{FP}} \left[1 + L(t/c) + 100(t/c)^4 \right] R_{L.S.} \quad (2.5)$$

Where, $C_{f_{FP}}$ = Flat plate skin friction coefficient, Reference 7 or 6, function of Mach number and Reynolds number

L = Thickness location parameter

= 1.2 for $(t/c)_{max}$ located @ $x > 0.3c$

= 2.0 for $(t/c)_{max}$ located @ $x < 0.3c$

$R_{L.S.}$ = Lifting surface correction factor (Figure 2.1)

$R_{fus.}$ = Fuselage correction factor (Figure 2.1)

Q = Interference factor,

= 1.0, nacelles and external stores mounted out of the local wing velocity field

= 1.25, external stores mounted symmetrically on the wing tip

= 1.3, nacelles and external stores if mounted in proximity of the wing

= 1.5, nacelles and external stores mounted flush with wings or nacelle or external stores flush mounted to fuselage

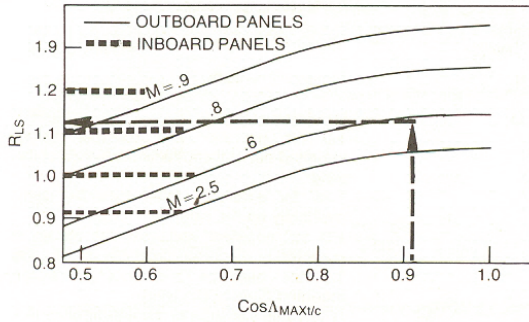
FR = Fineness ratio,

= l/d for circular cross-section

= $l/\sqrt{h \cdot w}$ for irregular cross sections and nacelles

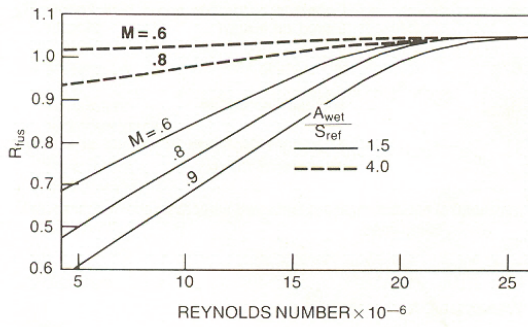
Subsonic-Component Correction Factors

Lifting Surface Correction



Fuselage Corrections

Apply ratio A_{wet}/S_{ref} value for the fuselage *plus* attached items (to respective sets of curves, dashed or solid).



For Mach ≤ 0.5

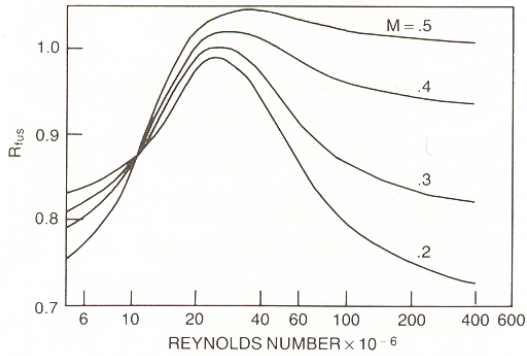


Figure. *Lifting surface and Fuselage correction factors*⁵

Method Overview				
Discipline	Design Phase	Method Title	Categorization	Author
Aerodynamics	Sizing	Subsonic partial laminar skin friction estimation	Semi-Empirical	Roskam, MACair
<p>Reference: Roskam, J., "Airplane Design Part VI: Preliminary Calculation of Aerodynamic, Thrust and Power Characteristics," DARcorporation, Lawrence, Kansas, 2003</p>				
<p>Brief Description</p> <p>Computation of the skin friction coefficient based on a given transitional Reynolds number for partial laminar flow airfoils. This method modifies the flat plate friction coefficient which can then be used method outlined by Smith.</p>				
<p>Assumptions</p> <p>Typical values</p>		<p>Applicability</p> <p>Subsonic aircraft</p>		
Execution of Method				
<p>Input</p> <p>R_{eT}, simple vehicle geometry and empirical constants</p>				
<p>Analysis description</p> <p>Estimate chord length of laminar flow from transitional Reynolds number.</p> $c_l = R_T \cdot \bar{c} / R_e$ <p>Estimate ratio of wing planform area for which the flow is laminar S_l / S_{ref}</p> <p>Compute the flat plate skin friction coefficients for the laminar and turbulent portion based on their respective characteristic lengths numbers (c_l for laminar section and MAC of the remaining area for turbulent)</p> $C_{fr} = \frac{0.482}{\text{Log}(R_e)}$ <p>Compute total flat plate friction coefficient</p> <p>Use the GD method for computing the total CD0</p>				
<p>Output:</p> <p>CD0,</p>				
Experience				
<p>Accuracy</p> <p>Unknown</p>		<p>Time to Calculate</p> <p>Unknown</p>	<p>General Comments</p> <p>When used in conjunction with the F-14 wing glove experiment for the transitional Re this method has proven to be accurate for current aircraft designs (B777-300ER, B787, A380, Embraer 170, etc.)</p>	

Further Description

Estimate chord length of laminar flow from transitional Reynolds number.

$$c_{TX} = R_{TX} \cdot \bar{c} / R_e$$

Estimate ratio of wing planform area for which the flow is laminar

If the laminar chord is less than the tip chord then the laminar portion can be approximated as a rectangle along the leading edge of the wing. Therefore,

$$S_l = c_{TX} \cdot b$$

$$\lambda_T = \frac{(c_t - c_{TX})}{(c_r - c_{TX})}$$

$$\bar{c}_T = \frac{2}{3}(c_r - c_{TX}) \frac{1 + \lambda_T + \lambda_T^2}{1 + \lambda_T}$$

If the laminar chord is greater than the tip then the laminar area will terminate at the trailing edge of the wing a certain spanwise location. In this case compute the spanwise location of the intersection and then compute the turbulent area (this shape will be a triangle). Then compute the turbulent mean aerodynamic chord as described above

ADD A FIGURE

Assuming that the ratio of laminar to turbulent planform area is equivalent to the ratio of wetted area then

$$S_{wet_t} = S_{wet} \frac{S_l}{S_{ref}}$$

Compute the flat plate skin friction coefficients for the laminar and turbulent portion based on their respective characteristic lengths numbers (c_L for laminar section and MAC of the remaining area for turbulent)

$$C_{f_T} = \frac{0.482}{\text{Log}\left(R_e \frac{\bar{c}_T}{\bar{c}}\right)}, C_{f_L} = \frac{1.328}{\text{Log}(R_{TX})}$$

Compute total flat plate friction coefficient based on the area ratios

$$C_f = C_{f_L} \frac{S_{wet_L}}{S_{wet}} + C_{f_T} \left(1 - \frac{S_{wet_L}}{S_{wet}}\right)$$

Use the GD method for computing the total CD0

Drag due to flaps and landing gear

Method Overview																
Discipline	Design Phase	Method Title	Categorization	Author												
Aerodynamics	Baseline Design	Initial Drag polar estimation	Semi-Empirical	Roskam												
Reference: Roskam, J., "Airplane Design Part I: Preliminary Sizing of Airplanes," DARcorporation, Lawrence, Kansas, 2003																
Brief Description Typical drag values for flaps effects in take-off and landing configurations																
Assumptions The entire method is an assumptions		Applicability Could be applied to any configuration														
Execution of Method																
Input Configuration (take-off or landing)																
Analysis description <table border="1" style="width: 100%; border-collapse: collapse;"> <thead> <tr> <th style="border-top: 1px solid black; border-bottom: 1px solid black;">Configuration</th> <th style="border-top: 1px solid black; border-bottom: 1px solid black;">ΔC_{D0}</th> <th style="border-top: 1px solid black; border-bottom: 1px solid black;">Δe</th> </tr> </thead> <tbody> <tr> <td>Clean</td> <td>0.0</td> <td>0.0</td> </tr> <tr> <td>Take-off</td> <td>0.010 - 0.020</td> <td>-0.05</td> </tr> <tr> <td>Landing</td> <td>0.015 - 0.025</td> <td>-0.10</td> </tr> </tbody> </table>					Configuration	ΔC_{D0}	Δe	Clean	0.0	0.0	Take-off	0.010 - 0.020	-0.05	Landing	0.015 - 0.025	-0.10
Configuration	ΔC_{D0}	Δe														
Clean	0.0	0.0														
Take-off	0.010 - 0.020	-0.05														
Landing	0.015 - 0.025	-0.10														
Output: ΔC_{D0} , Δe																
Experience																
Accuracy Unknown		Time to Calculate N/A	General Comments Use with care													

Method Overview				
Discipline Aerodynamics	Design Phase Baseline Design	Method Title Drag due to landing gear	Categorization Semi-Empirical	Author Roskam
Reference: Roskam, J., "Airplane Design Part I: Preliminary Sizing of Airplanes," DARcorporation, Lawrence, Kansas, 2003				
Brief Description Typical drag values for landing gear up or down				
Assumptions The entire method is an assumptions		Applicability Could be applied to any configuration		
Execution of Method				
Input Configuration (Landing gear up/down)				
Analysis description				
Configuration		ΔC_{D0}	Δe	
Clean		0.0	0.0	
Down		0.015 - 0.025	No Effect	
Output: ΔC_{D0}				
Experience				
Accuracy Unknown		Time to Calculate N/A	General Comments Use with care	

Wave drag

Method Overview				
Discipline	Design Phase	Method Title	Categorization	Author
Aerodynamics	Sizing	MAC wave drag approximation	Semi-Empirical	Czysz
Reference: McDonald Douglas circa 1970				
Brief Description From an assumed or computed critical mach number and K_0 (approximation of the area distribution to the sear hack body) the drag rise can be computed as a function of mach number				
Assumptions Critical Mach number, approximate area distribution		Applicability Any aircraft with the appropriate critical mach number and K_0 .		
Execution of Method				
Input $M_{cr}, K_0, \Lambda_{LE}, AR$				
Analysis description		<p>The graph plots the wave drag coefficient $\Delta C_{D_{wave}}$ on the y-axis (ranging from 0 to 0.56) against the wave drag parameter S_f/L^2 on the x-axis (ranging from 0 to 0.028). Five dashed lines represent different values of K_0: 1.0, 1.5, 2.0, 2.9, and 4.0. The lines show that $\Delta C_{D_{wave}}$ increases with both S_f/L^2 and K_0. A legend indicates symbols for different data sources: open circles for 'BASES OF REV.', open triangles for 'CURRENT AIRCRAFT', open squares for 'NASA TFV MODELS', and open diamonds for 'MDC TFV MODELS'. A note mentions 'SERIES-WAVE OPTIMUM BODY OF REVOLUTION'.</p>		
$\left(\Delta C_{D_{wave}}\right)_{S_F} = \frac{K_0}{10^3} \left[\frac{10 \cdot (M - M_{cr})}{\left(\frac{1}{\cos \Lambda_{LE}} - M_{cr}\right)^n} \right]$ $n = \frac{3}{1 + 1/AR}$ $\Delta C_{D_{wave}} = \left(\Delta C_{D_{wave}}\right)_{S_F} \frac{S_f}{S}$				
Output:				
$\Delta C_{D_{wave}} = \left(\Delta C_{D_{wave}}\right)_{S_F} \frac{S_f}{S}$				
Experience				
Accuracy Dependent on assumed values		General Comments Use the provided figure for guidance for K_0		

Induced Drag

Method Overview				
Discipline	Design Phase	Method Title	Categorization	Author
Aerodynamics	Sizing	Induced Drag	Semi-Empirical	Wilson
<p>Reference: "Aircraft Synthesis Analysis Program, Aerodynamics Module," Volume VI, LTV, Aerospace and Defense, Vought Aero Products Division, TX, 1988</p>				
<p>Brief Description</p> <p>Mach number corrections from Vought wind-tunnel testing to the induced drag method presented in DATCOM. In addition a separate method is presented for the lift curve slope based on VAC methods</p>				
<p>Assumptions</p> <p>Strait-tapered wings, round or sharp leading edge airfoils</p>		<p>Applicability</p> $2 \leq AR \leq 10.7$ $0 \leq \lambda \leq 0.713$ $19.1 \leq \Lambda_{LE} \leq 63.4$ $0.13 \leq M \leq 2.4$ $0.72 \times 10^6 \leq R_E \leq 16.6 \times 10^6$		
Execution of Method				
<p>Input</p> <p>Re, Mach, $C_{L\alpha}$, airfoil leading edge radius, wing sweep, taper ratio, aspect ratio</p>				
<p>Analysis description</p> <p>Estimate (R_1) and (R_2) from the methods described below</p> <p>Compute the Oswald's efficiency factor (e)</p>				
<p>Output:</p> <p>e</p>				
Experience				
<p>Accuracy</p> <p>Works well within range of applicability</p>		<p>Time to Calculate</p> <p>N/A</p>	<p>General Comments</p> <p>Have had limited success with the Citation X (See accuracy comment)</p>	

Further Description

For straight tapered wings the Oswald's efficiency is computed by the Equation below

$$e = \left[\frac{R_2 (C_{L\alpha} / AR)}{R_1 (C_{L\alpha} / AR) + (1 - R_1)\pi} \right] K_3 + \Delta e$$

Where the constant R_1 and R_2 are computed depending on flight Mach number. A linear interpolation is used for the transonic region.

Round Leading Edges

$$R_1 = \begin{cases} \text{Fig 2.6} & M \leq 0.8 \\ 0.0 & M \geq 1 / \cos \Lambda_{LE} \\ \text{Interpolate} & 0.8 \leq M \leq 1 / \cos \Lambda_{LE} \end{cases}, R_2 = 1.0$$

Sharp Leading Edges

$$R_1 = 0.0, R_2 = \begin{cases} 1.1 & M \leq 0.8 \\ 1.0 & M \geq 1.2 \\ \text{Interpolate} & 0.8 \leq M \leq 1.2 \end{cases}$$

The constants K_3 and Δe are used to account for supercritical wings, leading edge camber, vortex attenuation, trim drag, etc.

Lift Curve Slope

Method Overview				
Discipline	Design Phase	Method Title	Categorization	Author
Aerodynamics	Sizing	Lift Curve Slope	Semi-Empirical	Hoak
Reference: Hoak, D., Fink, R., "USAF Stability and Control DATCOM," Global Engineering Documents, CA, 1978				
Brief Description 3-D wing lift curve slope for strait tapered wings				
Assumptions Strait-tapered wings, incompressible flow			Applicability Strait-tapered wings in subsonic flow ($M < 0.8$)	
Execution of Method				
Input Mach, AR, airfoil lift curve slope, wing sweep				
Analysis description $\frac{C_{L\alpha}}{AR} = \left[\frac{2\pi}{2 + \sqrt{\frac{AR^2 \beta^2}{k^2} \left(1 + \frac{\tan^2 \Lambda_{LE}}{\beta^2} \right) + 4}} \right] \frac{(C_{L\alpha})_{test}}{(C_{L\alpha})_{pred}}$ $\beta = \sqrt{1 - M^2}$ $k = \frac{C_{l\alpha}}{2\pi}$ $\frac{(C_{L\alpha})_{test}}{(C_{L\alpha})_{pred}} \text{ from Figure 2.8}$				
Output: $C_{L\alpha}$				
Experience				
Accuracy Works well with in applicability		Time to Calculate N/A	General Comments	

SUBSONIC SPEEDS

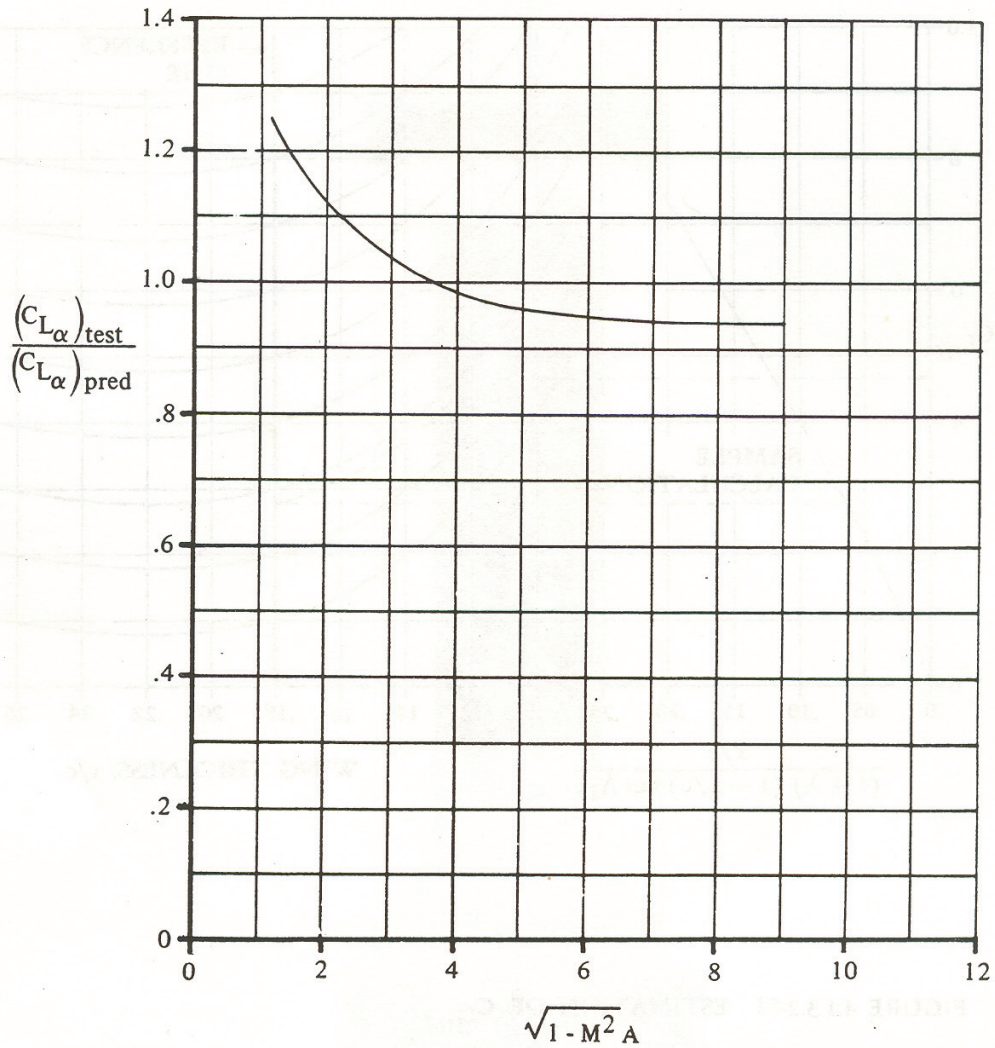


FIGURE 4.1.3.2-52 CORRELATION OF SUBSONIC LIFT-CURVE SLOPE FOR CRANKED PLANFORMS HAVING ROUND-NOSED AIRFOILS

Figure. 2.8 Lift-curve-slope correction factor (USAF DATCOM)

Maximum Lift Coefficient

Method Overview				
Discipline	Design Phase	Method Title	Categorization	Author
Aerodynamics	Sizing	Maximum Landing Lift Coefficient	Typical values	Roskam
<p>Reference: Roskam, J., "Airplane Design Part I: Preliminary Sizing of Airplanes," DARcorporation, Lawrence, Kansas, 2003</p>				
<p>Brief Description Selection of maximum lift coefficient based on similar aircraft</p>				
<p>Assumptions Typical values only, use caution</p>		<p>Applicability Homebuilt aircraft propeller aircraft, single engine propeller aircraft, twin engine propeller aircraft, agricultural aircraft, business jets, regional turboprop aircraft, transport jets, military trainers, fighters, military patrol, bomb and transport, flying boats, supersonic cruise aircraft</p>		
Execution of Method				
<p>Input Type of aircraft</p>				
<p>Analysis description Select value for maximum lift coefficient from Figure 3.1 on page 91</p>				
<p>Output: CL_{max}, CL_{TO}, CL_{LAND}</p>				
Experience				
<p>Accuracy Depends on selection</p>		<p>Time to Calculate Unknown</p>	<p>General Comments The selection of this variable drives the size and complexity of high-lift devices</p>	

Drag Polar Location Specification

Method Overview				
Discipline Aerodynamics	Design Phase Sizing	Method Title Lift to drag ratio	Categorization Analytic	Author Vinh
Reference: Vinh, N., "Flight Mechanics of High-Performance Aircraft," Cambridge Aerospace Series 4, "UK, 1995				
Brief Description Computes the L/D for a given location on the drag polar				
Assumptions Tail aft configuration or flying wing		Applicability Symmetric aircraft with 1 or 2 horizontal lifting surfaces (TAC, FWC)		
Execution of Method				
Input M, L', C_{D0}				
<p>Analysis description</p> $C_L = \sqrt{\frac{m}{m-1}} \sqrt{\frac{C_{D0}}{L'}}, \quad L/D = \frac{\sqrt{m(2-m)}}{2\sqrt{L' C_{D0}}}$				
Output: $C_L, L/D$				
Experience				
Accuracy	Time to Calculate	General Comments Useful for high speed aircraft which do not cruise at L/D_{max} due to the high thrust requirement		

PROPULSION

Specific fuel consumption

Method Overview								
Discipline	Design Phase	Method Title	Categorization	Author				
Propulsion	Baseline Design	Turbofans, Turbojet, and Turboprop SFC variation	Empirical	Mattingly				
<p>Reference: Mattingly., "Aircraft Engine Design," 2nd Edition, AIAA Educational Series, American Institute of Aeronautics and Astronautics, Virginia, 2002</p>								
<p>Brief Description Statistical regressions for SFC values for High bypass turbofans, Low bypass turbofans, Turbojets and Turboprop engines</p>								
<p>Assumptions Based propulsions systems circa 2002 to 2010</p>		<p>Applicability Current Turbofan, Turbojet and Turboprop propulsion systems (ADD MACH LIMITS)</p>						
Execution of Method								
<p>Input Type of propulsion system, relative bypass ratio, temperature ratio at a given altitude and Mach</p>								
<p>Analysis description</p> <table border="0" style="width: 100%;"> <tr> <td style="width: 50%; vertical-align: top;"> <p><u>High bypass Turbofan</u></p> $SFC = (0.45 + 0.54M_0)\sqrt{\theta}$ <p><u>Low bypass Turbofan</u></p> $SFC = (0.9 + 0.30M_0)\sqrt{\theta} \text{ mil power}$ $SFC = (1.6 + 0.27M_0)\sqrt{\theta} \text{ max power}$ </td> <td style="width: 50%; vertical-align: top;"> <p><u>Turbojet</u></p> $SFC = (1.1 + 0.30M_0)\sqrt{\theta} \text{ mil power}$ $SFC = (1.5 + 0.23M_0)\sqrt{\theta} \text{ max power}$ </td> </tr> <tr> <td style="width: 50%; vertical-align: top;"> <p><u>Turbofan</u></p> $SFC = (0.18 + 0.8M)\sqrt{\theta}$ </td> <td style="width: 50%; vertical-align: top;"> <p><u>Turbojet</u></p> $SFC = (0.18 + 0.8M)\sqrt{\theta}$ </td> </tr> </table>					<p><u>High bypass Turbofan</u></p> $SFC = (0.45 + 0.54M_0)\sqrt{\theta}$ <p><u>Low bypass Turbofan</u></p> $SFC = (0.9 + 0.30M_0)\sqrt{\theta} \text{ mil power}$ $SFC = (1.6 + 0.27M_0)\sqrt{\theta} \text{ max power}$	<p><u>Turbojet</u></p> $SFC = (1.1 + 0.30M_0)\sqrt{\theta} \text{ mil power}$ $SFC = (1.5 + 0.23M_0)\sqrt{\theta} \text{ max power}$	<p><u>Turbofan</u></p> $SFC = (0.18 + 0.8M)\sqrt{\theta}$	<p><u>Turbojet</u></p> $SFC = (0.18 + 0.8M)\sqrt{\theta}$
<p><u>High bypass Turbofan</u></p> $SFC = (0.45 + 0.54M_0)\sqrt{\theta}$ <p><u>Low bypass Turbofan</u></p> $SFC = (0.9 + 0.30M_0)\sqrt{\theta} \text{ mil power}$ $SFC = (1.6 + 0.27M_0)\sqrt{\theta} \text{ max power}$	<p><u>Turbojet</u></p> $SFC = (1.1 + 0.30M_0)\sqrt{\theta} \text{ mil power}$ $SFC = (1.5 + 0.23M_0)\sqrt{\theta} \text{ max power}$							
<p><u>Turbofan</u></p> $SFC = (0.18 + 0.8M)\sqrt{\theta}$	<p><u>Turbojet</u></p> $SFC = (0.18 + 0.8M)\sqrt{\theta}$							
<p>Output: SFC</p>								
Experience								
<p>Accuracy Works well for propulsion systems which fit nicely into these categories. Poor accuracy for medium bypass engines</p>		<p>Time to Calculate</p>	<p>General Comments Typically used for guidance when it is not yet known what type of propulsion system is required</p>					

Thrust variation

Method Overview				
Discipline	Design Phase	Method Title	Categorization	Author
Propulsion	Baseline Design	Turbofans, Turbojet, and Turboprop SFC variation	Empirical	Mattingly
<p>Reference: Mattingly, J., "Aircraft Engine Design," 2nd Edition, AIAA Educational Series, American Institute of Aeronautics and Astronautics, Virginia, 2002</p>				
<p>Brief Description</p> <p>Statistical regressions for thrust variation for High bypass turbofans, Low bypass turbofans, Turbojets and Turboprop engines</p>				
<p>Assumptions</p> <p>Based propulsions systems circa 2002 to 2010</p>		<p>Applicability</p> <p>Current Turbofan, Turbojet and Turboprop propulsion systems</p>		
Execution of Method				
<p>Input</p> <p>Type of propulsion system, relative bypass ratio, temperature and pressure ratio at a given altitude and Mach, throttle ratio</p>				
<p>Analysis description</p> <p>Select propulsion system, throttle ratio</p> <p>Use the appropriate statistical regression (See further description for more detail)</p>				
<p>Output:</p> $\frac{T}{T_{SL}}$				
Experience				
<p>Accuracy</p> <p>Works well for propulsion systems which fit nicely into these categories. Poor accuracy for medium bypass engines</p>		<p>Time to Calculate</p>	<p>General Comments</p> <p>Typically used for guidance when it is not yet known what type of propulsion system is required. Installation losses included</p>	

Further Description

These regressions are based on total temperature and pressure which are defined as,

$$\theta_0 = \frac{T_t}{T_{std}} = \theta \left(1 + \frac{\gamma-1}{2} M_0^2 \right)$$

$$\delta_0 = \frac{P_t}{P_{std}} = \delta \left(1 + \frac{\gamma-1}{2} M_0^2 \right)^{\frac{\gamma}{\gamma-1}}$$

High Bypass ratio Turbofan ($M_0 < 0.9$)

$$\theta_0 \leq TR, \frac{T}{T_{SL}} = \delta_0 \left(1 - 0.49\sqrt{M_0} \right)$$

$$\theta_0 > TR, \frac{T}{T_{SL}} = \delta_0 \left(1 - 0.49\sqrt{M_0} - \frac{3(\theta_0 - TR)}{1.5 + M_0} \right)$$

Low Bypass ratio Turbofan (Max power)

$$\theta_0 \leq TR, \frac{T}{T_{SL}} = \delta_0$$

$$\theta_0 > TR, \frac{T}{T_{SL}} = \delta_0 \left(1 - \frac{3.5(\theta_0 - TR)}{\theta_0} \right)$$

Turbojet (Max power)

$$\theta_0 \leq TR, \frac{T}{T_{SL}} = \delta_0 \left(1 - 0.3(\theta_0 - 1) - 0.1\sqrt{M_0} \right)$$

$$\theta_0 > TR, \frac{T}{T_{SL}} = \delta_0 \left(1 - 0.3(\theta_0 - 1) - 0.1\sqrt{M_0} - \frac{1.5(\theta_0 - TR)}{\theta_0} \right)$$

Turboprop

$$M_0 \leq 0.1 \quad \frac{T}{T_{SL}} = \delta_0$$

$$\theta_0 \leq TR, \frac{T}{T_{SL}} = \delta_0 \left(1 - 0.96(M_0 - 1)^{0.25} \right)$$

$$\theta_0 > TR, \frac{T}{T_{SL}} = \delta_0 \left(1 - 0.96(M_0 - 1)^{0.25} - \frac{3(\theta_0 - TR)}{8.13(M_0 - 0.1)} \right)$$

Low Bypass ratio Turbofan (Military power)

$$\theta_0 \leq TR, \frac{T}{T_{SL}} = 0.6\delta_0$$

$$\theta_0 > TR, \frac{T}{T_{SL}} = 0.6\delta_0 \left(1 - \frac{3.8(\theta_0 - TR)}{\theta_0} \right)$$

Turbojet (Military power)

$$\theta_0 \leq TR, \frac{T}{T_{SL}} = 0.8\delta_0 \left(1 - 0.16\sqrt{M_0} \right)$$

$$\theta_0 > TR, \frac{T}{T_{SL}} = 0.8\delta_0 \left(1 - 0.16\sqrt{M_0} - \frac{24(\theta_0 - TR)}{(9 + M_0)\theta_0} \right)$$

The throttle ratio TR defines the point at which the engine switches from operating at maximum compressor pressure ratio (π_c) to that of maximum turbine inlet temperature (T_{t4}).

Guidance TR: Early commercial and military aircraft use a $TR = 1$ which yields operating at both the maximum π_c and T_{t4} . Due to special requirements on more recent aircraft, such as supercruise ($TR = 1.151$), have required a deviation from this trend and thus operating at either maximum π_c or T_{t4} but never both. ***Typically a $TR = 1$ will suffice unless higher thrust is required at low altitudes and high mach numbers***

Propulsion system sizing

Method Overview				
Discipline	Design Phase	Method Title	Categorization	Author
Propulsion	Sizing	Turbofan engine preliminary design tool	Empirical	Svoboda
Reference: Svoboda, C., "Turbofan engine database as a preliminary design tool," Aircraft Design 3, Pergamon, 2000				
Brief Description Statistical regression for turbofan weight, dimensions and performance				
Assumptions Based on data for high-bypass ratio engines			Applicability High-bypass > 3 Turbofan engines	
Execution of Method				
Input Take-off thrust				
Analysis description $W_{dry}(lbs) = 250 + 0.175T_{to}(lbs)$ $L_{eng}(in) = 40 + 0.59\sqrt{T_{to}}(lbs)$ $D_{fan}(in) = 2 + 0.39\sqrt{T_{to}}(lbs)$ $D_{nac}(in) = 5 + 0.39\sqrt{T_{to}}(lbs)$ $T_{cr}(lbs) = 200 + 0.2T_{to}(lbs)$ $\alpha(-) = 3.2 + 0.01\sqrt{T_{to}}(lbs)$		Analysis description $P_{tot}(-) = 200 + 0.2T_{to}(lbs)$ $SFC_{TO}(lb / lbs / hr) = 0.49 - 0.0007\sqrt{T_{to}}(lbs)$ $SFC_{cr}(lb / lbs / hr) = 0.8 - 0.00096\sqrt{T_{to}}(lbs)$ $SFC_{TO}(lb / lbs / hr) = 0.71 - 0.15\sqrt{\alpha}$		
Output: $W_{dry}, L_{eng}, D_{fan}, D_{nac}, T_{cr}, \alpha, P_{tot}, SFC_{TO}, SFC_{CR}$				
Experience				
Accuracy Appears to work for the Citation X, However, the AE3007 is in the statistical database. See reference for accuracy of specific regressions		Time to Calculate Quick	General Comments See reference for accuracy of specific regressions	

PERFORMANCE

Stall

Method Overview				
Discipline	Design Phase	Method Title	Categorization	Author
Performance Matching	Baseline Design	Stall Speed Representation	Semi-Empirical	Roskam
<p>Reference: Roskam, J., "Airplane Design Part I: Preliminary Sizing of Airplanes," DARcorporation, Lawrence, Kansas, 2003</p>				
<p>Brief Description Given a design stall speed and various values of C_{Lmax}, the W/S requirements are calculated</p>				
<p>Assumptions C_{Lmax} is assumed based on type of aircraft and</p>		<p>Applicability Homebuilt aircraft propeller aircraft, single engine propeller aircraft, twin engine propeller aircraft, agricultural aircraft, business jets, regional turboprop aircraft, transport jets, military trainers, fighters, military patrol, bomb and transport, flying boats, supersonic cruise aircraft</p>		
Execution of Method				
<p>Input VS, CLmax,</p>				
<p>Analysis description $W / S = 1 / 2 \rho V_S^2 C_{Lmax}$</p>				
<p>Output: W/S</p>				
Experience				
<p>Accuracy Unknown</p>		<p>Time to Calculate Unknown</p>	<p>General Comments Stall and landing approach may impose similar constraints</p>	

Landing Distance

Method Overview				
Discipline	Design Phase	Method Title	Categorization	Author
Performance Matching	Sizing	Landing Distance Representation for FAR 25 aircraft	Semi-Empirical	Roskam
Reference: Roskam, J., "Airplane Design Part I: Preliminary Sizing of Airplanes," DARcorporation, Lawrence, Kansas, 2003				
Brief Description Given a landing field length and the approach speed is calculated using empirical data and the stall speed representation is used to compute the wing loading requirement with $C_{LMAX(Landing)}$				
Assumptions FAR 25 regulations used		Applicability FAR 25 business jets, regional turboprop aircraft, transport jets		
Execution of Method				
Input $C_{Lmax(Landing)}$, S_{FL}				
Analysis description $V_A = \sqrt{\frac{S_{FL}}{0.3}}$ $V_s = V_A/1.3$ $(W/S)_L = 1/2\rho V_s^2 C_{Lmax(landing)}$				
Output: W/S , V_A				
Experience				
Accuracy Accuracy based on past aircraft. Approximation only		Time to Calculate N/A	General Comments Based upon trend data. Integrated into AVDsizing PM_MD1_LAND.F90	

Take-off Distance

Method Overview				
Discipline	Design Phase	Method Title	Categorization	Author
Performance Matching	Sizing	Take-off Distance Representation for FAR 25 aircraft	Semi-Empirical	Roskam
<p>Reference: Roskam, J., "Airplane Design Part I: Preliminary Sizing of Airplanes," DARcorporation, Lawrence, Kansas, 2003</p>				
<p>Brief Description Given a take-off field length and various values of C_{Lmax}, the W/S requirements are calculated</p>				
<p>Assumptions FAR 25 regulations used</p>		<p>Applicability business jets, regional turboprop aircraft, transport jets</p>		
Execution of Method				
<p>Input Range of W/S, $C_{Lmax(TO)}$, S_{TOFL}</p>				
<p>Analysis description $T/W = \frac{37.5(W/S)}{\sigma C_{Lmax} S_{TOFL}} \text{ (add STOFL)}$</p>				
<p>Output: T/W=f(W/S)</p>				
Experience				
<p>Accuracy Accuracy based on past aircraft. Approximation only</p>		<p>Time to Calculate Unknown</p>	<p>General Comments Based upon trend data. Be sure the aircraft in question is to comply with FAR 25</p>	

Climb gradient requirement

Method Overview				
Discipline	Design Phase	Method Title	Categorization	Author
Performance Matching	Sizing	Climb performance matching for FAR 25 aircraft	Empirical	Loftin
<p>Reference: Loftin, L., "Subsonic Aircraft: Evolution and the Matching of Sizing to Performance," NASA RP1060, 1980</p>				
<p>Brief Description</p> <p>Climb requirements are calculated for take-off and balked landing. From basic drag polar estimations and given FAR 25 OEI climb gradient requirements, T/W is computed.</p>				
<p>Assumptions</p> <p>FAR 25 regulations used</p>		<p>Applicability</p> <p>Subsonic transonic aircraft</p>		
Execution of Method				
<p>Input</p> <p>Drag Polar and C_L for each condition, FAR climb gradient requirements (CGR), and</p>				
<p>Analysis description</p> <p>Compute L/D for each requirement</p> $L/D = \left(\frac{C_L}{C_{D0} + \Delta C_{Df} + \Delta C_{Ds} + \Delta C_{Dg} + \frac{C_L^2}{\pi AR \cdot e}} \right)$ <p>For each FAR 25 requirement compute</p> $T/W = \left(\frac{N}{N-1} \right) \left(\frac{1}{L/D} + CGR \right) \text{ for OEI and } T/W = \left(\frac{1}{L/D} + CGR \right) \text{ for AEI}$				
<p>Output:</p> <p>T/W for each requirement</p>				
Experience				
<p>Accuracy</p> <p>Accuracy based on drag polar accuracy</p>		<p>Time to Calculate</p> <p>Unknown</p>	<p>General Comments</p> <p>Loftin has a representation for rate of climb requirements under FAR 23 type aircraft</p>	

Method Overview				
Discipline Performance Matching	Design Phase Sizing	Method Title Take-off and Climb performance matching for FAR 25 aircraft	Categorization Semi-empirical	Author Coleman
Reference: Current Document..				
Brief Description Linking of take-off and climb performance matching through the required lift coefficient. Modification of the Loftin's Method which solves for W/S and T/W as a function of CL.				
Assumptions FAR 25 regulations used. Trim drag neglected		Applicability Subsonic transonic aircraft		
Execution of Method				
Input Drag Polar, FAR climb gradient requirements (CGR), T/TSL, take-off field length S_{TO} , altitude of runway.				
Analysis description Compute density ratio at altitude σ Compute take-off parameter (TOP) $TOP = \frac{37.5(W/S)_{TO}}{\sigma S_{TO}}$ Compute second segment climb lift coefficient $C_{L2} = \frac{-CGR + \sqrt{CGR^2 - 4 * L' \left(C_{D0} - \frac{N-1}{N} \frac{TOP}{1.44} \right)}}{2L'}$ Compute T/W required to satisfy Take-off and Second segment climb criterion $(T/W)_{TO} = \frac{T}{T_{SL}} \frac{N}{N-1} \left[\frac{1}{L/D} + CGR \right] \quad L/D = \frac{C_{L2}}{C_{D0} + L' C_{L2}^2} \quad C_{LTO} = 1.44 C_{L2}$				
Output: T/W during take-off at sea-level				
Experience				
Accuracy Accuracy based aerodynamic and propulsion methods.		Time to Calculate Unknown	General Comments This method computes the lift coefficient required for these mission requirements. Thus eliminated the need for an initial estimate of C_{LTO}	

Design cruise

Method Overview				
Discipline	Design Phase	Method Title	Categorization	Author
Performance Matching	Sizing	Cruise Matching	Analytic	Coleman/Loftin
<p>Reference: (Modified from) Loftin, L., "Subsonic Aircraft: Evolution and the Matching of Sizing to Performance," NASA RP1060, 1980</p>				
<p>Brief Description</p> <p>T/W=f(W/S) derived from the drag polar at the cruise flight condition. The altitude is also found for which allows the aircraft to fly at a specific location on the drag polar (Vihn). Modified from Loftin's Cruise Matching approach</p>				
<p>Assumptions</p> <p>Standard Atmosphere</p>		<p>Applicability</p> <p>Subsonic transonic aircraft</p>		
Execution of Method				
<p>Input</p> <p>M_c, m, Range of wing loadings</p>				
<p>Analysis description</p> <p>Match initial cruise altitude to required trim L/D from the aerodynamic L/D method from Vihn and the trim method from Coleman, for a given wing loading W/S by solving the follow expression for pressure. Use standard atmosphere tables for altitude.</p> $C_{L(L/D_{trim})} = \sqrt{\frac{m}{m-1}} \sqrt{\frac{C_{D0}}{L'}}, \quad L/D_{trim} = \frac{C_{L(L/D_{trim})}}{C_{D0} + L'_w C_{L_w}^2 + L'_h C_{L_h}^2}$ $W/S = C_{L(L/D_{trim})} M^2 \frac{q}{M^2} = C_{L(L/D_{trim})} M^2 \frac{\gamma}{2} p$ <p>At that altitude obtain T_c/T_{SL} from propulsion model</p> <p>Calculate $T/W = \frac{1}{(T_c/T_{SL})(L/D)_{max}}$</p> <p>Repeat for each W/S</p>				
<p>Output:</p> <p>(T/W)=f(W/S)</p>				
Experience				
<p>Accuracy</p> <p>Accuracy based on drag polar and propulsion model accuracy</p>		<p>Time to Calculate</p> <p>Unknown</p>	<p>General Comments</p> <p>Must use of design performance to make sure the match point is applicable across the flight envelope</p>	

Time to climb

Method Overview				
Discipline	Design Phase	Method Title	Categorization	Author
Performance Matching	Sizing	Climb requirements for jet powered aircraft	Semi-Empirical	Roskam/Coleman
<p>Reference: Roskam, J., "Airplane Design Part I: Preliminary Sizing of Airplanes," DARcorporation, Lawrence, Kansas, 2003</p>				
<p>Brief Description</p> <p>T/W as a function of W/S and initial climb speed and cruise altitude. Initial climb speed and cruise altitude are solved for iteratively during performance matching.</p>				
<p>Assumptions</p> <p>Linear relationship between rate of climb and altitude.</p> <p>Maximum rate of climb occurs at L/Dmax for shallow climbs</p>		<p>Applicability</p> <p>Any jet powered aircraft, can be used for climb to cruise altitude.</p>		
Execution of Method				
<p>Input</p> <p>Drag polar at climb speed and average altitude, T_0/T_{SL}, fuel fraction for take-off, start-up and taxi, time to climb to cruise altitude</p>				
<p>Analysis description</p> <p>Compute initial rate of climb required</p> $RC_0 = \frac{h_{max}}{t_c} \ln \left[\left(1 - \frac{h_{cruise}}{h_{max}} \right)^{-1} \right]$ <p>From initial climb speed compute L/D_{max} and velocity at L/D_{max}</p> $(T/W)_{TO} = \frac{W}{W_{TO}} \frac{T}{T_{SL}} \left[\frac{RC_0}{V_0} - \frac{1}{L/D} \right] \quad L/D = \frac{1}{2} \sqrt{\frac{1}{L' C_{D0}}} \quad V_0 = \sqrt{\frac{2(W/S)_{climb}}{\rho \sqrt{C_{D0}/L'}}$ <p>Iterate initial climb speed in with initial climb speed out until convergence</p>				
<p>Output:</p> <p>T/W</p>				
Experience				
<p>Accuracy</p> <p>Accuracy based on drag polar accuracy</p>		<p>Time to Calculate</p> <p>Unknown</p>	<p>General Comments</p> <p>V_0 must be iterated for the drag polar. If C_{D0} is assumed invariant with velocity then no iteration is required.</p>	

Descent performance

Method Overview				
Discipline	Design Phase	Method Title	Categorization	Author
Performance Matching	Sizing	Compute the range and time to descent	Semi-Empirical	Roskam
<p>Reference: Roskam, J., "Airplane Design Part VII: Determination of Stability, Control and Performance Characterizes: FAR and Military Requirements," DARcorporation, Lawrence, Kansas, 2003</p>				
<p>Brief Description</p> <p>Assume power reduced to flight idle (power off) the flight path angle, rate of descent range covered and time of descent from cruise altitude is computed.</p>				
<p>Assumptions</p> <p>Power off, descent at maximum L/D</p> <p>Maximum rate of climb occurs at L/Dmax for shallow climbs</p>			<p>Applicability</p> <p>Any aircraft</p>	
Execution of Method				
<p>Input</p> <p>Cruise altitude, Drag polar at initial decent altitude, wing loading</p>				
<p>Analysis description</p> <p>Compute descent angle</p> $\gamma = \tan^{-1}\left(-\frac{1}{L/D_{\max}}\right)$ <p>Rate of descent can be derived from the equations as</p> $RD = \sqrt{\frac{2(W/S)}{\rho} \left(\frac{C_D}{C_L}\right)^{2/3} \cos^3 \gamma}$ <p>Assuming descent at constant L/D the glide range and time in the air are</p> $R_{GL} = -h / \tan \gamma, t_{GL} = -h / RD$				
<p>Output:</p> <p>$\gamma, RD, R_{GL}, t_{GL}$</p>				
Experience				
<p>Accuracy</p>		<p>Time to Calculate</p> <p>Unknown</p>	<p>General Comments</p> <p>Used for an approximation of range and time of descent.</p>	

Maximum velocity

Method Overview				
Discipline	Design Phase	Method Title	Categorization	Author
Performance Matching	Baseline Design	Maximum velocity constraint for jet powered aircraft	Semi-Empirical	Roskam
<p>Reference: Roskam, J., "Airplane Design Part I: Preliminary Sizing of Airplanes," DARcorporation, Lawrence, Kansas, 2003</p>				
<p>Brief Description T/W requirement for a given wing loading and time to climb</p>				
<p>Assumptions</p>		<p>Applicability Any jet powered aircraft</p>		
Execution of Method				
<p>Input Drag polar at cruise, cruise altitude, velocity, ratio of maximum cruise speed weight to take-off weight (k), T_0/T_{SL}</p>				
<p>Analysis description</p> $\frac{T}{W} = C_{D_o} q \frac{1}{W/S} + \frac{(W/S)}{\pi AR q e}$ <p>Normalize to take-off weight and thrust</p> $(W/S)_{TO} = k(W/S)_C$ $(T/W)_{TO} = \left(\frac{T}{W}\right)_0 \frac{T_{SL}}{T_0} k$				
<p>Output: T/W=f(W/S) for maximum cruise speed</p>				
Experience				
<p>Accuracy Accuracy based on drag polar accuracy</p>		<p>Time to Calculate Unknown</p>	<p>General Comments Roskam has a representation for rate of climb requirements under FAR 23 type aircraft</p>	

Ceiling

Method Overview				
Discipline	Design Phase	Method Title	Categorization	Author
Performance Matching	Sizing	Ceiling requirements for jet powered aircraft	Semi-Empirical	Roskam
<p>Reference: Roskam, J., "Airplane Design Part I: Preliminary Sizing of Airplanes," DARcorporation, Lawrence, Kansas, 2003</p>				
<p>Brief Description</p> <p>T/W as a function of W/S and initial climb speed and cruise altitude. Initial climb speed and cruise altitude are solved for iteratively during performance matching.</p>				
<p>Assumptions</p> <p>Linear relationship between rate of climb and altitude.</p> <p>Maximum rate of climb occurs at L/Dmax for shallow climbs</p>		<p>Applicability</p> <p>Any jet powered aircraft, can be used for climb to cruise altitude.</p>		
Execution of Method				
<p>Input</p> <p>Drag polar at climb speed and average altitude, T_0/T_{SL}, fuel fraction for take-off, start-up and taxi, time to climb to cruise altitude, Rate of climb required at service ceiling.</p>				
<p>Analysis description</p> <p>Compute initial rate of climb required</p> <p>Based on CLmax compute velocity, and L/D at required service ceiling</p> $(T/W)_{TO} = \frac{W}{W_{TO}} \frac{T}{T_{SL}} \left[\frac{RC_{ceiling}}{V_0} - \frac{1}{L/D} \right] \quad L/D = \frac{1}{2} \sqrt{\frac{1}{L' C_{D_0}}} \quad V_{ceiling} = \sqrt{\frac{2(W/S)_{ceiling}}{\rho \sqrt{C_{D_0}} / L'}}$				
<p>Output:</p> <p>T/W</p>				
Experience				
<p>Accuracy</p> <p>Accuracy based on drag polar accuracy</p>		<p>Time to Calculate</p> <p>Unknown</p>	<p>General Comments</p> <p>Not generally a significant performance constraint for transports..</p>	

Fuel weight estimation/Trajectory

Method Overview				
Discipline	Design Phase	Method Title	Categorization	Author
Performance	Baseline Design	Initial fuel weight estimation	Semi-Empirical	Roskam
<p>Reference: Roskam, J., "Airplane Design Part I: Preliminary Sizing of Airplanes," DARcorporation, Lawrence, Kansas, 2003</p>				
<p>Brief Description</p> <p>Fuel fractions are calculated for each mission segment based on typical values or from the Breguet range and endurance equations with assumed L/D and SFC. This fuel fractions are then multiplied to give the total mission fuel fraction.</p>				
<p>Assumptions</p> <p>Assumed fuel fractions for warm-up, taxi, take-off, descent and landing. Climb, cruise and loiter from Breguet</p>		<p>Applicability</p> <p>Homebuilt aircraft propeller aircraft, single engine propeller aircraft, twin engine propeller aircraft, agricultural aircraft, business jets, regional turboprop aircraft, transport jets, military trainers, fighters, military patrol, bomb and transport, flying boats, supersonic cruise aircraft</p>		
Execution of Method				
<p>Input</p> <p>Type of aircraft, L/D, SFC, Range, time to climb, loiter time or range.</p>				
<p>Analysis description</p> <p>Assume values of fuel fractions for warm-up, taxi, take-off, descent and landing from Table 2.1</p> <p>Compute fuel fractions for climb, cruise and loiter from</p> $R = \frac{V_c}{SFC} \frac{1}{L/D} \ln\left(\frac{W_i}{W_f}\right) \text{ and } E = \frac{1}{SFC} \frac{1}{L/D} \ln\left(\frac{W_i}{W_f}\right)$ <p>Multiple fuel fractions together to get the total fuel fraction.</p> <p>Multiply total fuel fraction by take-off weight to get fuel weight.. Break climb and cruise into several small increments to increase accuracy.</p>				
<p>Output:</p> <p>T/W=f(W/S) for maximum cruise speed</p>				
Experience				
<p>Accuracy</p> <p>Accuracy based on drag polar and propulsion SFC accuracy</p>		<p>Time to Calculate</p> <p>Unknown</p>	<p>General Comments</p> <p>Roskam has a representation for rate of climb requirements under FAR 23 type aircraft</p>	

STABILITY AND CONTROL

Trim

Method Overview				
Discipline	Design Phase	Method Title	Categorization	Author
Performance Matching	Baseline Design	Approximate Trim Solution	Semi-Empirical	Coleman/ Torenbeek
Reference:				
Brief Description Simplified 2-D (Lift and pitching moment) trim solution to compute the corresponding basic (untrimmed aircraft) lift and the longitudinal control effectors (<i>LoCE</i>) lift contributions. Both are used in the appropriate drag polar				
Assumptions Tail aft configuration or flying wing		Applicability Symmetric aircraft with 1 or 2 horizontal lifting surfaces (TAC, FWC)		
Execution of Method				
Input $C_{L_{total}}$ required, SM, l/c , $C_{m_{ac}}$				
Analysis description $C_{L_{basic}}$ as a Given $C_{L_{LoCE}} = \frac{(C_{m_{ac}})_{wb} - C_{L_{total}} \frac{(x_{cg} - x_{ac})_{wb}}{\bar{c}}}{\frac{S_h}{S} \eta \frac{(x_{cg} - x_{ac})_{wb}}{\bar{c}} - V_h \eta}$ $C_{L_{wb}} = C_{L_{total}} - C_{L_{LoCE}} \frac{S_h}{S} \eta$				
Output: $C_{L_{total}}$, $C_{L_{basic}}$, $C_{L_{LoCE}}$, L/D				
Experience				
Accuracy Uncertain. Use only for showing relative effects of changing static margin.		Time to Calculate	General Comments This method shows small effects of trim on L/D for long coupled TAC. Reduce l/c to for close coupled configuration	

Method Overview				
Discipline Performance Matching	Design Phase Baseline Design	Method Title Approximate Trim Solution	Categorization Semi-Empirical	Author Hoak/ Torenbeek
<p>Reference: Hoak, D., Fink, R., "USAF Stability and Control DATCOM," Global Engineering Documents, CA, 1978</p> <p>Torenbeek, E., "Synthesis of Subsonic Airplane Design," Delft University Press, London, 1982</p>				
<p>Brief Description</p> <p>A combination of DATCOM and Torenbeek methods for estimating both the zero lift pitching moment and distance from the c.g. to the wing body aerodynamic center. For use with the <i>Approximate Trim Solution Method</i>.</p>				
Assumptions Tail aft configuration or flying wing		Applicability Symmetric aircraft with 1 or 2 horizontal lifting surfaces (TAC, FWC)		
Execution of Method				
Input				
<p>Analysis description</p> <p>Compute wing pitching moment about its aerodynamics center</p> <p>Adjust the pitching moment due to fuselage effects</p> <p>Compute the distance from the c.g. to the aerodynamic center</p>				
<p>Output:</p> <p>$C_{L_{total}}, C_{L_{basic}}, C_{L_{LoCE}}, L/D$</p>				
Experience				
Accuracy Uncertain. Use only for showing relative effects of changing static margin.		Time to Calculate	General Comments This method shows small effects of trim on L/D for long coupled TAC. Reduce l/c to for close coupled configuration	

Further Description

For a wing body combination the pitching moment about the wing body aerodynamic center can be written as,

$$(C_{mac})_{wb} = (C_{mac})_w + (C_{mac})_{fuse}$$

For strait tapered wings the pitching moment coefficient can be approximated by (DATCOM),

$$(C_{mac})_w = \frac{AR \cos^2 \Lambda_{c/4}}{AR + 2 \cos \Lambda_{c/4}} c_{m0} \left(\frac{C_{mac}}{C_{mac} M=0} \right) + \frac{\Delta C_M}{\Delta \theta}$$

Where, $\left(\frac{C_{mac}}{C_{mac} M=0} \right)$ from Figure 4.1.4.1-6
 $\frac{\Delta C_M}{\Delta \theta}$ from Figure 4.1.4.1-5

The fuselage effect can be estimated from (Torenbeek, based on Munk)

$$(C_{mac})_f = -1.8 \left(1 - \frac{2.5b_f}{l_f} \right) \frac{\pi b_f l_f}{4S\bar{c}} \frac{(C_{L0})_{wb@ \alpha_f=0.0}}{(C_{L\alpha})_{wb}}$$

The distance from the c.g. to the aerodynamic center can be written as

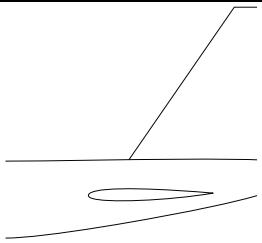
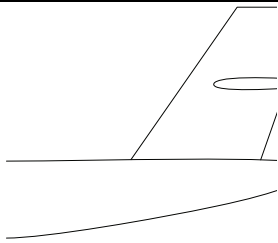
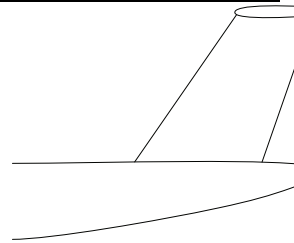
$$\frac{(x_{cg} - x_{ac})_{wb}}{\bar{c}} = SM + \frac{C_{LLoCE\alpha}}{C_{Lwb\alpha}} \left(1 - \frac{d\varepsilon}{d\alpha} \right) V_h \eta_h$$

Where the downwash gradient can be approximated by

$$\frac{d\varepsilon}{d\alpha} = \frac{C_{Lw\alpha}}{\pi AR (\lambda r)^{0.25} (1 - |m|)}$$

Where $r = \frac{2l_h}{b_w}$ and $m = \frac{2h_h}{b_w}$. The dynamic pressure ratio (η) and tail high constant (m) can be select according to Table 3.?

Table below: Guidance for dynamic pressure ratio and tail high constant based on H-T

location			
			
	0.85	0.95	1.0
	0.0	0.5	0.25

WEIGHT AND BALANCE

Structural Loads

Method Overview				
Discipline	Design Phase	Method Title	Categorization	Author
Structural Load estimation	Sizing Design	V-N diagram and structural limits for FAR 25 aircraft	Semi-Empirical	Roskam
Reference: Roskam, J., "Airplane Design Part V: Component Weight Estimation," DARcorporation, Lawrence, Kansas, 2003				
Brief Description Construction of the maneuvering and guest V-N diagram based on design trend for FAR 25 commercial transports.				
Assumptions		Applicability		
		FAR 25 aircraft		
Execution of Method				
Input CLmax, w/s, maneuvering altitudes				
Analysis description Compute maneuvering and guest load factor limit lines Compute maneuvering and guest design velocities Construct V-N maneuvering and guest diagrams				
Output: V-N maneuvering and guest diagrams, design load factor and velocity limits				
Experience				
Accuracy		Time to Calculate	General Comments	
		Unknown	Required data for both weight estimation and cost regressions	

Further Description

For FAR 25 aircraft the positive and negative limited load factors can be approximated from Equations 5.1 to 5.4

Maneuvering limits

$$n_{\lim_{pos}} = 2.1 + \frac{24,000 \text{ lbs}}{TOGW + 10,000 \text{ lbs}}, \quad 2.5 \leq n_{\lim_{pos}} \leq 3.8$$

$$n_{\lim_{neg}} = \begin{cases} -1 & V_C \geq V \\ \text{Varies linearly to 0 at } V_D & V_C < V \leq V_D \end{cases}$$

Gust limits

$$n_{\lim} = 1 \pm \frac{K_g U_{de} V C_{L\alpha}}{498(W/S)}$$

$$\text{Where, } K_g = \frac{0.88 \mu_g}{5.3 + \mu_g}$$

$$\mu_g = \frac{2(W/S)}{\rho \bar{c} g C_{L\alpha}}$$

The derived guest velocity (U_{de}) depends on the gust limit line as follows (Equations 5.5 to 5.7)

V_B Gust Line

$$U_{de} = \begin{cases} 66 \text{ ft/s} & h \leq 20,000 \text{ ft} \\ 84.67 - 0.000933h & 20,000 \text{ ft} < h \leq 50,000 \text{ ft} \end{cases}$$

V_C Gust Line

$$U_{de} = \begin{cases} 50 \text{ ft/s} & h \leq 20,000 \text{ ft} \\ 66.67 - 0.000833h & 20,000 \text{ ft} < h \leq 50,000 \text{ ft} \end{cases}$$

V_D Gust Line

$$U_{de} = \begin{cases} 25 \text{ ft/s} & h \leq 20,000 \text{ ft} \\ 33.34 - 0.000417h & 20,000 \text{ ft} < h \leq 50,000 \text{ ft} \end{cases}$$

Design gust velocities

The design speed for maximum gust intensity (V_B) corresponds between the intersection of the V_B gust line and the maximum normal force curve.

The 1-g stall speed can be expressed as (Equation 5.8)

$$V_{S1} = \sqrt{\frac{2(W/S)}{\rho C_{N_{\max}}}}$$

For load factors greater than 1 (Equation 5.9)

$$V = V_{S1} n^{1/2}$$

Equating Equation 5.9 to the positive V_B gust line yields an expression for V_B (Equation 5.10)

$$V_B = \frac{KV_{S1}^2 + V_{S1}\sqrt{K+4}}{2}$$

Where, $K = \frac{K_g U_{de} C_{L\alpha}}{498(W/S)}$ from the gust load factor equation

The cruise velocity (V_C) is the greater of design cruise velocity or $V_C = V_B + 43kts$

The design dive speed (V_D) can be determined from either Equation 5.11 or 5.12

$$V_D = 1.25V_C$$

$$M_D = 1.25M_C$$

The design gust speed VG, VF and VE are determined from the negatives of the VB, VC and VD gust lines respectively. Note, for VG use the maximum negative normal force

Design maneuvering velocities

The design maneuvering speed (V_A) can be found from Equation 5.9 where the maximum normal force curve meets the maximum maneuvering load factor

With these points and lines the following V-N Maneuver and Gust diagrams can be constructed

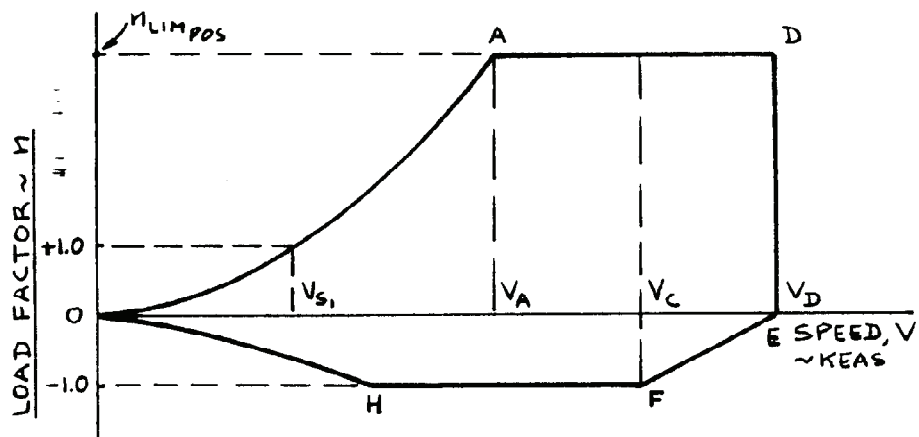
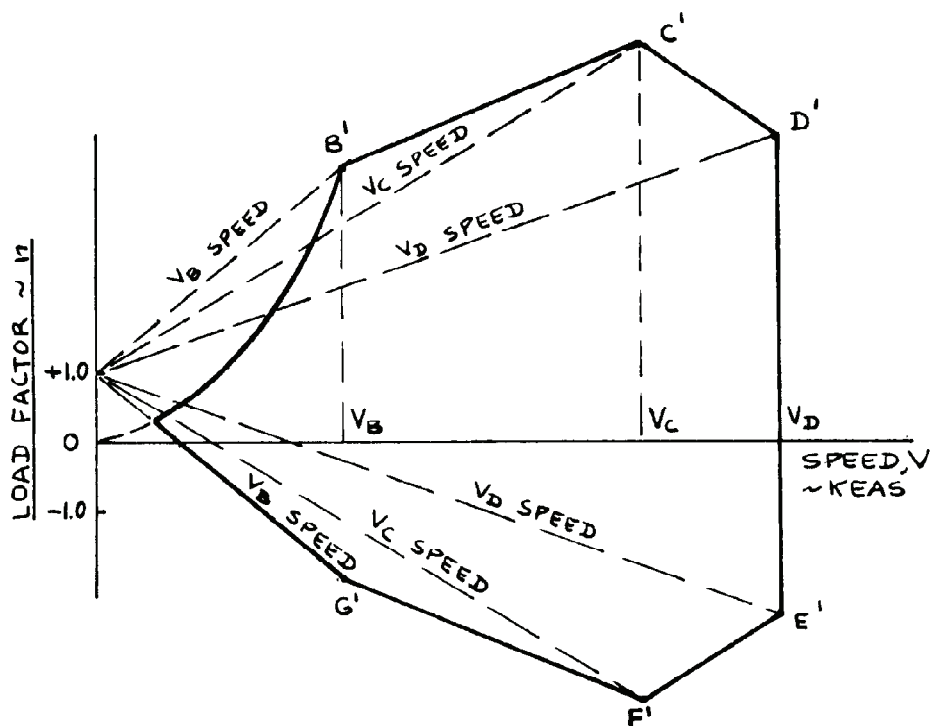


Figure 4.2a V-n Maneuver Diagram According to FAR 25



Empty Weight and Volume Formulation

Method Overview				
Discipline	Design Phase	Method Title	Categorization	Author
Weight Estimation	Parametric Sizing	Convergence Empty weight estimation	Empirical	Coleman/ Czysz
Reference: Dissertation				
Brief Description A modification of the hypersonic convergence method for estimating the converged empty weight based on volume and mass. This method has been modified to allow for the incorporation of additional methods for structural, propulsion, systems and operational item weights beyond what are presented in hypersonic convergence				
Assumptions Wing area is not constant		Applicability Any aircraft our launcher configuration. Applicability depends on the methods used for the structural, propulsion and systems weight		
Execution of Method				
Input $WR, T/W,$				
Analysis description Solve the below system for S_{pln} and OEW Weight Budget: $OEW = \frac{W_{str} + W_{sys} + W_{oper} + (T/W)_{max} WR / E_{TW} (W_{pay} + W_{crew})}{\frac{1}{1+\mu_a} - f_{sys} - (T/W)_{max} WR / E_{TW}}$ Volume Budget: $OEW = \frac{\tau \cdot S_{pln}^{1.5} (1 - k_{vw} - k_{vs}) - V_{fix} - V_{pay} - V_{crew}}{\frac{WR-1}{\rho_{fuel}} + k_{ve} (T/W)_{max} WR}$ Use the additional methods for W_{str} , W_{sys} , W_{oper} and ETW				
Output: OEW, TOGW, OWE, S_{pln}				
Experience				
Accuracy Depends upon additional methods		Time to Calculate Unknown	General Comments Works well for any configuration. Is at the heart of AVDsizing. The convergence logic will take the output and feed it back through the geometry trajectory and constraints until convergence	

Structural weight

Method Overview				
Discipline	Design Phase	Method Title	Categorization	Author
Weight Estimation	Sizing	Wing Structure Group Weight Fraction Method	Empirical	Nicolai
Reference: Nicolai, Leland. "Fundamentals of Aircraft Design," METS Inc., San Jose, CA, 2008.				
Brief Description Estimation of structural weight fraction in terms of ultimate load factor, wing dimensions, and Max Take-off Gross Weight, Max Zero Fuel Weight,				
Assumptions Includes the weight of leading edge slats, flower/single slotted flaps & ailerons. Valid for Mo range of 0.4 to 0.8, t/c range of 0.08 to 0.15 and aspect ratio AR range of 4 to 12. Valid for metallic materials		Applicability Commercial Transport		
Execution of Method				
Input S_w, M_o (max Mach), $W_{TO}, n_{ult}, \Lambda_{1/2}, t/c_{avg}$,				
Analysis description				
$W_w/S_w = 0.00428 \frac{AR^{1.0} M_o^{0.43} \lambda^{0.14} (W_{TO} n_{ult})^{0.84}}{(100 * t/c)_{avg}^{0.76} \cos^{1.54}(\Lambda_{1/2}) S_w^{0.52}}$				
Assume 20% reduction for composite materials				
Output: W_w/S_w (lb/ft ²)				
Experience				
Accuracy Unknown.		Time to Calculate Unknown	General Comments Roskam attributes this method to GD. Input by A. Walker	

Method Overview				
Discipline Weight Estimation	Design Phase Sizing	Method Title Fuselage mass estimation	Categorization Empirical	Author Howe
Reference: Howe, D., "Aircraft Conceptual Design Synthesis," Professional Engineering Publishing Limited, UK, 2000				
Brief Description Fuselage mass based on basic geometry and structural constraints				
Assumptions			Applicability See recommended mass coefficients	
Execution of Method				
Input For Pressurized transport fuselage: p, B, L, h, C_2 , For other aircraft: C_2, V_D, L, B, H				
Analysis description Pressurized transport fuselage $M_{fuselage} = C_2 p (9.75 + 5.84B) \left(\frac{2L}{b+H} - 1.5 \right) (b+h)^2 \quad [\text{kg}]$ Other fuselage $M_{fuselage} = C_2 [L(B+H)V_D^{0.5}]^{1.5} \quad [\text{kg}]$				
Output: $M_{fuselage}$				
Experience				
Accuracy Unknown. Has worked well for the Citation X	Time to Calculate Unknown	General Comments Use typical values for ultimate load factor and dive speed. Use a %15 correction factor for composite materials.		

Method Overview				
Discipline	Design Phase	Method Title	Categorization	Author
Weight Estimation	Sizing	Tail Structure Group Weight Fraction Method	Empirical	Torenbeek
Reference: Torenbeek, E. "Synthesis of subsonic airplane design," Delft University Press, Rotterdam, 1976.				
Brief Description Estimation of structural weight fraction in terms of ultimate load factor, wing dimensions, and Gross Weight.				
Assumptions If tailplane area not yet known, tail weight is assumed between 3.5% and 4.0% of empty weight.			Applicability Turbine-powered Transport	
Execution of Method				
Input k_{tail} , S_{tail} , Λ_{tail} , V_D , tail dimensions				
Analysis description				
$W_{HT}/S_{HT} = k_{HT} \left\{ 3.81 \left[\frac{S_{HT}^{0.2} V_D}{1000 \left(\cos \Lambda_{\frac{1}{2}HT} \right)^{0.5}} \right] - 0.287 \right\}$			$k_{HT} = 1.0$ for fixed stabilizer $= 1.1$ for variable-incidence tails; add 8% for a bullet of appreciable size	
$W_{VT}/S_{VT} = k_{VT} \left\{ 3.81 \left[\frac{S_{VT}^{0.2} V_D}{1000 \left(\cos \Lambda_{\frac{1}{2}VT} \right)^{0.5}} \right] - 0.287 \right\}$			$k_{VT} = 1.0$ for fuselage-mounted horizontal tailplanes $= 1 + 0.15 \left(\frac{S_{HT} h_{HT}}{S_{VT} b_{VT}} \right)$ for fin-mounted stabilizers (e.g. T-Tail)	
Use Figure 8-5, Normalized specific horizontal tailplane weight, to iterate upon correlated values of $\frac{W_{tail}}{k_{tail} S_{tail}}$ and $\frac{S_{tail}^2 V_D / 1000}{\sqrt{\cos \Lambda_{tail}}}$				
Output: Horizontal and Vertical Tail Loading (wt/area)				
Experience				
Accuracy Unknown.		Time to Calculate Unknown	General Comments For transport category aircraft and executive jets the Design Dive speed V_D has dominant effect on tail weight. Input by A. Walker	

Method Overview				
Discipline Weight Estimation	Design Phase Parametric Sizing	Method Title Raymer cargo/transport aircraft Nacelle Weight Method	Categorization Empirical	Author Roskam
Reference: Raymer, P., Aircraft Design: A Conceptual Approach," 4 th Edition, AIAA Education Series, American Institute of Aeronautics and Astronautics, Reston, VA, 2006				
Brief Description Empirical weight estimation for turbojet and turbofan engines				
Assumptions Unknown		Applicability Cargo/Transport aircraft		
Execution of Method				
Input $K_{ng}, N_{Lt}, N_w, N_z, W_{ec}, N_{en}, S_n$				
Analysis description $W_n = 0.6724 K_{ng} N_{Lt}^{0.10} N_w^{0.294} N_z^{0.119} W_{ec}^{0.611} N_{en}^{0.984} S_n^{0.224}$ [lbs]				
Output: W_n				
Experience				
Accuracy Unknown. Appears to have worked well for commercial transports ranging from the Embraer 170 to the A380.		Time to Calculate Unknown	General Comments	

Further Description

K_{ng} = 1.017 for pylon mounted engines
= 1.0 otherwise

N_{Lt} = Nacelle Length (ft)

N_w = Nacelle width (ft)

N_Z = Ultimate load factor

W_{ec} = Weight of engines and contents (lbs)

N_{en} = Number of engines

S_n = Nacelle wetted area (ft²)

Method Overview				
Discipline Weight Estimation	Design Phase Parametric Sizing	Method Title Torenbeek commercial transport landing gear weight	Categorization Empirical	Author Roskam
Reference: Torenbeek, E. <i>Synthesis of Subsonic Airplane Design</i> . Boston : Delft University, 1982.				
Brief Description Empirical landing gear weight estimation for transport type aircraft				
Assumptions Tricycle landing gear		Applicability Cargo/Transport aircraft Jet trainers Business Jets		
Execution of Method				
Input $W_{TO}, K_{gr}, A_g, B_g, C_g, D_g$				
Analysis description $W_g = K_{gr} \left(A_g + B_g \cdot W_{TO}^{3/4} + C_g \cdot W_{TO} + D_g \cdot W_{TO}^{3/2} \right) \quad [\text{lbs}]$				
Output: W_g				
Experience				
Accuracy Unknown. Appears to have worked well for commercial transports ranging from the Embraer 170 to the A380.		Time to Calculate Unknown	General Comments	

Further Description

$K_{gr} = 1.0$ for low wing aircraft

= 1.08 for high wing aircraft

Empirical Constants

Aircraft Type	Gear Type	Gear Component	A_g	B_g	C_g	D_g
Jet trainers & Business Jets	Retractable	Main	3.0	0	0	0.
		Nose	2.0	0	0	0.
		Tail	1.0	0	0	0.
Other Civil Aircraft	Fixed	Main	0.0	0	0	0.
		Nose	5.0	0	0	0.
		Tail	1.0	0	0	0.
	Retractable	Main	0.0	0	0	1.
		Nose	0.0	0	0	2.
		Tail	1.0	0	0	0.

Propulsion system weight

Method Overview				
Discipline	Design Phase	Method Title	Categorization	Author
Weight Estimation	Sizing	Power plant mass estimation	Empirical	Howe
Reference: Howe, D., "Aircraft Conceptual Design Synthesis," Professional Engineering Publishing Limited, UK, 2000				
Brief Description Correction factor to dry propulsion system weight for installation (nacelles, pods, cowlings, propeller, etc.)				
Assumptions			Applicability See recommended mass coefficients	
Execution of Method				
Input M_{ENG}, C_3				
Analysis description $M_{POWERPLANT} = C_3 M_{ENG}$ [kg]				
Type of Aircraft		C_3		
Executive jets and jet transports		1.56		
Supersonic aircraft with variable geometry intakes		2.0		
Turboprop transports		2.25		
Propeller turbine trainers		2.0		
General aviation, twin piston-engine types		1.80		
All other types		1.40		
Output: $M_{POWERPLANT}$				
Experience				
Accuracy		Time to Calculate	General Comments	
Unknown. Has worked well for the Citation X		Unknown		

Further Description

The mass of the engine should be taken from actual engine data. If data is not available the following T/W of typical engines may be used in the sizing process (Table 5.4).

Table: 5.4: Guidelines for typical engine thrust to weight ratio's Fuselage Weight

Estimation (Howe)

Turbojet / Turbofan engines	T/W_{ENG}
Military combat engines	
Basic dry thrust rating	4.5 – 6.5
With typical afterburner	7 – 9
With provision for vectoring nozzles, etc.	4 – 6
Civil transport engines (usually high bypass ratio turbofans)	
Sea level static rating	5.0 – 6.5
Propeller driven propulsion	$(P/W_{ENG}$
	[kW/N]
Advanced turboprop engines, including gear box	0.34 – 0.42
Turboshaft engines, with gear box	0.5 – 0.8
Piston engines	0.034
no supercharger, power < 150 kw	0.057(1+
	0.006kw)
no supercharger, Power > 150	0.12
Supercharged, Power > 150 kw	0.1
Small rotary engines	0.135

Fixed equipment weight

Method Overview				
Discipline	Design Phase	Method Title	Categorization	Author
Weight Estimation	Sizing	Refined Hydraulic and/or Pneumatic Group Weight Method	Empirical	Roskam
Reference: Roskam, J., "Airplane Design Part V: Component Weight Estimation," DARcorporation, Lawrence, Kansas, 2003				
Brief Description Estimation of Hydraulic sys weight in terms of gross-take-off weight.				
Assumptions Weight of hydraulics usually included in the flight controls group		Applicability Commercial Transport		
Execution of Method				
Input W_{TO}				
Analysis description				
Aircraft Type		W_{hyd}/W_{TO}		
Business Jets		0.0070 – 0.0150		
Regional turboprops		0.0060 – 0.0120		
Commercial Transports		0.0060 – 0.0120		
Military Patrol, transport, bombers		0.0060 – 0.0120		
Fighter, Attack		0.0050 – 0.0180		
Output: Hydraulic System Group weight (lb)				
Experience				
Accuracy Based on 1980s data		Time to Calculate short	General Comments Input by A. Walker	

Method Overview				
Discipline Weight Estimation	Design Phase Sizing	Method Title Refined Instrumentation Group Weight Method	Categorization Empirical	Author Torenbeek
Reference: Roskam, J., "Airplane Design Part V: Component Weight Estimation," DARcorporation, Lawrence, Kansas, 2003				
Brief Description Estimation of instrumentation, aviations and electrical n weight in terms of number of engines, pilots, pax, take-off weight, empty weight.				
Assumptions			Applicability Multiple aircraft	
Execution of Method				
Input $W_{TO}, W_E, R, N_{pil}, N_e$				
Analysis description				
Speed Range	Aircraft Type	Equation		
General Aviation	Single Engine Prop	$W_{instr} = 33N_{pax} \text{ [lb]}$		
	Multi-Engine Prop	$W_{instr} = 40 + 0.008W_{TO} \text{ [lb]}$		
Commercial Transport	Regional turboprops	$W_{instr} = 120 + 20N_e + 0.006W_{TO} \text{ [lb]}$		
	Jet Transports	$W_{instr} = 0.575W_E^{0.556}R^{0.25} \text{ [lb]}$		
Output: Hydraulic System Group weight (lb)				
Experience				
Accuracy Based on 1980s data		Time to Calculate short	General Comments Input by A. Walker	

Method Overview				
Discipline Weight Estimation	Design Phase Sizing	Method Title APU weight Method	Categorization Empirical	Author Roskam
Reference: Roskam, J., "Airplane Design Part V: Component Weight Estimation," DARcorporation, Lawrence, Kansas, 2003				
Brief Description Typical weight fraction values for APU weight. General approximation only				
Assumptions			Applicability Transport and patrol type aircraft. Both Civil and Military	
Execution of Method				
Input W_{TO}				
Analysis description $W_{apu} = K_{apu} W_{TO}$ Where, $K_{apu} = 0.004 - 0.013$				
Output: W_{apu}				
Experience				
Accuracy		Time to Calculate	General Comments General approximation only, more thorough analysis of the electrical needs of the aircraft is required.	

Method Overview				
Discipline	Design Phase	Method Title	Categorization	Author
Weight Estimation	Sizing	Furnishings weight Method	Empirical	Torenbeek
Reference: Roskam, J., "Airplane Design Part V: Component Weight Estimation," DARcorporation, Lawrence, Kansas, 2003				
Brief Description Furnishing weight based on correlation with maximum zero fuel weight				
Assumptions		Applicability Commercial transports		
Execution of Method				
Input W_{TO}, W_f				
Analysis description $W_{fur} = 0.211(W_{TO} - W_f)$				
Output: $W_{fur} = 0.211$				
Experience				
Accuracy General results only		Time to Calculate	General Comments This method is primary applicable for initial studies only, more refined method required for c.g. estimation.	

Method Overview				
Discipline	Design Phase	Method Title	Categorization	Author
Weight Estimation	Sizing	Baggage handling equipment weight Method	Empirical	Roskam
<p>Reference: Roskam, J., "Airplane Design Part V: Component Weight Estimation," DARcorporation, Lawrence, Kansas, 2003</p>				
<p>Brief Description Empirical correlation for baggage and cargo handling equipment for use in military and commercial freighters.</p>				
Assumptions			Applicability	
			Military and Commercial transports	
Execution of Method				
Input				
<p>Analysis description For Military Transports the General Dynamics method is suggested, $W_{bc} = K_{bc} (N_{pax})^{1.456}$ Where $K_{bc} = 0.0646$ without preload provisions $= 0.316$ with preload provisions</p> <p>For commercial transports the Torenbeek method is suggested $W_{bc} = 3S_{ff}$ where S_{ff} is the freight flow area in ft^2</p> <p>For baggage and cargo containers, $W_{Containers} = 1.6 \cdot V_{caontainer s}$</p>				
Output:				
Experience				
Accuracy		Time to Calculate	General Comments	

Operational items weight

Method Overview				
Discipline	Design Phase	Method Title	Categorization	Author
Weight Estimation	Sizing	Operational items mass estimation	Empirical	Howe
Reference: Howe, D., "Aircraft Conceptual Design Synthesis," Professional Engineering Publishing Limited, UK, 2000				
Brief Description Mass estimation for operating items including crew personal items, safety equipment, freight equipment, water and food, residual fuel				
Assumptions			Applicability See recommended mass coefficients	
Execution of Method				
Input $N_{crew}, F_{op}, PAX, PAY$				
Analysis description <u>Passenger aircraft</u> $M_{op} = 85N_{crew} + F_{op}PAX$ [kg]				
Type of transport		C_4		
Short haul		7		
Medium range		12		
Very long range and executive		16		
<u>Freight aircraft</u> $M_{op} = 600 + 0.03PAY$ [kg]				
<u>Other types</u> 77 kg per person for light aircraft, 100 kg for combat				
Output: M_{sys}				
Experience				
Accuracy Unknown. Has worked well for the Citation X		Time to Calculate Unknown	General Comments	

COST

Life Cycle Cost Formulation

Method Overview				
Discipline	Design Phase	Method Title	Categorization	Author
Cost Estimation	Sizing, CE,	Life Cycle cost	Empirical	Roskam
Reference: Roskam, J., "Part VII: Airplane Cost Estimation: Design, Development, Manufacturing and Operation," DARcorporation, Kansas, 2003				
Brief Description Life Cycle cost is estimated from the summation of Research, Development, Testing and Engineering Cost (RDTE), Acquisition cost (ACQ), Operations Cost (OPS), and Disposal (DISP)				
Assumptions		Applicability		
		Commercial and Military Aircraft		
Execution of Method				
Input $C_{RDTE}, C_{ACQ}, C_{OPS}, C_{DISP}$				
Analysis description Estimate $C_{RDTE}, C_{ACQ}, C_{OPS}, C_{DISP}$ Life Cycle Cost (LCC) $LCC = C_{DRDTE} + C_{ACQ} + C_{OPS} + C_{DISP}$				
Output: LCC				
Experience				
Accuracy		Time to Calculate	General Comments	
		Unknown		

RDT&E estimation

Method Overview				
Discipline	Design Phase	Method Title	Categorization	Author
Cost Estimation	Sizing, CE,	RAND DAPCA IV RDT&E and Production Cost Model	Empirical	Hess
<p>Reference: Hess, R.W., Ronmanoff, H.P., "Aircraft Airframe Cost Estimating Relationships," Rand Corp., Rept. R-3255-AF, Santa Monica, CA, 1987.</p> <p>(VIA: Raymer, D., "Aircraft Design: A Conceptual Approach," Third Edition, AIAA Educational Series, 1999</p>				
<p>Brief Description</p> <p>DAPCA is comprised of Cost Estimating Relationships (CER's) for RDT&E and production broken down by, (1) Engineering, (2) tooling, (3) manufacturing, (4) quality control, (5) development support, (6) flight-testing and (7) manufacturing material costs. This model is a generic model, working reasonably well for most aircraft types. See Rand Corp for more mission specific models.</p>				
<p>Assumptions</p> <p>Based on data for n-stealth, non-composite fighters, trainers, transports and bombers.</p>		<p>Applicability</p> <p>DAPCA IV was developed from statistical data for non-stealth, non-composite fighters, trainers, transports and bombers; It does not handle most advanced designs well (approx 20-40% error). Over predicts commercial transports by approx 10%</p>		
Execution of Method				
<p>Input</p> <p>$TOGW, V_{max}, Q, FTA, N_{eng}, T_{max}, M_{max}, It4, C_{avionics}$</p>				
<p>Analysis description</p> <p>Estimate engineering, tooling, manufacturing, and quality control hours.</p> <p>Estimate hourly rates for engineering, tooling, manufacturing, and quality control hours.</p> <p>Estimate development support, flight testing manufacturing materials, engine production and avionics cost directly</p>				
<p>Output:</p> <p>RDT&E+flyaway costs, per unit costs</p>				
Experience				
<p>Accuracy</p> <p>Has worked, QST SSBJ and Dassault Tri-jet SSBJ.</p> <p>Typically, 20-40% error for advanced military aircraft and 10% error for commercial transports</p>		<p>Time to Calculate</p> <p>Unknown</p>	<p>General Comments</p> <p>Use for fighters/high-speed aircraft only</p>	

Further Description

Engineering (E), Tooling (T), Manufacturing (M) and quality control (QC) hours CER's

$$H_E = \begin{cases} 7.07(OWE)^{0.777} V_{\max}^{0.894} Q^{0.163} & lbs, ft / s \\ 7.53(OWE)^{0.777} V_{\max}^{0.894} Q^{0.163} & kgs, m / s \end{cases}$$

$$H_T = \begin{cases} 8.71(OWE)^{0.777} V_{\max}^{0.696} Q^{0.263} & lbs, ft / s \\ 10.5(OWE)^{0.777} V_{\max}^{0.696} Q^{0.263} & kgs, m / s \end{cases}$$

$$H_M = \begin{cases} 10.72(OWE)^{0.820} V_{\max}^{0.484} Q^{0.641} & lbs, ft / s \\ 15.20(OWE)^{0.820} V_{\max}^{0.484} Q^{0.641} & kgs, m / s \end{cases}$$

$$H_{QC} = \begin{cases} 0.076 & \text{Cargo} \\ 0.133 & \text{Other} \end{cases}$$

Table: 6.1: Hourly rates (R) for Engineering, Tools, Manufacturing and Quality Control

Hourly CER's	(1999 \$)/hr
Engineering	86.00
Tooling	88.00
Manufacturing	81.00
Quality Control	73.00

Development support (D), Flight Test (F), Manufacturing materials (MM), Engine production cost (ENG), avionics and interiors CER's (Equations 6.1.5 through 6.1.10)

$$C_D = \begin{cases} 66.0(OWE)^{0.630} V_{\max}^{1.3} & lbs, ft / s \\ 47.7(OWE)^{0.630} V_{\max}^{1.3} & kgs, m / s \end{cases}$$

$$C_F = \begin{cases} 1807.1(OWE)^{0.325} V_{\max}^{0.822} FTA^{1.21} & lbs, ft / s \\ 1408.0(OWE)^{0.325} V_{\max}^{0.822} FTA^{1.21} & kgs, m / s \end{cases}$$

$$C_M = \begin{cases} 16.0(OWE)^{0.921} V_{\max}^{0.621} Q^{0.799} & lbs, ft / s \\ 22.6(OWE)^{0.921} V_{\max}^{0.621} Q^{0.799} & kgs, m / s \end{cases}$$

$$C_E = \begin{cases} 2241.0[0.043T_{MAX} + 243.25M_{\max} + 0.969T_{t4} - 2228] & lbs, ft / s \\ 2251.0[9.660T_{MAX} + 243.25M_{\max} + 1.740T_{t4} - 2228] & kN, m / s \end{cases}$$

$$C_{avionics} = K_{avionics} OWE \quad \text{or} \quad = K_{RTD\&E+Flyaway} (RTD \& E + Flyaway)$$

$$C_{interiors} = \begin{cases} \$2,500 / Pax & \text{Long-haul transport} \\ \$1,250 / Pax & \text{Regional transport} \\ \$625 / Pax & \text{General aviation} \end{cases}$$

Combining yields the total estimate of RTD&E+Flyaway costs (Equation 6.11) where

$K_{avionics}$ and $K_{RTD\&E+Flyaway}$ can be estimated from Table 6.1.2

$$RTD \& E + Flyaway = H_E R_E + H_T R_T + H_M R_M + H_{QC} R_{QC} + C_D + C_F + C_M + QC_{ENG} N_{ENG} + C_{avionics} + C_{interiors}$$

Table: 6.1.2: Avionics constants

Avionics constants	
$K_{avionics}$	3,000 to 6000 \$/lbs (\$7 to \$ 13 \$/g) in 1999 dollars
$K_{RTD\&E+Flyaway}$	5 to 25 % of RTD&E+Flyaway costs depended on complexity

This model is based on the design and manufacturing of aluminum airframes. The following correction factors for design, tooling, manufacturing, and quality control are recommended for materials with more difficult design and fabrication (Table 6.1.3)

Table: 6.1.2: Material design and fabrication correction factors

Material	Correction factor
Aluminum	1.0
Graphite-epoxy	1.1 – 1.8
Fiberglass	1.1 – 1.2
Steel	1.5 – 2.0
Titanium	1.3 – 2.0

Manufacturing and acquisition

Method Overview				
Discipline	Design Phase	Method Title	Categorization	Author
Cost Estimation	Sizing, CE,	Method for estimating manufacturing and acquisition cost	Semi-Empirical	Roskam
<p>Reference: Roskam, J., "Part VII: Airplane Cost Estimation: Design, Development, Manufacturing and Operation," DARcorporation, Kansas, 2003</p>				
<p>Brief Description Build-up of manufacturing and acquisition costs</p>				
<p>Assumptions Based on data from military and commercial aircraft</p>		<p>Applicability Military and commercial aircraft, preliminary design purposes only</p>		
Execution of Method				
<p>Input</p>				
<p>Analysis description Estimate engineering, tooling, manufacturing, and quality control hours. $C_{ACQ} = C_{man} + C_{pro}$ Where manufacturing cost is broken down into $C_{man} = C_{aed_m} + C_{apc_m} + C_{fto_m} + C_{fin_m}$ See further description for more detail The unit price per aircraft can be computed from $AEP = C_{man} + C_{pro} + C_{RDTE} / N_m$ </p>				
<p>Output: C_{ACQ}, AEP</p>				
Experience				
<p>Accuracy</p>		<p>Time to Calculate Unknown</p>	<p>General Comments</p>	

Further Description

The following are suggested methods of estimating the manufacturing cost components

$$C_{man} = C_{aed_m} + C_{apc_m} + C_{fito_m} + C_{fin_m} \quad 6.2.4$$

Airframe engineering and design

$$C_{aed_m} = MHR_{aed_{prog}} R_{e_m} - C_{aed_r}$$

Where,

R_{e_m} = engineering man-hour rate per hour for entire aircraft program

$MHR_{aed_{prog}}$ = engineering man-hours the entire aircraft program

$$= 0.0396 W_{amp_r}^{0.791} V_{max}^{1.526} N_{program}^{0.183} F_{diff} F_{CAD}$$

$N_{program}$ = Number of aircraft built for entire program

Aircraft program production cost

$$C_{apc_m} = C_{E\&A_m} + C_{int_m} + C_{man_m} + C_{mat_m} + C_{qc_m}$$

Engine and avionics cost

$$C_{E\&A_m} = (C_e N_e + C_p N_p + C_{avionics}) N_m \quad 6.2.5$$

Where,

C_e = Cost per engine

N_e = number of engine per aircraft

C_p = Cost per propeller

N_p = number of propellers aircraft

$C_{avionics}$ = avionics cost per aircraft

N_m = number of aircraft manufacture

$$= N_{program} - N_r$$

Manufacturing cost

$$C_{man_m} = MHR_{man_{program}} R_{m_{program}} - C_{man_r} \quad 6.2.6$$

Where,

$R_{m_{program}}$ = manufacturing labor rate for program

R_{m_r} = manufacturing labor rate for RDTE

$$MHR_{man_{program}} = 28.984 W_{amp_r}^{0.740} V_{max}^{0.543} N_{program}^{0.524} F_{diff}$$

Manufacturing material cost

$$C_{mat_m} = 37.632 F_{mat} W_{amp_r}^{0.689} V_{max}^{0.624} N_{program}^{0.792} CEF - C_{mat_r} \quad 6.2.7$$

Where,

- F_{mat} = 1.0 for airframes made primarily of conventional aluminum alloys
= 1.5 for stainless steel airframes
= 2.0 – 2.5 for 'conventional' composite material, Li/Al, alloys or ARAL
= 3.0 for carbon composite aircraft

Tooling cost

$$C_{tool_r} = MHR_{tool\ program} R_{t_m} - C_{tool_r} \quad 6.2.8$$

Where,

- R_{t_m} = tooling labor rate per man hour
= 1.5 for stainless steel airframes
= 2.0 – 2.5 for 'conventional' composite material, Li/Al, alloys or ARAL
= 3.0 for carbon composite aircraft
- $MHR_{tool\ program}$ = $4.0127 W_{amp_r}^{0.764} V_{max}^{0.889} N_{rdie}^{0.178} N_{program}^{0.066} F_{diff}$
 N_r = RDTE production rate per month (typically 0.33)

Quality control cost

$$C_{qc_m} = 0.13 C_{man_m}$$

Production flight test operation cost

$$C_{fto_m} = N_m C_{ops/hr} T_{pft} F_{ftoh} \quad 6.2.6$$

Where,

- $C_{ops/hr}$ = operating cost per hour
- T_{pft} = Number of flight test hours flown by the manufacture before aircraft is delivered to customer
= 2 hrs for general aviation
= 10 hrs for jet transports
= 20 hrs for military aircraft
- F_{ftoh} = overhead factor associated with production flight test activates
= 4.0 (suggested value)

Manufacturing Finance cost

$$C_{fin_m} = F_{fin_m} C_{man} \quad 6.2.6$$

Where,

- F_{fin_m} = financing factor
= 0.1 to 0.2 depending on the interest rates which are available

Manufacturing Profit

$$C_{pro_m} = F_{pro} \cdot C_{man}$$

6.2.11

Where,

F_{pro}

= profit margin

= average 0.10, See Table 2.1 in Roskam

Direct Operating Cost

Method Overview				
Discipline	Design Phase	Method Title	Categorization	Author
Cost Estimation	Sizing, CE	Direct Operating Cost for Commercial Airplanes: DOC	Semi-Empirical	Roskam
<p>Reference: Roskam, "Airplane Design, Part VIII: Airplane Cost Estimation: Design, Development, Manufacturing and Operating", DARcorporation, Kansas, 2002</p>				
<p>Brief Description</p> <p>This method is an adaptation of ATA-method which decomposes direct operating cost into 5 components, (1) Flight, (2) Maintenance, (3) depreciation, (4) landing fees, navigation fees, registry taxes, and (5) financing direct operating costs.</p>				
Assumptions			Applicability	
			Commercial, corporate and private transports	
Execution of Method				
Input				
<p>Analysis description</p> $DOC = DOC_{flt} + DOC_{maint} + DOC_{depr} + DOC_{lnr} + DOC_{fin}$				
DOC component	Breakdown	DOC component	Breakdown	
Flying DOC_{flt}	Crew	Depreciation DOC_{depr}	Airframe	
	Fuel		Engine	
	Insurance		Prop(s)	
Maintenance DOC_{maint}	Airframe Labor		Avionics	
	Engine Labor		Airframe spare parts	
	Airframe material		Engine spare parts	
	Engine materials	Landing fees, Navigation fees/ Registry taxes DOC_{lnr}	Landing	
	Applied maintenance burden		Navigation	
		Finance DOC_{fin}	Registration	
			Finance	
Output:				
DOC				
Experience				

Accuracy	Time to Calculate	General Comments
Has worked well for the Citation X, QST SSBJ and Dassault Tri-jet SSBJ.	Unknown	DOC estimates at this design phase are for comparison purposes only, Depreciation table not applicable for business jets.

Further Description

Flying DOC

Flying DOC is estimated from the crew (C_{crew}), fuel and oil (C_{pol}) and airframe insurance (C_{ins}) direct operating costs (Equation 6.2.1)

$$DOC_{flt} = C_{crew} + C_{pol} + C_{ins}$$

Crew costs can be estimated from Equation 6.2.2. Where j indicates the crew member (1 = Captain, 2 = Co-pilot, 3 = Flight engineer, 4 = maintenance personal).

$$C_{crew} = \sum_{j=1}^{j=4} n_{c_j} \frac{1+k_j}{V_{bl}} \frac{SAL_j}{AH_j} + \frac{TEF_j}{V_{bl}}$$

Where,

- n_c = number of crew members
 - = 1 for scheduled block times < 10 hours
 - = 2 for scheduled block times > 10 hours
 - = 0 for personal aircraft
- k = factor accounting for vacation pay, training costs, crew premium, insurance and taxes
 - = 0.26 (typical value)
- V_{bl} = Block velocity
- SAL = crew member annual salary (see Table 6.2.1)
- AH = number of flight hours per year for flight crew
 - = 800 hrs for jet domestic flights
 - = 900 hrs for props domestic flights
 - = 750 hrs for jet international flights
 - = 850 hrs for prop international flights
- TEF = travel expense for each flight crew member
 - = 7.0 \$/block hour domestic flights (1989 dollars)
 - = 11.0 \$/block hour international flights (1989 dollars)

Table: 6.2.1: Annual Salaries by operators in 1989 dollars

Aircraft type	Captain	Co-pilot	Flight Engineer
Jet transport (BAC 111 – B747)	\$35,000 – \$144,000	\$24,000 – \$67,000	\$20,000 – \$62,000
Corporate jet transport (Learjet 23 – G III)	\$30,000 – \$72,000	\$22,000 – \$52,000	-
Corporate turboprop (MU-2 - King air 300)	\$25,000 – \$52,000	\$20,000 – \$32,000	-
Regional turboprop (DHC-6 - F-27)	\$20,000 – \$25,000	\$11,000 – \$21,000	-
Corporate Recipes (single – twin)	\$20,000 – \$47,000	\$19,000 – \$26,000	-
Cabin crew (all aircraft types)	\$19,000 - \$32,000		

To convert from 1989 dollars to then dollars use the following relationship (Equation 6.2.3)

$$COST_{Then\ year} = COST_{1989} \frac{CEF_{Then\ year}}{CEF_{1989}}$$

Where,

CEF = Cost escalation factor (use current data)

Fuel and oil costs can be estimated from equation 6.2.4.

$$C_{pol} = \frac{W_{bl}}{R_{bl}} \frac{FP}{FD} + \frac{W_{obl}}{R_{bl}} \frac{OLP}{OD}$$

Where,

W_{Fbl} = Block fuel weight, same as mission fuel

FP = Fuel price per gallon (use current data)

FD = Fuel density

W_{obl} = Block oil weight

= $W_{Fbl} / 70$ for reciprocating engines

= $0.70 n_{eng} t_{bl}$ for turbine engines

n_{eng} = number of engines
 t_{bl} = block time
 OP = Oil price per gallon (use current data)
 OD = Oil density

Table 6.2.2 shows the densities for aviation fuel, and oils

Table: 6.2.2: Aviation fuels and oil densities

Fuel	Density (lbs/US gallon)
Aviation Gasoline	
Grades 100/130	6.00
Grades 108/135	5.90
Grades 115/145	5.80
Petroleum	
JP-1	6.70
JP-2	6.65
JP-3	6.45
JP-4	6.55
JP-5	6.82
Jet A	6.74

Insurance cost can be estimated from equation 6.2.5.

$$C_{ins} = \frac{f_{ins_{hull}} AMP}{U_{ann_{bl}} V_{bl}}$$

Where,

$f_{ins_{hull}}$ = annual hull insurance rate in USD/USD aircraft price/aircraft/year
 = ranges from 0.005 to 0.030 USD/USD/aircraft/year
 AMP = aircraft market price
 $U_{ann_{bl}}$ = Annual block hour utilization
 V_{bl} = Block velocity

Or an alternative method can be utilized from Equation 6.2.6

$$C_{ins} = 0.02DOC$$

Maintenance DOC

Maintenance DOC is estimated from the airframe labor ($C_{lab/af}$), engine labor ($C_{lab/eng}$), airframe maintenance materials ($C_{mat/af}$), engine maintenance materials ($C_{mat/eng}$) and applied maintenance burden (Equation 6.2.7).

$$DOC_{maint} = C_{lab/af} + C_{lab/engl} + C_{mat/ap} + C_{mat/eng} + C_{amb}$$

Airframe labor cost can be estimated from Equation 6.2.8

$$C_{lab/af} = 1.03 \frac{MHR_{mapbl} R_{lap}}{V_{bl}}$$

Where,

MHR_{mapbl} = number of airframe and systems maintenance man hours need per block

$$= MHR_{mapflt} t_{flt} / t_{bl}$$

Lacking more precise data,

= $3.0 + 0.067 (OWE - n_{eng} W_{eng}) / 1000$ for turbine engine aircraft (weight in lbs)

= $1.7 + 0.067 (OWE - n_{eng} W_{eng}) / 1000$ for recip. enge aircraft (weight in lbs)

R_{lap} = aircraft maintence labor rate per man hour. (use current data)

Engine labor cost can be estimated from Equation 6.2.9

$$C_{lab/af} = 1.03 \frac{1.3 N_{eng} MHR_{mengbl} R_{1eng}}{V_{bl}}$$

Where,

MHR_{mengbl} = number of engine maintenance man hours need per block

$$= MHR_{mengflt} t_{flt} / t_{bl}$$

Lacking more precise data,

= $\left(0.718 + 0.0317 \frac{T_{to} / n_{eng}}{1,000} \right) \frac{1,100}{TBO} + 0.10$ for turbjet of turbofan engines

= $\left(0.4956 + 0.0532 \frac{SHP_{TO} / n_{eng}}{1,000} \right) \frac{1,100}{TBO} + 0.10$ for turboprop engines

= $\left(0.0765 \left(\frac{W_{eng}}{1,000} \right)^2 + 0.2495 \frac{W_{eng}}{1,000} \right) \frac{0.70}{TBO} + 0.30$ per reciprocating engine

R_{1eng} = engine maintence labor rate per man hour. (use current data)

TBO = Time between overalls (hrs)

Airframe maintenance materials cost can be estimated from Equation 6.2.10

$$C_{mat/af} = 1.03 \frac{C_{mat/apblhr}}{V_{bl}}$$

Where,

$C_{mat / apblhr}$ = airframe and systems maintenance materials cost per aircraft block hour in USD/hr

$$= 30.0 \frac{CEF_{\text{then year}}}{CEF_{1989}} ATF + 0.79 \times 10^{-5} AFP \quad \text{for turbine engine aircraft}$$

$$= 36.0 \frac{CEF_{\text{then year}}}{CEF_{1989}} ATF + 0.475 \times 10^{-5} AFP \quad \text{for recip. engine aircraft}$$

ATF = aircraft type factor
 = 1.0 for 10,000 < TOGW
 = 0.5 for 5,000 < TOGW < 10,000
 = 0.25 for TOGW < 5,000 lbs
 AFP = airframe price

Engine maintenance materials cost can be estimated from Equation 6.2.11

$$C_{mat / eng} = 1.03 \frac{1.3 n_{eng} C_{mat / engblhr}}{V_{bl}}$$

Where,

$C_{mat / engblhr}$ = Engine maintenance materials cost per aircraft block hour in USD/hr
 = $(5.43 \times 10^{-5} EP \cdot ESPPF - 0.47) / K_{Hem}$ for turbine engine aircraft
 = $(0.0004274 (EP/1,000)^2 + 0.08263 (EP/1,000)) (0.10 + 0.9 / K_{Hem})$ for recip. engine aircraft

engine aircraft

EP = Engine price
 $ESPPF$ = Engine spare parts price factor
 = 1.5 (typically)
 K_{Hem} = Time between overalls correction factor
 = $0.021(TBO/100) + 0.769$ for turbine engines
 = $0.076(TBO/100) + 0.164$ for recip. engines
 TBO = Time between overalls (hrs) (use current data)

Applied maintenance burned cost can be estimated from Equation 6.2.12

$$C_{amb} = \frac{1.03 \left[f_{amb / lab} \left(MHR_{mapbl} R_{1ap} + n_{eng} MHR_{engbl} R_{1eng} \right) + f_{amb / mat} \left(C_{mat / apblhr} + n_{eng} C_{mat / engblhr} \right) \right]}{V_{bl}}$$

Where,

$f_{amb / lab}$ = overhead distribution factor for labor, building, lighting, heating and administrative costs

$f_{amb/mat}$ = overhead distribution factor for materials, building, lighting, heating and administrative costs

Table 6.2.3 gives typical values for overhead distribution costs

Table: 6.2.3: Typical labor and materials overhead distribution factors

	Personal aircraft	Corporate	Commercial
f	0.80 – 0.90	0.90 – 1.00	1.00 – 1.40
$f_{amb/lab}$			
f	0.20 – 0.30	0.30 – 0.40	0.40 – 0.70
$f_{amb/mat}$			

Depreciation DOC

Depreciation DOC is estimated from the airframe depreciation (C_{dap}), engine depreciation (C_{deng}), propeller depreciation (C_{dpp}), avionics depreciation (C_{dav}), airframe spare parts depreciation (C_{dafsp}) and engine spare parts depreciation (C_{dengsp}). Equation 6.2.13

$$DOC_{maint} = C_{daf} + C_{deng} + C_{dpp} + C_{dav} + C_{dafsp} + C_{dengsp}$$

Airframe depreciation cost can be estimated from Equation 6.2.13

$$C_{daf} = \frac{F_{daf}(AFP - N_e EP - N_p PP - ASP)}{DP_{af} U_{annbl} V_{bl}}$$

Where,

- F_{daf} = airframe depreciation factor (Table 6.2.4)
- ASP** = avionics price
- PP** = propeller price
- N_p = number of propellers
- DP_{af} = airframe depreciation period (Table 6.2.4)

Engine depreciation cost can be estimated from Equation 6.2.14

$$C_{deng} = \frac{F_{deng} n_{eng} EP}{DP_{eng} U_{annbl} V_{bl}}$$

Where,

- F_{deng} = engine depreciation factor (Table 6.2.4)
- DP_{eng} = engine depreciation period (Table 6.2.4)

Propeller depreciation cost can be estimated from Equation 6.2.15

$$C_{dprop} = \frac{F_{dprop} n_p PP}{DP_{pp} U_{annbl} V_{bl}}$$

Where,

- F_{dprp} = propeller depreciation factor (Table 6.2.4)
- DP_{prp} = propeller depreciation period (Table 6.2.4)
- n_p = number of propellers

Avionics depreciation cost can be estimated from Equation 6.2.16

$$C_{dav} = \frac{F_{dav} ASP}{DP_{av} U_{anbl} V_{bl}}$$

Where,

- F_{dav} = avionics depreciation factor (Table 6.2.4)
- DP_{av} = avionics depreciation period (Table 6.2.4)

Airframe spare parts depreciation cost can be estimated from Equation 6.2.17

$$C_{dafsp} = \frac{F_{dafsp} F_{afsp} AFP}{DP_{afsp} U_{annbl} V_{bl}}$$

Where,

- F_{dafsp} = airframe spare parts depreciation factor (Table 6.2.4)
- F_{afsp} = airframe spare parts factor
- =0.10 (typical value)
- DP_{afsp} = airframe spare parts depreciation period (Table 6.2.4)

Engine spare parts depreciation cost can be estimated from Equation 6.2.18

$$C_{dengsp} = \frac{F_{daengsp} F_{engsp} n_{eng} EP \cdot ESPPF}{DP_{engsp} U_{annbl} V_{bl}}$$

Where,

- $F_{daengsp}$ = engine spare parts depreciation factor (Table 6.2.4)
- F_{engsp} = engine spare parts factor
- =0.50 (typical value)
- $ESPPF$ = engine spare parts price factor (Table 6.2.4)
- = 1.0 if all parts a purchased with engine
- = 1.5 otherwise (typical value)
- DP_{engsp} = engine spare parts depreciation period (Table 6.2.4)

Table: 6.2.4: Typical depreciation periods and factors

Item	Depreciation period <i>DP</i> (yrs)	Residual value (%)	Depreciation factor f_d
Airframe	10	15	0.85
Engines	7	15	0.85
Propellers	7	15	0.85
Avionics	5	0	1.00
Airplane spare parts	10	15	0.85
Engine spare parts	7	15	0.85

Landing fees, Navigation fees, and Registry taxes DOC

Landing fees (C_{lf}), Navigation (C_{nf}) and Registry taxes (C_{rt}) DOC is estimated from Equation 6.2.19

$$DOC_{lnr} = C_{lf} + C_{nf} + C_{rt}$$

Landing fees DOC can be estimated from Equation 6.2.20

$$C_{lf} = \frac{C_{aclf}}{t_{bl}V_{bl}}$$

Where,

C_{aclf} = airplane landing fee per landing

Lacking actual landing fee data
=0.002TOGW (USD/lbs) 1989 dollars

Or

$$C_{lf} = (0.036 + 4 \times 10^{-8} TOGW) DOC \text{ (TOGW in lbs)}$$

Navigation fees DOC can be estimated from Equation 6.2.21

$$C_{nf} = \frac{C_{acnf}}{t_{bl}V_{bl}}$$

Where,

C_{acnf} = airplane landing fee per flight

= 0.0 operations in the USA

=10.0 USD/flight operations outside the USA (1989 dollars)

Or

$$C_{lf} = (0.001 + 1 \times 10^{-8} TOGW) DOC \text{ (TOGW in lbs)}$$

Taxes DOC can be estimated from Equation 6.2.22

$$C_{rt} = f_{rt}DOC$$

Where,

f_{rt} = tax rate depends on aircraft size, state and country where the aircraft is registered

$$= 0.001 + TOGW10^{-8} \text{ lacking better information}$$

Financing DOC

If the designer wishes to include financing DOC the following rule of thumb is suggested

$$DOC_{fin} = 0.07DOC$$

Block Mission

Method Overview				
Discipline	Design Phase	Method Title	Categorization	Author
Cost Estimation	Sizing, CE	Block mission for commercial transport	Semi-Empirical	Roskam
Reference: Roskam, "Airplane Design, Part VIII: Airplane Cost Estimation: Design, Development, Manufacturing and Operating", DARcorporation, Kansas, 2002				
Brief Description This method estimates the block, range, speed and time for DOC computation purposes				
Assumptions		Applicability Commercial, corporate and private transports		
Execution of Method				
Input Block range R_{bl} , cruise speed V_{cr} , Take-off gross weight ($TOGW$)				
Analysis description				
Output: block velocity, block time, utilization flight and block hours				
Experience				
Accuracy		Time to Calculate Unknown	General Comments DOC	

Further Description

The average block velocity is defined as (Equation 6.3.1)

$$V_{bl} = \frac{R_{bl}}{t_{bl}}$$

Where, $t_{bl} = t_{gm} + t_{cl} + t_{cr} + t_{de}$

$$R_{bl} = R_{cr} + R_{cl} + R_{de} + R_{man}$$

Climb and descent (R_{cl} , t_{cl} and R_{de} , t_{de}) are determined from performance analysis. Time for ground maneuvering t_{gm} , (Equation 6.3.2) and range covered during air traffic control constraints can be determined by R_{man} (Equation 6.3.3)

$$t_{gm} = 0.51 \times 10^{-6} TOGW + 0.125 \text{ [hrs]} ,$$

$$R_{man} = V_{man} \cdot t_{man}$$

Where,

$$V_{man} = \begin{cases} 250 \text{ kts} & \text{below 10,000 ft} \\ V_{cr} & \text{above 10,000 ft} \end{cases}$$

$$t_{man} = 0.25 \times 10^{-6} TOGW + 0.0625$$

Solving for cruise time (t_{cr}) (Equation 6.3.6) and range (R_{cr}) (Equation 6.3.7)

$$t_{cr} = \begin{cases} (1.06R_{bl} - R_{cl} - R_{de} + R_{man})/V_{cr} & \text{Domestic operations} \\ (1.01R_{bl} - R_{cl} - R_{de} + R_{man})/V_{cr} & \text{International operations} \end{cases}$$

$$R_{cr} = V_{cr} \cdot t_{cr}$$

The average flight speed and time can be computed from the following (Equation 6.3.8 -6.3.9)

$$t_{flt} = t_{cl} + t_{cr} + t_{de}$$

$$V_{flt} = V_{cr} \frac{t_{cr}}{t_{flt}}$$

Annual utilization in block hours may be approximated by Equation 6.3.10 or from typical values given in Table 6.3.1

$$U_{annbl} = \begin{cases} 10^3 \left(3.4546t_{bl} + 2.994 - \sqrt{12.289t_{bl}^2 - 5.6626t_{bl} + 8.964} \right) & \text{Passenger transports} \\ 10^3 \left(6.053t_{bl} + 5.70 - \sqrt{37.771t_{bl}^2 - 13.494t_{bl} + 32.490} \right) & \text{Cargo transports} \end{cases}$$

Table: 6.3.1: Typical annual utilization block hours

Type of operation	Long haul $t_{bl} > 5$ hrs	Medium haul $2 < t_{bl} < 5$ hrs	Short haul $0.5 < t_{bl} < 2$ hrs
Jet transport	3,600 – 4,400	2,100 – 3,300	1,000 – 3,000
Regional transport	-	2,000 – 3,000	1,000 – 2,500
Corporate transport	500 – 1,500	400 – 1,200	300 – 1,000
Personal transport	-	200 - 800	200 – 800
Agricultural	-	-	500 – 1,000
Trainers	-	-	1,000 – 2,500

To express annual utilization in flight hours use the following conversion (Equation 6.3.11).

$$U_{ann, flt} = U_{ann, bl} \frac{V_{bl}}{V_{flt}}$$

B.2 BLENDED WING BODY CONFIGURATION TRANSPORT METHODS

GEOMETRY

Method Overview				
Discipline	Design Phase	Method Title	Categorization	Author
Geometry	Parametric sizing	Blended wing body parameterization	Analytical	Coleman
Reference: Dissertation				
Brief Description Derivation of the blended wing-body configuration's geometry, wetted area and volume for use in the AVDsizing logic. At the time when the geometry module uses the given planform area and Kuchemann's slenderness parameter to derive the remainder of the geometry of the current aircraft				
Assumptions 3 segmented wing Transonic operation.		Applicability Transonic Blended wing body configuration		
Execution of Method				
Input $S_{pln}, \tau, AR_{cab}, AR_o, \lambda_c, \lambda_b, \lambda_t, \eta_b, (t/c)_t, (x/c), h_{cab}$				
Analysis description Compute planform area's Compute span parameters Compute root chord length Compute cabin thickness ratio Iteratively solve for root cabin t/c to meet the required volume. If the root cabin height is smaller than the outboard cabin height set the root height to outboard and account the excess volume as void. The next iteration through the logic will account for the increase in void volume.				
Output: $S_{cab}, S_l, S_o, b_w, \eta_1, \eta_2, c_r, (t/c)_r, (t/c)_c$				
Experience				
Accuracy	Time to Calculate		General Comments	

Further Description

The flying wing configuration (FWC) or blended wing body (BWB) presents the challenge of combining the primary volume supply, lift supply and control into one lifting surface. The coupling of these surfaces requires the wing thickness to vary to meet current τ and planform values. As with tail aft aircraft the wing thickens is coupled to the wing sweep angle through critical Mach number effects. This creates an aircraft which is very geometrically responsive to changes in planform area and τ . The build up the analytic equations for the Blended Wing Body (BWB) is broken down into (1) inner wing planform, (2) outer wing planform and (3) total volume (below).

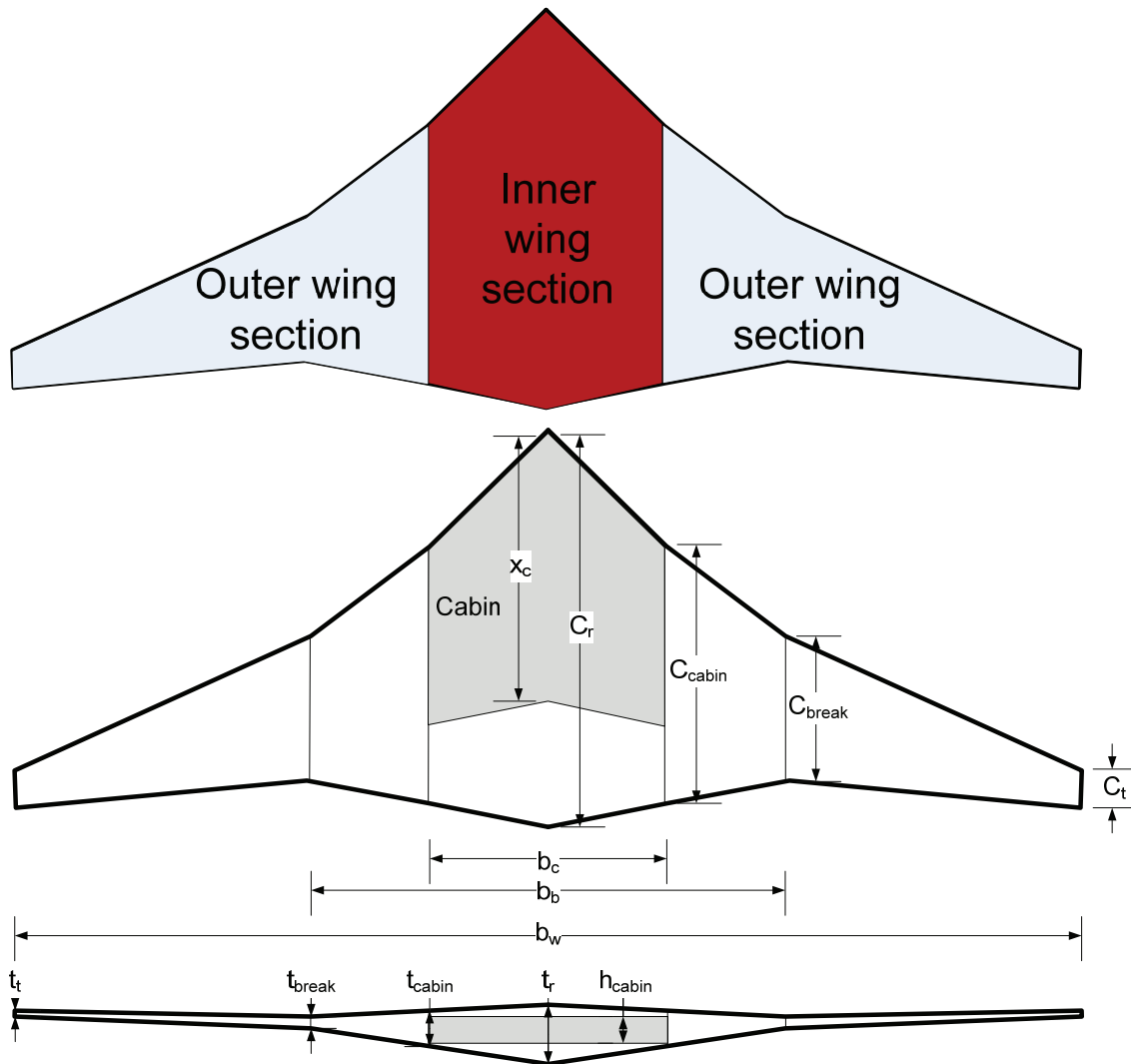


Fig: Definition of the planform of a generic blending wing body.

Definition of the inner wing planform

The inner wing planform consists of two parts, the cabin and aft section (above). The cabin presents the first constraints for the BWB in terms of (1) cabin height (2).cabin floor area and (3) cabin aspect ratio The cabin height requires that the outboard section of the cabin must be sufficiently thick to accommodate the required cabin height. This constraint does not explicitly apply to the root where the airfoil thickness could be higher than required for cabin

height. In the AVD^{sizing} process the required passenger volume is known and thus by specifying cabin height the cabin floor area is known. The cabin aspect ratio controls the shape of the cabin floor for passenger cabin evacuation. If the cabin aspect ratio is too low a sufficient number exits will not be possible out the side of the aircraft in case of an emergency. Leibeck⁽²⁷⁾ states, as a rule of thumb, that the cabin aspect ratio should be greater than 4.0 for proper cabin evacuation. This provides 3 geometric relationships. (below).

Cabin height $t_c = h_{cab} \Rightarrow \left(\frac{t}{c}\right)_c = \frac{h_{cab}}{c_r \lambda_c} \cdot (h_{cab}/t_c)_{req}$ 5.7

Cabin floor $S_{cab} = V_{pax} / h_{cab}$ 5.8

Cabin Aspect ratio $AR_{cab} = \frac{b_c^2}{S_{cab}} \Rightarrow b_c = \sqrt{AR_{cab} S_{cab}}$ 5.9

The final piece required to define the cabin section is the percent of the chord to which the cabin occupies (x/c). With chord occupation of the cabin defined the cabin area plus the aft body area (S_I) and wing area can be defined as shown in Figure below.

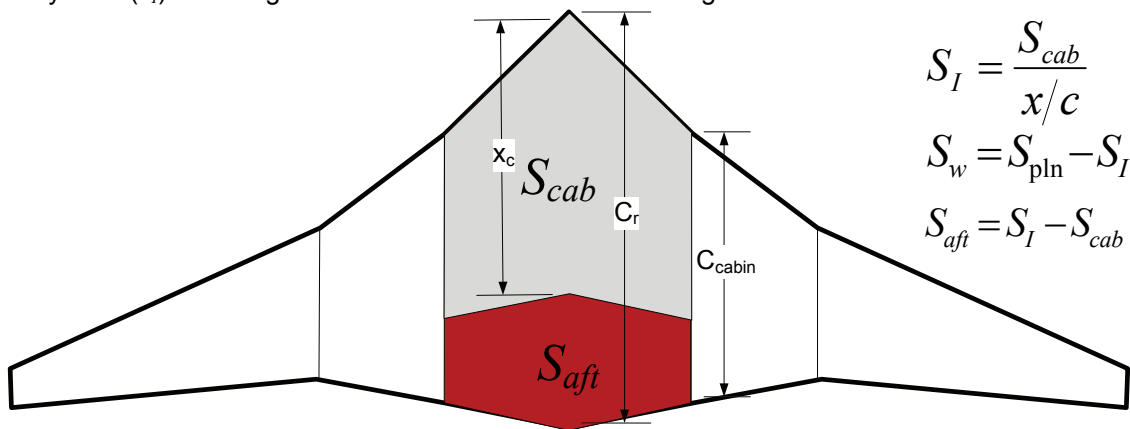


Fig Wing area breakdown for the BWB.

In summary the cab and aft section of the BWB are controlled by with the height cabin (h_{cab}), the cabin chord wise occupation (x/c) and cabin aspect ratio (AR_{cab}).

Definition of wing section planform

To define the wing planform a new variable is introduces η_b which is defined along with the outer wing taper ratios relative to the chord length at the edge of the cabin (Figure below).

This is done to allow for typical taper ratios of transonic transport wings.

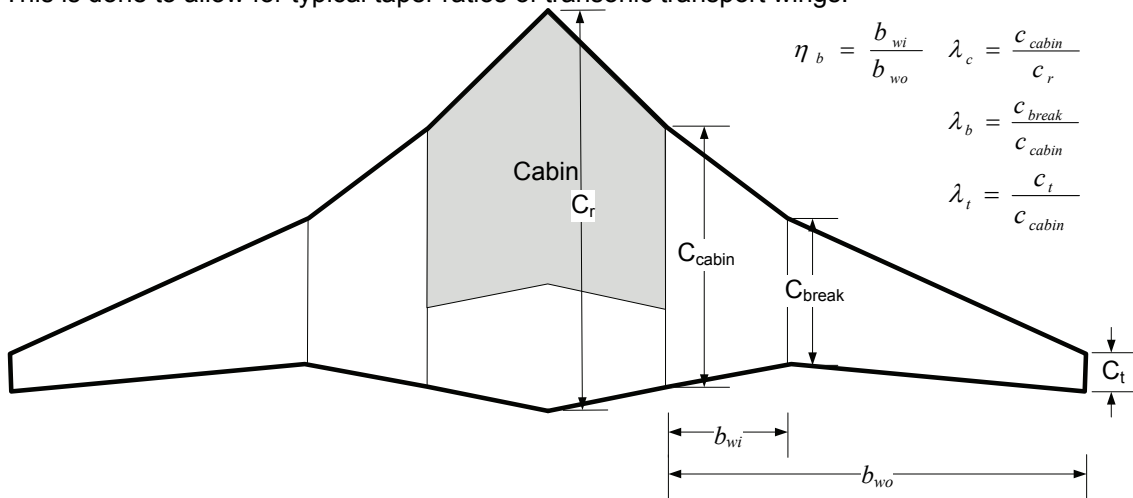


Fig: definition of outer wing.

By specifying the outer wing AR and given the current estimate of planform area required the total span breakdown can be computed.

Total Volume Definition

Starting from the volume of an irregular truncated prism with a defined the thickness (t) and length (c) all that is required is a shape variable (k_{st}) describing the area (Figure below. Typical shape variables are listed in Table below.

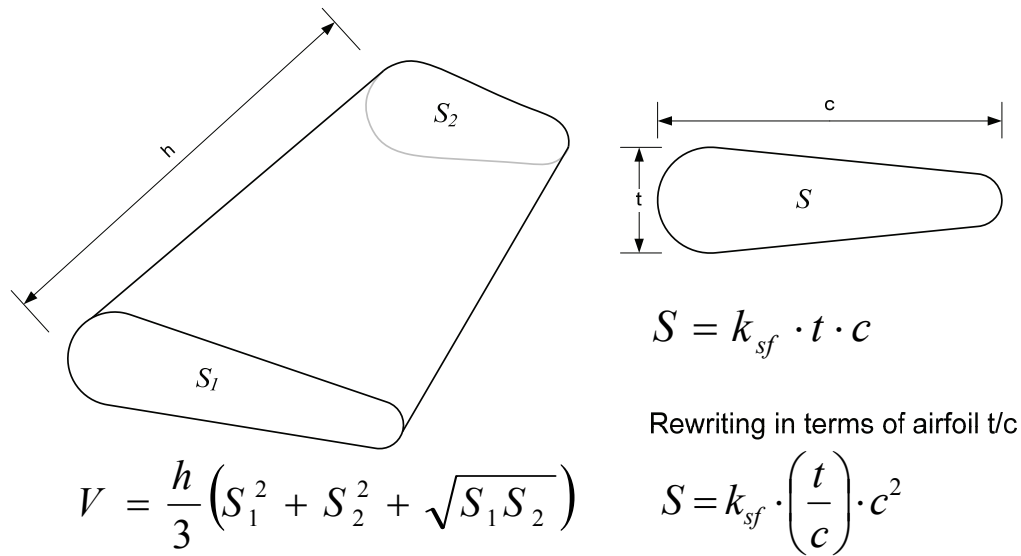
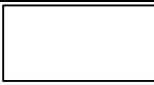
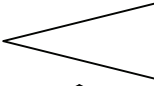
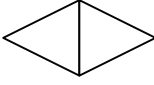



Fig 5-11: Definition of the volume of an irregular prism⁽²⁵⁾.

Table: typical shape factors for geometric shapes

Shape		k_{sf}
Square		1
Triangle		1/2
Diamond		1/2
Torenbeek approximation of a fuel tank within a wing structure ⁽¹⁹⁾		0.54

$$V_{total} = k_{sf} c_r^2 b \left[\begin{aligned} & \eta_1 \left(\frac{t}{c}\right)_r (1 + \lambda_c^2 + \lambda_c) + \\ & + \lambda_c^2 \left((\eta_2 - \eta_1) \left(\left(\frac{t}{c}\right)_c + \left(\frac{t}{c}\right)_t \lambda_b^2 + \sqrt{\left(\frac{t}{c}\right)_c \left(\frac{t}{c}\right)_t} \right) \lambda_b \right) + \\ & + (1 - \eta_2) \left(\left(\frac{t}{c}\right)_c \lambda_b^2 + \left(\frac{t}{c}\right)_t \lambda_t^2 + \left(\frac{t}{c}\right)_t \lambda_b \lambda_t \right) \end{aligned} \right] \quad 5.7$$

Table: Planform definitions for the blended wing body

Variable	Description	
η_1	Ratio of span location of cabin to total span to	$\eta_1 = \frac{b_c}{b_w}$
η_2	Ratio of wing break to total span	$\eta_2 = \frac{b_b}{b_w}$
$\left(\frac{t}{c}\right)_r$	Airfoil thickness ratio at root	
$\left(\frac{t}{c}\right)_c$	Airfoil thickness ratio at edge of cabin	
$\left(\frac{t}{c}\right)_t$	Airfoil thickness ratio at wing break point and wing tip	
λ_c	Tapper ratio at the edge of cabin	$\lambda_c = \frac{c_{cabin}}{c_r}$
λ_b	Tapper ratio at the wing break	$\lambda_b = \frac{c_{break}}{c_r}$
λ_t	Tapper ratio at the wing tip	$\lambda_b = \frac{c_t}{c_r}$

With the inner and outer wing planforms defined the only variables left to be solved for are the wing thicknesses. The thickness ratios utilized in the sizing logic to geometrically fit the volume required to the volume available for the current estimate of planform area and value of τ . However, currently we have one equation (volume, Equation 5.7) and 2 unknown. (t/c_r and t/c_t). Recall, from the cabin height requirement (Equation 5.7) yields a required t/c at the edge of the cabin.

To enable a closed form solution an additional equation is required. Assuming a thickness to chord distribution provides such an equation. Assuming a similar thickness distribution as Liebeck⁽²⁷⁾, the thickness to chord ratio decreases linearly from the root to the outer wing break point and is then constant to the wing tip as shown in

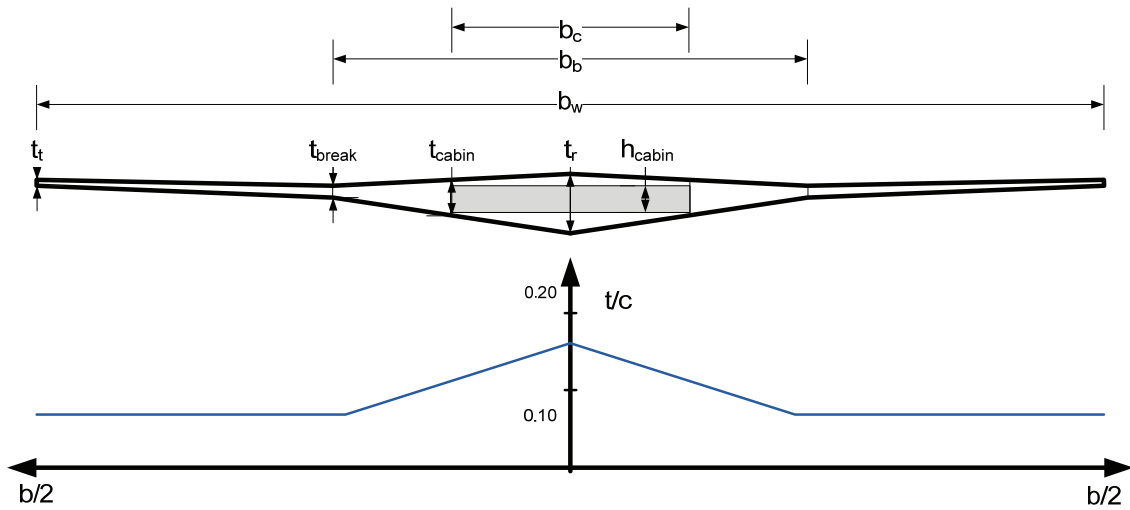


Fig: Assumed thickness distribution

To completely describe the distribution one of the following must be defined: (1) t/c_r , (2) t/c_t or (2) the slope of t/c from root to wing break. Of these three options the most reasonable appears to be the outer wing thickness which can be selected based on past transonic wing designs. Therefore in order to meet the required volume specified by τ and planform area the root thickness to chord ratio and the slope of the thickness to chord ratio are solved for simultaneously via a numerical solution.

AERODYNAMICS

Fiction and form drag

Same as TAC method

Drag due to flaps and landing gear

Same as TAC method

Wave drag

Same as TAC method

Induced Drag

Same as TAC method

Lift Curve Slope

Same as TAC method

Maximum Lift Coefficient

Same as TAC method

Drag Polar Location Specification

Same as TAC method

PROPULSION

Specific fuel consumption

Same as TAC method

Thrust variation

Same as TAC method

Propulsion system sizing

Same as TAC method

PERFORMANCE

Landing Distance

Same as TAC method

Take-off Distance

Same as TAC method

Climb gradient requirement

Same as TAC method

Design cruise

Same as TAC method

Time to climb

Same as TAC method

Descent performance

Same as TAC method

Maximum velocity

Same as TAC method

Ceiling

Same as TAC method

Fuel weight estimation/Trajectory

Same as TAC method

STABILITY AND CONTROL

Trim

Modification of TAC method, wing twist is utilized as an approximation to a camber control device, method will be included in final dissertation.

WEIGHT AND BALANCE

Structural Loads

Same as TAC method

Empty Weight and Volume Formulation

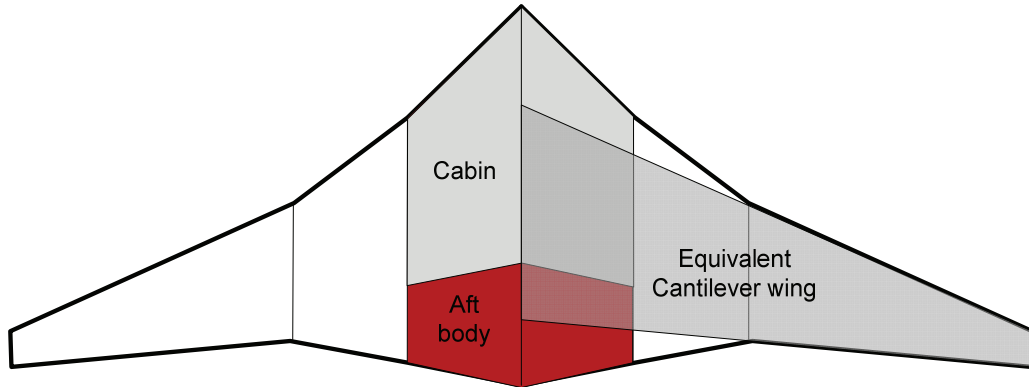
Same as TAC method

Structural weight

Method Overview				
Discipline	Design Phase	Method Title	Categorization	Author
Weight Estimation	Sizing	BWB Wing mass estimation	Semi-empirical	Coleman / GD
<p>Reference: Howe, D., "Aircraft Conceptual Design Synthesis," Professional Engineering Publishing Limited, UK, 2000</p>				
<p>Brief Description</p> <p>Based on the empirical wing structural weight estimation from General Dynamics. This method is applied to the BWB by approximating the wing box as an extrapolation from the outboard wing section to the centerline and then treating this wing as a cantilever beam. Estimating ideal primary structure, secondary structure and corrected with statistics.</p>				
<p>Assumptions</p> <p>The BWB primary wing structure is similar to that of a cantilever wing</p> <p>The applied loads are similar to that of conventional cantilever transports</p> <p>Load distribution over the wing is similar to cantilever wings (this one is iffy)</p>		<p>Applicability</p> <p>BWB transonic transports with classical trapezoidal wing box</p>		
Execution of Method				
<p>Input</p> <p>$AR, M_o, \lambda, W_{to}, N_{ult}, t/c_{avg}, \Lambda_{0.5}, S_w$</p>				
<p>Analysis description</p> <p>Where M_{allows} for increments due to secondary structure and variations of the primary wing structure (Table 5.3).</p> $W_w/S_w = 0.00428 \frac{AR^{1.0} M_o^{0.43} \lambda^{0.14} (W_{TO} n_{ult})^{0.84}}{(100 * t/c)_{avg}^{0.76} \cos^{1.54}(\Lambda_{1/2}) S_w^{0.52}}$ <p>S_{struct} and AR_{struct} refer to the wing area and Aspect ratio of the projected trapezoidal wing from centerline out to wing tip. See Further Description</p>				
<p>Output:</p> <p>W_w</p>				
Experience				
<p>Accuracy</p> <p>When combined with the cabin and aft-body weight estimate the total OEW agrees with the Boeing BWB-800 estimates.</p>		<p>Time to Calculate</p> <p>Unknown</p>	<p>General Comments</p> <p>Unsure if this method is physically sound however it has proven useful for 1st order BWB studies. Being applied to 225, 325, 555 and 325 pax BWB studies in the AVD Lab</p>	

Further Description

The structural aspect ratio and wing area are defined to approximate an equivalent cantilever wing as shown below



Method Overview				
Discipline	Design Phase	Method Title	Categorization	Author
Weight Estimation	Parametric Sizing	BWB Fuselage and aft-body weight estimation	Empirical	Bradley
<p>Reference: Bradley, Kevin R., "A Sizing Methodology for the Conceptual Design of Blended-Wing-Body Transports," NASA/CR-2004-213016, Langley Research Center, Hampton, Virginia, 2004.</p>				
<p>Brief Description</p> <p>Empirical estimates on Fuselage mass based on FEA regressions from BWB geometry, incorporated into FLOPS.</p>				
<p>Assumptions</p> <p>The weight of the aft center body and wing are lumped together, and the weight of the fuselage is the weight of the pressurized cabin.</p>			<p>Applicability</p> <p>BWB</p>	
Execution of Method				
<p>Input</p> <p>N_e (number of engines supported by the center body), S_{emp} (planform area of the aft center body), λ_{emp} (taper ratio), S_{cabin} (planform area of the pressurized cabin)</p>				
<p>Analysis description</p> <p>Pressurized transport fuselage</p> $W_{Fuse} = 0.316422 * K_s * W_{TO}^{0.166552} * S_{cabin}^{1.061158} \text{ [lb]}$ $W_{Empennage} = (1 + 0.05 * N_e) * 0.53 * S_{emp} * W_{TO}^{0.2} * (\lambda_{emp} + 0.5) \text{ [lb]}$				
<p>Output:</p> $W_{Structure} = W_{Fuselage} + W_{Empennage} \text{ [lb]}$				
Experience				
<p>Accuracy</p> <p>Has worked well in comparison to Boeing estimates</p>		<p>Time to Calculate</p> <p>Unknown</p>	<p>General Comments</p> <p>Incorporated into FLOPS 6.03. Input by A. Walker</p>	

Propulsion system weight

Same as TAC method

Fixed equipment weight

Same as TAC method

Operational items weight

Same as TAC method

COST

Life Cycle Cost Formulation

Same as TAC method

RDT&E estimation

Same as TAC method

Manufacturing and acquisition

Same as TAC method

Direct Operating Cost

Same as TAC method

Block Mission

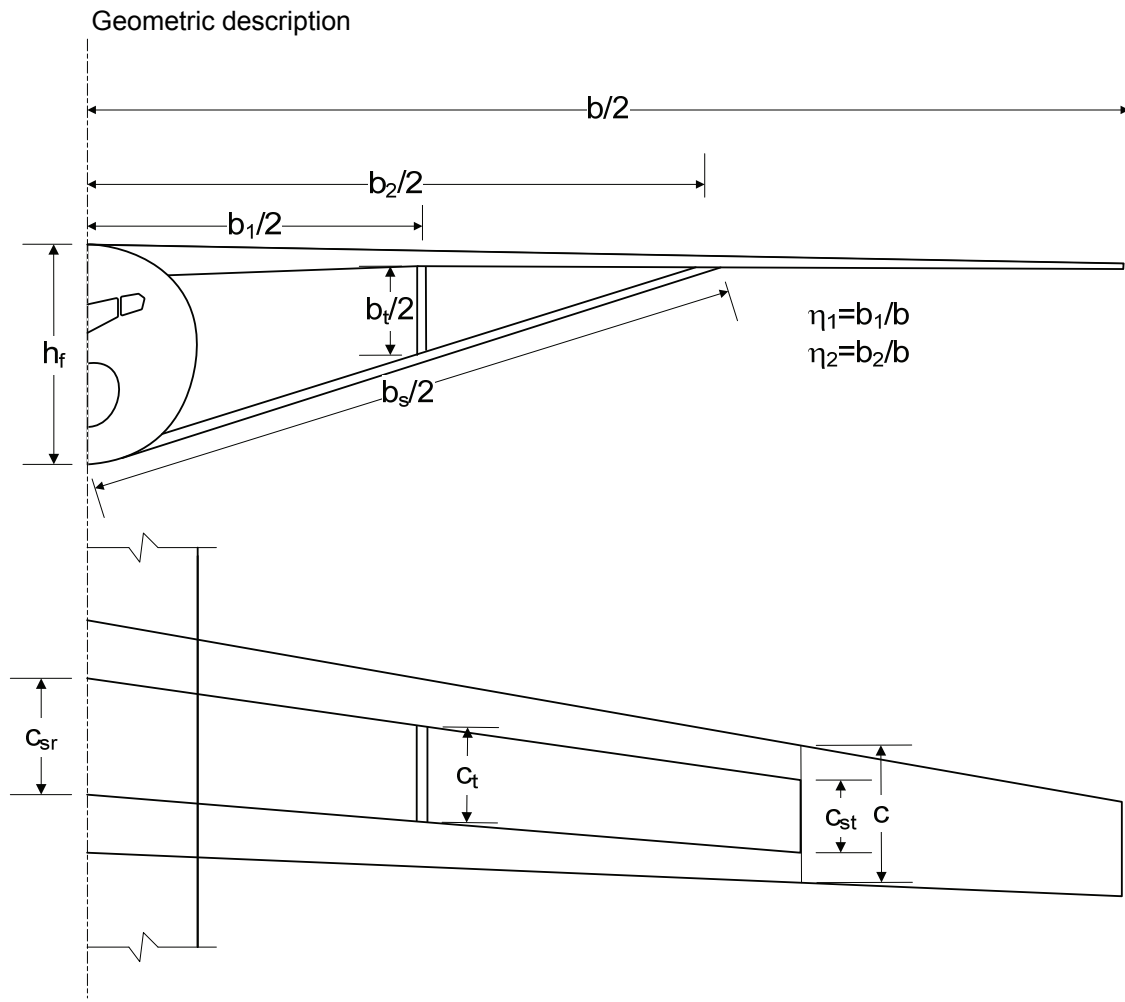
Same as TAC method

B.3 STRUT-BRACED WING CONFIGURATION TRANSPORT METHODS

GEOMETRY

Method Overview				
Discipline	Design Phase	Method Title	Categorization	Author
Geometry	Parametric sizing	Strut/Truss braced geometry simplification	Analytical	Coleman
Reference: Dissertation				
Brief Description Based on the TAC, the SBW/TBW geometry computes the span, chord length, wetted area and volume of a single strut or a 2 member truss.				
Assumptions High wing configuration Strut is connected at the bottom of the fuselage Strut sweep is equal to wing sweep Strut taper ratio same as wing. Truss taper ratio is set to 1 and has no sweep.			Applicability Transonic/Subsonic SBW/TBW	
Execution of Method				
Input Same as TAC with c_s/c , η_1 , η_2 , $(t/c)_{min}$, $(t/c)_{max}$				
Analysis description In addition to the wing, fuselage, nacelle and empennage computations from TAC Compute span and chord lengths Compute thickness requirement based on sweep angle and critical Mach number, min and maximum thickness ratios are also specified. Compute volume and wetted area.				
Output:				
Experience				
Accuracy	Time to Calculate		General Comments Same parametric definition as TAC wing planform	

Further Description



AERODYNAMICS

Fiction and form drag

Same as TAC method

Strut Interference drag

Method Overview				
Discipline	Design Phase	Method Title	Categorization	Author
Aerodynamics	Sizing	Subsonic wing strut interference drag	Semi-Empirical	Hoerner
Reference: Hoerner, F.S., "Fluid-Dynamic Drag", 1965				
Brief Description Empirical estimation of wing-strut intersections for strut-braced aircraft. The wing body intersection is typically accounted for in the profile drag estimation.				
Assumptions Subsonic flow, negligible sweep effects. No compressibility effects accounted for.		Applicability Subsonic strut-braced aircraft		
Execution of Method				
Input $b, C_r, c_t, (t/c)_w, (t/c)_s, S_{ref}, \eta, C_L, b_{strut}$				
Analysis description To compute wing-strut interference $\Delta(C_D)_{WS-strut} = (17.0(t/c)_{avg}^4 - 0.005(t/c)_{avg}^2)(c_t)_s^2 / S_{ref}, \quad (t/c)_{avg} = \frac{1}{2}((t/c)_w + (t/c)_s)$ $\Delta(C_D)_{WS-CL} = (0.1C_L)^2(c_t)_s^2 / S_{ref}$ $\Delta(C_D)_{WS-inc} = (0.000006\beta^2 + 0.0015\beta) \cdot (c_t)_s^2 / S_{ref} \quad \beta = \cos^{-1} D_{fus} / b_{strut}$ $\Delta(C_D)_{WS} = \Delta(C_D)_{WS-strut} + \Delta(C_D)_{WS-CL}$				
Output: $\Delta C_{Dws}, \Delta C_{Dsf}$				
Experience				
Accuracy Unknown		Time to Calculate N/A	General Comments Appears to agree with VT SBW and TBW studies, however, this study has neglected transonic effects as well	

Method Overview				
Discipline Aerodynamics	Design Phase Sizing	Method Title Subsonic strut fuselage interference drag	Categorization Semi-Empirical	Author Hoerner
Reference: Hoerner, F.S., "Fluid-Dynamic Drag", 1965				
Brief Description Empirical estimation of strut-fuselage intersections for strut-braced aircraft. The wing body intersection is typically accounted for in the profile drag estimation.				
Assumptions Subsonic flow, negligible sweep effects. No compressibility effects accounted for.		Applicability Subsonic strut-braced aircraft		
Execution of Method				
Input $b, c_r, c_t, (t/c)_w, (t/c)_s, S_{ref}, \eta, C_L, b_{strut}$				
Analysis description To compute wing-strut interference $\Delta(C_D)_{WS-strut} = (17.0(t/c)_s^4 - 0.0003)(c_t)_s^2 / S_{ref}, \quad (t/c)_{avg} = \frac{1}{2}((t/c)_w + (t/c)_s)$ $\Delta(C_D)_{WS-CL} = (0.1C_L)^2 (c_t)_s^2 / S_{ref}$ $\Delta(C_D)_{WS-inc} = (0.000006\beta^2 + 0.0015\beta) \cdot (c_t)_s^2 / S_{ref} \quad \beta = \cos^{-1} D_{fus} / b_{strut}$ $\Delta(C_D)_{WS} = \Delta(C_D)_{WS-strut} + \Delta(C_D)_{WS-CL}$				
Output: $\Delta C_{Dws}, \Delta C_{Dsf}$				
Experience				
Accuracy Unknown		Time to Calculate N/A	General Comments Appears to agree with VT SBW and TBW studies, however, this study has neglected transonic effects as well	

Drag due to flaps and landing gear

Same as TAC method

Wave drag

Same as TAC method

Induced Drag

Same as TAC method

Lift Curve Slope

Same as TAC method

Maximum Lift Coefficient

Same as TAC method

Drag Polar Location Specification

Same as TAC method

PROPULSION

Specific fuel consumption

Same as TAC method

Thrust variation

Same as TAC method

Propulsion system sizing

Same as TAC method

PERFORMANCE

Landing Distance

Same as TAC method

Take-off Distance

Same as TAC method

Climb gradient requirement

Same as TAC method

Design cruise

Same as TAC method

Time to climb

Same as TAC method

Descent performance

Same as TAC method

Maximum velocity

Same as TAC method

Ceiling

Same as TAC method

Fuel weight estimation/Trajectory

Same as TAC method

STABILITY AND CONTROL

Trim

Same as TAC method

WEIGHT AND BALANCE

Structural Loads

Same as TAC method with the empirical correction for strut as shown in chapter 3

Empty Weight and Volume Formulation

Same as TAC method

Structural weight

Propulsion system weight

Same as TAC method

Fixed equipment weight

Same as TAC method

Operational items weight

Same as TAC method

COST

Life Cycle Cost Formulation

Same as TAC method

RDT&E estimation

Same as TAC method

Manufacturing and acquisition

Same as TAC method

Direct Operating Cost

Same as TAC method

Block Mission

Same as TAC method

B.3 HYPERSONIC CRUISER METHODS

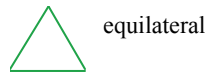
GEOMETRY

Method Overview				
Discipline	Design Phase	Method Title	Categorization	Author
Aerodynamics	Sizing	HC geometry	Semi-Empirical	Czysz
<p>Reference: Curran, E., Murthy, S., "Sramjet Propulsion, Chapter 16: Czysz, P., Vandekerckhove, J., "Transatmospheric Launcher Sizing," , Progress in Astronautics and Aeronautics, American Institute of Aeronautics and Astronautics, Inc., Virginia, 2000</p>				
<p>Brief Description</p> <p>Geometric description of hypersonic gliders and cruisers with delta wing planforms for varies base geometries. By select the planform geometric shape (sweep angle, spatula width) and the base area (circular, trapezoidal, triangular, etc (the remainder of the geometry can be derived.</p>				
<p>Assumptions</p> <p>Simplified geometry</p>		<p>Applicability</p> <p>General glider and air breather configuration</p>		
Execution of Method				
<p>Input: S_{pIn}, t, K_s, c/s, Λ_{LE}</p>				
<p>Analysis description</p> $\frac{S_{wet}}{S_{pIn}} = K_w = \text{See further description}$ $l = \sqrt{\frac{S_{pIn} \tan \Lambda_{LE}}{1 + c/s}}$ $s = l / \tan \Lambda_{LE}$ $c = c/s \cdot s$ $b = 2s + c$ $K_{w_{c/s>0}} = K_{w_{c/s=0}} \left(1 + \frac{c/s K_s}{1 + c/s} \right),$ $K_s = \begin{cases} 0.154 & \text{triangular} \\ 0.2413 & \text{elliptical} \end{cases}$ $S_f = \pi \cdot e s^2 + e s c, \quad e = a/b = \text{see further description}$				
<p>Output: K_w, l, s, c, b, S_f</p>				
Experience				

Accuracy	General Comments
Dependent on assumed values	Use the provided figure for guidance for K_0

Further Description

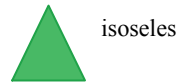
The ratio of the width at the base top to the base bottom ranges from zero (a triangle) to one (a rectangle). The blunted cone adds volume without a significant increase in the wetted area for the nose radius to base radius shown (zero to 0.30) and that is given on the next page.



equilateral
 $K_w = 3.291 - 2.714 \tau + 12.194 \tau^2$



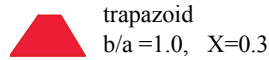
b/a = 0.30
 $K_w = 2.386 - 3.489 \tau + 27.664 \tau^2$



isoseles
 $K_w = 3.483 - 2.102 \tau + 9.482 \tau^2$



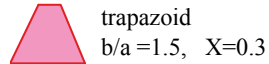
b/a = 0.30
 $K_w = 2.517 - 1.957 \tau + 13.178 \tau^2$



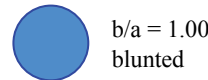
trapazoid
 b/a = 1.0, X = 0.3
 $K_w = 2.769 - 3.038 \tau + 17.314 \tau^2$



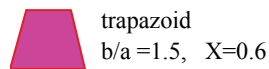
b/a = 1.00
 $K_w = 3.404 - 1.427 \tau + 4.930 \tau^2$



trapazoid
 b/a = 1.5, X = 0.3
 $K_w = 3.184 - 1.995 \tau + 9.449 \tau^2$



b/a = 1.00
 blunted
 $K_w = 3.394 - 1.364 \tau + 4.896 \tau^2$

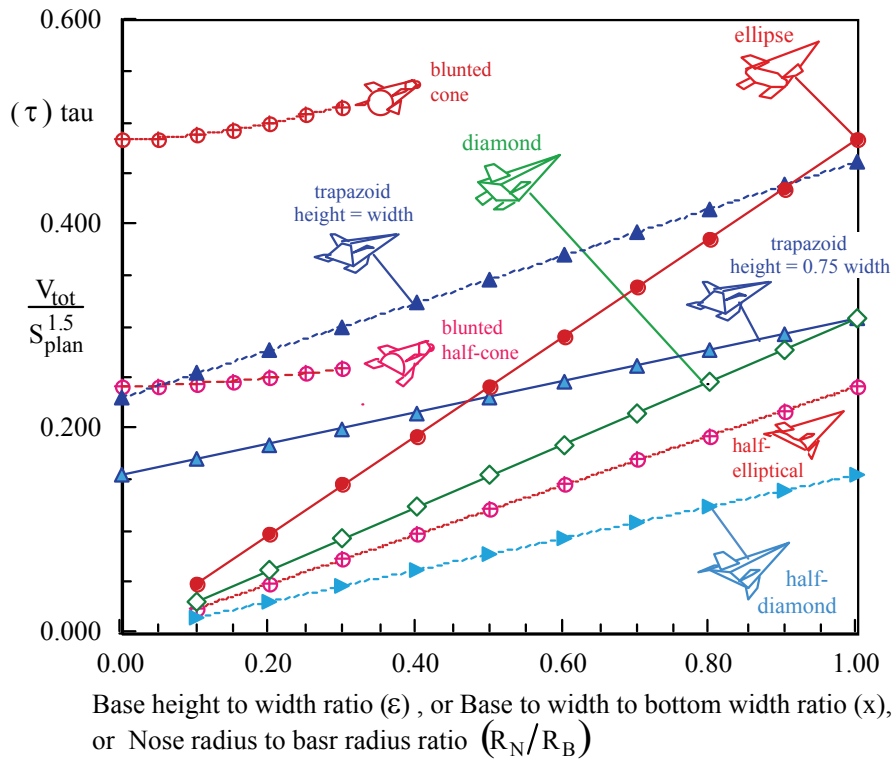


trapazoid
 b/a = 1.5, X = 0.6
 $K_w = 3.351 - 1.482 \tau + 6.826 \tau^2$

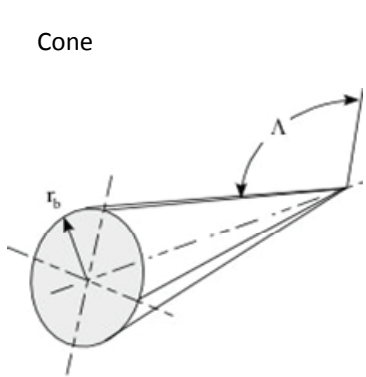
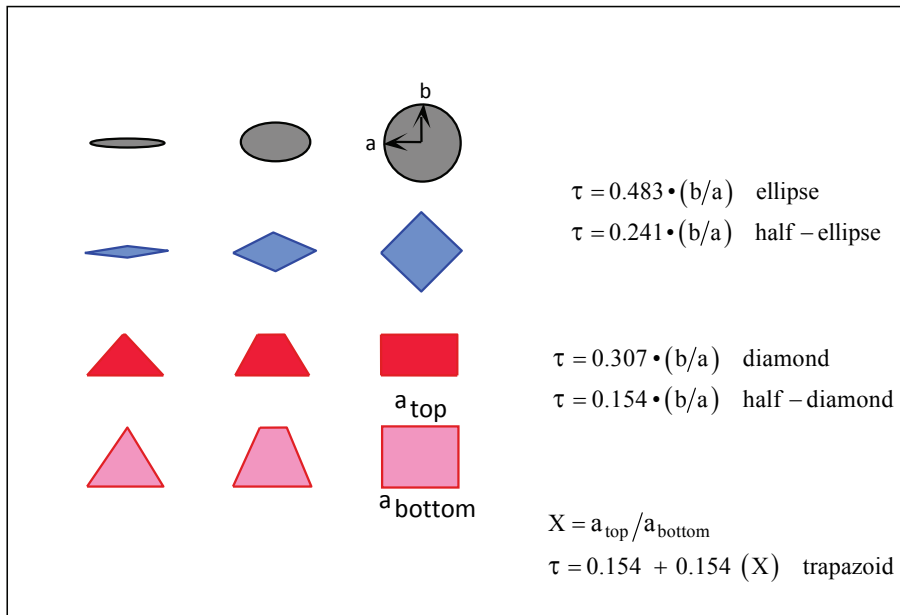


b/a = 0.50
 $K_w = 2.194 - 1.414 \tau + 10.312 \tau^2$

These generalized fixed sweep planforms with variable cross sections span a wide range of wetted area ratio and tau. Figure below shows graphically the range of τ for the range of base geometry variation.



Each base has the same width, and it is used as the reference dimension to normalize the area and volume characteristics. These shapes have no control surfaces integrated into the configuration, so are the basic shapes devoid of control surfaces. The configurations are good for hypersonic gliders, but generally do not make acceptable airbreathing configurations. It is not possible to have the required propulsion performance by merely attaching an airbreathing engine to a rocket derived configuration. It is possible to use some of these configurations for airbreathing rocket concepts, such as deeply cooled and LACE propulsion concepts that are limited to Mach numbers less than six, and use the rocket engine for airbreathing engine. The key to a successful airbreathing concept is the maintenance of sharp leading edges.



$$0.54 \leq \tau \leq 0.39$$

$$A_{\text{base}} = \pi r^2$$

$$S_{\text{plan}} = r^2 \tan \Lambda$$

$$S_{\text{wet}} = \pi r^2 \left(1 + \frac{1}{\cos \Lambda} \right)$$

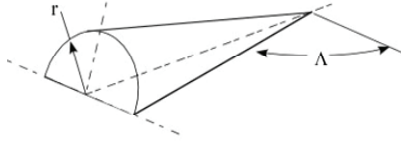
$$V_{\text{tot}} = \frac{\pi r^3}{3} \tan \Lambda$$

$$K_w = \pi \left(\frac{1}{\tan \Lambda} + \frac{1}{\sin \Lambda} \right)$$

$$\tau = \frac{\pi}{3 \sqrt{\tan \Lambda}}$$

$$\tan \Lambda = \left(\frac{\pi}{3 \cdot \tau} \right)$$

Half Cone



$$A_{\text{base}} = \frac{\pi r^2}{2}$$

$$S_{\text{plan}} = r^2 \tan \Lambda$$

$$S_{\text{wet}} = \frac{\pi r^2}{2} \left(1 + \frac{1}{\cos \Lambda} \right) + r^2 \tan \Lambda$$

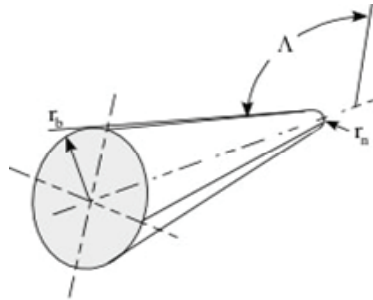
$$V_{\text{tot}} = \frac{\pi r^3}{6} \tan \Lambda$$

$$K_w = \frac{\pi}{2} \left(\frac{1}{\tan \Lambda} + \frac{1}{\sin \Lambda} \right) + 1$$

$$\tau = \frac{\pi}{6 \sqrt{\tan \Lambda}}$$

$$\tan \Lambda = \left(\frac{\pi}{6 \tau} \right)$$

Blunted cone



$$A_{\text{base}} = \frac{\pi r_b^2}{2}$$

$$S_{\text{plan}} = r_b^2 \cdot \tan \Lambda \cdot \left[1 + \left(\frac{r_n}{r_b} \right)^2 \right] + \frac{\pi r_b^2}{2} \cdot \left(\frac{r_n}{r_b} \right)^2$$

$$S_{\text{wet}} = \pi r_b^2 \cdot \left[1 + \frac{1 + \left(\frac{r_n}{r_b} \right)^2}{\cos \Lambda} + 2 \left(\frac{r_n}{r_b} \right)^2 \right]$$

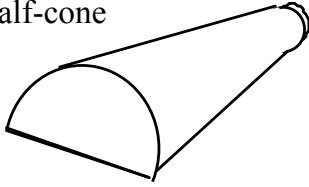
$$V_{\text{tot}} = \frac{\pi r_b^3}{3} \cdot \left(1 - \frac{r_n}{r_b} \right) \cdot \left[1 + \frac{r_n}{r_b} + \left(\frac{r_n}{r_b} \right)^2 \right] \cdot \tan \Lambda$$

$$+ \frac{\pi r_b^3}{2} \cdot \left(\frac{r_n}{r_b} \right)^3$$

$$(K_w)_{78^\circ} = 4.600 \cdot \left(\frac{r_n}{r_b} \right)^2 - 2.350 \cdot \frac{r_n}{r_b} + 4.111$$

$$\tau_{78^\circ} = 0.3048 \cdot \left(\frac{r_n}{r_b} \right)^2 + 0.01875 \cdot \frac{r_n}{r_b} + 0.04826$$

blunted
half-cone



$$A_{\text{base}} = \frac{\pi r_b^2}{4}$$

$$S_{\text{plan}} = r_b^2 \tan \Lambda \left[1 \checkmark \left(\frac{r_n}{r_b} \right)^2 \right] + \frac{\pi r_b^2}{2} \left(\frac{r_n}{r_b} \right)^2$$

$$S_{\text{wet}} = \frac{\pi r_b^2}{2} \left[1 + \frac{1 + \left(\frac{r_n}{r_b} \right)^2}{\cos \Lambda} + 2 \left(\frac{r_n}{r_b} \right)^2 \right] + S_{\text{plan}}$$

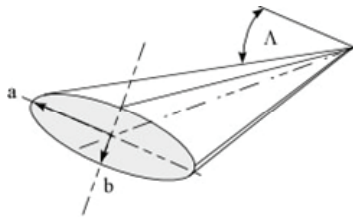
$$V_{\text{tot}} = \frac{\pi r_b^3}{6} \left[\left(1 \checkmark \frac{r_n}{r_b} \right) \left[1 + \frac{r_n}{r_b} + \left(\frac{r_n}{r_b} \right)^2 \right] \tan \Lambda + 2 \left(\frac{r_n}{r_b} \right)^3 \right]$$

$$\tau_{78^\circ} = 0.1381 \left(\frac{r_n}{r_b} \right)^2 + 0.01643 \frac{r_n}{r_b} + 0.2409$$

$$0.2409 \leq \tau_{78^\circ} \leq 0.258$$

$$(K_w)_{78^\circ} = 58.592 \left(\frac{r_n}{r_b} \right)^2 \checkmark 25.755 \frac{r_n}{r_b} + 5.970$$

Ellipse



$$A_{\text{base}} = \pi a^2 e$$

$$S_{\text{plan}} = a^2 \tan \Lambda$$

$$S_{\text{wet}} = \pi a^2 \frac{(1+e)}{\cos \Lambda} \left(1 + \frac{R^2}{4} + \frac{R^4}{64} + \frac{R^6}{256} \right) + \pi a^2 e$$

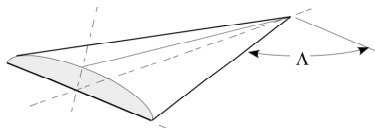
$$V_{\text{tot}} = \frac{\pi a^3 e}{3} \tan \Lambda$$

$$e = b/a \quad R = \frac{1-e}{1+e}$$

$$(K_w)_{78^\circ} = 2.404 \tau^2 + 2.920 \tau + 2.174$$

$$\tau_{78^\circ} = 0.4826 \left[\frac{b}{a} \right]$$

Half-ellipse



$$A_{\text{base}} = \pi a^2 e/2$$

$$S_{\text{plan}} = a^2 \tan \Lambda$$

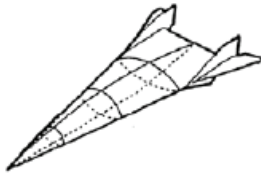
$$S_{\text{wet}} = \frac{\pi a^2}{2} \left\{ \frac{(1+e)}{\cos \Lambda} \left(1 + \frac{R^2}{4} + \frac{R^4}{64} + \frac{R^6}{256} \right) + e \right\} + S_{\text{plan}}$$

$$V_{\text{tot}} = \frac{\pi a^3 e}{6} \tan \Lambda$$

$$e = b/a \quad R = \frac{1-e}{1+e}$$

$$\tau_{78^\circ} = 0.2413 \left[\frac{b}{a} \right]$$

$$(K_w)_{78^\circ} = 2.226 + 2.917 \left[\frac{b}{a} \right] + 4.689 \left[\frac{b}{a} \right]^2$$



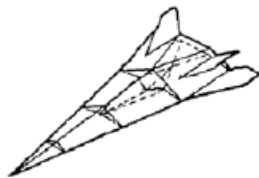
$$K_w = -62.217 \cdot \tau^3 + 29.904 \cdot \tau^2 - 1.581 \cdot \tau + 2.469$$

Blended Body, McDonnell Douglas circa 1965



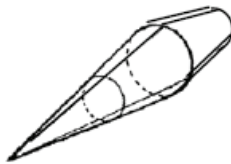
$$K_w = -93.831 \cdot \tau^3 + 58.920 \cdot \tau^2 - 5.648 \cdot \tau + 2.821$$

Wing-Body



$$K_w = -533.451 \cdot \tau^3 + 220.302 \cdot \tau^2 - 22.167 \cdot \tau + 3.425$$

Nonweiler Waverider, circa 1960



$$\tau_{78^\circ} = 0.383$$

$$(K_w)_{78^\circ} = 3.622$$

Truncated Double Cone, circa 1965



$$\tau_{78^\circ} = 0.404$$

$$(K_w)_{78^\circ} = 3.963$$

Right Circular Cone

AERODYNAMICS

The aerodynamic relationships presented were developed by McDonnell aircraft circa 1960 from various experimental aircraft and wind-tunnel tests

Subsonic drag polar

Method Overview				
Discipline	Design Phase	Method Title	Categorization	Author
Aerodynamic	Sizing	Subsonic drag polar for wing-body and blended body configurations	Empirical	MACair
Reference: Czysz, P.A., "Hypersonic Convergence," AFRL-VA-WP-TR-2004-3114, 2004 HYFAC reports				
Brief Description From empirical correlations between maximum trimmed $L/\max D$ and τ and L' (induced drag coefficient) and τ the subsonic drag polar is developed.				
Assumptions. Highly swept planform Wing body or blended body hypersonic configurations. Use only to start the design cycle		Applicability Wing body or blended body hypersonic configurations.		
Execution of Method				
Input τ, M				
Analysis description From slenderness (t) and mach number (M) the appropriate trimmed L/D_{\max} and induced drag coefficient are derived. From this C_{D0} is determined via $C_{D0} = \frac{1}{4 \cdot L' \cdot (L/D)^2}$ See further description for the appropriate correlations				
Output: $C_{D0}, L', L/D$				
Experience				
Accuracy Data correlates well within the range of τ and mach number		General Comments Has worked well for both the Sanger II wing body and LAPCAT blended body		

Future Description

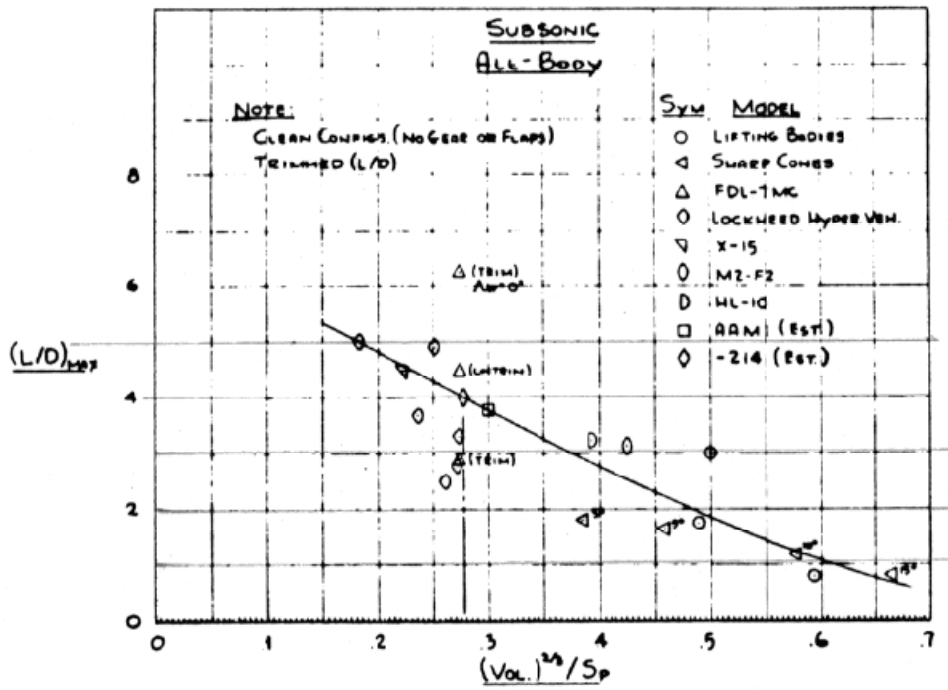


Figure 161. Subsonic Blended Body L/D Correlations

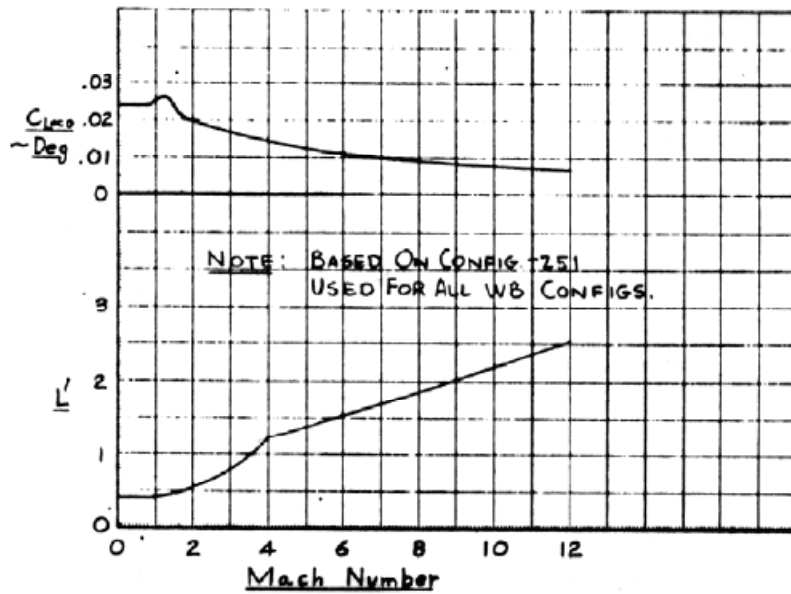


Figure 147. Wing-Body Configurations

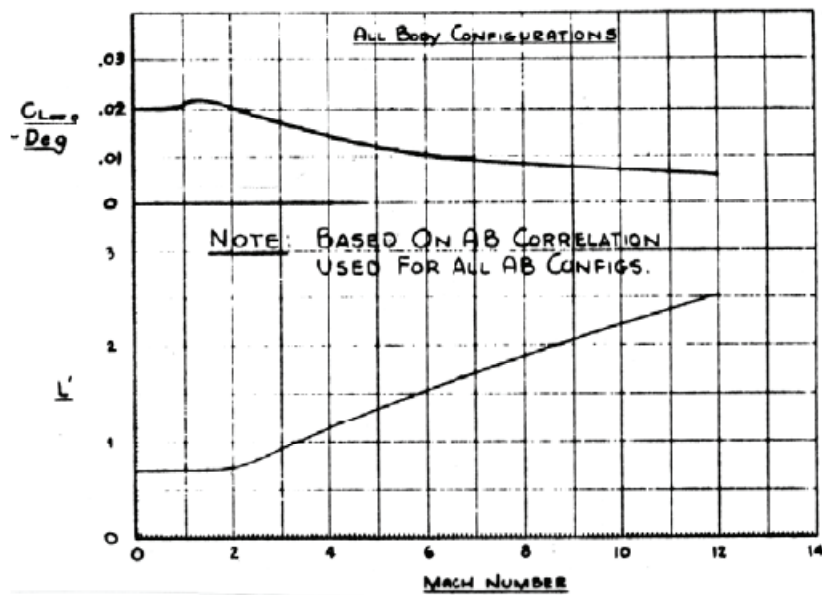


Figure 148. Blended-Body Configurations

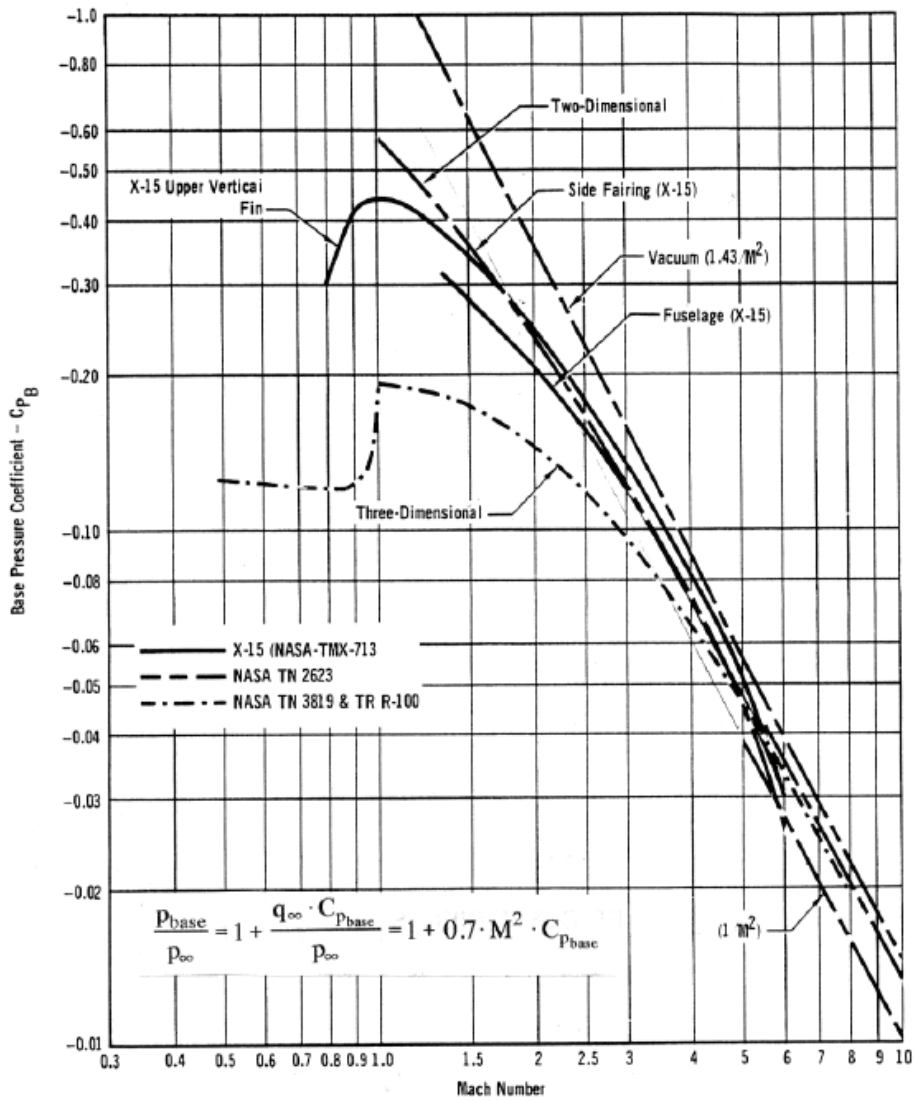
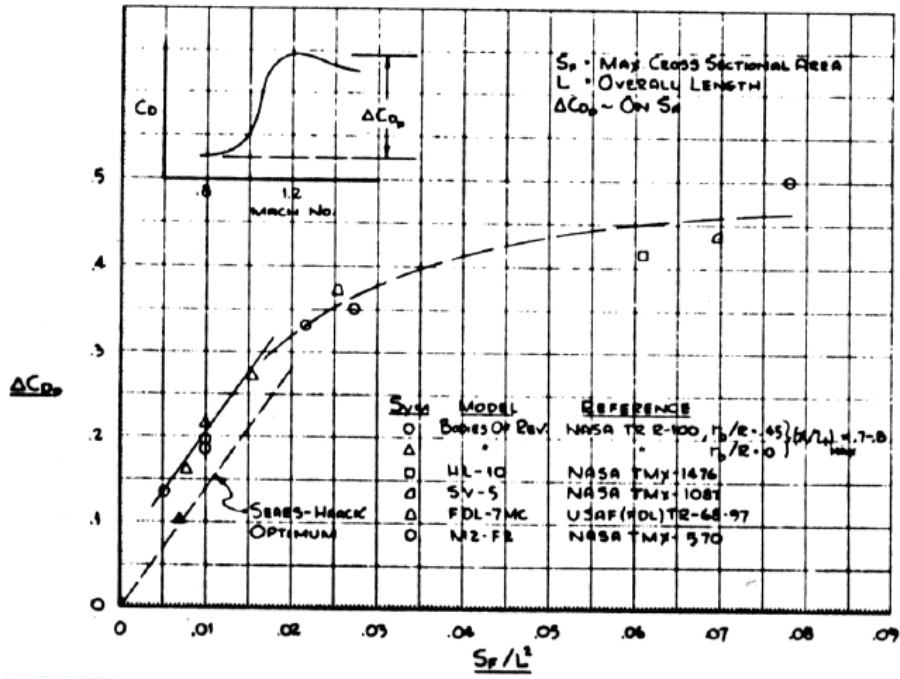


Figure 154. Representative Base Pressure Coefficient

Transonic drag rise

Method Overview				
Discipline	Design Phase	Method Title	Categorization	Author
Aerodynamic	Sizing	Subsonic drag polar for wing-body and blended body configurations	Empirical	MACair
Reference: Czysz, P.A., "Hypersonic Convergence," AFRL-VA-WP-TR-2004-3114, 2004 HYFAC reports				
Brief Description The maximum drag rise is computed using an empirical correlation between the aircrafts frontal area				
Assumptions. Highly swept planform Wing body or blended body hypersonic configurations.			Applicability Wing body or blended body hypersonic configurations.	
Execution of Method				
Input S_{front} , aircraft length (L)				
Analysis description From the ratio of S_{front}/L^2 of various wing body and blended body correlations the following curve fit is determined for the maximum drag rise. If $S_{front}/L^2 < 0.015$ then $(C_{Dwave})_{max} = \frac{S_{front}}{S_{pln}} \left[1.3862 \left(\frac{S_{front}}{L^2} \right) + 0.067 \right]$ If $S_{front}/L^2 > 0.015$ then $(C_{Dwave})_{max} = \frac{S_{front}}{S_{pln}} \left[0.9536 \left(\frac{S_{front}}{L^2} \right)^3 - 1.916 \left(\frac{S_{front}}{L^2} \right)^2 + 1.3651 \left(\frac{S_{front}}{L^2} \right) + 0.1119 \right]$ Interpolate from zero wave drag at mach 0.8 to max at mach 1.2. Interpolate from wave drag at Mach 1.2 to supersonic wave drag at Mach 2 See further description for correlation data				
Output: ΔC_{Dwave}				
Experience				
Accuracy Data correlates well within the range of frontal area's			General Comments Has worked well for both the Sanger II wing body and LAPCAT blended body	

Further Description



Supersonic/Hypersonic Drag Polar

Method Overview				
Discipline Aerodynamic	Design Phase Sizing	Method Title Supersonic/Hypersonic drag polar for wing-body and blended body configurations	Categorization Empirical	Author MACair
Reference: Czysz, P.A., "Hypersonic Convergence," AFRL-VA-WP-TR-2004-3114, 2004				
Brief Description Maximum trimmed L/D Correlations from blended bodies and wing bodies and as a function of τ at mach numbers of at 2, 6 and 12 are used to build a 2-D look-up table				
Assumptions. Highly swept planform Wing body or blended body hypersonic configurations.			Applicability Wing body or blended body hypersonic configurations.	
Execution of Method				
Input τ, M				
Analysis description From the required Mach number and τ , L/D max is interpolated from the data shown in further description (a cubic spline interpolation is suggested). Combining this with the same induced drag correlation is utilized in subsonic method (which extends to Mach 12) the zero lift drag coefficient is determined via, $C_{D0} = \frac{1}{4 \cdot L' \cdot (L/D)^2}$ See further description for correlation data				
Output: $C_{D0}, L', L/D$				
Experience				
Accuracy Data correlates well within the range of applicability			General Comments Has worked well for both the Sanger II wing body and LAPCAT blended body	

Further Description

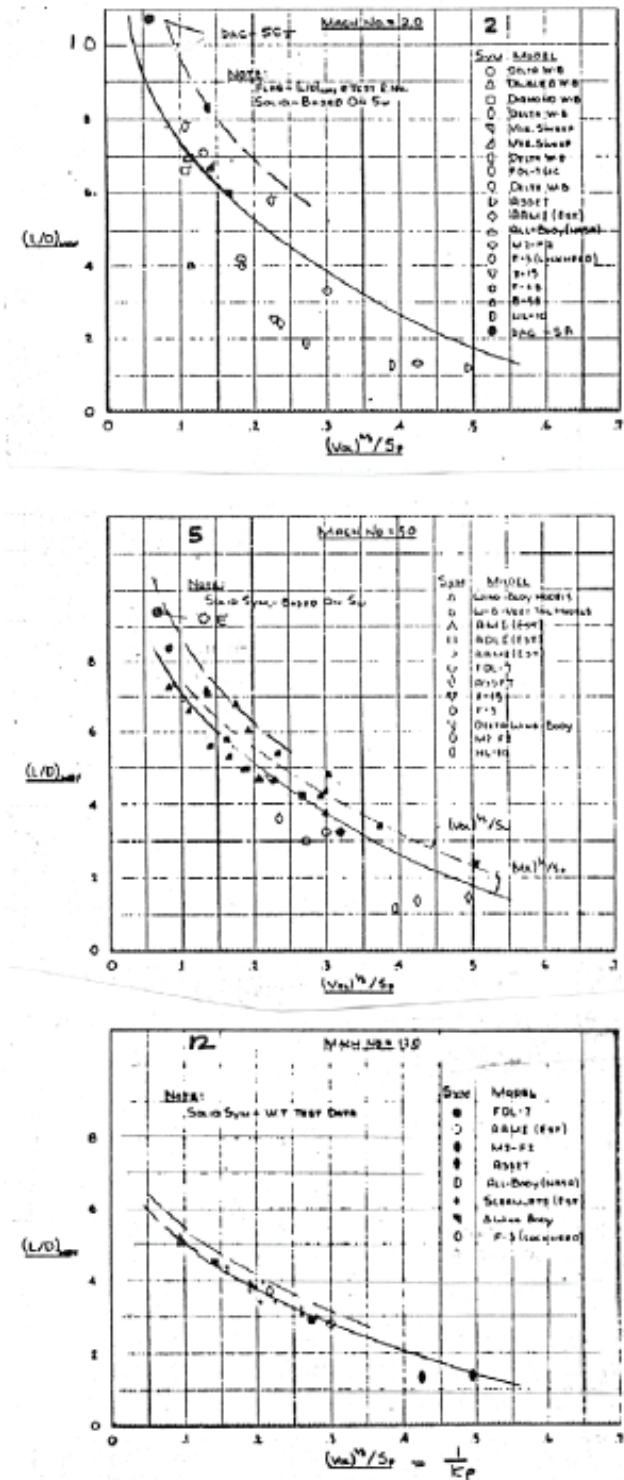


Figure 163. McDonnell Aircraft Lift-to-Drag Ratio Correlations

Drag due to flaps and landing gear
Same as TAC

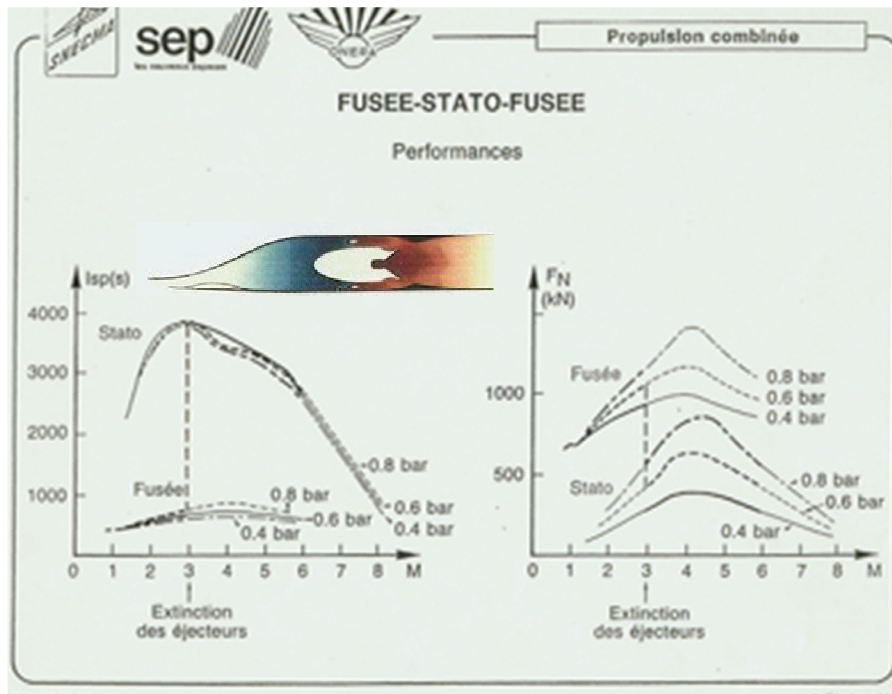
PROPULSION

Specific fuel consumption / Specific impulse / Thrust Available

Method Overview				
Discipline	Design Phase	Method Title	Categorization	Author
Propulsion	Sizing	ONERA Ejector Ramjet data	Empirical	ONERA
Reference: SNECMA-ONERA-SEP Combined Propulsion Studies in France. s.l. Presentation, 1986.				
Brief Description Experimental data from an ejector ramjet module is used to predict the I_{sp} and thrust available as a function of mach number and dynamic pressure.				
Assumptions. Represents Typically Ejector ramjet performance. Use only to start the design cycle		Applicability Ejector ramjet vehicles which operate from $0 < Mach < 8$ $0.4 < q < 0.8 \text{ bar}$		
Execution of Method				
Input M, q				
Analysis description Use the data presented in Further description as a look-up table				
Output: I_{sp}, T_{avl}				
Experience				
Accuracy Unknown, believed to be from a viable ejector ramjet design. use as typical data only		General Comments Use as typical data only. From the thrust		

Further Description

The propulsion systems Isp and Thrust available tables are derived from the following figure as a function of mach number and dynamic pressure.

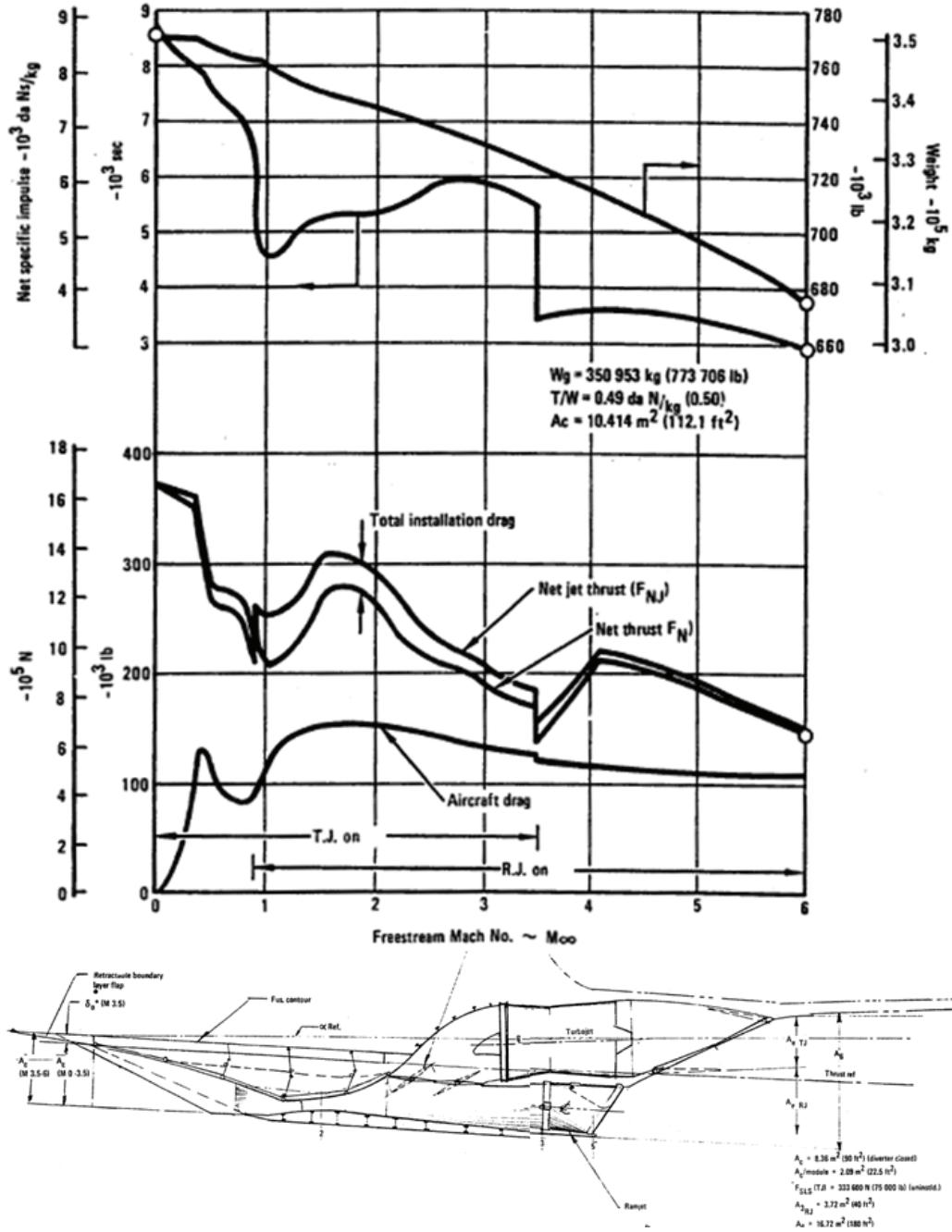


Specific fuel consumption / Specific impulse / Thrust Available

Method Overview				
Discipline	Design Phase	Method Title	Categorization	Author
Propulsion	Sizing	HYCAT Turboramjet data	Empirical	Morris
Reference: Morris, R., Brewer, G. <i>Hypersonic Cruise Aircraft Propulsion Integration Study, Volume I</i> . Burbank : NASA CR-158926-1, NASA Langely Research Center, 1979.				
Brief Description Experimental data from an ejector ramjet module is used to predict the I_{sp} and thrust available as a function of mach number and dynamic pressure.				
Assumptions. Fixed capture area of 10.414 m ² per engine Vehicle operates on similar trajectory to HYCAT study (see reference)		Applicability Ejector ramjet vehicles which operate from $0 < \text{Mach} < 6$ Along a similar trajectory to the HYCAT study		
Execution of Method				
Input M ,				
Analysis description Use the data presented in Further description as a look-up table				
Output: I_{sp}, T_{avl}				
Experience				
Accuracy Unknown, believed to be from a viable turbo-ramjet design. use as typical data only		General Comments Use as typical data only. From the thrust		

Further Description

The propulsion systems Isp and Thrust available tables are derived from the following figure as a function of mach number and dynamic pressure.



PERFORMANCE

Landing Distance

Same as TAC method

Take-off Distance

Same as TAC method

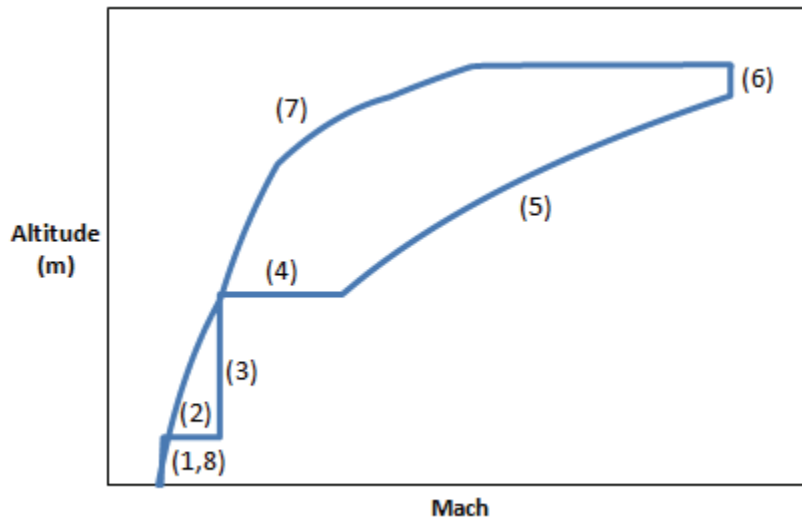
Total Trajectory thrust requirement and fuel requirement

Method Overview				
Discipline	Design Phase	Method Title	Categorization	Author
Propulsion	Sizing	Hypersonic Cruiser Trajectory	Numerical	HYFAC
Reference: Czysz, P.A., "Hypersonic Convergence," AFRL-VA-WP-TR-2004-3114, 2004				
Brief Description				
From an assumed segmented trajectory, an energy integration is performed to compute the fuel weight required. From the computed drag and propulsion system performance data the thrust required at sea-level is compute at each step. The largest thrust requirement is utilized for the				
Assumptions.			Applicability	
Step climb up to transonic acceleration Constant altitude transonic acceleration Constant dynamic pressure climb to cruise altitude Cruise-climb (constant C_L) and Max L/D descent			Air-breathing Hypersonic or supersonic cruisers or first stage launchers.	
Execution of Method				
Input				
Trajectory, C_{D0} , L' , T/Tsl , n_{max} , I_{sp} at each step				
Analysis description				
At each point the following equation is utilized to compute to compute the total fuel burn and thrust requirement (see, further description) Each segment is then integrated based on constant, altitude, velocity, or dynamic pressure The total fuel fraction is then summed for weight and volume convergence The largest thrust to weight ratio is used for engine weight estimation.				
Output:				
$WR, (T/W)_{TO}$				
Experience				
Accuracy		General Comments		
Depends on aero and propulsion system accuracy		This type of trajectory tends to yield the lowest thrust requirement due to the constant altitude transonic acceleration. Transonic acceleration is typically what sets the vehicles thrust requirement.		

Further Description

Assumed trajectory:

(1) climb to 10,000 ft, (2) constant altitude acceleration to 0.8 M, (3) constant Mach climb to 12,000, (4) constant altitude acceleration through the transonic region to maximum dynamic pressure, (5) constant dynamic pressure climb to cruise altitude, (6) cruise-climb to altitude, (7) maximum L/D descent, and (8) landing, see below.



At each integration step (i) (each segment of the trajectory is broken down by predefined step size) the following is computed

Gravity relief

$$\frac{L}{W} = 1 - \frac{V^2}{g(R_e + h)}$$

Aerodynamic efficiency

$$C_L = \frac{L}{W} \frac{W_i}{TOGW} \frac{(W/S)_{TO}}{\bar{q}}$$

$$\frac{L}{D} = \frac{C_L}{C_{D0} + L'C_L^2}$$

Required T/W

$$\left(\frac{T}{W}\right)_i = n_{max} + \frac{1}{L/D}$$

$$\left(\frac{T}{W}\right)_{TO} = \frac{1}{T/T_{SL}} \left(\frac{T}{W}\right)_i$$

Energy at step i

$$E_i = \frac{h_i R_e}{h_i + R_e} + \frac{V_i^2}{2g}$$

Compute derivatives

$$\dot{E}_i = V_i \cdot n_{max}$$

$$\Delta t = \frac{E_i - E_{i-1}}{\dot{E}_i}$$

$$\Delta R = V_i \cdot \Delta t$$

$$\frac{\Delta W_i}{TOGW} = -\Delta T \frac{T/W}{I_{SP}}$$

Next step

$$t_{i+1} = t_i + \Delta t$$

$$R_{i+1} = R_i + \Delta R$$

$$\frac{W_{i+1}}{TOGW} = \frac{W_i}{TOGW} + \frac{\Delta W_i}{TOGW}$$

STABILITY AND CONTROL

Trim

Accounted for in empirical aerodynamic method

WEIGHT AND BALANCE

Structural Loads

Not required for weight estimation

Empty Weight and Volume Formulation

Method Overview				
Discipline	Design Phase	Method Title	Categorization	Author
Weight Estimation	Parametric Sizing	Convergence Empty weight estimation	Empirical	Coleman/ Czys
Reference: Dissertation				
Brief Description A modification of the hypersonic convergence method for estimating the converged empty weight based on volume and mass. This method has been modified to allow for the incorporation of additional methods for structural, propulsion, systems and operational item weights beyond what are presented in hypersonic convergence				
Assumptions Wing area is not constant		Applicability Any aircraft our launcher configuration. Applicability depends on the methods used for the structural, propulsion and systems weight		
Execution of Method				
Input $WR, T/W, W_{pay}, W_{crew}, V_{pay}, V_{crew}$				
Analysis description Solve the below system for S_{pln} and OEW Weight Budget: $OEW = \frac{W_{str} + W_{sys} + W_{oper} + (T/W)_{max} WR / E_{TW} (W_{pay} + W_{crew})}{\frac{1}{1+\mu_a} - f_{sys} - (T/W)_{max} WR / E_{TW}}$ Volume Budget: $OEW = \frac{\tau \cdot S_{pln}^{1.5} (1 - k_{vw} - k_{vs}) - V_{fix} - V_{pay} - V_{crew}}{\frac{WR-1}{\rho_{fuel}} + k_{ve} (T/W)_{max} WR}$ Use the additional methods for $W_{str}, W_{sys}, f_{sys}, W_{oper}$ and E_{TW}				
Output: $OEW, TOGW, OWE, S_{pln}$				
Experience				
Accuracy Depends upon additional methods		Time to Calculate Depends on structural weight estimation	General Comments Works well for any configuration. Is at the heart of AVDsizing. The convergence logic will take the output and feed it back through the geometry trajectory and constraints until convergence	

Further Description

Additional volumetric relationships

$$V_{pay} = W_{pay} / \rho_{pay}$$

$$V_{crew} = N_{crew} (V_{pcrv} + k_{crew})$$

$$V_{void} = k_{vv} V_{tot}$$

$$V_{ppl} = W_{OE} \left(\frac{W_R - 1}{\rho_{ppl}} \right)$$

$$48 \leq \rho_{pay} \leq 130 \text{ kg/m}^3$$

$$0.9 \leq k_{crew} \leq 2.0 \text{ m}^3/\text{person}$$

$$6.0 \leq V_{pcrv} \leq 5.0 \text{ m}^3/\text{person}$$

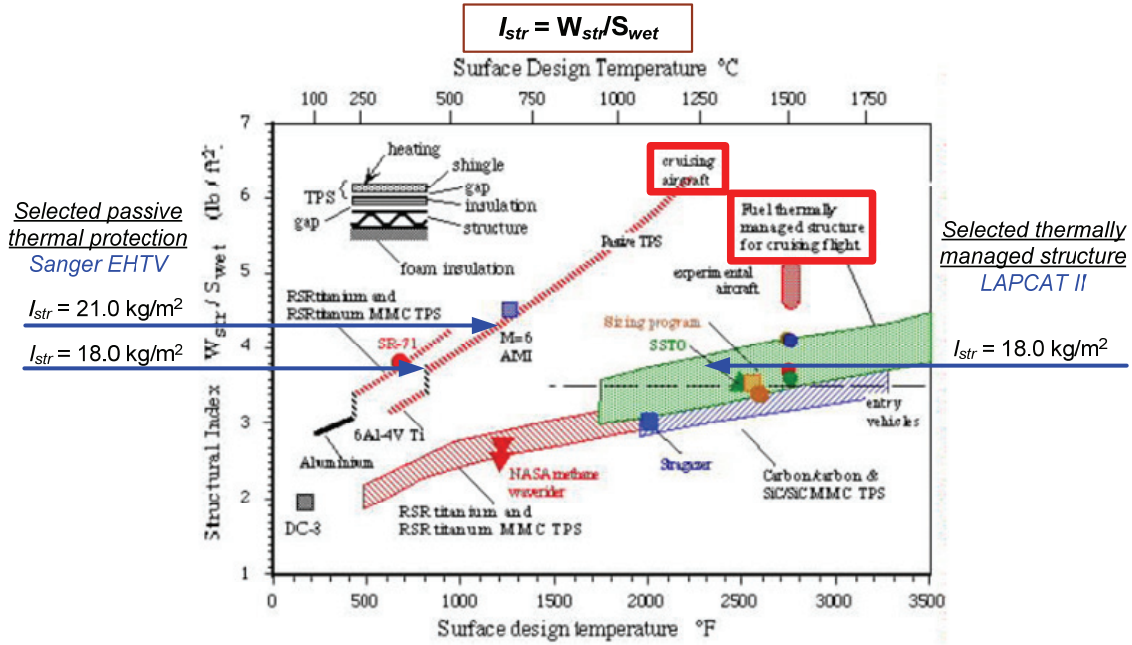
$$0.10 \leq k_{vv} \leq 0.20 \text{ m}^3/\text{m}^3$$

Structural weight

Method Overview				
Discipline	Design Phase	Method Title	Categorization	Author
Structure	Sizing	Structural Index	Empirical	Czysz
Reference: Czysz, P.A., "Hypersonic Convergence," AFRL-VA-WP-TR-2004-3114, 2004				
Brief Description The structural index, W_{str}/S_{wet} is selected based on the thermal environment.				
Assumptions Blended body or wing body hypersonic cruiser or launch vehicle. Integrated thermal projection and structural sandwich			Applicability Both passive and actively cooled structures Hypersonic cruisers and launch vehicles	
Execution of Method				
Input I_{str}, S_{wet}				
Analysis description Select Structural index (see further description) compute structural weight $W_{str} = I_{str} \cdot S_{wet}$				
Output: W_{str}				
Experience				
Accuracy Has worked well for a variety of hypersonic cruisers projects at MAC. Proves valid for the Sanger II		General Comments Due to the transition from hot to cold structure the structural index does not need to be greater than 18 kg/m ² . The rule of thumb at MAC was 21 kg/m ² was used for demonstrators (with cheap and heavier materials) and 18 kg/m ² was used for operational vehicles		

Further Description

The structural index is selected from the figure below from the predicted maximum



Propulsion system weight and volume

Method Overview				
Discipline	Design Phase	Method Title	Categorization	Author
Weight Estimation	Parametric Sizing	Propulsion system weight and volume estimation	Empirical	Czysz
Reference: Czysz, P.A., "Hypersonic Convergence," AFRL-VA-WP-TR-2004-3114, 2004				
Brief Description The propulsion system weight and volume estimation is performed through selected the appropriate engine thrust to weight ratio and volume coefficient.				
Assumptions Installed engine thrust to weight ratio Installed engine volume coefficient		Applicability Launch vehicles and hypersonic cruisers		
Execution of Method				
Input <i>Type of propulsion system</i>				
Analysis description Select ETW and Kve. Substitute into weight and volume budget Weight: $W_{eng} = \frac{TW_o W_R}{E_{TW}} (W_{dry} + W_{pay} + W_{crew})$ $10 \leq E_{TW} \leq 25$ kg thrust/kg weight Volume: $V_{eng} = k_{ve} (T/W)_{max} W_R W_{OE}$ $0.25 \leq k_{ve} \leq 0.75$; m ³ /ton thrust See further description for guidance				
Output: E_{TW}, k_{ve}				
Experience				
Accuracy Depends upon additional methods		Time to Calculate	General Comments Has worked well for several hypersonic studies at MAC. Has proven valid for several transonic applications as well	

Further Description

The figure below from Hypersonic Convergence shows typical values of engine thrust to weight ratio for various propulsion cycles.

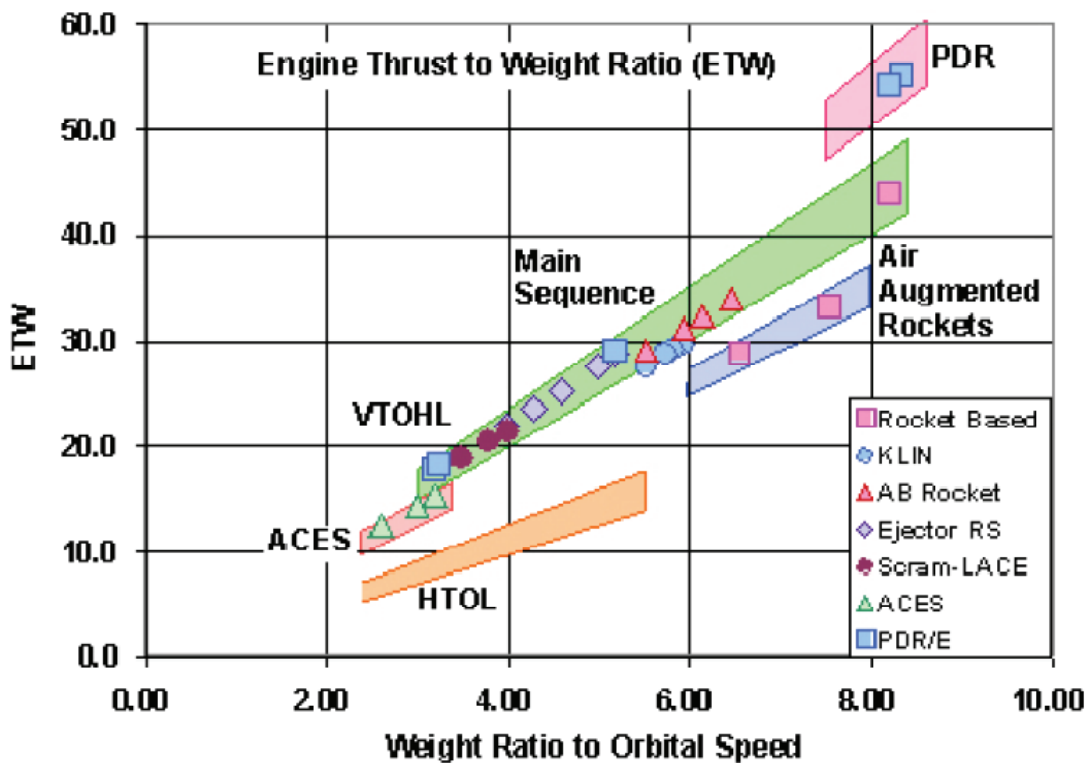


Table: Definitions of possible accelerator cycles

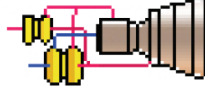
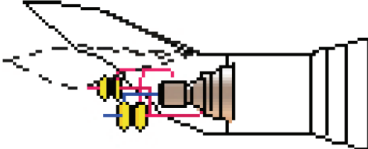

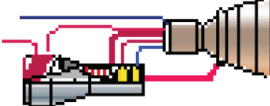
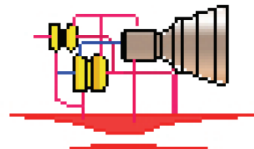
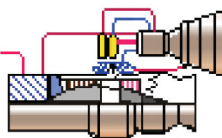
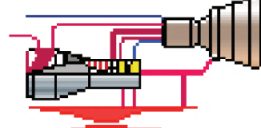
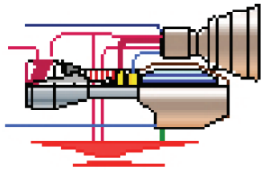
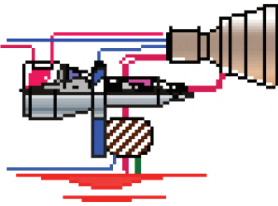
Cycle	Description	
Rocket	Conventional liquid propellant rocket	 <p data-bbox="1006 430 1209 451">Liquid-Propellant Rocket</p>
Air –Augmented Rocket	Rocket enclosed in an inlet duct to act as a high-energy ejector	 <p data-bbox="1128 619 1299 661">Air-Augmented Rocket Ram-Rocket</p>
Airbreathing Rocket	<p data-bbox="576 672 860 724">LACE – Liquid Air Cycle Airbreathing Rocket.</p> <p data-bbox="576 756 917 871">An inlet heat exchanger boils liquid hydrogen to liquefy the incoming air for storage and later use in the rocket</p>	 <p data-bbox="990 819 1274 840">Liquid Air Cycle Airbreathing Rocket</p>
Airbreathing Rocket	<p data-bbox="576 882 747 903">Deeply cooled</p> <p data-bbox="576 934 933 1113">An inlet heat exchanger boils liquid hydrogen to cool the incoming air just short of saturation. A turbocompressor pumps the high-pressure cold air to the rocket chamber</p>	 <p data-bbox="998 1029 1274 1050">Deeply Cooled Airbreathing Rocket</p>
Ejector Ram-Scramjet-Rocket	Rocket ejectors integral in the ramjet struts provide both thrust and compression	
Thermally integrated combined cycle propulsion	<p data-bbox="576 1312 933 1365">KLIN – Deeply cooled turbojet rocket</p> <p data-bbox="576 1396 868 1501">Analogues deeply cooled rocket with a turbojet for improved low-speed performance</p>	 <p data-bbox="1015 1491 1169 1512">Figure 368 KLIN Cycle</p>
Airbreathing Rocket	Deeply cooled Ram/Scramjet	 <p data-bbox="998 1669 1218 1690">Deeply Cooled Ram/Scramjet</p>

Table: Definitions of possible accelerator cycles (continued)

Cycle	Description	
ACES ejector-ram-scramjet-rocket	<p data-bbox="573 310 727 340">LACE-ACES</p> <p data-bbox="573 367 950 640">LACE system with the liquid air separated into 'nitrogen-poor air' and 'oxygen-poor nitrogen'. The 'nitrogen-poor' air is stored for use in the rocket engine and the oxygen-poor nitrogen is introduced into the ramjet for increased mass-flow and thrust.</p>	
	<p data-bbox="573 640 831 682">Deeply Cooled ACES</p>	

Systems weight and volume

Method Overview				
Discipline	Design Phase	Method Title	Categorization	Author
Weight Estimation	Parametric Sizing	System weight and volume estimation	Empirical	Czysz
Reference: Czysz, P.A., "Hypersonic Convergence," AFRL-VA-WP-TR-2004-3114, 2004				
Brief Description The systems weight and volume estimation is performed through selected the appropriate fixed and variable systems weight and volume coefficients.				
Assumptions Installed engine thrust to weight ratio Installed engine volume coefficient		Applicability Launch vehicles and hypersonic cruisers		
Execution of Method				
Input <i>Type of propulsion system</i>				
Analysis description				
Weight: $W_{sys} = C_{sys} + f_{sys}W_{dry}$		$0.16 \leq f_{sys} \leq 0.24$ ton/ton		
$C_{sys} = C_{un} + f_{mnd}N_{crew}$		$1.9 \leq C_{un} \leq 2.1$ ton		
		$1.45 \leq f_{mnd} \leq 1.05$ ton/person		
Volume: $V_{sys} = V_{fix} + k_{vs}V_{tot}$		$0.02 \leq k_{vs} \leq 0.04$ m ³ /m ³		
$V_{fix} = V_{un} + f_{crew}N_{crew}$		$5.0 \leq V_{un} \leq 7.0$ m ³		
		$11.0 \leq f_{crew} \leq 12.0$ m ³ /person		
Note: $W_{dry} = W_{OE} - W_{pay} - f_{crew}N_{crew}$				
Output: W_{sys}, V_{sys}				
Experience				
Accuracy These coefficients were derived by VDK in the 60's and 70's through collaboration with several European collaborators		Time to Calculate	General Comments Has worked well for several hypersonic studies at MAC. This method is also in agreement with the AVD Lab Sanger II study.	

COST

Life Cycle Cost Formulation

Not computed

RDT&E estimation

Not computed

Manufacturing and acquisition

Not computed

Direct Operating Cost

Not computed

Block Mission

Not computed

APPENDIX C

EXAMPLE AVDSIZNG INPUT FILE: B777-300ER MODEL

!*****

```
<- APAXD
325.0
<- APAXMAX
370.0
<- CREW
16.0
<- WPAX [KG]
97.52
<- WCREW [KG]
92.0
<- WCARGO [KG]
6474.0
<- WCARGO_MAX [KG]
69853.0
<- NCRUISE
1.0
<- D_RANGE (KM)
14075.2 5000.0
<- D_MACH
0.84 0.84
<- D_WR
1.0 0.5
<- TOFL [m]
3048.0
<- ALT_TO
0.0
<- ALT_LAND
0.0
<- SLAND [m]
1767.84
<- ALT_ICLIMB [m]1
3048.0
<- ALT_SCEILING [m]
12000.0
<- NTTC
0
<- TTC [hr]
1.2
<- RC_CEILING [m/s]
0.5
```

Fuel Selection input

!Variable description*****

!FUEL_DEN Fuel density (kg/m^3)

!*****

```
<- FUEL_DEN (kg/m^3)
```

780.0

Regulation input

!Variable description*****
!TO_CGR Take-off climb gradient
!TO_OEI Take-off with OEI (1=yes, 2=no) NOT IN USE
!ALAND_CGR Landing climb gradient
!ALAND_OEI Landing with OEI (1=yes, 2=no) NOT IN USE
!ALAND_WR Maximum Landing weight ratio
!ALTRES Cruise altitude for reserve fuel/divert
!R_MACH velocity for reserve fuel/divert
!TIMERES loiter time for reserve fuel/divert
!N_ETOPS ETOPS switch
! =0 ETOPS not required
! =1 ETOPS required
!*****

<- TO_CGR [RAD]
 0.024
<- TO_OEI [RAD]
 1
<- ALAND_CGR [RAD]
 0.021
<- ALAND_OEI [RAD]
 1
<- ALAND_WR
 0.714
<- ALTRES [KM] ****double check****
 3048.0
<- TIMERES [MIN]
 60.0
<- N_ETOPS
 1

Convergece input

!Variable description*****
!NPM Performance matching method switch
! =1 Cruise Climb (Altitude Free)
! =2 Cruise Climb (Altitude Fixed)
!*****
<- NPM
 1
!LOFTIN metod *****
!SREF Inital wing area guess
!ALT(5) Initial cruise altitude guess

```

!D_MVIHN          Location on drag polar for cruise (1 = L/D max)[NCRUISE]
!CLCRUISE        Initial cruise lift coefficient guess (for trim solution)
!TAU             Kuchemann's tau slenderness parameter
!*****

```

```

<- SREF(m^2)
  500.0
<- ALTC (m)
  8229.6  8229.6
<- D_MVIHN
  1.0  0.2
<- CLCRUISE
  0.52
<- TAU
  0.21
<- AISTR
  32.7

```

```

*****
Sizing input
*****

```

```

!Variable description*****
!WSINITIAL        Initial wing loading
!WSFINAL          Final wing loading
!WSSTEP           Wing loading step
!*****

```

```

<- WSINITIAL
  450
<- WSFINAL
  700
<- WSSTEP
  25

```

```

*****
Configuration input
*****

```

```

!Variable description*****
!NFUSE            Number of fuselages or external bodies
! FUSAPEX         Fuselage Nose location (1-X, 2-Y, 3-Z)
! FUSE_FILE       Fuselage file name (NFUSE)
! NFP             Number of fuselage polar coordinates
! AFTC_DF         Ratio of tail length to max fuselage diameter
! AFNC_DF         Ratio of nose length to max fuselage diameter
!NENGINES         Number of propulsion systems
!NPROPELLER       Number of Propellers (total)
!NNAC             Number of Nacelles
! NAC_REF         Reference location indicator
!                =1 Fuselage Noise
!                =2 Wing apex

```

```

!ANAPEX          Nacelle apex location repeat (NNAC times) (1-X, 2-Y-, 3-Z)
!
!                IF NAC_REF =1 THEN
!                  X - percent fuselage length(positive aft)
!                  Y - percent fuselage width (positive right from top view)
!                  Z - Percent fuselage high (positive up)
!                IF NAC_REF =2 THEN
!                  X - percent local chord location (positive aft)
!                  Y - percent span (positive out the right wing)
!                  Z - Percent nacelle high (positive down, zero corresponds to
center of nacelle at wing LE)
! NAC_FILE       Nacelle file
! NWING          Number of wings
! NAFW           Airfoil file index
!               1-39 AIRFOILS FROM FILES (NOT RECOMMEND FOR BWB
visualization)
!               40 - NACA 4 digit
!               41 - NACA 4 Digit modified
!               63 - NACA 63 SERIES (Thickness and camber from sizing results)
!               64 - NACA 64 SERIES          "
!               65 - NACA 65 SERIES          "
!               :
!               67 - NACA 67 SERIES          "
! WINGAPEX       Wing apex(1-X, 2-Y, 3-Z) (1-X/ALFUS, 2-Y/DMAX, 3-Z/DMAX)
! NHT            Number of Horizontal tails (canard, H-T, etc.)
! NAFH           Airfoil file index
!               1-39 AIRFOILS FROM FILES (NOT RECOMMEND FOR BWB
visualization)
!               40 - NACA 4 digit
!               41 - NACA 4 Digit modified
!               63 - NACA 63 SERIES (Thickness and camber from sizing results)
!               64 - NACA 64 SERIES          "
!               65 - NACA 65 SERIES          "
!               :
!               67 - NACA 67 SERIES          "
! HTAPEX         Horizontal tail apex (1-X/ALFUS, 2-Y/DMAX, 3-Z/DMAX) (reference to
fuselage nose)
! NVT            Number of vertical tails
! NAFV           Airfoil file index
!               1-39 AIRFOILS FROM FILES (NOT RECOMMEND FOR BWB
visualization)
!               40 - NACA 4 digit
!               41 - NACA 4 Digit modified
!               63 - NACA 63 SERIES (Thickness and camber from sizing results)
!               64 - NACA 64 SERIES          "
!               65 - NACA 65 SERIES          "
!               :
!               67 - NACA 67 SERIES          "
! VTAPEX         Vertical tail apex(1-X/ALFUS, 2-Y/DMAX, 3-Z/DMAX)
! NAFDD          Number of airfoils in database (MAX 10)
! AIRFOIL_FILE  Airfoil ordinates file names
! MLG_REF       main landing gear reference location
!               =1 Wing mounted

```



```

!                                     =2 Fuselage mounted
!*****

!*****
!** FUSELAGE
!*****
<- NFUSE
  1
<- FUSAPEX
  0.000 0.000 0.000
<- FUSE_FILE
  RF-A320A.DAT
<- NFP
  48
<- AFTC_DF
  3.46
<- AFNC_DF
  1.6

!*****
!** PROLUSION
!*****
<- NENGINES
  2
<- NPROPELLER
  0
<- NNAC
  2
<- NAC_REF
  2
<- ANAPEX
  -0.5 0.3 0.55
  -0.5 -0.3 0.55
<- NAC_FILE
  GONDEL1.DAT
<- NNP
  48

!*****
!** WING SECTIONS
!*****
<- NWING
  1
<- NAFW
  63
<- WINGAPEX
  0.34 0.0 -0.35
<- NHT
  1
<- NAFH
  2
<- HTAPEX
  0.85 0.0 0.15

```

```

<- NVT
1
<- NAFV
1
<- VTAPEX
0.85 0.0 0.40
!*****
!** AIRFOIL DATABASE
!*****
<- NAFDD
2
<- AIRFOIL_FILE
N64012.DAT
N64008A.DAT

!*****
!** LANDING GEAR
!*****
<- MLG_REF
1
<- ANG
0.08 0.0 -0.5
<- AMG
0.85 0.10 0.0

*****
Geometry input
*****

!METHOD SELECTION *****
!MGEO Geometric sizing method
! = 1 manual input of required geometry
! = 2 wing thickness computed from cruise lift coefficient
! Mach number and sweep anlge to yield a wing critical
! Mach number of 0.04 above the cruise Mach number (Howe). The
! empennage sweep is computed as inputted increment above the
! wing sweep (Shaufele) and the empennage thickness is compute to
yield
! a critical mach number 0.05 above the wing critical mach
! number (Roskam)
! = 3 vehicle sized with tau, using constant fuselage l/d and wing AR
! = 4 vehicle sized with tau, using constant fuselage l/d and wing s/l
!*****

<- MGEO
3

!WING *****
!wing span and AR, specify one and leave the other as 0.0
! ARW(5) Wing Aspect ratio [max 5]
! BW(5) Wing Span [max 5]
!S_LWING ratio of wing semi-span to fuselage length

```

```

!TRW(5)          Wing Taper ratio [max 5]
!ALW(5)          Wing sweep
!AXCW(5)         chord location of wing sweep (x/c)
!***TCW(5)       Wing airfoil thickness (/c) [max 5]      (NOT REQUIRED FOR
MGEO=2)
!TWISTW(5)       Wing twist (deg) [max 5]
!DIHEDW          Wing dihedral
!*****

```

```

<- ARW
  9.00
<- BW [M] (NO LONGER IN USE Initial guess)
  0.0
<- S_LWING
  0.50
<- TRW
  0.15
<- ALW
  35.0
<- AXCW
  0.0
<- TCW
  0.11
<- TWISTW (deg)
  -3.0
<- TCT_MAX
  0.05
<- DIHEDW
  6.0

```

```

!Horizontal tail*****
!HT span and AR, specify one and leave the other as 0.0
!ARH(5)          HT Aspect ratio
!TRH(5)_TRW      HT Tapper ratio per wing TRW
!DALH            increment of H-T sweep from wing sweep
!Volume quotient, specify two and leave one blank
! VH(5)          HT volume quotient
! SHSREF(5)      HT area ratio(Sh/Sref)
! ALCH(5)        Lever arm from HT ac to Wing ac (l/c)
!VTTYPE          configuration correction factor
!                =1.0000, fuselage mounted tail
!                =0.8440, T-tail low wing
!                =1.3500, T-tail high wing
!DIHEDH          HT dihedral
!*****

```

```

<- ARH
  4.5
<- TRH_TRW
  2.33
<- DALH
  0.0

```

```

<- VH
0.93581
<- VTTYPE
1.000
<- SHSREF
0.2256
<- ALCH
0.0
<- DIHEDH
1.0

```

```

!Vertical tail*****
!VT span and AR, specify one and leave the other as 0.0
! ARV(5)          VT Aspect ratio
! BV(5)          VT Span
!TRV(5)_TRW      VT Tapper ratio per wing TR
!DALV           increment of V-T sweep from wing sweep
!Volume quotient, specify two and leave one blank
! VV(5)          VT volume quotient
! SVSref(5)      VT area ratio(Sh/Sref)
! ALCV(5)        Lever arm from VT ac to Wing ac (l/c)
!**SWETV(5)      VT wetted area
!**SEXPV(5)      VT exposed area
!**SFV(5)        VT frontal area
!*****

```

```

<- ARV
1.75
<- TRV_TRW
2.0
<- DALV
0.0
<- VV
0.067478
<- SVSREF
0.1220
<- ALCV
0.0
<- DIHEDV
90.0

```

```

!FUSELAGE*****
!INFUSE_FINE      Fuselage fineness ratio used
                  = 0 constant Fineness ratio
                  = 1 Constant cabin cross-section
!ALFUS_DFUS(5)    Fuselage length to max diameter
!HFUS_WFUS(5)     Fuselage height to width
!CHFUS           Fuselage cross-sectional height (required if ALFUS_DFUS=0)
!CWFUS           Fuselage cross-sectional width (required if ALFUS_DFUS=0.0)
!B2L(5)          Ratio of wing half span to fuselage length (Kuchemann's s/L)
!**DMAX(5)        Fuselage maximum diameter
!**FRFUS(5)       Fuselage fineness ratio

```

```

!ALCAB(5)          Length of cabin
!WCAB(5)           Width of cabin
!HCAB(5)           Height of cabin
!**VCAB(5)         Volume of cabin
!**SWETfuse(5)    Fuselage wetted area
!**SFfuse(5)      Fuselage frontal area
!*****

```

```

<- NFUSE_FINE
  1
<- ALFUS_DFUS [-]
  11.787
<- HFUS_WFUS [-]
  1.0
<- CHFUS
  6.20
<- CWFUS
  6.20
<- B2L
  0.0
<- ALCAB [m]
  10.94
<- HCAB [m]
  2.0
<- WCAB [m]
  5.47

```

```

!Nacelles (INTIAL GUESS IF MSPROP = 1) *****
!ALNAC(10)          Nacelle length
!HNAC(10)           Nacelle height
!WNAC(10)           Nacelle width
!DLNAC(10)          Inner Nacelle diameter
!ALNAC_CORR         Nacelle length correction factor
!                   =1.0 for non-mixed turbofan
!                   =1.8 for mixed flow turbofan (AE 3007)
!*****

```

```

<- ALNAC (m)
  7.212 7.212
<- HNAC (m)
  3.960 3.960
<- WNAC (m)
  3.960 3.960
<- DLNAC(m)
  3.960 3.960
<- ALNAC_CORR
  1.0

```

```

*****
AERODYNAMICS input
*****

```

```

!Method Selection *****
!MCDFRIC      Skin friction method
!              =1 General Dynamics method (additional input required)
!              =2 General Dynamics method (additional input required)
!MCDI         Induced drag method
!              =1 VAC/DATCOM symetric drag polar method
!MCDTWAVE     Transonic Wave drag method
!              =1 McDonald Douglas method (MD, additional input required)
!              =2 Grassmeyer method via Mason Configuration Aerodynamics
!MCDTRIM      Trim drag method
!              =1 Torenbeek/Coleman (additional input required)
!MCD_LG       Landing gear drag method
!              =1 Roskam (additional input required)
!MCD_Flaps    Flaps drag Method
!              =1 Roskam (additional input required)
!MCL_MAX      Maximum lift coefficient
!              =1 Roskam (additional input required)
!MCLA         Lift curive slope method
!              =1 DATCOM (additional input required)
!*****

```

```

<- MCDFRIC
  2
<- MCDI
  1
<- MCDTWAVE
  2
<- MCDTRIM
  1
<- MCD_LG
  1
<- MCD_FLAP
  1
<- MCL_MAX
  1
<- MCLA
  1

```

```

!CDfric GD Method *****
!ALGD         airfoil thickness location parameter
!              =1.2 x >= 0.30c
!              =2.0 x < 0.30c
!RFUS         Fuselage Correction factor, Fig III B.2-2a GD handbook
!QNAC         Nacelle interference factor
!*****

```

```

<- ALGD
  1.2
<- APDF
  100.0
<- RFUS
  1.1

```

```

<- QNAC
  1.0
<- NF14
  0
<- RXTW
  2.65E6
<- RXTF
  0.25E6
<- AMAX_LFC
  0.60
<- TURB_LAM_LS
  1.0
<- TURB_LAM_FUS
  1.0
<- WIF
  1.0

```

```

!CLA DATCOM Method *****
!CLAFW(5)      Wing Airfoil lift curve slope
!CLAFH(5)      HT Airfoil lift curve slope
!*****

```

```

<- CLAFW
  6.30
<- CLAFH
  6.13

```

```

!CDI VAC/DATCOM Method *****
!ALERW(5)      Wing Airfoil leading edge radius over chord length, rle/c
!ALERH(5)      Wing Airfoil leading edge radius over chord length, rle/c
!IROUNDW(5)    Wing airfoil leading edge shape
!              =1 round
!              =0 sharp
!IROUNDH(5)    Wing airfoil leading edge shape
!              =1 round
!              =0 sharp
!DECORRECT     OSWALDS EFFICIENCY FACTOR CORRECTION FOR
SUPERCRITICAL WINGS
!              LEADING EDGE CAMBER, VORTEX ATTENUATION, ETC.
!*****

```

```

<- ALERW
  0.007
<- ALERH
  0.007
<- IROUNDW
  1
<- IROUNDH
  1
<- DECORRECT
  1.05

```

```

!CDTWAVE MD Method *****
!MCRIT_H          Critical Mach number switch
!                = 0 manual input of critical Mach Number
!                = 1 Computation of Critical Mach number (Howe)
!AMACHCR          CRITICAL MACH NUMBER (See Corning/GD hand-book) (Not
required for MCRIT_H=1
!AK0              Approximation to the Sears-Haak Body, See methods library
!*****

<- MCRIT_H
  0
<- AMACHCR
  0.80
<- AK0
  1.5

!CD_LG ROSKAM Method *****
!CD_LG            Drag increment due to landing gear (See Table ?? in Drag Methods)
!CD_DE            Oswald efficiency factor increment due to landing gear
!*****

<- CD_LG
  0.015
<- DE_LG
  0.0

!CD_flap ROSKAM Method *****
!CD_FLAP_TO      Drag increment due to Flaps in take-off position
!DE_FLAPTO       Oswald efficiency factor increment due to T-O flaps
!CD_FLAP_TO      Drag increment due to Flaps in take-off position
!DE_FLAPLAND     Oswald efficiency factor increment due to Landing flaps
!*****

<- CD_FLAP_TO
  0.02
<- DE_FLAPTO
  -0.010
<- CD_FLAP_LAND
  0.075
<- DE_FLAPLAND
  -0.015

!CL_Max ROSKAM Method *****
!CL_MAXMAXR      Maximum Lift Coefficient (See Figure 3.1 in ROSKAM)
!CL_LANDR        MAXIMUM Lift Coefficient during LANDING
!CL_MAXNCLEANR   MAXIMUM NEGATIVE Lift Coefficient (FOR VN DIAGRAM)
!*****

<- CL_MAXLANDR
  2.95
<- CL_MAXCLEANR
  1.5

```



```
<- CL_MAXNCLEANR
-1.0
```

```
!APPROXIMATE TRIM DRAG Coleman Method *****
!CM0AF      Approximate wing airfoil zero lift pitching moment
!ANH        Dynamic pressure ratio compared to free-stream at HT
!AMH        Height of the HT from wing normalized to half span
            AMH=H/(B/2)
            (SEE METHODS LIBRARY FOR SUGGESTED VALUES)
!*****
```

```
<- CM0AF
-0.0175
<- ANH
0.85
<- AMH
0.0
```

```
*****
PROPULSION input
*****
```

```
!Method Selection *****
!MTSFC      Thrust specific fuel consumption
!           =1 Turbojet/Turbofan, Howe PROP_MD1
!           =2 Turboprop, Howe PROP_MD2
!           =3 Turbojet, fan, or prop, Mattingly PROP_MD3
!           =4 GASTURB ENGINE DECK
!MTSL_TALT  Ratio of thrust at altitude to thrust at sea-level
!           =1 Turbojet/Turbofan, Howe PROP_MD4
!           =2 Turboprop, Howe PROP_MD5
!           =3 Turbofan, Turbojet or turboprop Mattingly PROP_MD6
!           =4 GASTURB ENGINE DECK
!MSPROP     Method of sizing propulsion system
!           =0 Fixed
!           =1 Svoboda statistics
!*****
```

```
<- MTSFC
3
<- MTSL_TALT
3
<- MSPROP
1
<- SFCC
1.00
<- TTSLC
1.00
```

```
!PROP_MD3 MATTINGLY SFC for Turbojets, Turbofans and Turboprops*****
!NMSOP      Propulsion system option
            =1 High bypass turbofan
```

```

=2 Low bypass turbofan at mil power (max non-afterburning)
=3 Low bypass turbofan at max power (max afterburning)
=4 Turbojet at mil power (max non-afterburning)
=5 Turbojet at max power (max afterburning)
=6 Turboprop
=7 Manual input of statistical constants
!AK1M      1st constant (ONLY REQUIRED FOR NMSOP=7)
!AK2M      2nd constant (ONLY REQUIRED FOR NMSOP=7)
!          (AK1M+AK1M*MACH)*SQRT(THETA0)
!*****

```

```

<- NMSOP
  7
<- AK1M
  0.23
<- AK2M
  0.48

```

```

!PROP_MD6 MATTINGLY T/Tsl for Turbojets, Turbofans and Turboprops*****
!NMTOP      Propulsion system option
            =1 High bypass turbofan
            =2 Low bypass turbofan at mil power (max non-afterburning)
            =3 Low bypass turbofan at max power (max afterburning)
            =4 Turbojet at mil power (max non-afterburning)
            =5 Turbojet at max power (max afterburning)
            =6 Turboprop
!TRM        Throttle ratio
!AK2M      2nd constant (ONLY REQUIRED FOR NMSOP=7)
!          (AK1M+AK1M*MACH)*SQRT(THETA0)
!*****

```

```

<- NMTOP
  1
<- TRM
  1.0

```

```

*****
Structural Load Estimation input
*****

```

```

!Method Selection *****
!MVN        Velocity-Load factor diagram (V-N)
!          =0 none
!          =1 FAR25 STRUCT_MD1
!NGLA       Gust load alleviation switch (using max maneuvering as limit)
!          =0 no gust load alleviation
!          =1 gust load alleviation
!*****

```

```

<- MVN
  1
<- NGLA

```

0

Weigh Estimation input

!Method Selection *****
!MFF Fuel fraction estimation (SWITCH INACTIVE, ROSKAM DEFAULT)
! =0 VDK
! =1 Roskam WB_MD1 (additional input required)
!MWING_STRUC Wing weight method (IF MWING_STRUC = 0 ISTR INPUT IS USED)
! =0 VDK
! =1 Howe WB_MD2(additional input required)
! =2 Howe Physical WB_MD7 (additional input required)
! =3 General Dynamics Method WB_MD9 (additional input required)
!MFUSE_STRUC Fuselage weight method
! =0 VDK
! =1 Howe WB_MD 3 (additional input required)
! =2 Torenbeek (additional input required)
!MHT_STRUC Horizontal tail/empennage weight method
! =0 VDK
! =1 Howe WB_MD 8(additional input required)
! =2 Torenbeek (additional input required)
!MVT_STRUC Vertical tail weight method
! =0 VDK
! =1 Howe WB_MD 8(no additional input required, must use Howe for
HT)
! =2 Torenbeek (additional input required)
!MNAC_STRUC Nacelle/Pylon structure
! =0 VDK
!MOPER Operational items
! =0 VDK
! =1 Howe WB_MD6
!MEQP Equipment weight
! =0 VDK
! =1 Howe WB_MD6
!MLG_STUC Landing Gear
! =0 VDK
! =1 Torenbeek (additional input required)
!MSYS Fixed systems weight
! =0 VDK
! =1 Torenbeek (VDK is still active, set systems values to zero)
!MBALANCE c.g. estimation method
! =0 no balance computed, constant SM assumed
! =1 Roskam (ADDITIONAL INPUT REQUIRED)
!*****

<- MFF
1
<- MWING_STRUC
3
<- MFUSE_STRUC

```

1
<- MHT_STRUC
2
<- MVT_STRUC
2
<- MPROP
2
<- MOPER
0
<- MEQP
0
<- MLG_STRUC
1
<- MSYS
1
<- MBALANCE
1

```

```

!WEIGHT_MD1 ROSKAM FUEL FRACTION*****
!WR_ST          start up weight ratio
!WR_TAX         Taxi weight ratio
!WR_TO         Take-off weight ratio
!WR_DE         Descent weight ratio
!WR_L          Landing weight ratio
!climb, cruise and reserve weight ratios are computed internally
!*****

```

```

<- WR_ST
0.990
<- WR_TAX
0.995
<- WR_TO
0.995
<- WR_L
0.992

```

```

!WEIGHT_MD9 GENERAL DYNAMICS EMPRICAL WING WEIGHT *****
!REFERENCE FOR AMCORRECT IS AN ALUMINUM AIRFRAME WITH THE FOLLOWING TE
AND LE BOXS
!LE BOX        SLAT
!TE BOX        FOWLER/DOUBLE SLOTTED FLAPS
!              SPOILERS
!              AILERONS
!AMCORRECT_GD  Statistical correction to the wing weight fraction (SEE HOWE TABLE
AD4.1A)
!ENGMT         Inertial relief factor for wing mounted engines
!              =0.12 no wing-mounted engines
!              =0.2 2 wing-mounted engines
!              =0.22 4 wing mounted engines
!WING_MAT_GD   Material correction factor (multiplication)
!*****

```

```
<- AMCORRECT_GD
0.007
<- ENGMT_GD
0.2
<- WINGMAT_GD
1.0
```

```
!WEIGHT_MD12 TORENBECK EMPRICAL HT WEIGHT *****
!AKHT          Statistical constant (see methods library)
!              =1.0, fixed HT
!              =1.1, variable incidence
!HTCORR        Horizontal tail correction factor
!*****
```

```
<- AKHT
1.1
<- HTCORR
1.0
```

```
!WEIGHT_MD13 TORENBECK EMPRICAL VT WEIGHT *****
!ZH_BV         Vertical height of horizontal tail / span of vertical
!              =0.0 for fuselage mounted HT
!VTCORR        Horizontal tail correction factor
!*****
```

```
<- ZH_BV
0.0
<- VTCORR
1.0
```

```
!WEIGHT_MD3 HOWE FUSELAGE WEIGHT *****
!NPRES        PRESSURIZED FUSELAGE SWITCH
!              =0, NON PRESSURIZED FUSELAGE
!              =1, PRESSURIZED FUSELAGE
!C2           Statistical constant (see methods library)
!ALTCP        CABIN PRESSURE EQUIVLENT ALTITUDE (REQUIRED FOR NPRES=1
ONLY)
!*****
```

```
<- NPRES
1.0
<- C2
0.79
<- ALTCP (m)
3000.0
```

```
!WEIGHT_MD5 HOWE SYSTEMS, EQUIPMENT AND LG WEIGHT *****
!C4           Statistical constant (see methods library)
!*****
```

```
<- C4
0.16
```

```

!WEIGHT_MD14 Torenbeek Landing gear WEIGHT *****
!AGNG          Statistical constants for noise gear (see methods library)
!BGNG
!CGNG
!DGNG
!AKNR
!AGMG          Statistical constant for main gear(see methods library)
!BGMG
!CGMG
!DGMG
!AKMR
!*****

```

```

<- AGNG
  20.0
<- BGNG
  0.10
<- CGNG
  0.00
<- DGNG
  2.0e-6
<- AKNR
  1.0
<- AGMG
  40.0
<- BGMG
  0.16
<- CGMG
  0.019
<- DGMG
  1.5e-5
<- AKMR
  1.0

```

```

!WEIGHT_MD6 HOWE OPERATIONAL ITEMS WEIGHT *****
!NPAX_CARGO    PASSENGER OR CARGO SWITCH
!              =1 PASSENGER
!              =2 CARGO
!FOP          Statistical constant (see methods library)
!*****

```

```

<- NPAX_CARGO
  1
<- FOP
  16.0

```

```

!WEIGHT_MD15 TORENBECK FIXED SYSTEMS WEIGHT*****
!AKFCS        Statistical constant for flight control system
!AKHPS        Statistical constant for Hydraulic and pneumatic system
!AKFUR        Statistical constant for furnishings
!AOX          Statistical constant for oxygen system

```

!BOX Statistical constant for oxygen system
!AKAPU Statistical constant for APU
!AKBC Statistical constant for baggage handling equipment
!AKAUX Statistical constant for auxiliary systems

!*****

<- AKFCS
0.44
<- AKHPS
0.006
<- AKFUR
0.211
<- AOX
40.0
<- BOX
2.4
<- AKAPU
0.013
<- AKBC
0.0
<- AKAUX
0.01

!WEIGHT DP2 VDK METHOD FOR COMMERCIAL TRANSPORTS*****

!FPRV passenger provisions (kg/person)
!ETW Engine thrust to weight ratio (kg thrust/kg)
!ETW_SC Scramjet thrust to weight ratio (kg thrust/kg)
!AKVE_TJ Turbojet specific volume (m³/kg thrust)
!AKVE_SC Scramjet specific volume (m³/kg thrust)
!AMU Minimum OWE weight margin
!FSYS variable system weight coefficient (kg/kg)
!CUN Unmanned system weight (kg)
!VUN Unmanned fixed system volume (m³)
!FMND crew system specific weight (kg/person)
!AKVV void volume coefficient (m³/m³)
!AKVS system volume coefficient (m³/m³)
!FCRW Fixed crew member specific volume(m³/person)

!VPCRW crew provisions volume (m³/person)
!AKCRW crew member volume (m³/person)
!V_PAX Passenger volume (m³/pax)
!RHO_CARGO Cargo density (kg/m³)
!EBAND Error band around the structural fraction EBAND (+/- 0.049)

!*****

<- FPRV
16.0
<- ETW
5.98
<- AKVE
0.000
<- AMU

```

0.00
<- FSYS
0.0
<- CUN
0.0
<- VUN (5 cu m VOID)
0.0
<- FMND
0.0
<- AKVV
0.20
<- AKVS
0.05
<- FCRW !ACCOUNTED FOR IN PAYLAOD AND CREW VOLUME
1.0
<- VPCRW
1.5
<- AKCRW
2.0
<- V_PAX
2.0
<- RHO_CARGO
326.72
<- EBAND
-0.049

```

```

*****
c.g estimation input
*****

```

```

!Roskam method *****
!ISM Target Static margin
!XCG_TOGW_D Initial TOGW c.g. location (% MAC)
!XCG_MLW Initial MLW c.g. location (% MAC)
!CRW_CG Crew c.g. (x, y, z)
! X - FRACTION OF NOISE
! Y - FRACTION OF WIDTH (FROM CENTERLINE)
! Z - FRACTION OF HEIGHT (FROM CENTERLINE)
!OP_CG Operating items c.g. (x, y, z)
! X - FRACTION OF FUSELAGE LENGTH
! Y - FRACTION OF FUSELAGE HEIGHT (FROM
CENTERLINE)
! Z - FRACTION OF FUSELAGE WIDTH (FROM CENTERLINE)
!APAY_D_CG Design Payload c.g. (x, y, z)
! X - FRACTION OF CABIN LENGTH
! Y - FRACTION OF WIDTH
! Z - FRACTION OF HEIGHT (FROM CENTERLINE)
!APAY_MAX_CG Max Payload c.g. (x, y, z)
! X - FRACTION OF CABIN LENGTH
! Y - FRACTION OF WIDTH (FROM CENTERLINE)
! Z - FRACTION OF HEIGHT (FROM CENTERLINE)

```


!FUEL_CG_W	Wing Fuel c.g. (x, y, z)
!	X - FRACTION OF CHORD LEGHTH
!	Y - FRACTION OF SPAN/2
!	Z - FRACTION OF THICKNESS
!FUEL_CG_F	Fuselage fuel c.g. (x, y, z)
!	X - FRACTION OF FUSELAGE LENGTH
!	Y - FRACTION OF FUSELAGE HIGHT (FROM CENTERLINE)
!	Z - FRACTION OF FUSELAGE WIDTH (FROM CENTERLINE)
!WING_CG	Wing structure c.g. (x, y, z)
!	X - FRACTION OF CHORD LEGHTH
!	Y - FRACTION OF SPAN/2
!	Z - FRACTION OF THICKNESS
!HT_CG	Horizontal tail structure c.g. (x, y, z)
!	X - FRACTION OF CHORD LEGHTH
!	Y - FRACTION OF SPAN/2
!	Z - FRACTION OF THICKNESS
!VT_CG	Vertical tail structure c.g. (x, y, z)
!	X - FRACTION OF CHORD LEGHTH
!	Y - FRACTION OF THICKNESS
!	Z - FRACTION OF SPAN/2
!FUSE_CG	Fuselage structure c.g. (x, y, z)
!	X - FRACTION OF FUSELAGE LENGTH
!	Y - FRACTION OF FUSELAGE HEIGHT (FROM
CENTERLINE)	
!	Z - FRACTION OF FUSELAGE WIDTH (FROM CENTERLINE)
!NACC_CG	Nacelle structure c.g. (x, y, z)
!	X - FRACTION OF NAC LENGTH
!	Y - FRACTION OF NAC WIDTH (FROM CENTERLINE)
!	Z - FRACTION OF NAC HEIGHT (FROM CENTERLINE)
!ENG_CG	Engine c.g. (x, y, z)
!	X - FRACTION OF NAC LENGTH
!	Y - FRACTION OF NAC WIDTH (FROM CENTERLINE)
!	Z - FRACTION OF NAC HEIGHT (FROM CENTERLINE)
!ANG_CG	Noise gear c.g. (x, y, z)
!	X - FRACTION OF STRUT LENGTH
!	Y - FRACTION OF STRUT HEIGHT (FROM CENTERLINE)
!	Z - FRACTION OF STRUT WIDTH (FROM CENTERLINE)
!AMG_CG	Main gear c.g.(x, y, z)
!	X - FRACTION OF STRUT LENGTH
!	Y - FRACTION OF STRUT HEIGHT (FROM CENTERLINE)
!	Z - FRACTION OF STRUT WIDTH (FROM CENTERLINE)
!FC_CG	Flight control system c.g.(x, y, z)
!	X - FRACTION OF FUSELAGE LENGTH
!	Y - FRACTION OF FUSELAGE WIDTH (FROM CENTERLINE)
!	Z - FRACTION OF FUSELAGE HEIGHT (FROM
CENTERLINE)	
!HPS_CG	Hydraulic and pneumatic system c.g.(x, y, z)
!	X - FRACTION OF FUSELAGE LENGTH
!	Y - FRACTION OF FUSELAGE WIDTH (FROM CENTERLINE)
!	Z - FRACTION OF FUSELAGE HEIGHT(FROM
CENTERLINE)	
!ELS_CG	Electrical system c.g.(x, y, z)


```
<- XCG_C_TOGW_D
0.285
<- XCG_C_MLW
0.15
<- CRW_CG
0.95 0.00 0.00
<- OP_CG
0.45 0.00 0.00
<- APAY_D_CG
0.65 0.00 0.00
<- APAY_MAX_CG
0.65 0.00 0.00
<- FUEL_CG_W
0.45 0.50 0.00
<- FUEL_CG_F
0.55 0.00 0.00
<- WING_CG
0.45 0.40 0.00
<- HT_CG
0.42 0.38 0.00
<- VT_CG
0.42 0.00 0.40
<- FUSE_CG
0.45 0.00 0.00
<- ANACC_CG
0.40 0.00 0.00
<- ENG_CG
0.50 0.00 0.00
<- ANG_CG
0.50 0.00 0.00
<- AMG_CG
0.50 0.00 0.00
<- FC_CG
0.61 0.00 0.00
<- HPS_CG
0.60 0.00 0.00
<- ELS_CG
0.60 0.00 0.00
<- AIAE_CG
0.60 0.00 0.00
<- API_CG
0.10 0.00 0.00
<- APU_CG
0.91 0.00 0.00
<- OX_CG
0.50 0.00 0.00
<- FUR_CG
0.65 0.00 0.00
<- BC_CG
0.65 0.00 0.00
<- AU_CG
0.41 0.00 0.00
```

<- PT_CG
0.50 0.00 0.00

COST input

!Method Selection *****

!MRDTE_FA RDT&E and Fly away Costs
! =1 Hess/Raymer (additional input required)
! =2 levenson/Roskam (additional input required)
! =3 Roskam (ballpark method, additional input required)
!MBLOCK Block mission method
! =1 Roskam (additional input required)
!MFLYDOC Flying Direct operating cost
! =1 Roskam (additional input required)
!MMDOC MAINTAINENCE Direct operating cost
! =1 Roskam (additional input required)
!MDEPDOC Depreciation operating cost
! =1 Roskam (additional input required)
!MLNTFDOC LANDING, NAVIATION, TAXES AND FINANCING operating cost
! =1 Roskam (additional input required)
!*****

<- MRDTE_FA
1
<- MBLOCK
1
<- MFLYDOC
1
<- MMDOC
1
<- MDEPDOC
1
<- MLNTFDOC
1

!COST_MD1_DAPCA RDT&E+FLYAWAY COST *****

!QUANT Quantify of aircraft produced
!FTA Number of flight test aircraft
!TT4 Total temperature at turbine inlet (for engine cost)
!RE Engineering costs per man hour (1999 dollars)
!IRT tooling costs per man hour (1999 dollars)
!IRM Manufacturing costs per man hour (1999 dollars)
!CPAX Interior cost per passenger
!IAVIONICS Aviations cost switch
! =1 per OWE
! =0 per RDT&E+Flyaway cost
!CAVOWE Cost per OWE (required if IAVIONICS = 1)
!CAVRD Cost per RDT&E+flyaway cost (required if IAVIONICS = 0)
!AINFLAT Adjustment from 1999 dollars to then dollars
!PRFMARG Required profit margin for the manufacturer

```

!ICARO      Cargo aircraft switch
!           = 0 no
!           = 1 yes
!CORMAT     Correction factor for materials (See Method Library)
!*****

```

```

<- QUANT
  350.0
<- FTA
  2
<- TT4
  2500.0
<- RE
  86.0
<- RT
  88.0
<- RM
  81.0
<- CPAX
  2500.0
<- IAVIONICS
  0
<- CAVOWE (NOT IN USE)
  3000.0
<- CAVRD
  0.25
<- AINFLAT
  1.279
<- PRFMARG
  0.20
<- ICARGO
  0
<- CORMAT
  1.0

```

```

!COST_MD10_RACUNIT A/C UNIT COST BALLPARK METHOD(ROSKAM) *****
!AUNITQ           CORRELATION COEFFICIENT
!BUNITQ           CORRELATION COEFFICIENT
! ACUNIT(1989)=10^(AUNITQ+BUNITQ*LOG(TOGW))
!AINFLATQ         INFLATION CORRECTION FROM 1989 TO THEN DOLLARS
!*****

```

```

<- AUNITQ
  3.3191
<- BUNITQ
  0.8043
<- AINFLATQ
  1.7575

```

```

!COST_MD2_RBLOCK BLOCK MISSION (ROSKAM) *****
!R_BLOCK         block range

```

```

!IFLIGHT          Domestic or international flight
!IAUTIL           Specification of Annual utilization
!                = 1 for commercial transport (based on block time)
!                = 0 manual input of annual flight hours
!UANNFLT          Annual flight hours (required if IAUTIL = 0)
!*****

<- R_BLOCK [KM]
  14075.2
<- IFLIGHT
  2
<- IAUTIL
  1
**<- UANNFLT [HRS/year]
  400.0

!COST_MD3_RFD0C Flying DOC (ROSKAM) *****
!ANCREW(4)        number of crew
!                ANCREW(1) = number of cabins
!                ANCREW(2) = number of copilots
!                ANCREW(3) = number of flight engineers
!                ANCREW(4) = number of flight attendants
!AVTIT(4)         Correction factor for vacation, training, insurance and taxes
!                AVTIT(1) = number of cabins
!                AVTIT(2) = number of copilots
!                AVTIT(3) = number of flight engineers
!                AVTIT(4) = number of flight attendants
!SAL(4)           Salary
!                SAL(1) = number of cabins
!                SAL(2) = number of copilots
!                SAL(3) = number of flight engineers
!                SAL(4) = number of flight attendants
!AH(4)            Number of flight hours per year
!                AH(1) = number of cabins
!                AH(2) = number of copilots
!                AH(3) = number of flight engineers
!                AH(4) = number of flight attendants
!TEF(4)           Travel expense for each flight crew member
!                TEF(1) = number of cabins
!                TEF(2) = number of copilots
!                TEF(3) = number of flight engineers
!                TEF(4) = number of flight attendants
!FUEL_P           Fuel price (per gallon)
!FUEL_D           Fuel density
!OLP              Oil price (per gallon)
!OD               Oil density
!FINSHULL         Annual hull insurance rate
!AINFDOC          Correct for flying DOC to then dollars
!*****

<- ANCREW (4)
  1.0 1.0 0.0 14.0

```

```

<- AVTIT (4)
  0.26 0.26 0.0 0.0
<- SAL (4) [$/year]
  85000.0 50000.0 0.0 32000.0
<- AH [HRS/year]
  750.0 750.0 0.0 750.0
<- TEF
  11.0 11.0 0.0 11.0
<- FUEL_P ($/liter) (approx $5.00/gallon, 1 U.S. $/ US gallon = 0.264172052 U.S. $/ liter)
  1.32086
<- FUEL_D_KGLIT (kg/liter)
  0.80763
<- OLP ($/liter)
  0.0
<- OD
  0.87063
<- FINSHULL
  0.05
<- AINFDOC
  1.0

```

```

!COST_MD4_RMDOC Maintenance DOC (ROSKAM) *****
!RAFM           Airframe maintence labor rate per man hour
!ICAFL         airframe man hours switch
!              = 0 Compute from OWE
!              = 1 Compute from airframe maintenance man hrs / fit hr
!AMHRAF_FLT    Number of airframe and systems man hours per flight hour
!AMHRAF_BL     Number of airframe and systems man hours per block hour
!RENM          Engine maintence labor rate per man hour
!ICENG         Engine man hours switch
!              = 0 Manual input of engine maintenance man hrs / block hr
!              = 1 Compute from engine maintenance engine weight and TBO
!AMHREN_FLT    Number of engine maintenance man hours per flight hour
!TBO           Time between engine overhauls
!AINMDOC       Inflation rate between 1989 and then dollars
!ESPPF         Engine spare parts factor
!FAMLB         Overhead distribution factor for labor, building, etc.
!FAMMAT        Overhead distribution factor for labor, building, etc.
!*****

```

```

<- RAFM [$/hr]
  16.0
<- ICAFL
  0
<- AMHRAF_FLT (NOT USED)
  6.0
<- RENM [$/hr]
  16.0
<- ICENG
  1
<- AMHREN_FLT (NOT USED)
  0.45

```

```

<- TBO [HRS] (assumed!!!!)
16000.0
<- AINMDOC [THEN YEARS/1989]
1.27
<- ESPPF
1.5
<- FAMLB
1.10
<- FAMMAT
0.60

!COST_MD5_RDEPDOC Depreciation DOC (ROSKAM) *****
!FDAF           Airframe depreciation factor
!DPAF           Airframe depreciation period
!FDENG         Engine depreciation factor
!DPEN          Engine depreciation period
!FDPROP        Propeller depreciation factor
!DPPROP        Propeller depreciation period
!FDAV          Avionics depreciation factor
!DPAV          Avionics depreciation period
!FDAFSP        Airframe spare parts depreciation factor
!FAPSPAF       Airframe spare parts factor
!DPAFSP        Airframe spare parts depreciation period
!FDENSP        Engine spare parts depreciation factor
!FENSPAF       Engine spare parts factor
!ESPPF         Engine spare parts price factor
!DPENSP        Engine spare parts depreciation period
!*****

<- FDAF
0.85
<- DPAF [YRS]
20.0
<- FDEN
0.85
<- DPEN [YRS]
15.
<- FDPROP
0.85
<- DPPROP [YRS]
7.
<- FDAV
1.00
<- DPAV [YRS]
5.
<- FDAFSP
0.5
<- FAFSPAF
0.10
<- DPAFSP [YRS]
20.
<- FDENSP

```



```

0.85
<- FENSPAF
0.25
<- ESPPFD (part included in engine price, otherwise 1.5)
1.0
<- DPENSP [YRS]
7.

!COST_MD6_RLNTF LANDING,NAV,TAXES,FIN DOC (ROSKAM)
*****
!ICACLF          Landing fees switch
!                =0 manual input
!                =1 based on TOGW
!CACLF          airport landing fee per landing
!CACNF          aircraft landing fee per flight
!IFRT           tax rate switch
!              = 0 manual input
!              = 1 based on TOGW
!FRT            tax rate/DOC
!CFIN_DOC       fraction of finance fees per DOC
!*****

<- ICACLF
1
<- CACLF (NOT USED)
1.0
<- CACNF
10.0
<- IFRT
1
<- FRT (NOT USED)
1.0
<- CFIN_DOC
0.07

```

REFERENCES

1. Spreen, W. *Marketing in the international Aerospace Industry*. Burlington : Ashgate Publishing Company, 2007.
2. Chudoba, B., Coleman G.,. *Conceptual Design assessment of a Suborbital Space Access Vehicle.*: The Aeronautical Journal,, 2008. Vol. 112, 1135.
3. Braslow, A. *A History of Suction-Type Laminar-Flow Control with Emphasis on Flight Research*. Washington, DC : NASA History Division Office of Policy and Plans, 1999.
4. Urie, D., Reaser, J. *Aerodynamic Development of a Small Horizontal Tail for an Active Control Relaxed Stability Transport Applications*. AIAA-79-1653, American Institute of Aeronautics and Astronautics, 1979.
5. Ko, A., Schetz, J., Mason, W. *Assesemtn of the Potential Advantages of Distributed-Propulsion for Aircraft*. Blackburg: Multidisciplinary Analysis and Design Center for Advanced Vehicles, Virginia Polytechnic Institute and State Univeristy, 203. ISABE-2003-1094.
6. Schetz, J.A., et al. *Multidisciplinary Design Optimization of Truss Braced Wing Airplanes*. Hampton, VA: Truss Braced Wing Workshop, 2009.
7. Heinze, W.,. *Ein Beitrag zur Quantitativen Analyse der Technischen und Wirtschaftlichen Auslegungsgrenzen Verschiedenster Flugzeugkonzepte fur den Transport grober Nutzlasten*. Braunschweig, Germany, PhD. Dissertation, Technical University Braunschweig, 1994.
8. Sobieszczanski-Sobieski, J, Hafka, R.T. Multi-disciplinary Aerospace Design Optimization: Survey of Recent Developments. *Structural Optimization* 14, 1-23, Pringer-Verlag, 1997.
9. Chudoba, B. *Stabiliy and Control Oof Conventional and Unconventional Aircraft Configurations A Generic Approach*. s.l. : BoD-Books on Demand, 2001.
10. Xiao, H. *A Prototype Computerized Synthesis Methodology for Generic Space Access Vehicle (SAV) Conceptual Designq*. Norman, OK : PhD. Dissertation, University of Oklahoma, 2006.
11. Warner, E. *Airplane Deisgn: Performance*. New York : McGraw-Hill, 1936.
12. Wood, K.D. *Aerospace Vehilce Design Volume I, Aircraft Design*. Boulder, Colorado : Johnson Publishing Company, 1963.
13. Brunk, S. *Handbook for Preliminary Design Engineers*. Fort Worth, Convair, a Division of General dynamics.

14. Louthan, J. *Parametric Airplane Design and Sizing*. Grand Prairie, Chance- Vought Corporation, Aeronautics and Mission Division, 1961.
15. Corning, G. *Supersonic and Subsonic Airplane Design*. Ann Arbor, Michigan : Edwards Brothers, Inc., 1953.
16. Loftin, L.K. *Subsonic Aircraft: Evolution and the Matching of Sizing to Performance*. Hampton, Virginia, NASA RP 1060m, NASA Langley Research Center, 1980.
17. Kossira, H. *Arbeitsblätter Zur Vorlesung, Flugzeugbau I*, Teil I. s.l. : Lehrstuhl und Institut für Flugzeugbau und Leichtbau, 1980.
18. Torenbeek, E. *Synthesis of Subsonic Airplane Design*. Boston : Delft University, 1982.
19. Stinton, D. *Design of the Aeroplane*. Oxford, England : BSP Professional Books, 1983.
20. Nicolai, L. *Fundamentals of Aircraft Design*. Ohio : METS, Inc., 1975.
21. Renner, A. Vorlesungsmitschrift zum Fach, Luft- und Raumfahrzeuge I. Ausgabe : Ditte, überarbeitete Ausgabe, 1984.
22. Hienemann, E. *Aircraft Design*. Baltimore : Nautical and Aviation Publishing Co., 1985.
23. Roskam, J. *Airplane Design, Parts I - VII*. Lawrence, Kansas : DARcorporation, 2003.
24. Whitford, R. *Design for Air Combat*. London : Janes, 1987.
25. Shevell, R. *Fundamentals of Flight*. New Jersey : Prentice-Hall, 1983.
26. Czysz, P. *Flight Vehicle Analysis and Design*. St Louis Course notes, Parks College, 1994.
27. Madelung. *Skriptum zur Vorlesung, Luftfahrttechnik II*. München, TU München, 1994.
28. Fielding, J. *Introduction to Aircraft Design*. Cambridge : Cambridge University Press, 1999.
29. Huenecke, K. *Modern Combat Aircraft Design*. Reston : American Institute of Aeronautics and Astronautics, 2006.
30. Kroo, I. *Aircraft Design Synthesis and Analysis*. [Online] September 2006. [Cited: November 1, 2009.] adg.stanford.edu/aa241/AircraftDesign.html.
31. Scholz, D. *Skript Zur Vorlesung, Flugzeugentwurf*. Hamburg Fachhochschule Hamburg, Fachbereich Fahrzeugtechnik, 1999.
32. Thomas, F. *Fundamentals of Sailplane Design*. College Park : College Park Press, 1993.
33. Jenkinson, L., Simpkin, P., Rhodes, D.,. *Civil Jet Aircraft Design*. Reston, Virginia : AIAA Education Series, 1999.
34. Heinze, W. *Aircraft Design Course Material*. Braunschweig, Technische Universität Braunschweig, 1999.
35. Whitford, R. *Fundamentals of Fighter Design*. London : Airlife, 2000.

36. Howe. *Aircraft Conceptual Design Synthesis*. s.l. : Professional Engineering Publishing Ltd., 2000.
37. Schaufele, R. *The Elements of Aircraft Preliminary Design*. Santa Ana, California : Aries Publications, 2000.
38. —. *Aircraft Preliminary Design and Performance*. Long Beach Aerospace Engineering Department, California State University Long Beach, 2003.
39. Vout-Nitschmann, R. *Einführung in die Luftfahrttechnik*. Stuttgart, IFB Institut Für Flugzeugbau, Universität Stuttgart, 2001.
40. Throbeck, J. *Manuskript zur Integrierten Lehrveranstaltung Flugzeugentwurf I und II*. Berlin, Technische Universität Berlin, 2001.
41. Mason, W. *Airplane Design, AOE 4065/4066*. Blacksburg, Virginia Polytechnic Institute, Department of Aerospace and Ocean Engineering, 2002.
42. Corke, T. *Design of Aircraft*. Upper Saddle River : Prentice Hall, 2003.
43. Raymer, D. *Aircraft Design: A Conceptual Approach, 3rd Edition*. Reston, Virginia : AIAA Educational Series, 1999.
44. Roskam, J. Anematt, W. *AAA (Advanced Aircraft Analysis): A user-friendly Approach to Preliminary Aircraft Design*. ICAS-90-2.10.2, ICAS, 1991.
45. Bargetto, R., Mazzetti, B., Garbolino, G. *Aircraft Configuration Analysis/Synthesis Expert System: A New Approach to Preliminary Sizing of Combat Aircraft*. ICAS 88-1.112, 1988.
46. Anon. *Aircraft Synthesis Analysis Program Description Volumes II - IX*. Dallas, Texas : LTV Aerospace and Defense, Vought Aero Products Division, 1985. 2-52400/5R-17.
47. Gelhausen, P. *ACSYNTH - A Standards-Based Systems for Parametric Computer Aided Conceptual Design of Aircraft*. Irvine, CA : AIAA 92-1268, American Institute of Aeronautics and Astronautics, 1992.
48. Hale, M., Mavis, D. Dennis, C. *The Implementation of a Conceptual Aerospace Systems Design and Analysis Toolkit*. s.l. : SAE/AIAA 1999-01-5639, 1999.
49. Wallace, R.E. *A Computerized System for the Preliminary Design of Commercial Airplanes*. AIAA 72-793, 1972.
50. Marinopolous, S., Jackson, D., Shupe, J., Mistree, F. *Compromise: An Effective Approach for Conceptual Aircraft Design*. AIAA 87-2965, 1987.
51. McCullers, L.A. *Aircraft Configuration Optimization Including Optimized Flight Profiles*. Hampton Virginia : Kentron International, Inc., 1987. N87-117743.
52. Seffinga, B. *Development of an interactive Computerized Aircraft Design System*. Los Angeles, AIAA 96-5529, World Aviation Congress, 1996.

53. Mavris, D.,N., DeLaurentis, D. *Methodology for Examining the Simultaneous Impact of Requirments, Vehilce Characteristics, and Technologies on Military Aircraft Design*. Atlanta, GA : ICAS 145.1, 2000.
54. Reith, D. *Technology Assessment with Mulit-Diciplinary Aircraft Design Tools on the Next Generation Supersonic Commerical Transport*. ICASE 96-3.5.1, 1996.
55. Daberkow, D., Mavris, D. *New Approaches to Conceptual and Preliminary Aircraft Design: A Comparative Assessment of a Neural Network Formulation and a Response Surface Methodolgoy*. 1998, AIAA 98-5509.
56. Dirks, G., Schneegans, A. *Scenario Based Aircraft Design Using Knowledge Based Software Methods*. ICAS 2000 Congress,pp 5103.1-5103.10, 2000.
57. Braun, R., Kroo, I. *Post-Optimality Analysis in Aerospace Vehilce Design*. AIAA 93-3932, 1993.
58. Simos, D. *Piano - Competitor Evaluation and Project Definition of Commerical Aircraft*. At your desktop. Lissys Research, 1991.
59. Raymer, D. *RDS Integrated Softward for Aircraft Design & Analysis - Presentation*. Playa del Rey, CA : Conceptual Research Corp. (www.aircraftdesign.com), 2010.
60. Lee, V., Ball, G., Wadsworth, E., Moran, W., and McLeod, J. *Computerized Aircraft Synthesis*. Journal of Aircraft, Vol. 4, No. 5, Sept-Oct 1967, pp. 402-408, 1967.
61. Cousin, J., Metcalfe, M. *The BAe (Commerical Aircraft) Ltd Transport Aircraft Synthesis and Optimization Program (TASOP)*. AIAA 90-3295, 1990.
62. Ardema, M., Williams, L. *Automated Synthesis of Transonic Transport*. AIAA 72-794, 1972.
63. Bouchard, E. *Concepts for a Future Aircraft Design Environment*. AIAA 92-1188, 1992.
64. Czysz, P.A.,. *Hypersonic Convergence - Volume 1*. Dayton, Ohio : AFRL-VA-WP-TR-2004-3114, Air Force Research Laboratory, 2004.
65. Simpson, T., Peplinski, J., Koch, P., Allen, J. *Metamodels for Computer-based Engineering Design: Survey and Recommendations*. London : Engineering with Computers, Springer-Verlag, 2001.
66. LANGLEY, N. *Vehicle sketch pad, .NASA Langley Software Platform for Rapid Aircraft Geometry*. Hampton, VA : http://www.sbir.nasa.gov/SBIR/STTR_05_P1, 2005.
67. Chudoba, B., Huang, X. *Development of a Dedicated Aerospace Vehicle Conceptual Design Knowledge Based System*. Reno AIAA 2006-0225, 44th Aerospace Sciences Meetign and Exhibit, 2006.
68. Davis, R. *Knowelege Based Systems in Artifical Intelegents, Part 2: TEIRESIAS, Applications of Meta Level Knowledge*. McGraw-Hill, 1982.
69. Chudoba, B., Coleman, G. *Generic Stability and Contorl for Aerospace Flight Vehilce Conceptual Design*. The Aeronautical Journal, 2008. Vol. 112, 1132.

70. Coleman, G. *A Generic Stability and Control Tool for Flight Vehicle Conceptual Design: Software Development*. Arlington, TX : Masters Thesis, The University of Texas at Arlington, 2007.
71. Chudoba, B., Coleman, G., Huang, X. *Conceptual Design Assessment of Suborbital Tourist Space Access Vehicle (SAV)*. Reno AIAA 2006-1240, 44th AIAA Aerospace Sciences Meeting and Exhibit, 2006.
72. Chudoba, B., Coleman, G., Czysz, P. *Feasibility Study of a Supersonic Business Jet Based on the LearJet Airframe*. The Aeronautical Journal, Volume 112, Number 1132, 2008, 2009.
73. Chudoba, B. Coleman, G., et al. *Development of Advanced Commercial Transport Aircraft Configurations (N+3 and Beyond Through the Assessment of Past, Present and Future Technologies - Final Report*. Langley : AVD Research Report, Presented at the National Institute of Aerospace, 2009.
74. Miller, J. *The X-Planes, X-1 to X-45 3rd Edition*. s.l. : Allan, Ian Publishing, 2001.
75. Droste, C., Walker, J. *The General Dynamics Case Study on the F-16 Fly-By-Wire Flight Control System*. Reston, VA : American Institute of Aeronautics and Astronautics, AIAA Professional Series.
76. Mead, L., Coppi, C., Strakosch, J.,. *A Case Study By Gruman Aerospace Corporation and Gulfstream American Corporation on the Gulfstream III*. Reston, VA : American Institute of Aeronautics and Astronautics, AIAA Professional Study Series, 1980.
77. Hiscocks, R. *A Case Study on the De Havilland Family of STOL Commuter Aircraft*. Reston, VA : American Institute of Aeronautics and Astronautics, AIAA Professional Series.
78. Nassi, I., and Schniederman, B. *Flowchart Techniques for Structured Program*. New York, New York : SIGPLAN Notices, Department of Computer Science, State University of New York, 1973.
79. Coleman, G. *AVD Parametric Sizing Methods Library*. Arlington : AVD Lab internal report, Publication pending , 2010.
80. Hahn, A. *Personal Communication*. 2009.
81. Schetz, J., Kapania, R., Mason, W. *Virginia Tech Truss-Braced Wing Team (Initial Structural Analysis Study)*. Jan. 2008.
82. Vihn, N. *Flight Mechanics of High-Performance Aircraft*. Cambridge, UK : Cambridge University Press, 1999.
83. Mason, W.H. *Transonic Aerodynamics of Airfoils and Wings*. Blacksburg, Virginia : Course Notes: Configuration Aerodynamics, http://www.aoe.vt.edu/~mason/Mason_f/ConfigAeroTransonics.pdf, 2009.
84. Morris, J., Ashford, D. *Aircraft Fuselage Configuration Studies Point to Use of Multideck Fuselages*. s.l. : SAE 670370, 1967.

85. Liebeck, R. *Design of the Blended-Wing-Body Subsonic Transport*. s.l. : AIAA 2002-0002, American Institute of Aeronautics and Astronautics , 2002.
86. Anon. *Aircraft Analysis Cessna Citation X*. Wichita, KA : Cessna Aircraft Company, Sales Engineering, Citation Marketing, July, 2005.
87. —. *A380 Airplane Characteristics*. Blangac Cedex, France : Airbus S.A.S Customer Services, January, 2008.
88. —. *Embraer 170 Specification Sheet*. s.l. : Embraer, January, 2006.
89. —. *737 Airplane Characteristics for Airport Planning*. Seattle, WA : Boeing, October, 2005.
90. —. *777-200LR/-300ER/ Freighter Airplane Characteristics for Airport Planning*. Seattle, WA : Boeing, December 2007.
91. *Boeing 787 Dreamliner Will Provide New Solutions for Airlines, Passengers*. *Boeing.com*. [Online] Boeing. [Cited: April 7, 2010.] <http://www.boeing.com/commercial/787family/background.html>.
92. *PurePower, PW1000G Engine*. 2009.
93. Chudoba, B., Coleman, G. *Thrust Vector Control (TVC) for Transport Aircraft*. Hampton, VA : Aerospace Vehicle Design Lab, University of Texas at Arlington, Presented at the NASA/NIA Truss Braced Wing (TBW) Synergistic Efficiency Technologies Workshop, 2009.
94. Bradley, K. *A Sizing Methodology for the Conceptual Design of Blended Wing-Body Transports*. Langley NASA/CR-20004-2130 16, National Aeronautics and Astronautics Administration, 2004.
95. Mason, W. *Original Werner Pfenniger Research*. s.l. : Presented at the NIA TBW Workshop, Multidisciplinary Analysis and Design Center for Advanced Vehicles, Virginia Tech, August, 2009.
96. Mukhopadhyay, V., et al. *Truss Braced Wing (TBW): NASA/NIA Cooperative Research on N+3 Generation Concepts*. 2009 Annual Meeting Fundamental Aeronautics Program Subsonic Fixed Wing Project, 2009.
97. Hoerner, S.F. *Fluid Dynamic Drag; Practical Information on Aerodynamic Drag and Hydrodynamic Resistance*,. 1965.
98. Chudoba, B., Coleman, G., Oza, A., Czysz, P. *What price supersonic speed? A design anatomy of supersonic transportation*, Part 1. s.l. : The Aeronautical Journal, 2008.
99. Chudoba, B., Oza, A., Coleman G., Czysz, P. *What price supersonic speed? An applied market research case study - Part 2*. The Aeronautical Journal, 2008.
100. Ingenito, A., Gulli, S., Bruno, C., Coleman, G., Oza, A. Chudoba B, Czysz P. *Sizing of TBCC Powered Hypersonic Vehicles*. Journal of Aircraft, TBD. Vol. TBD, TBD [Submitted].

101. Paulson, M. *Developments - Putting a 'Q' into supersonic flight*. Professional Pilot, September 2007, 2007.
102. Antonov, V., Gordon, Y., et al. *OKB Sukhoi - A history of the design bureau and its aircraft*, 1st edition. Midland Publishing Limited, 1996.
103. Deremaux, Y. *Intermediate aircraft configuration families*, Issue-1.: HISAC-T-5-27-1, Dassault Aviation, 2007.
104. Kuchemann, D. *The Aerodynamic Design of Aircraft*. Elmsford, New York : Pergamon Press, LTD., 1978.
105. Koelle, D.E. *On the Optimum Cruise Speed of a Hypersonic Aircraft*. Munich Messerschitt-Bolkow-BLohm (MBB), 1995.
106. Steelant, J. *LAPCAT: High-Speed Propulsion Technology*. Neuilly-sur-Seine, France : *Advances on Propulsion Technology for High-Speed Aircraft* (pp 12-1 to 12-28). Educational Notes RTO-EN-AVT-150, Paper 12. Available from <http://www.rot.nato.int>.
107. Ingenito, A., Bruno, C., Gulli, S. *Conceptual Design of a Mach 8 Vehicle, definition and Analysis of an Air TBCC+SCRJ Powered Vehicle*. Rome University of Rome, 2009.
108. Nonweiler, T.R.F. *Aerodynamic Problems of Manned Space Vehicles*. J. R. Aeronautical Society, 1959. Vol. 63, 521.
109. Morris, R., Brewer, G. *Hypersonic Cruise Aircraft Propulsion Integration Study, Volume I*. Burbank NASA CR-158926-1, NASA Langley Research Center, 1979.
110. Anon. *SNECMA-ONERA-SEP Combined Propulsion Studies in France*. Presentation, 1986.
111. *Falcon Hypersonic Technology Vehicle-2 (HTV-2)*. Tactical Technology Office. [Online] DARPA. [Cited: April 9, 2010.] www.darpa.mil/tto/programs/falcon.
112. Coleman, G., Chudoba, B., Huang, X. *Assessment of Current Space Access Vehicle Tourism Regulations and Their Implications on Design*. Reno AIAA-2006-1528, 44th AIAA Sciences Meeting and Exhibit, 2006.

BIOGRAPHICAL INFORMATION

Gary Coleman graduated with a Degree in Aerospace Engineering from the University of Oklahoma in 2004. After graduation he began his master's research in the Aerospace Vehicle Design Lab at the University of Oklahoma. During this time he was involved in the conceptual design of the Rocketplane LTD.'s Model XP space tourism vehicle and a technical feasibility study of a supersonic business jet with SpritWing aviation. After transferring to the University of Texas at Arlington with the AVD Lab in 2005, he continued work on the SpritWing Supersonic business jet and completed his master's research in the development of a generic stability and control for conceptual design.

Upon completed his masters degree he began the current research in an adaptable parametric sizing tool for aerospace conceptual design. During this research he was involved in the NASA LaRC future commercial transport program and supported the conceptual design Mach 8 commercial transport with the University of Rome.

During both his masters and PhD research he was the Graduate Teaching Assistant for the Aerospace senior design class where he developed a design analysis lab and advised students during several senior design projects.